



ELECTRON TRANSFER PROCESSES IN THE PHOTOLYSIS OF
TRANSITION METAL N-HETROCYCLIC COMPLEXES

by

GHULAM MOHAMMAD MALIK,
M.Sc. (PUNJAB), PAKISTAN.

A Thesis submitted to the University of Adelaide in
partial fulfillment of the requirements for the degree of
Doctor of Philosophy

Department of Physical and Inorganic Chemistry

The University of Adelaide

April, 1979

Awarded 9th Nov. 1979.

ON THE QUEST FOR TRUTH

I know from my own painful searching, with many blind alleys, how hard it is to take a reliable step, be it ever so small, towards the understanding of that which is truly significant.

Albert Einstein

This Thesis contains no material previously submitted for a degree or diploma in any University, and to the best of my knowledge and belief, contains no material previously published or written by another person, except where the due reference is made in the text.

G.M. Malik

ACKNOWLEDGEMENTS

It gives me immense pleasure to acknowledge with thanks the invaluable help, benevolent guidance, and continued encouragement of my supervisor, Dr. G.S. Laurence. I express gratitude to Professor D.O. Jordan in whose department this work was carried out and the other staff members. I wish to thank Dr. A.T. Thornton, Dr. K.D. Whitburn, Dr. M. Dwyer and Mr. G. Boehm, for their help and friendship.

I acknowledge the award of a Columbo Plan Scholarship and grant of duty leave by the Punjab Government.

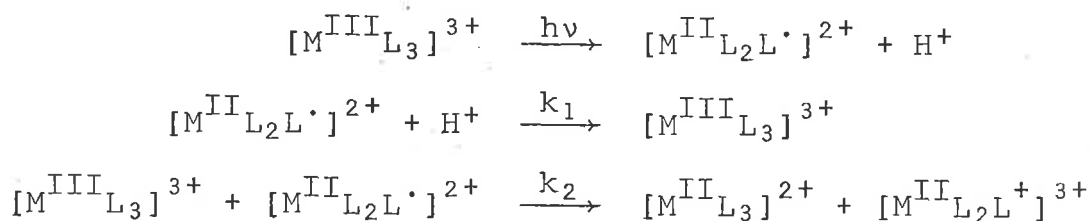
My sincere thanks are due to Ms. P. Ramos for her help, continued friendship and typing this manuscript. Thanks are also due for the help of Messers A. Bowers, G. Duthie, K. Shepherdson, R. Morris and Mrs. B. Hogg.

An acknowledgement will be incomplete without thanking my wife Kubra for her love, understanding and patience for taking charge of the family, while I have been away for four years.

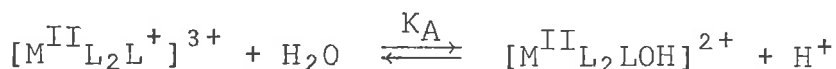
ABSTRACT

The photochemistry of transition metal complexes of the type $[M^{III}L_3]^{3+}$ ($M = Fe(III), Co(III)$ and $Ru(III)$; $L = 2,2'$ -bipyridine, 1,10-phenanthroline or its related ligands) has been studied over the acid range 0.2 - 10 M $HClO_4$ by flash photolysis technique. The complexes undergo two stage photoreductions: a primary photo-reaction is followed by secondary thermal reactions.

The initial photochemical product is a $M(II)$ -ligand-radical complex $[M^{II}L_2L\cdot]^{2+}$. The $[M^{II}L_2L\cdot]^{2+}$ species decays by two competitive electron transfer processes, one leading to further reduction of $[M^{III}L_3]^{3+}$ complex and the other, by an acid catalysed path regenerating the original complex. A fast post-equilibrium converts the $[M^{II}L_2L^+]^{3+}$ species to a proposed hydroxy-ligand



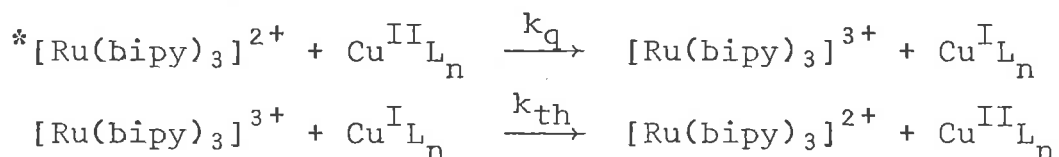
product $[M^{II}L_2LOH]^{2+}$. The rates of the intramolecular (k_1) and



outer-sphere intermolecular (k_2) electron transfer are of the order of $(0.5 - 1.0) \times 10^2 \text{ s}^{-1}$ and $10^6 \text{ M}^{-1} \text{ s}^{-1}$ respectively. The overall quantum yield approaches zero in concentrated (10 M) $HClO_4$ due to the competition between the two thermal reactions, although the primary quantum yield remains constant at all acidities. The intraligand $\pi \rightarrow \pi^*$ bands are photochemically active and the ligand is the electron donor. Internal quenching of the ligand's luminescence by an intramolecular electron transfer is probably

responsible for the observed photoreduction of the $[M^{III}L_3]^{3+}$ complexes.

The quenching of the luminescent excited state of $[Ru(bipy)_3]^{2+}$ by a series of Cu(II) complexes of varying ligands, charge, geometry and redox potential was studied using a N_2 pulsed-laser excitation source. Flash photolysis experiments show the quenching to be by electron transfer.



The bimolecular quenching rate constants, k_q , and the rate constants (k_{th}) for the thermal back electron transfer reactions fall in the range $10^7 - 10^9 M^{-1} s^{-1}$ and $10^8 - 10^9 M^{-1} s^{-1}$ respectively. For the quenchers used, the rates (k_q and k_{th}) have been found to be insensitive to the nature of ligand/s, charge and geometry of the complex, probably due to the dynamic Jahn-Teller effects. The experimental data are discussed in terms of current approaches to theories of outer-sphere electron transfer reactions.

FOREWORD

This thesis is a study of the electron transfer processes in the photolysis of transition metal N-heterocyclic complexes and involves the fields of photochemistry of transition metal complexes of polypyridine ligands and oxidation-reduction reactions of copper complexes, induced by the excited state tris(2,2'-bipyridine)ruthenium(II). For this reason the experimental results and discussion has been divided into two parts. Part I deals with the photochemistry of transition metal N-heterocyclic complexes while Part II contains the oxidation-reductions of copper complexes. To make the discussion sections more fluent, the results which were not considered crucial have been placed as an Appendix and should be considered as supplementary.

TABLE OF CONTENTS

	Page No.
LIST OF ABBREVIATIONS	(i)
LIST OF TABLES	(ii)
LIST OF FIGURES	(v)
 PART 1: PHOTOCHEMISTRY OF TRANSITION METAL N-HETROCYCLIC COMPLEXES	
CHAPTER 1 - INTRODUCTION	1
<u>Section 1</u>	
I.1 Absorption and Emission Spectra of Transition Metal N-Hetrocyclic complexes	2
I.1.1 $[M(\text{bipy})_3]^{2+}$ Spectra	2
I.1.2 Emission Spectra	6
I.1.3 $[ML_3]^{3+}$ Spectra	8
<u>Section 2</u>	
I.2 Oxidation-Reduction Photochemistry	9
I.2.1 Reduction of the Metal Centre	12
(i) Primary Photoreaction	12
(ii) Secondary Thermal Reactions	13
(a) Radical-Substrate Reactions	18
(b) Radical-Product Reactions	18
I.2.2 Oxidation of Metal Centres	19
(i) Primary Photoreaction	19
(ii) Secondary Thermal Reactions	20
I.2.3 Communication between Excited States	22
(i) Intersystem Crossing between Charge Transfer States	22
(ii) Communication between Charge Transfer and Intraligand Excited States	23

	(iii) Communication between Charge Transfer and Ligand Field Excited States	25
	<u>Section 3</u>	
I.3	Coordinated Ligand Radicals	26
I.3.1	Photolytic Generation of Coordinated Ligand Radicals	26
I.3.2	Formation of Coordinated Ligand Radicals by Pulse Radiolysis	29
	(i) \bar{e}_{aq} Adducts	29
	(ii) Reactions of Hydroxyl Radical with Metal Complexes	32
	(a) Hydroxyl Radical Adducts	32
	(b) Hydrogen Atom Abstraction	32
	<u>Section 4</u>	
I.4	Thermal Oxidation-Reduction Reactions	36
I.4.1	Outer-Sphere Mechanism	36
I.4.2	Marcus Theory	37
	<u>Section 5</u>	
I.5	Redox Reactions of Polypyridine Transition Metal Complexes	40
I.5.1	Outer-Sphere Reactions	40
I.5.2	Intramolecular Oxidation Reduction Reactions.....	41
CHAPTER 2	- EXPERIMENTAL	45
II.1	Materials	45
II.1.1	$[\text{Fe}(\text{phen})_3]^{3+}$	45
II.1.2	$[\text{Fe}(\text{bipy})_3]^{3+}$	45
II.1.3	$[\text{Fe}(\text{Me}_4\text{-phen})_3]^{3+}$	46
II.1.4	$[\text{Co}(\text{phen})_3]^{3+}$	46

II.1.5	[Co(phen) ₃] ²⁺	47
II.1.6	[Ru(bipy) ₃] ²⁺	47
II.1.7	[Cu(II)diene]	47
II.1.8	[Cu(en) ₂] ²⁺	47
II.1.9	[Cu(H ₂ EDTA)] ²⁻	48
II.1.10	[Cu(Me ₆ -tren)(ClO ₄)] ¹⁺	48
II.1.11	Cu(II) N-hetrocyclic Diimine Complexes	48
II.1.12	Cu(I) Complexes	48
II.1.13	Other Reagents	49
II.2	Preparation and Standardization of Solutions	50
II.3	Apparatus	54
II.3.1	Flash Photolysis Apparatus	54
II.3.1.1	Excitation Source	54
II.3.1.2	Detection System	56
II.3.1.3	Data Acquisition	57
II.3.1.3.1	The Digital Voltmeters	57
II.3.1.3.2	Biomation 610B	57
II.3.1.3.3	AR-11	58
II.3.2	Laser Photolysis Apparatus	60
II.3.2.1	Excitation Source	60
II.3.2.2	Detection System	62
II.3.2.3	Data Acquisition	63
II.3.2.4	Data Processing	63
II.3.3	(i) Computer System	63
	(ii) Data Treatment	64
II.4	Experimental Methods	66
II.4.1	Flash Photolysis	66
II.4.2	Laser Photolysis	67

CHAPTER 3	- LITERATURE SURVEY	68
III.1	Chromium Complexes	68
III.2	Iron Complexes	71
III.3	Cobalt Complexes	74
III.4	Copper Complexes	76
III.5	Silver Complexes	77
III.6	Ruthenium Complexes	78
III.7	Rhodium Complexes	80
III.8	Iridium Complexes	81
III.9	Platinum Complexes	82
CHAPTER 4	- RESULTS	83
	<u>Section 1</u>	
IV.1	General	83
	(a) Stage I	83
	(b) Stage II	83
	(c) The Effect of Acid Concentration	85
	(d) The Photolysis Products	85
	(e) The Transient Species	85
	(f) Flash Photolysis of $[\text{Co}(\text{phen})_3]^{3+}$	86
	<u>Section 2 - Preliminaries</u>	87
IV.2.1	Thermal Stability of the Complexes	87
IV.2.2	Effect of Monitoring Light	87
IV.2.3	Oxygen Purgig	88
IV.2.4	Photochemical Reactions and Products	90
	<u>Section 3 - Stoichiometry of the Reaction</u> ...	93
IV.3.1	Difference Spectra	93
	(i) $[\text{Fe}(\text{phen})_3]^{3+}$	93
	(ii) $[\text{Fe}(\text{Me}_4\text{-phen})_3]^{3+}$	93
	(iii) $[\text{Fe}(\text{bipy})_3]^{3+}$	97
	(iv) $[\text{Ru}(\text{bipy})_3]^{3+}$	97
	(v) Changes in Intraligand Absorbance	99

IV.3.2	Stoichiometry.....	105
	<u>Section 4</u> - Kinetics of the Secondary Thermal Reactions.....	112
IV.4.1	Introduction.....	112
IV.4.2	Kinetics of the Secondary Thermal Reactions at Low Acid Concentration (0.50 - ca. 5 M H ⁺)	114
IV.4.3	Kinetics of the Secondary Thermal Reactions at High Acid Concentrations	124
IV.4.4	Summary of the Effect of Acidity.....	142
IV.4.5	The effect of the Concentration of [M ^{III} L ₃] ³⁺ at Constant Acid Concentration	145
IV.4.6	Influence of Ionic Strength.....	147
	<u>Section 5</u> - The Nature of the Intermediate Species	150
IV.5.1	Chemical Scavenging Experiments.....	150
IV.5.2	Scavenging of Hydroxyl Radicals.....	151
	(i) Alcohol Scavengers	151
	(ii) Halide Ion Scavenging	154
IV.5.3	Cu ²⁺ _(aq) Scavengers	157
IV.5.4	The Intermediate.....	159
CHAPTER 5	- DISCUSSION	160
V.1	The photochemical and Thermal Reactions	160
V.2	Transient Species and Photochemical Products	164
V.3	Kinetic Analysis.....	171
V.4	Thermal Intramolecular and Intermolecular Electron Transfers.....	175
V.5	Differences between the Steady State and Flash Photolysis of [Fe(phen) ₃] ³⁺	179
V.6	The Effects of Viscosity, Ionic Strength and Water Activity.....	183
V.6.1	Effect of Viscosity	183
	(i) Effect of Viscosity on the Primary Quantum Yield.....	184
	(ii) Effect of Viscosity on the Photophysics.....	185
	(iii) Effect of Viscosity on the Thermal Reactions.....	186

V.6.2	Effects of Ionic Strength and Water Activity	187
V.7	The Primary Photochemistry of $[ML_3]^{3+}$ Complexes .	190
V.7.1	Photophysics of Phenanthroline and Bipyridine Ligands	190
V.7.2	Energy Levels of the $[ML_3]^{3+}$ Complexes	195
V.7.3	The Primary Photochemical Reaction	196
V.7.4	Conclusion	202

PART 2: OXIDATION-REDUCTION REACTIONS OF COPPER COMPLEXES

CHAPTER 6	- REACTIONS OF EXCITED $[Ru(bipy)_3]^{2+}$ WITH COPPER COMPLEXES	204
-----------	---	-----

Section 1

VI.1	Introduction	204
	(a) Electron Transfer Reactions of $*[Ru(bipy)_3]^{2+}$	204
	(b) Electron Transfer Reactions of Cu(II) Species	207

Section 2

VI.2	Redox Properties of $*[Ru(bipy)_3]^{2+}$	209
------	--	-----

Section 3

VI.3	Oxidation-Reduction Reactions of Copper Complexes	212
VI.3.1	Reductions of Cu(II) Complexes	212
VI.3.2	Oxidations of Cu(I) Complexes	215
VI.3.3	The Self Exchange Rates of Cu(I) and Cu(II) Complexes	217

Section 4

VI.4	Experimental	219
VI.4.1	Solutions and Apparatus	219
VI.4.2	Laser Excitation - Measurements of the Quenching Rate Constants	219
VI.4.3	Flash Photolysis - Measurements of the Thermal Back Electron Transfer Rates	219

VI.4.4	Measurements of the Activation Energies for the Quenching Rate Constants	221
	<u>Section 5</u>	
VI.5	Results	222
	<u>Section 6</u>	
	Discussion	225
IV.6.1	General Observations	225
IV.6.2	Current Approaches to Theories of Electron Transfer Rates	225
	(i) The Marcus Theory	225
	(ii) The Rehm-Weller Treatment	228
VI.6.3	Rate Constants, Activation Parameters and the Marcus Theory	232
IV.6.4	The Relationship Between k_{12} and K_{12}	236
IV.6.5	Estimation of Cu(I)-Cu(II) Self Exchange Rates	236
APPENDIX A	248
REFERENCES	258

LIST OF ABBREVIATIONS

BA	Benzoate
bipy	2,2'-bipyridine
But	butyl
Cl-phen	5-chloro-1,10-phenanthroline
CyDTA	trans-1,2-diaminocyclohexanetetraacetate
diene	5,5,7,12,12,14-hexamethyl-1,4,8,11-tetraaza-cyclodeca-4,11-diene
dmb	4,4'-dimethyl-2,2'-bipyridine
DMF	dimethylformamide
dmp	2,9-dimethyl-1,10-phenanthroline
EDTA	ethylenediaminetetraacetate
Et	ethyl
Me	Methyl
Me ₄ -phen	3,4,7,8-tetramethyl-1,10-phenanthroline
Me ₆ -tren	tris(dimethyl-aminoethyl)amine
MNBA	meta-nitrobenzoate
NBA	nitrobenzoate
NCA	nitrocinnamate
NO ₂ -phen	5-nitro-1,10-phenanthroline
ONBA	ortho-nitrobenzoate
ox	oxatate
PDTA	propylenediaminetetraacetate
ph	phenyl
phen	1,10-phenanthroline
PNBA	para-nitrobenzoate
Py	pyridine
terpy	terpyridine
tet-b	5,5,7,12,12,14-hexamethyl-1,4,8,11-tetraazacyclotetradecane
tu	thiourea

LIST OF TABLES

Table	Page
1. Summary of Primary Radicals and Metallo- fragments	14
2. Transients in the Photolysis of Oxalato- Complexes	27
3. Rates of Intramolecular Electron Transfers	34
4. Molar Absorbances used in the Standardization of Solutions	51
5. The Effect of Oxygen	89
6. Looking for Possible Photodissociation	91
7. Isosbestic Points for the Difference Spectra of the Final Products of Photolysis in the Intraligand band	104
8. Data for Stoichiometry Determining Experiments ...	107
9. Absorption Spectral Data used in Stoichiometric Calculations	109
10. Relative Changes in Absorbance for Stage I and Stage II	110
11. Relative Quantum Yield with Increasing Acid Concentration	113
12. Data for Variation of k_{obs} (Stage II) with Increasing Acid Concentration	121
13. Rate Constants for Stage II	122

Table	Page
14. Second Order Rate Constants for the Oxidation of $\text{Fe}_{(\text{aq})}^{2+}$ by Various Transition Metal N-Heterocyclic Complexes at 25°C	123
15. Data for k_{obs} with Increasing Acid Concentration for the Transient Decay to Reform M(III) Complexes	137
16. Effect of Activity of Water on the Decay of the Transient to Reform M(III) Complexes	139
17. Primary Quantum Yields	141
18. Activity of Water in Different Acids	143
19. Activity Coefficients of Acids	144
20. Effect of Ionic Strength	147
21. Effect of Alcohol Scavengers on Stage II reaction	151
22. Summary of Rate Constants for Reactions of OH Radicals with $[\text{ML}_3]$ Complexes	153
23. A Search for Hydroxyl Radicals	156
24. Effect of $\text{Cu}_{(\text{aq})}^{2+}$ as Scavenger	158
25. Photophysical Properties of Phenanthroline and Bipyridine	193
26. Spectra of Fe(III) and Ru(III) Complexes of Bipyridine	195
27. Redox Potentials for the M(III) Complexes and pK_a Values of the Ligands	201
28. Stereochemistry of Copper Complexes	205

Table	Page
29. Rates of Reduction of Cu(II) Complexes by Ferrocytochrome c	214
30. Rate Constants for Self Exchange of Copper Complexes	218
31. Quenching and Thermal Electron Transfer Rates Data	223
32. Activation Parameters for Quenching by Copper Complexes	224
33. Estimates of Photochemical and Thermal Self Exchange Rate Constants for Copper Complexes - Marcus Theory	238
34. Estimates of Photochemical and Thermal Self Exchange Rate Constants for Copper Complexes - Weller Treatment	241
35. Data for ΔG_{12}^\ddagger and ΔG_{12}^0	244
36. Rate Constants for Acid Hydrolysis of M(II) Complexes of Bipyridine and Terpyridine Ligands	254

LIST OF FIGURES

Figure		Page
1.	Ultraviolet-Visible Spectra of Bipyridine and Phenanthroline Ligands	3
2.	Molecular Orbital Diagram for Classifying Electronic Transitions in Metal Complexes	4
3.	Absorption and Emission Spectra of M(II) and M(III) Complexes	5
4.	Electronic Absorption Spectra of Fe(III) Complexes	7
5.	Diagram for the Photophysical and Photochemical Processes of $[\text{Ir}(\text{phen})_2\text{Cl}_2]^+$ ion	10
6.	Hypothetical diagram for the photochemistry of $[\text{Rh}(\text{NH}_3)_5\text{I}]^{2+}$	24
7.	Block Diagram of Flash Photolysis Apparatus....	55
8.	Block Diagram of Laser Photolysis Apparatus....	61
9.	The Two stages of Photoreduction	84
10.	Difference Spectra of the Initial and Final Products of Photolysis of $[\text{Fe}(\text{phen})_3]^{3+}$ and that of $[\text{Fe}(\text{phen})_3]^{2+}$ and $[\text{Fe}(\text{phen})_3]^{3+}$	94
11.	Difference Spectra of the Initial and Final Products of Photolysis of $[\text{Fe}(\text{Me}_4\text{-phen})_3]^{3+}$ and that of $[\text{Fe}(\text{Me}_4\text{-phen})_3]^{2+}$ and $[\text{Fe}(\text{phen})_3]^{3+}$	95
12.	Difference Spectra of the Initial and Final Products of Photolysis of $[\text{Fe}(\text{bipy})_3]^{3+}$ and the Difference Spectra of $[\text{Fe}(\text{bipy})_3]^{2+}$ and $[\text{Fe}(\text{bipy})_3]^{3+}$	96

Figure	Page
13. Difference Spectra of the Initial and Final Products of Photolysis of $[\text{Ru}(\text{bipy})_3]^{3+}$ including the Difference Spectra of $[\text{Ru}(\text{bipy})_3]^{2+}$ and $[\text{Ru}(\text{bipy})_3]^{3+}$	98
14. Difference Spectra of the Final Products of Photolysis of M(III) Complexes in the intra-ligand band	100
15. The Slow (Stage II) Reaction in the Photolysis of M(III) Complexes	115
16. Plots of Pseudo-first Order Rate Constants versus $[\text{M}^{\text{III}}\text{L}_3]^{3+}$ concentration	
17. "Kinetic Isosbestic Effect" in the Photolysis of M(III) Complexes	125
18. Plots of Variation of Relative Quantum Yield with Increasing Acid	130
19. Variation of the Pseudo-first Order Rate Constant (k_{obs}) for the Slow Formation of M(II) Complexes (Stage II) with Increasing Acid Concentration	131
20. Decay of the Transient Absorbance (Stage I) to Reform M(III) Complexes	133
21. Plots of $k_{(\text{obs})}$ Versus Acid Concentration	138
22. Graphs Showing the Effect of Water Activity. Plots of $k_{(\text{obs})}/[\text{Acid}]$ versus $a_{\text{H}_2\text{O}}$	140
23. Flash Pictures Showing the Effect of $[\text{Fe}(\text{phen})_3]^{3+}$ Concentration at 3 M HClO_4 on the Photolysis of $[\text{Fe}(\text{phen})_3]^{3+}$	146

Figure		Page
24.	Flash Picture Showing the Effect of Ionic Strength (5.5 M) on the Photolysis of $[\text{Fe}(\text{phen})_3]^{3+}$	148
25.	Traces Showing the Changes in Absorbance at 273 nm in the Absence and Presence of Added Chloride Ions in the Photolysis of $[\text{Fe}(\text{phen})_3]^{3+}$ without Silica Filter.....	155
26.	Variation of $\phi_{+\text{Fe(II)}}/\phi_{-\text{Fe(III)}}$ with Sulphuric Acid and Methylmethacrylate Concentrations	167
27a	Diagram for the Photophysics of Bipyridine	191
27b	and Phenanthroline Ligands	192
28.	An unlikely Hypothetical Diagram to Explain the Photoreduction of $[\text{Fe}(\text{phen})_3]^{3+}$ by Excitation in the Intraligand ($\pi \rightarrow \pi^*$) band.....	197
29.	The Proposed Diagram for the Photoreduction of $[\text{Fe}(\text{phen})_3]^{3+}$ by Excitation in the Intraligand ($\pi \rightarrow \pi^*$) band by Internal Quenching of the Ligand's Phosphorescence by an Intramolecular Ligand to Metal Electron Transfer - An Exemplary Case for M(III) Complexes.....	199
30.	Absorbance changes at 436 nm in the Photolysis of $[\text{Ru}(\text{bipy})_3]^{2+}$ (10 μM) and $[\text{Cu}(\text{Me}_6\text{-tren})(\text{H}_2\text{O})]^{2+}$ (4 mM) at the Natural pH	220
31.	The Marcus Theory's Predicted Behaviour of $\log k_{12}$ versus ΔGr^0	227
32.	The Rehm-Weller Treatment's Predicted Behaviour of $\log k_q$ versus ΔGr^0	230

Figure	Page
33. Plot of $\log k_{12}$ versus $\log K_{12}$ for the Copper Complexes Used as Quenchers	233
34. Plots of ΔG_{12}^\ddagger versus ΔG_{12}^0	237
35. Plots of the Photochemical (k_{ex}^ϕ) and Thermal (k_{ex}^{th}) Exchange Rates (calculated from the Marcus Theory) versus ΔG^0	239
36. Plots of the Photochemical (k_{ex}^ϕ) and Thermal (k_{ex}^{th}) Exchange Rates (calculated from the Weller Treatment) versus ΔG^0	243
37. Absorption Spectra of $[\text{Co}(\text{phen})_3]^{3+}$, Flash Photolysed $[\text{Co}(\text{phen})_3]^{3+}$ and after Shaking the Photolysed Solution with Chloroform	250
38. Three Stages of Reactions in the Flash Photolysis of $[\text{Co}(\text{phen})_3]^{3+}$ Ion	252

PART I

PHOTOCHEMISTRY OF TRANSITION METAL
N-HETROCYCLIC COMPLEXES



INTRODUCTION

Transition metal complexes of 2,2'-bipyridine, 1,10-phenanthroline and related ligands are particularly interesting for the study of photo-induced oxidation-reduction reactions owing to their intense visible absorption bands. They are substitutionally inert and can be reduced or oxidized without change of their molecular geometry. The research interest in the photo-redox reactions of these complexes stems from the facts that their photochemical behaviour has not been determined with any certainty to date and that the electron transfer reactions of the excited states of polypyridine transition metal complexes are promising reactions for the conversion of solar energy into chemical energy. In addition these reactions allow one to check the theories of electron transfer reactions over a wide range of free energy change (ΔG°). Transport of electrons through molecules is of fundamental chemical importance, relating to the intramolecular pathways for the transfer of electrons through the large biological molecules involved in the redox process which occur in chloroplasts and mitochondria. The study of photo-reactions of polypyridine metal complexes may also help in the understanding of the factors that govern the rate of intra-molecular electron transfer from a coordinated ligand radical to a metal centre in the oxidation-reduction process of biologically important systems.

SECTION 1

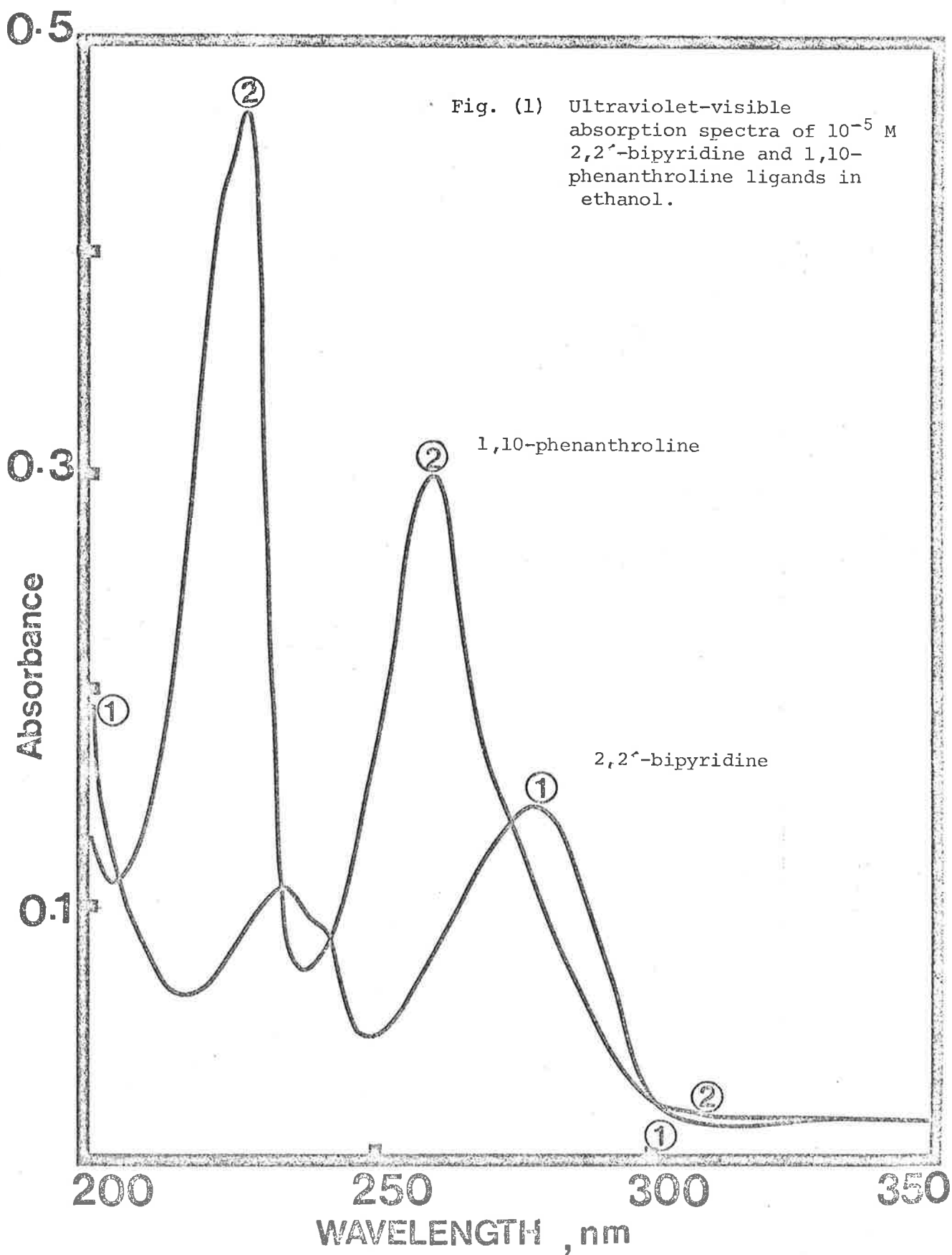
I.1 ABSORPTION AND EMISSION SPECTRA OF POLYPYRIDINE TRANSITION METAL COMPLEXES

The ultraviolet-visible spectra of the free ligands consists of absorption maxima at 280 nm and 235 nm (bipyridine) and at 290 nm, 265 nm and 226 nm (phenanthroline) [Fig. (1)]. The bands correspond essentially to $\pi \rightarrow \pi^*$ transitions (Favini & Gamba, 1966; Gil, Moraga & Brunel, 1967; Kiss & Császár, 1963). Kiss and Császár consider an $n \rightarrow \pi^*$ transition to lie under the long wavelength tail of the bipyridine spectrum.

Coordination of these bases to metal ions results in a red shift of the ligand spectrum (Favini & Gamba, 1966; Ito, 1956; Kiss & Császár, 1963; Martin, McWhinnie & Waing, 1961 and Sone Krumholtz & Stammreich, 1955). Analysis and assignment of the absorption spectra of the transition metal complexes is very difficult due to the complexity of electronic structure of these molecules but a simplified schematic molecular orbital diagram, resulting from combination of metal and ligand orbitals of appropriate symmetry is a usual convenient way of classifying electronic transitions. It should be pointed out that the energy ordering of the various orbitals may be different from that shown in Fig. 2.

I.1.1 $[M(\text{bipy})_3]^{2+}$ Spectra

The absorption and emission spectra of $[\text{Ru}(\text{bipy})_3]^{2+}$ are shown in Fig. 3. By comparison with the spectrum of protonated bipy (Lyttle & Hercules, 1969) the band at 285 nm have been assigned to the $1L \pi \rightarrow \pi^*$ transition. The shoulders at 322 and



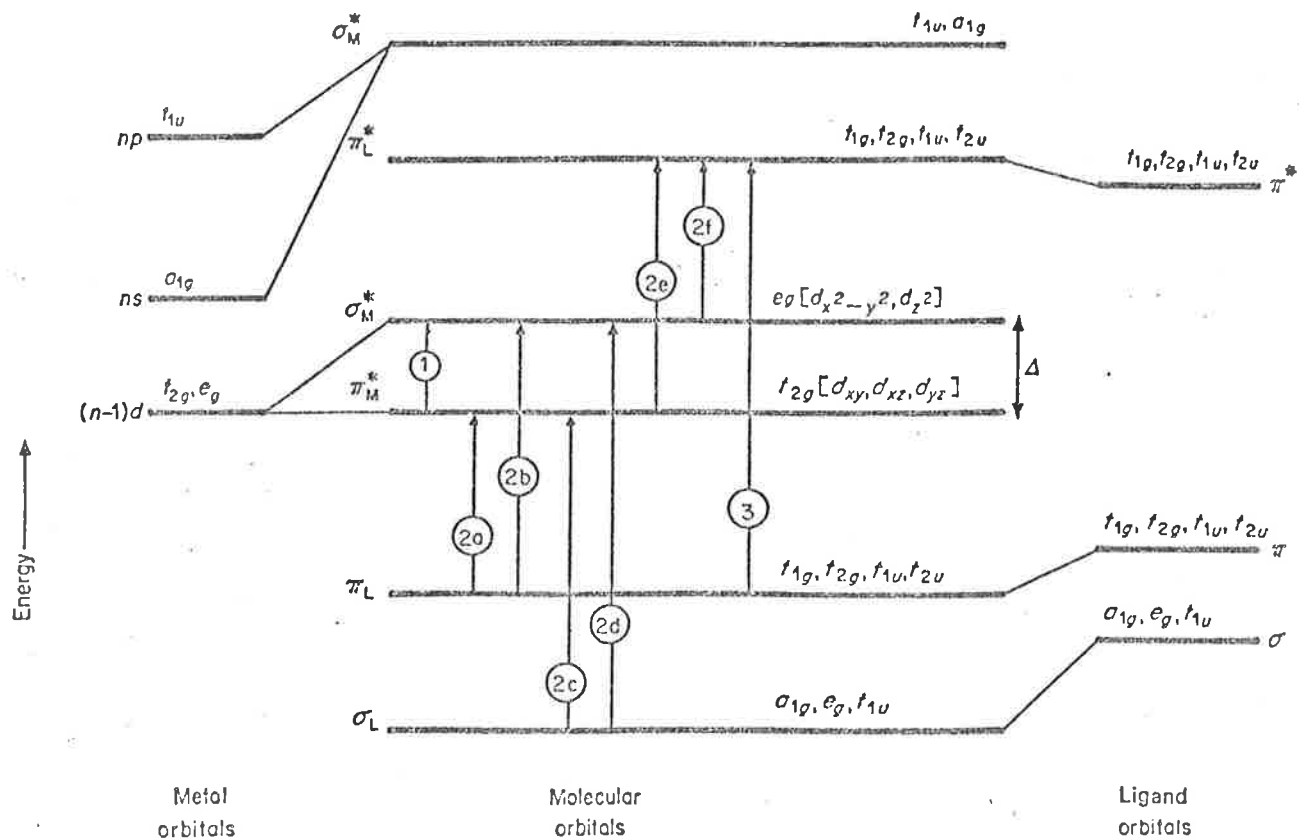


FIG. 2 Schematic orbital energy diagram representing various types of electronic transitions in octahedral complexes. A line connects an atomic orbital to that MO in which it has the greatest participation. The asterisk of π_M is put into parentheses since this orbital may have bonding, non-bonding, or antibonding character, depending on the particular metal and ligands involved. 1: ligand field transitions; 2a, 2b, 2c, 2d: ligand-to-metal charge transfer transitions; 2e, 2f: metal-to-ligand charge transfer transitions; 3: internal ligand transitions.

Reference: Balzani & Carassiti, 1970.

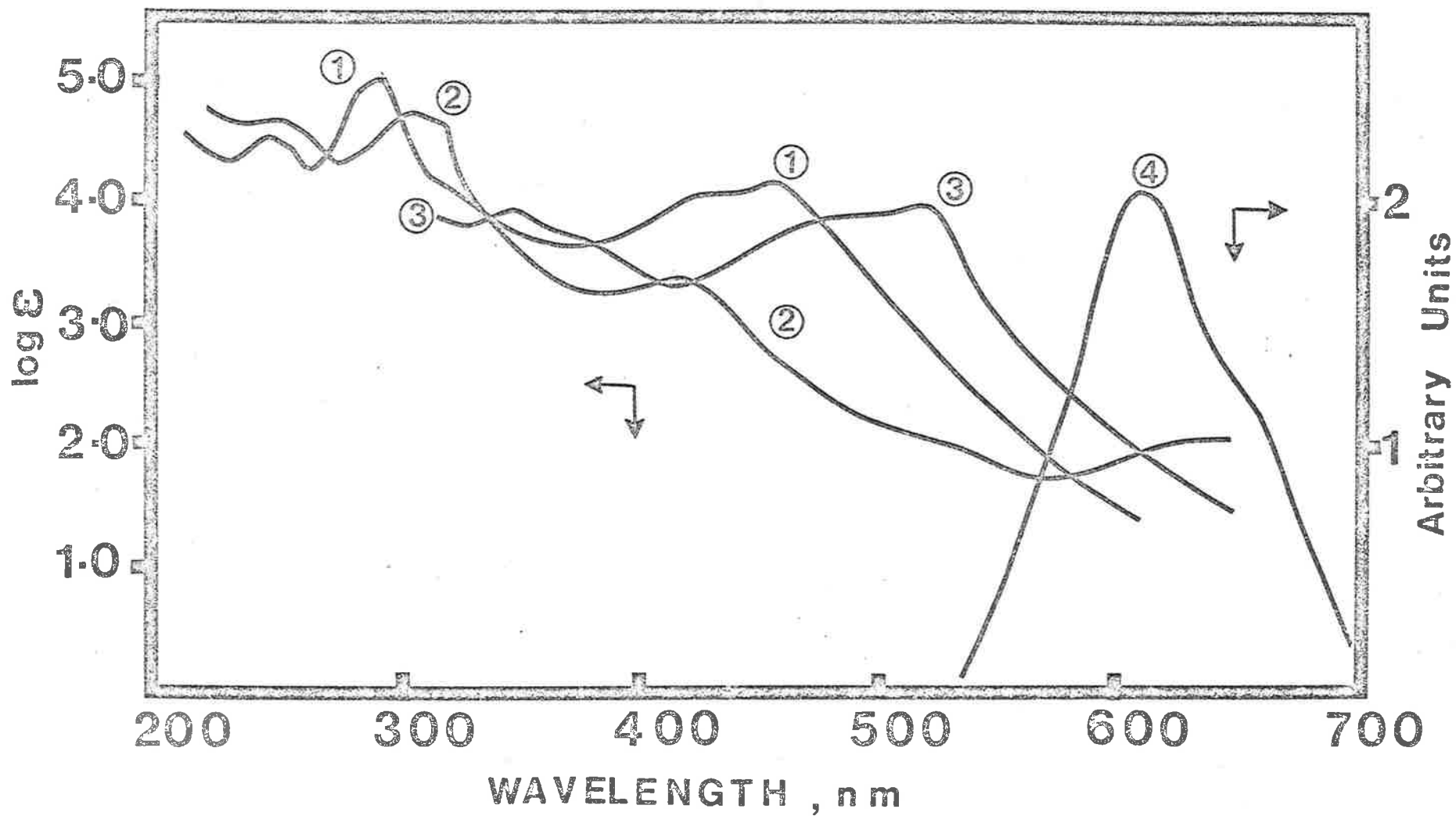


Fig. (3) Absorption and emission spectra of M(II) and M(III) complexes. (1) $[\text{Ru}(\text{bipy})_3]^{2+}$ (in H_2O), (2) $[\text{Ru}(\text{bipy})_3]^{3+}$ (in 5M HClO_4), (3) $[\text{Fe}(\text{bipy})_3]^{2+}$ (in H_2O) and (4) the emission spectra of $[\text{Ru}(\text{bipy})_3]^{2+}$ (in H_2O).

344 nm could probably arise due to LF/d-d transitions.

The two remaining bands at 240 (UV region) and 450 nm are due to MLCT $d \rightarrow \pi^*$ transitions, each one showing two vibronic components which can be resolved at room temperature (Lyttle & Hercules, 1969). The assignment of the absorption at $\lambda > 500$ nm has been a matter of conjecture. In this complex 1L π^* orbital is the lowest energy empty MO instead of the 1L σ^* orbital (Tokel-Tokovoryan & Hemingway & Bard, 1973).

The spectrum of $[\text{Fe}(\text{bipy})_3]^{2+}$, both in crystal and solution, is very similar to that of $[\text{Ru}(\text{bipy})_3]^{2+}$ (Palmer & Piper, 1966). The entire spectrum is shifted about ~ 65 nm to lower energy relative to that of ruthenium complex (Fig. 3) (Bryant, Ferguson & Powel, 1971). Other than this, the only difference in the Ru(II) spectrum appears to be the absence of a weak shoulder corresponding to the $[\text{Fe}(\text{bipy})_3]^{2+}$ band at 870 nm (there is a shoulder at 556 nm, but its extinction coefficient is much higher than that of the Iron(II) complex; Palmer & Piper, 1966).

I.1.2 Emission Spectra

The extent of the spin-orbit coupling in a molecule containing a Ru(II) ion should make for a large rate of intersystem crossing, thus significantly populating the lowest triplet level and partially removing the spin forbiddenness of phosphorescence (Watts & Crosby, 1972). As a consequence $[\text{Ru}(\text{bipy})_3]^{2+}$ luminesces in fluid solution at room temperature while $[\text{Fe}(\text{bipy})_3]^{2+}$ is non-luminescent. The nature of the emitting state of $[\text{Ru}(\text{bipy})_3]^{2+}$ is now definitely established as MLCT but the spin label, usually taken as a triplet, cannot really be defined because of the dominant role of spin-orbit coupling (Lyttle & Hercules, 1969;

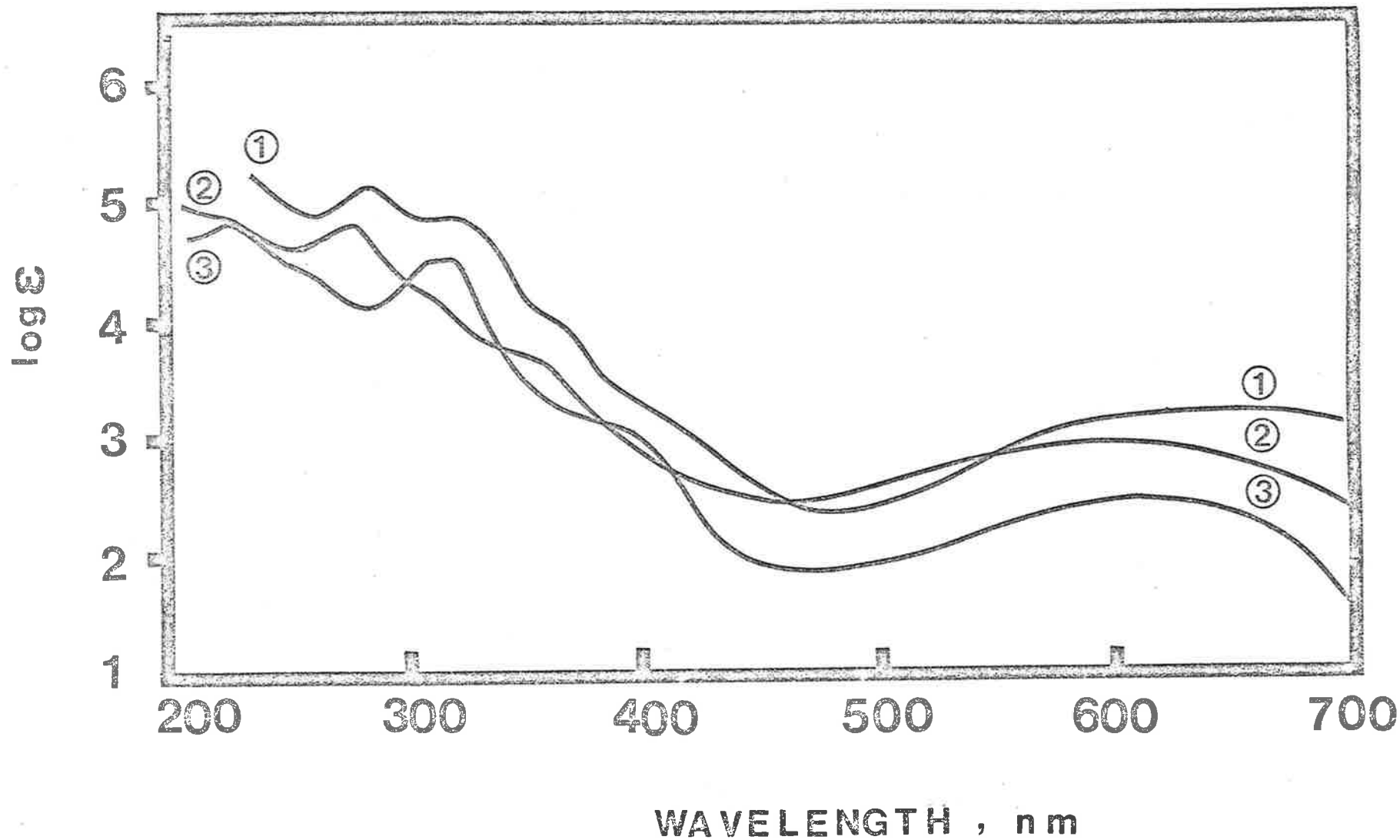


Fig. (4) Electron absorption spectra of Fe(III) complexes. (1) $[\text{Fe}(\text{Me}_4\text{-phen})_3]^{3+}$, (2) $[\text{Fe}(\text{phen})_3]^{3+}$ and (3) $[\text{Fe}(\text{bipy})_3]^{3+}$. All the spectra in 10 M HClO_4 .

Hipps & Crosby, 1975). The spectrum of $[\text{Fe}(\text{phen})_3]^{2+}$ is also similar to $[\text{Fe}(\text{bipy})_3]^{2+}$ and $[\text{Ru}(\text{bipy})_3]^{2+}$ in the visible region but slightly different in the UV-region (the 1L band).

I.1.3 $[\text{ML}_3]^{3+}$ Spectra

The assignment of the intense electronic absorption bands in the spectra of $[\text{ML}_3]^{3+}$, metal ions in the trivalent state (d^5 , low-spin), is more complex than those of $[\text{M}(\text{bipy})_3]^{2+}$ complexes. The spectra (Fig. 3, 4) in the UV-region consists of a band near 238 nm ($\epsilon > 10^4 \text{ M}^{-1} \text{ cm}^{-1}$) and a band resolved into two components, 307 and 316 nm ($\epsilon > 2 \times 10^4$), is assigned to 1L $\pi-\pi^*$ transition. The splitting could be due to vibrational effects (Bryant & Ferguson, 1971) or to the splitting of the π -orbitals of the ligand by the symmetry of the metal orbitals (Mason & Norman, 1969; Orgel, 1961; Ferguson, Hawkins, Kane-Maguire & Lip, 1969). Similar bands have been assigned to $[\text{Fe}(\text{phen})_3]^{3+}$ (Day & Sanders, 1967).

The visible spectra of $[\text{M}(\text{bipy})_3]^{3+}$ complexes consist of a weak band below 530 nm ($\epsilon < 10^3 \text{ M}^{-1} \text{ cm}^{-1}$). The band has been assigned to LMCT transition, and a similar assignment has been made for phenanthroline complexes (Day & Sanders, 1967). The spectra of $[\text{ML}_3]^{3+}$ complexes are shown in Figs. 3 and 4. All these d^5 complexes are non-luminescent.

SECTION 2

I.2 OXIDATION-REDUCTION PHOTOCHEMISTRY

The photochemical behavior of a molecule is determined by a complicated balance of chemical and spectroscopic factors (Balzani & Carassiti, 1970). When the complexes are irradiated their electronically excited states are reached. The electronic energy can be dissipated chemically (photoreaction) or physically (heat or luminescence). Although the electronic configuration of the excited state, reached by direct irradiation, plays an important role in the photochemical and photophysical behaviour of the molecule it is not always possible to explain the observed photoreaction from the initial excitation.

A common feature of all photo-processes is the communication between excited states. The relative populations of each state are a function of the intersystem crossing, back intersystem crossing and internal conversion efficiencies. These efficiencies are dependent on the experimental conditions (solvent, temperature, ionic strength etc.), the nature of the metal ion and the ligands involved (Fig. 5).

It is difficult to formulate rules predicting the reaction mode (which is controlled by the nature of the excited state) when a particular absorption band is irradiated. The generalization that charge transfer excited states lead to redox process and the ligand field excited states cause photo-substitution does not always hold good but it is convenient to discuss oxidation-reduction photochemistry in terms of irradiation of the complexes in their charge transfer bands.

Irradiation of the charge transfer bands of coordination complexes causes radial redistribution of the electron density

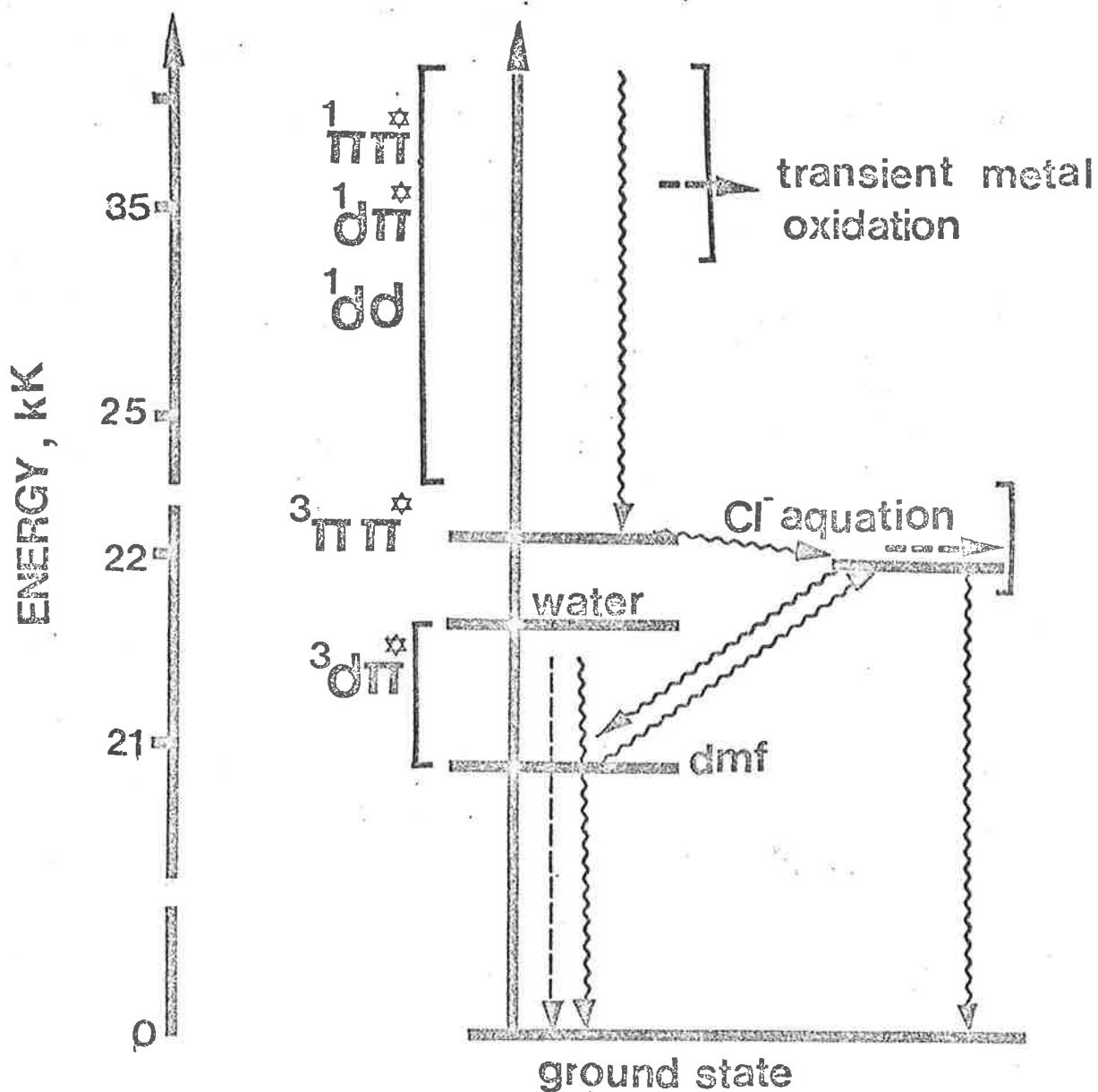
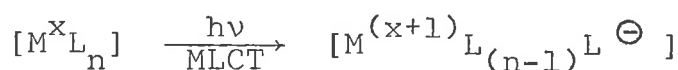


Fig. 5 Diagram for the Photophysical and Photochemical Processes of $[\text{Ir}(\text{phen})_2\text{Cl}_2]^+$ ion following the photoexcitation. Reference: Hoffman, Balzani et al. 1975.

between the metal centre and the ligands. This can result in a variety of chemical reactions of which the most characteristic are redox processes. Charge transfer photochemistry is complicated by the overlap of charge transfer (CT), ligand field (d-d) and intraligand bands (IL).

Two basic photoredox processes are recognized depending upon whether the electron transfer is from the ligand to the metal or vice versa. LMCT and MLCT charge transfer excited states commonly involve intramolecular electron transfers resulting in the oxidation or reduction of the metal centres with concurrent ligand reduction or oxidation (Adamson, 1960a; Doering, Porter & Karanka, 1962; Wehry, 1967; Klänning & Symons, 1959, 1960; Fleischauer & Adamson, 1975).



Examples are known where charge transfer to solvent (Matheson et al., 1963; Lachisch, Schafferman & Stein, 1976; Waltz & Adamson, 1969; Samotus, 1973a & 1973b) and intermolecular charge transfer between ion pairs (Malone & Endicott, 1972; Endicott & Hoffman, 1965; Wells & Endicott, 1971; Elsgernnd & Beattie, 1968) occur:



The photoredox processes are largely dependent on the stabilities of the initial and final chemical systems, the ligands involved and the conditions of the medium. Due to the electron

transfer, the charge transfer excited states may become more susceptible towards nucleophilic attack which may lead to the conversion of a substitutionally inert complex to its reduced or oxidized counterpart. Photoredox reactions of complexes with protogenic ligands are expected to be strongly affected by the acidity of the medium (Malik & Laurence, 1978).

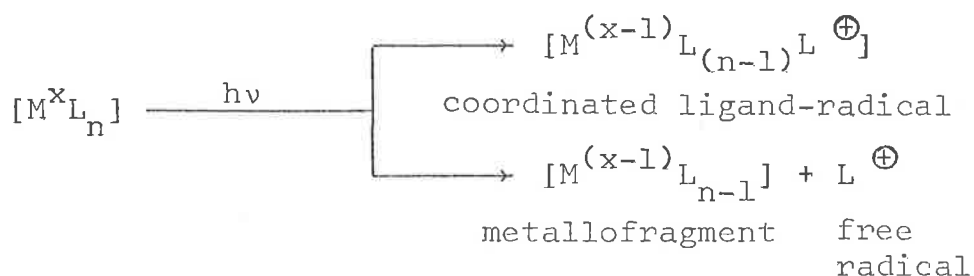
It is generally judicious to combine perturbation (flash photolysis, laser photolysis or pulse radiolysis) and chemical scavenging techniques in order to facilitate the identification of primary transient species. Recently electrochemical (Lilie et al., 1971; Gatzel et al., 1969, 1973; Patterson & Perone, 1972) and conductance (Lilie & Fessenden, 1973) techniques have also been used in such perturbation studies.

1.2.1 REDUCTION OF THE METAL CENTRE

This section describes the general concepts of LMCT photochemistry and by no means gives a comprehensive review of the subject. Included here are those systems where coordinated ligand-radicals, observed in the present study, have been proposed or tentatively identified.

(i) Primary Photoreaction

Irradiation of coordination compounds in their LMCT bands generally leads to the formation of one electron reduced species (metallo-fragment) and an equivalent oxidation of the ligand to produce a radical pair as the primary photoproduct.



Primary metallo-fragments and radicals have been proposed or identified in many redox reactions of Co(III), Fe(III) and Ru(III) complexes. These results are summarized in Table (1).

One particularly clear instance of the identification of metallo-fragment and primary radical is given in the flash photolysis of $[\text{PtCl}_6]^{2-}$ by Wright and Laurence (1972). The



spectrum of the transient (ca. $\lambda > 400$ nm), decaying by second order kinetics, was found to be identical with that of the pulse radiolytically generated Pt(III) species, and $\text{Cl}\cdot$ was detected as Cl_2^- ($\lambda_{\text{max}} \sim 360$ nm, $\epsilon_{\text{max}} \sim 8 \times 10^3 \text{ M}^{-1} \text{ cm}^{-1}$) in



the presence of added chloride ions.

(ii) Secondary Thermal Reactions

The observed overall quantum yield of a photoredox reaction may be different from the primary quantum yield because primary products can react thermally. The radical pair can undergo geminate recombination in the solvent cage and after escaping from the solvent cage whereas coordinated ligand-radicals react intramolecularly. Some of these radicals are stable while other more reactive species can undergo a large variety of reactions: radical-radical coupling, bimolecular disproportionation, hydrogen atom abstraction or solvolysis yielding simpler or more stable species. Examples are known where radical-substrate or radical-product reactions have been observed.

Secondary thermal reactions can also arise from the scavenging experiments. Although chemical scavenging techniques are useful in providing information about the nature and identity of

Table (1)

SUMMARY OF PRIMARY RADICALS AND METALLO-FRAGMENTS IDENTIFIED OR PROPOSED
 FOLLOWING DIRECT LMCT EXCITATION OF TRANSITION METAL COMPLEXES

Complex Irradiated	Primary Radical	Probable Metallofragment	Reference
$[\text{Co}(\text{NH}_3)_6]^{3+}$	NH_3^+	$[\text{Co}(\text{NH}_3)_5]^{2+}$	Endicott & Hoffman, 1965
$[\text{Co}(\text{NH}_3)_5\text{H}_2\text{O}]^{3+}$	NH_3^+	$[\text{Co}(\text{NH}_3)_4]^{2+}$	Endicott & Hoffman, 1965
$[\text{Co}(\text{NH}_3)_5\text{NCS}]^{2+}$	$\cdot\text{NCS}$	$[\text{Co}(\text{NH}_3)_5]^{2+}$	Adamson & Sporer, 1958
$[\text{Co}(\text{NH}_3)_5\text{N}_3]^{2+}$	$\cdot\text{N}_3$	$[\text{Co}(\text{NH}_3)_4]^{2+}$	Ferrandi & Endicott, 1973a Adamson & Sporer, 1958 Endicott, Hoffman & Beres, 1970
$[\text{Co}(\text{NH}_3)_5\text{O}_2\text{R}]^{2+}$	$\cdot\text{R}$	$[\text{Co}(\text{NH}_3)_5]^{2+}$	Cooper & DeGraff, 1972 Campano, Kantrowitz, Hoffman & Weinberg, 1974
$[\text{Co}(\text{NH}_3)_5\text{ox}]^{2+}$	$\text{C}_2\text{O}_4^-/\text{CO}_2^-$	$[\text{Co}(\text{NH}_3)_5]^{2+}$	Vaudo, Kantrowitz, Hoffman, Papaconstantinou & Endicott, 1972 Hoffman & Simic, 1973 Vaudo, Kantrowitz & Hoffman, 1971
$[\text{Co}(\text{NH}_3)_5\text{OCO}_2]^{2+}$	CO_3^-	$[\text{Co}(\text{NH}_3)_5]^{2+}$	Cope & Hoffman, 1972 Cope, Chen & Hoffman, 1973 Chen, Cope & Hoffman, 1973

Table (1) (Cont....)

$[\text{Co}(\text{NH}_3)_5\text{OOCH}]^{2+}$	$\cdot\text{H}$	$[\text{Co}(\text{NH}_3)_5]^{2+}$	Kantrowitz, Hoffman & Schilling, 1972
$[\text{Co}(\text{NH}_3)_5\text{Cl}]^+$	NH_3^+ or $\dot{\text{Cl}}$	$[\text{Co}(\text{NH}_3)_5]^{2+}$	Caspari, Hughes, Endicott & Hoffman, 1970
$[\text{Co}(\text{NH}_3)_5\text{Br}]^{2+}$	$\text{Br}\cdot$	$[\text{Co}(\text{NH}_3)_5]^{2+}$	Malone & Endicott, 1972 Penkett & Adamson, 1965
$[\text{Co}(\text{NH}_3)_5\text{I}]^{2+}$	$\text{I}\cdot$	$[\text{Co}(\text{NH}_3)_5]^{2+}$	Malone & Endicott, 1972 Penkett & Adamson, 1965
$[\text{Co}(\text{NH}_3)_5\text{NO}_2]^{2+}$	NO_2	$[\text{Co}(\text{NH}_3)_5]^{2+}$	Balzani, Ballardini, Sabbatini & Moggi, 1968 Scandola, Bartocci & Scandola, 1968
$[\text{Co}(\text{en})_3]^{3+}$	en^+	$[\text{Co}(\text{en})_2]^{2+}$	Klein & Moeller, 1965
$[\text{Co}(\text{CN})_5\text{NCS}]^{3-}$	$\dot{\text{NCS}}$	$[\text{Co}(\text{CN})_5]^{3-}$	Ferrandi & Endicott, 1973 Endicott, Ferrandi & Barber, 1975
$[\text{Co}(\text{CN})_5\text{N}_3]^{3-}$	$\cdot\text{N}_3$	$[\text{Co}(\text{CN})_5]^{3-}$	Ferrandi & Endicott, 1973 Endicott, Ferrandi & Barber, 1975
$[\text{Co}(\text{CN})_5\text{I}]^{3-}$	$\text{I}\cdot$	$[\text{Co}(\text{CN})_5]^{3-}$	Ferrandi & Endicott, 1973 Endicott, Ferrandi & Barker, 1975
$[\text{Co}(\text{EDTA})]^{1-}$	$\cdot\text{Y}^{\text{a}}$	$[\text{Co}^{\text{II}}(\cdot\text{Y})]^-$	Natarajan & Endicott, 1973a, b & c
$[\text{Co}(\text{HEDTA})\text{Cl}]^-$	$\cdot\text{Y}^{\text{a}}$	$[\text{Co}^{\text{II}}(\cdot\text{Y})]^-$	Natarajan & Endicott, 1973a, b & c
$[\text{Co}(\text{HEDTA})\text{Br}]^-$	$\cdot\text{Y}^{\text{a}}$	$[\text{Co}^{\text{II}}(\cdot\text{Y})]^-$	Natarajan & Endicott, 1973a, b & c

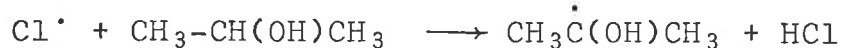
Table (1) (Cont....)

$[\text{Co}(\text{N}_4)\text{Cl}_2]^{1+\text{b}}$	$\text{Cl}\cdot$	$[\text{Co}(\text{N}_4)]^{2+}$	Malone & Endicott, 1972
$[\text{Co}(\text{N}_4)\text{Br}_2]^{1+\text{b}}$	$\text{Br}\cdot$	$[\text{Co}(\text{N}_4)]^{2+}$	Malone & Endicott, 1972
$[\text{Rh}(\text{NH}_3)_5\text{CNS}]^{2+}$	$\cdot\text{NCS}$	$[\text{Rh}(\text{NH}_3)_4]^{2+}$	Ferrandi, Endicott & Barker, 1975
$[\text{Rh}(\text{NH}_3)_5\text{N}_3]^{2+}$	$\cdot\text{N}$	$[\text{Rh}(\text{NH}_3)_4\text{NH}]^{3+}$	Ferrandi & Endicott, 1973 Ferrandi, Endicott & Barber, 1975 Reed, Wang & Basolo, 1972 Reed, Gafney & Basolo, 1974
$[\text{Rh}(\text{NH}_3)_5\text{Cl}]^{2+}$	$\text{Cl}\cdot$	$[\text{Rh}(\text{NH}_3)_4]^{2+}$	Kelly, 1971
$[\text{Rh}(\text{NH}_3)_5\text{Br}]^{2+}$	$\text{Br}\cdot$	$[\text{Rh}(\text{NH}_3)_4]^{2+}$	Kelly, 1971
$[\text{Rh}(\text{NH}_3)_5\text{I}]^{2+}$	$\text{I}\cdot$	$[\text{Rh}(\text{NH}_3)_4]^{1+}$	Kelly & Endicott, 1972
$[\text{Ir}(\text{NH}_3)_5\text{N}_3]^{2+}$	$\cdot\text{NH}$	$[\text{Ir}(\text{NH}_3)_5\text{NH}_3]^{3+}$	Gafney, Reed & Basolo, 1973
$[\text{PtCl}_6]^{2-}$	$\text{Cl}\cdot$	$[\text{PtCl}_5]^{2-}$	Wright & Laurence, 1972
$[\text{Fe}(\text{OH}_2)_5\text{Br}]^{2+}$	$\cdot\text{Br}$	$[\text{Fe}(\text{OH})_6]^{2+}$	Thornton & Laurence, 1970 Thornton & Laurence, 1973
$[\text{Fe}(\text{OH}_2)_4\text{ox}]^+$	C_2O_4^-	$[\text{Fe}(\text{H}_2\text{O})_6]^{2+}$	Cooper & DeGraff, 1972
$[\text{Ru}(\text{NH}_3)_5\text{X}]^{2+}$	-	-	Wells & Endicott, 1971

^a $\cdot\text{Y}$ = N-methyleneethylenediaminetriacetate. It is presumed that this radical remains coordinated to the reduced metal centre after the primary photochemical reaction.

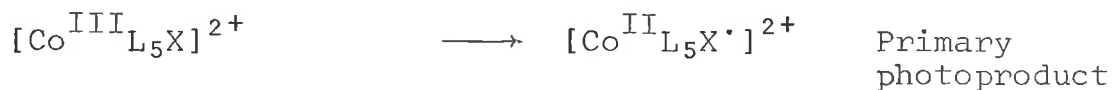
^b For (N_4) , a cyclic tetradentate nitrogen donor ligand; ligands include 5,7,7,12,14,14-hexamethyl-1,4,8,11-tetraazacyclodeca-4,11-diene and amine analogues.

the primary products they present some inherent difficulties owing to the possible formation of reactive radicals involving scavengers (Thomas, 1965; Latimer, 1952; Woodruff & Margerum, 1973; Malone & Endicott, 1972; Lilie, Beck & Henglein, 1971). Secondary thermal reactions of these radicals (e.g. $\text{CH}_3\dot{\text{C}}(\text{OH})\text{CH}_3$

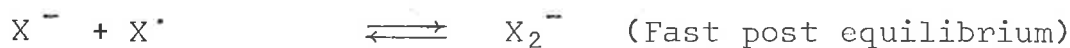
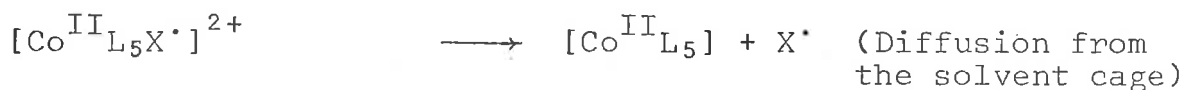
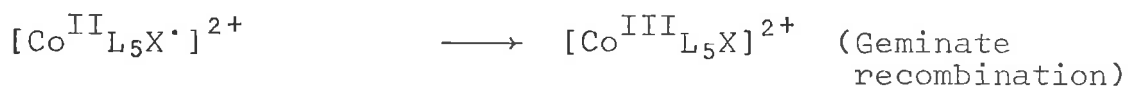


or $\text{CH}_3\dot{\text{C}}\text{HOH}$ etc.) may lead to the deviation from the stoichiometric (1:1 correspondence) and even irreproducible product yields. The actual reaction modes of these radicals are controlled by the thermodynamic feasibilities and mechanistic propensities.

In the much studied cases of photoreduction of Co(III)-acidopentamine complexes, by LMCT excitation, in aqueous halide solution, the formation of X_2^- and $\text{Co}^{2+}(\text{aq})$ can be represented as: primary photoreaction



secondary thermal reactions



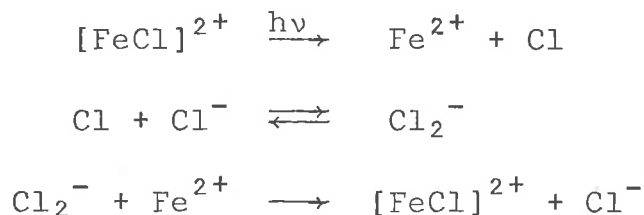
The entity $[\text{Co}^{\text{II}}\text{L}_5]^{2+}$ is labile ($t_{1/2} < 0.1 \mu \text{ sec}$) and high-spin so that reaction between the radical (X_2^-) and metallo-fragment



is impossible, while the oxidation of $\text{Co}^{2+}(\text{aq})$ by X_2^- ion is known to be too inefficient (Thornton & Laurence, 1973).

(a) Radical-Substrate Reactions

Radical-substrate reactions are known to occur where reactive radicals and reasonably stable metallo-fragments are formed



Haim and Taube (1963) demonstrated an efficient iodine atom reduction of $[\text{Co}(\text{NH}_3)_5\text{X}]^{2+}$. Recently (Malone & Endicott, 1972; Balzani & Carassiti, 1970) it has been shown that the reduction is due to I_2^- with a rate constant of $10^5 \text{ M}^{-1} \text{ sec}^{-1}$. Reduction of $\text{Co}(\text{NH}_3)_5\text{X}^{2+}$ by Br_2^- is less efficient due to small overall free energy change (Thornton & Laurence, 1973; Marcus, 1964). Such radical reductions of the substrate have been demonstrated to be very efficient for oxalatoferrates (Cooper & DeGeraff, 1971 & 1972; Patterson & Perone, 1973; Parkar & Hatchard, 1959) and the Iron(III) and Co(III) EDTA complexes (Natarajan & Endicott, 1973 a, b & c).

In the case of polydentate chelate complexes the primary radical may be incorporated into the metallofragment. Photo-reduction of $\text{Co}(\text{EDTA})^-$, in acidic solution, is believed to proceed through the formation of a coordinated ligand radical. Failure to observe the transient species, $(\text{CoL}\cdot)^-$, has been attributed to the rapid intramolecular fragmentation of the primary photoproduct.

(b) Radical-product Reactions

Radical-product reactions are most likely to occur with

relatively stable and substitutionally inert metallo-fragments. This has been the case with pentacyano-cobalt(III), $\text{Co}(\text{CN})_5^{2-}$ (Litelpo & Endicott, 1971; Ferrandi, Endicott & Barber, 1975), and Co(III) complexes with the partially unsaturated tetradentate macrocyclic ligands, $[\text{Co}(\text{N}_4)]^{3+}$, complexes. The geminate recombination reactions of $[\text{Co}(\text{N}_4)]^{2+}$ with X_2^- ($\text{X} = \text{Cl}, \text{Br}, \text{I}$) and $\dot{\text{C}}\text{H}_3$, are known to occur at nearly diffusion controlled rates (Litelpo & Endicott, 1971 and Roche & Endicott, 1972, 1974). Such radical metallofragment reactions have also been observed in the photoreduction of Rh(III) ammine complexes (Ferrandi, Endicott & Barber, 1975; Kelly & Endicott, 1972a and Kelly, 1971) and found to be efficient. The efficiency of the geminate recombination process could be the reason for the overall low photoredox quantum yield in Rh(III) complexes.

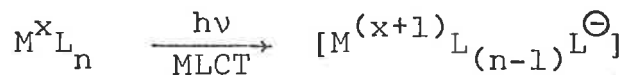
I.2.2 OXIDATION OF METAL CENTRES

In contrast to excitation in the LMCT band where labilization of the coordinated ligands is the usual reactivity for the conversion of M(III) complexes to high spin M(II) series, excitation in MLCT band, accompanying promotion of a d-electron to the lowest lying empty ligand orbital does not normally lead to labilization because the higher oxidation state of transition metals are usually low spin and substitutionally inert. If the photoredox process occurs, oxidation of the metal centre with concurrent ligand reduction would be an expected pathway for MLCT excited state.

(i) Primary Photoreaction

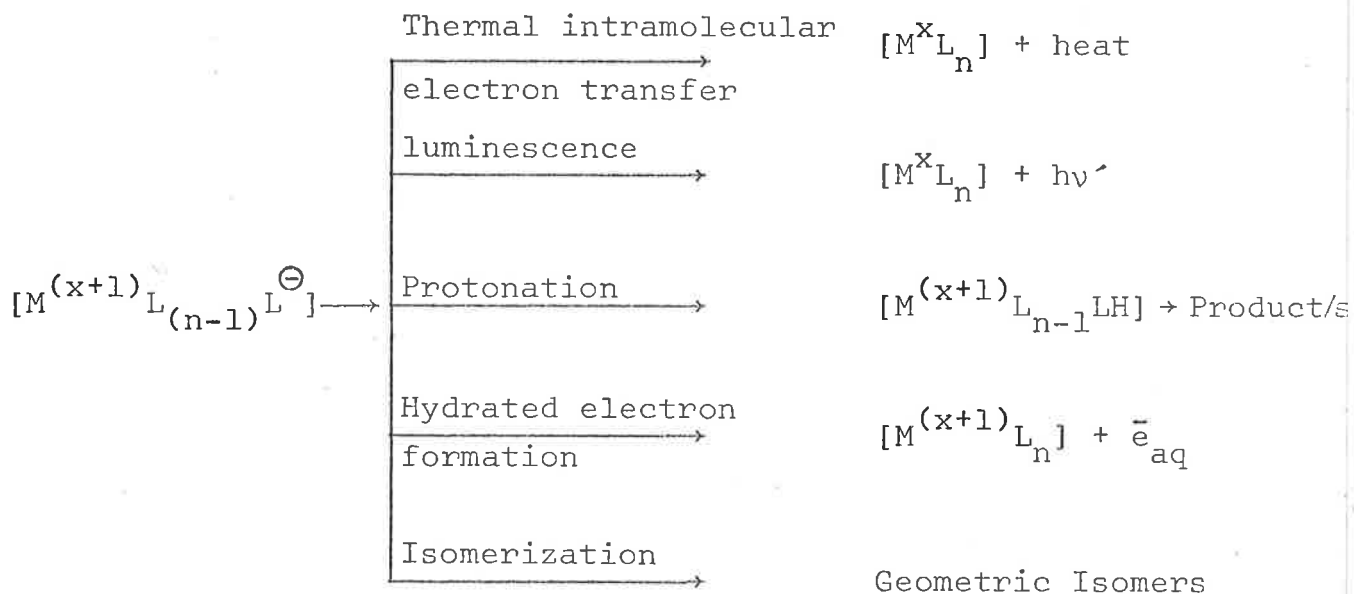
The primary photoproduct under MLCT excitation can be conceptualized as an oxidized metal centre and a radical anion in the

coordination complex.



(ii) Secondary Thermal Reactions

Secondary thermal reactions of primary photoproduct may be summarized as:

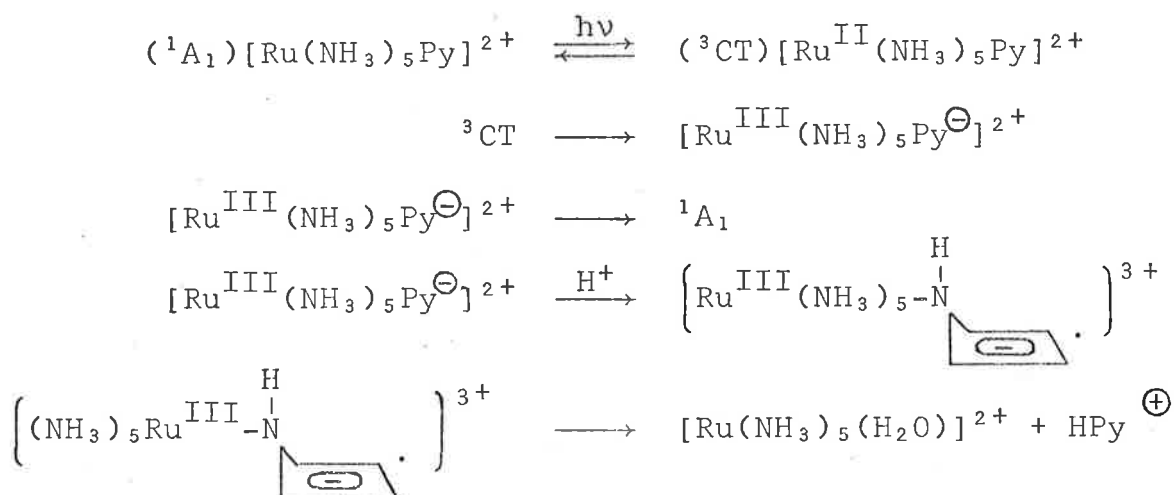


The observed secondary thermal mode is controlled by the nature of the metal centre and the ligands.

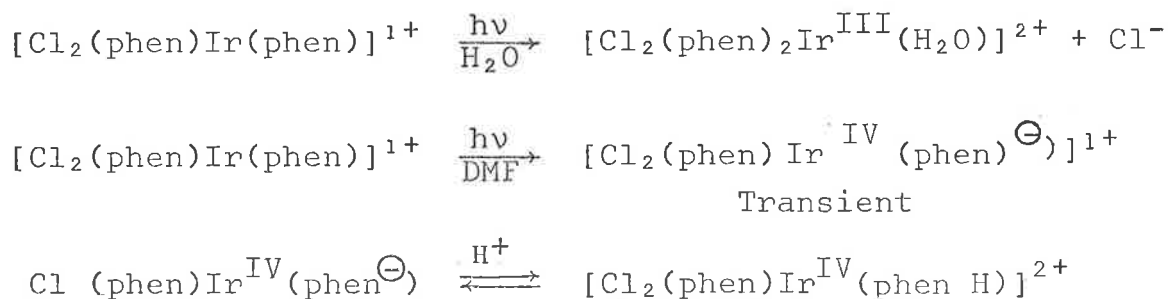
Due to the dominant role of spin-orbit coupling in the heavier metal ions [Ru(II), Ir(III), Os(II) and Rh(III)] luminescence, as a secondary thermal reaction, in the complexes of phen, bipy, terpy and related ligands has been observed (Lyttle & Hercules, 1969; Hoffman, Balzani et al., 1975; DeArmond & Hillis, 1971; Demas & Crosby, 1971; Crosby, Watts & Carsten, 1970; Watts & Crosby, 1972; Carsten & Crosby, 1970).

When Ru(II) complexes of the type $Ru(NH_3)_5L$, where L represents Py, acetonitrile, benzonitrile or dinitrogen, which all have intense MLCT bands (Ford, Rudd, Gaunder & Taube, 1968; Clark & Ford, 1970 and Treitel, Flood, Marsh & Gray, 1969), are irra-

diated in their MLCT bands an extensive ligand aquation occurs (Natarajan & Endicott, 1972; Chaisson et al., 1972; Ford, Chaisson & Stuermer, 1971). On the basis of variation of quantum yield with pH of the solution two independent photoaquation paths have been invoked. The pH dependent path is believed to proceed through the protonation of a coordinated pyridine-anion radical to give the final products. Natarajan & Endicott (1972) in their flash photolysis experiments with $[\text{Ru}(\text{NH}_3)_5\text{Py}]^{2+}$ observed a transient absorbance decaying slowly to the substrate and attributed it to $[\text{Ru}^{\text{III}}(\text{NH}_3)_5\text{Py}^\ominus]^{2+}$



Similar behaviour has also been observed for $[\text{Ir}(\text{phen})_2\text{Cl}_2]^{1+}$ photolysis where release of Cl^- and protonation of the radical anion ligand was found to occur (Hoffman, Balzani et al., 1975) fairly close to the pKa value of the free phen ligand.



Irradiation of $[\text{Ru}^{\text{II}}(\text{bipy})_2(4\text{-Stilbazolc})_2]^{2+}$ and

$[\text{RuCl}(\text{bipy})_2(4\text{-stilbazole})]^{1+}$ in butyronitrile solution in the visible region (405, 436, 546 nm) corresponding to excitation in the MLCT band causes complete conversion of the cis-isomer to the trans-isomer (Zarnegar, Bock & Whitten, 1973). The isomerization processes arising from MLCT excited state are thought to be due to the transfer of an electron from the lowest antibonding orbital of 4-stilbazole ligand. The intersystem crossing from the $\pi_L \rightarrow \pi_L^*$ state may be slow enough to compete with the observed photoreaction and the internal conversion to the ground state.

I.2.3 COMMUNICATION BETWEEN EXCITED STATES

As mentioned earlier, communication between excited states is common to all photoprocesses. Such communications can result in a variety of photochemical processes following the excitation in the charge transfer bands. Communication between excited states can be divided here into communication between different charge transfer excited states, between charge transfer and ligand field and between charge transfer and intra-ligand excited states.

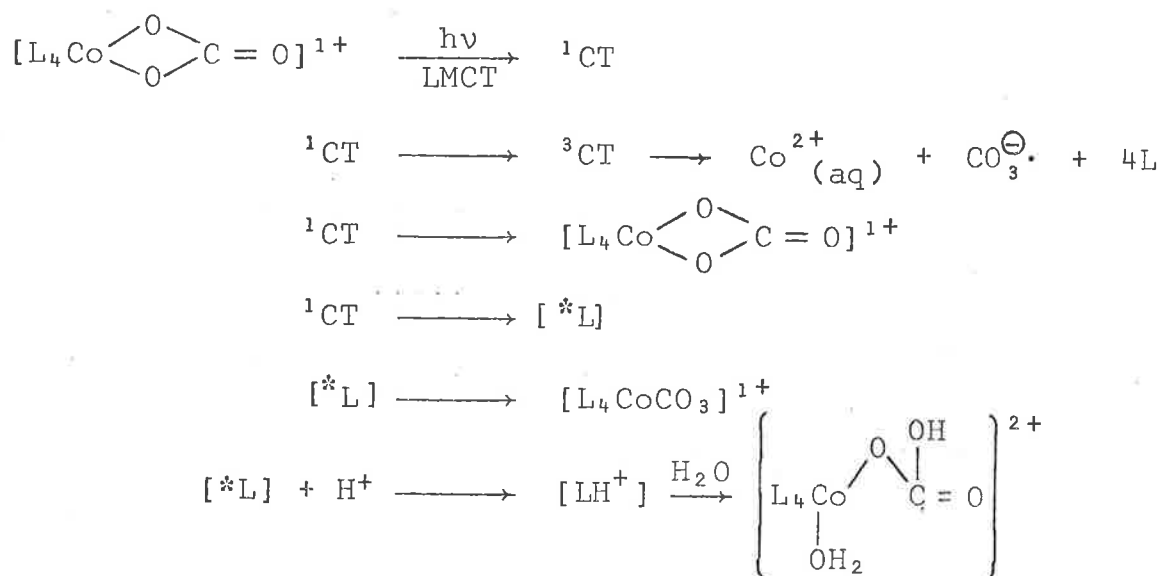
(i) Intersystem Crossing between Charge Transfer States

In the much studied cases of Co(III) complexes, excitation in the LMCT bands leads to a single reaction mode (photoreduction) but $[\text{Co}(\text{CN})_5\text{N}_3]^{3-}$ and $[\text{Co}(\text{CN})_5\text{I}]^{3-}$ are the exceptions. Excitation of $[\text{Co}(\text{CN})_5]^{3-}$ in the low energy LMCT band leads to the formation of $[\text{Co}(\text{CN})_5]^{4-}$ and X \cdot while higher energy excitation results in several processes including CN^- oxidation (Ferrandi & Endicott, 1973; Endicott, Ferrandi & Barber, 1975). Nitrene formation from $[\text{Rh}(\text{NH}_3)_5\text{N}_3]^{2+}$ occurs over a narrow range of excitation energies in the LMCT band (Endicott, Ferrandi & Barber,

1975a) and this has been attributed to the relaxation of higher charge-transfer states without populating the state responsible for nitrene formation which arises from an exceptionally isolated state.

(ii) Communication between Charge Transfer and Intraligand Excited States

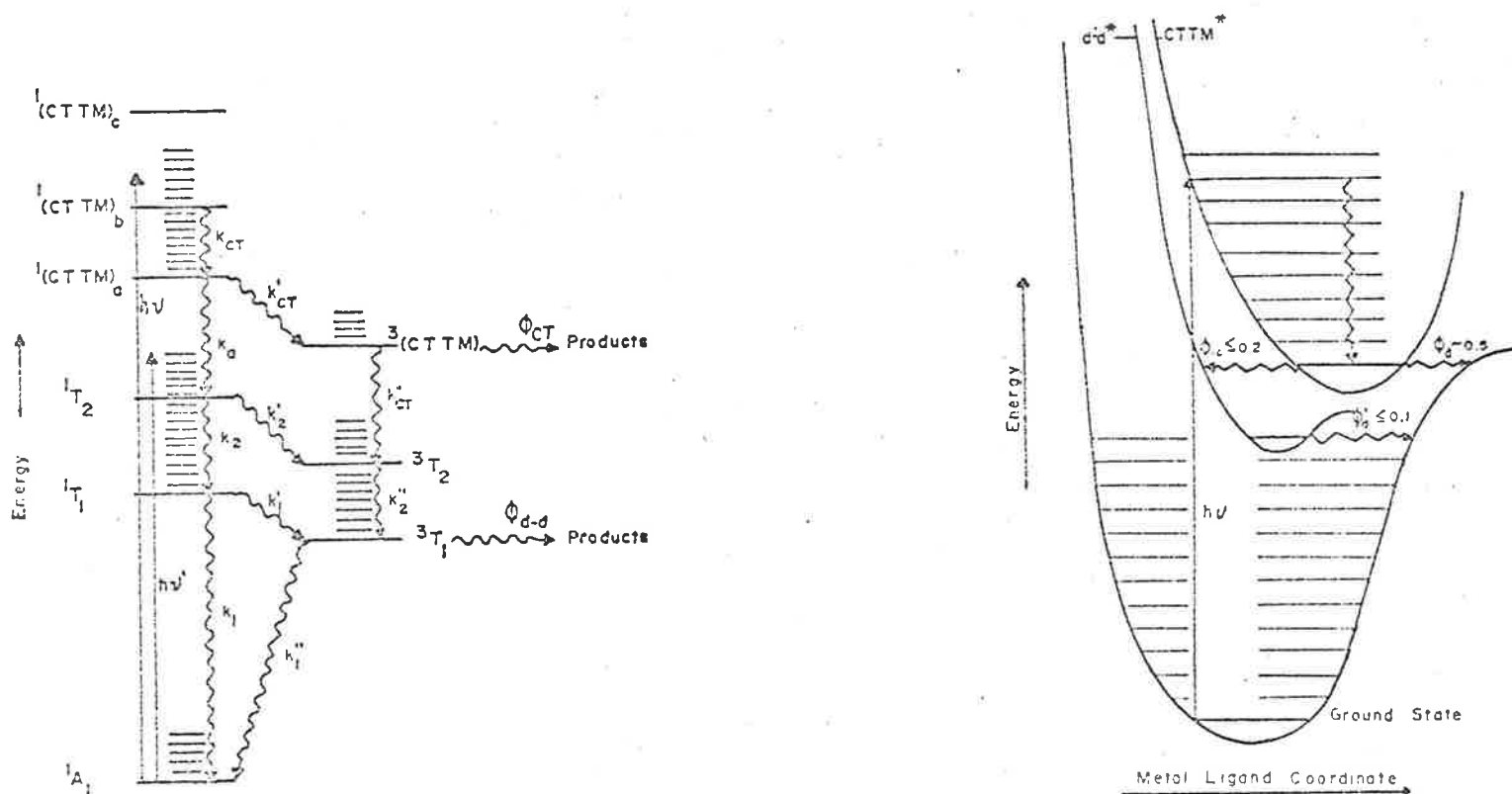
Photoexcitation of the bidentate carbonato Co(III) complexes in the intense LMCT bands has been said (Cope, Chen & Hoffman, 1973) to produce a ^1CT state which decays through intersystem crossing to a ^3CT state and a competitive intraligand excited state ($^*\text{L}$). The ^3CT state is thought to be the precursor to the redox process while protonation of the carbonate ligand in the $^*\text{L}$ excited state is considered to cause aquation.



A very similar mechanism has been proposed for the photochemistry of $[\text{Co}(\text{NH}_3)_5\text{OOCH}]^{2+}$ which is also found to lead to photo-reduction and production of a c-bonded isomer (Campano, Kantrowitz, Hoffman & Weinberg, 1974).

Communication between CT and intraligand excited states may explain the cis-trans isomerization of $[\text{Ru}(2,2'\text{-bipy})(4\text{-stilbazole})_2]^{2+}$ and $\text{Ru}(2,2'\text{-bipy})(4\text{-stilbazole})\text{Cl}]^{1+}$ complexes.

Fig. 6 Hypothetical diagram for the photochemistry of $[\text{Rh}(\text{NH}_3)_5\text{I}]^{2+}$



(a) Hypothetical energy level scheme for a low-spin d^6 complex of O_h symmetry. Solid lines indicate typical initial excitations into CTM or ligand-field (d-d) excited-state manifolds. The triplet CTM state, ${}^3(\text{CTM})$, is intended to be representative. Wavy lines indicate the various, competitive radiationless decay modes of the thermally equilibrated excited states.

(b) Hypothetical potential energy manifolds for an nd^6 complex. For simplicity, all states have been assumed to have the same spin multiplicity. Relative yields are indicated for the various internal conversion processes inferred from the photochemistry of $[\text{Rh}(\text{NH}_3)_5\text{I}]^{2+}$.

Reference: Kelly & Endicott, 1972a.

MLCT excitation gives mainly trans-isomers whereas $\pi\pi^*$ excitation produces predominantly cis-isomers. It has been suggested that $\pi\pi^*$ and MLCT excitation produce a common intermediate, a ligand-radical anion species which transforms to the thermodynamically more stable isomer (Zarnegar, Bock & Whitten, 1973).

The quantum yield for the photoreduction of $[\text{Fe}(\text{phen})_3]^{3+}$ is less than 10^{-4} in the visible region ($\lambda_{\text{max}} = 602 \text{ nm}$) which corresponds to a spin allowed $\pi-t_2$ LMCT transition but rises sharply in the intraligand band (Baxendale & Bridge, 1955; Wehry & Ward, 1971; Malik & Laurence, 1978) [c.f. Chapters 4 & 5].

(iii) Communication between Charge Transfer and Ligand Field Excited States

An inefficient communication between LMCT and LF excited states occurs in $[\text{Rh}(\text{NH}_3)_5\text{I}]^{2+}$ photolysis (Kelly & Endicott, 1972b). Excitation in the LMCT band causes both ammonia aquation ($\phi = 0.2$) and redox ($\phi \approx 0.2$) process while ligand field excitation of this complex results in trans-ammonia aquation with a quantum yield of about 0.9. It is concluded that at least 50% of the time LMCT excited states relax directly to the ground state without populating the lower energy ligand field excited states [Fig.(6)].

Arguments have also been advanced for an inefficient inter-system crossing between LMCT and ligand field excited states for Co(III) complexes (Adamson & Sporer, 1958; Adamson, 1960b; Vogler & Adamson, 1968).

SECTION 3

I.3 CO-ORDINATED LIGAND RADICALS

It is appropriate to include a section on the nature and reactions of co-ordinated ligand radicals because thermal intermolecular and intramolecular reactions of co-ordinated phen and bipy radical ligands have been observed in the present work.

Co-ordination ligand radicals have been proposed as precursors of the reaction products in some intermolecular electron transfer reactions of metal complexes, in particular, when one of the ligand contains a system of conjugated double bonds (Taube & Gould, 1969). The presence of the conjugation resonance stabilizes the radicals and allows the study of the spectral and kinetic behaviour of these species. Co-ordinated ligand radicals have also been postulated or identified in the flash photolysis and pulse radiolysis of metal complexes.

I.3.1 Photolytic Generation of Coordinated Ligand Radicals

There is increasing evidence for the formation of co-ordinated ligand radicals in the photolysis of transition metal complexes (Balzani & Carassiti, 1970; Adamson & Fleischauer, 1975). The participation such radicals (e.g. $[\text{Co}^{\text{III}}(\text{EDTA}^{\ominus})]$, $[\text{Ru}^{\text{III}}(\text{NH}_3)_5\text{Py}^{\ominus}]$ $[\text{Cl}_2(\text{phen})\text{Ir}^{\text{IV}}(\text{phen}^{\ominus})]^{1+}$ in the thermal reactions following the excitation in the CT bands of the metal complexes has already been discussed (c.f. oxidation-reduction photochemistry).

The LMCT photochemistry of Iron(III), Cobalt(III) and Uranium(VI) - oxalato-complexes have been studied using stationary state photolysis, flash photolysis and electrochemical detection techniques. The transient spectra show the formation of a ligand-

Table (2)

TRANSIENTS IN THE PHOTOLYSIS OF OXALATO COMPLEXES

e = electrochemical detection; s = spectral data; i = inferred from flash data

Complex Irradiated	Transient Species	Reference
[Fe(ox) ₃] ³⁻	ox ⁻ (s,e)	1,2,3,4,5
	CO ₂ ⁻ (s,e)	1,2,5
	Unidentified metastable state (s)	4
	(ox) ₂ Fe ^{III} $\left. \begin{array}{l} \diagup \text{O}-\overset{\cdot}{\text{C}}=\text{O} \\ \diagdown \text{O}-\overset{\cdot}{\text{C}}=\text{O} \end{array} \right\}^{3-}$ (e)	1,5
	[(ox) ₂ Fe ^{II} (CO ₂)] ³⁻ (s)	1,5
[Fe(ox)] ¹⁺	$\dot{\cdot}$ (s)	6
	[Fe(ox)] (s)	6
[Co(ox) ₃] ³⁻	ox ⁻ (s)	6
	[(ox) ₂ Co ^{II} (ox ⁻)] ³⁻ (s)	7,8
	[(ox) ₂ Co ^{II} (ox ⁻)] ⁴⁻ (s)	7,8
	\bar{e}_{aq} (i)	7
	[(ox) ₂ Co ^{II} (ox ⁻)(H ₂ O)] ³⁻ (s)	7
	[(ox) ₃ Co ^{II} (ox ⁻)] ⁵⁻ (s)	8
	[(NH ₃) ₅ Co ^{II} -CO $\dot{\cdot}$ O] ¹⁺ (s)	8
[Co(NH ₃) ₅ ox] ¹⁺		
[Co(NH ₃) ₄ ox] ¹⁺	[(NH ₃) ₄ Co ^{II} -CO $\dot{\cdot}$ O] ¹⁺ (s)	9,10
[Co(en) ₂ ox] ¹⁺	[(en) ₂ Co-COO] ¹⁺ (s)	9,10
[Cr(ox) ₃] ³⁻	none (s)	5
[UO ₂ ²⁺ -ox ²⁻]	transient species not identified (s,e)	3,4

Table (2) (Cont...)

References

- (1) Jamieson & Perone, J.Phys.Chem., 76, 830 (1972).
- (2) Cooper & DeGraffe, J.Phys.Chem., 75, 2897 (1971).
- (3) Paszyc & Norvish, Roczn.Chem., 37, 1305 (1963).
- (4) Parker & Hatchard, J.Phys.Chem., 63, 22 (1959).
- (5) Patterson & Perone, J.Phys.Chem., 77, 2437 (1973).
- (6) Cooper & DeGraffe, J.Phys.Chem., 76, 2618 (1972).
- (7) Cordeman et al., J.Phys.Chem., 78, 1361 (1974).
- (8) Rowan, Hoffman & Milburn, J.Amer.Chem.Soc., 96, 6060 (1974).
- (9) Endicott et al., J.Amer.Chem.Soc., 94, 6655 (1972).
- (10) Vaudo, Kantrowitz & Hoffman, J.Amer.Chem.Soc., 93, 6698 (1971).

radical complex concurrently with the reduction of the metal centre. The transient species found in the photolysed solutions of oxalato complexes are summarized in Table (II).

Recently the study of the reactions of Ni(II) and Cu(II)-tetra-aza macrocyclic complexes with OH radicals, generated by flash photolysis, has suggested that the oxidation of the complexes by OH proceeds by H-atom abstraction (Kevin D. Whitburn, 1976) from the ligand. The spectra of the transient species were found to be more characteristic of M(II) ligand-radical complex than that of M(III) macrocyclic complexes.

I.3.2 Formation of Co-ordinated Ligand Radicals by Pulse Radiolysis

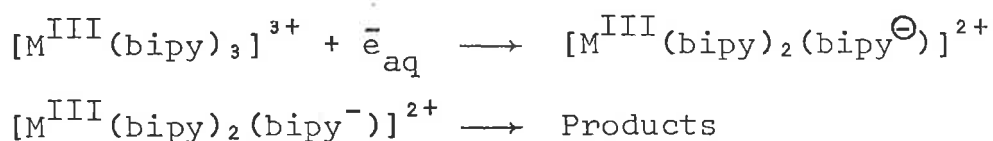
Pulse radiolytically generated species such as \bar{e}_{aq} , OH, CO_2^- and H can react with metal complexes to produce coordinated ligand radicals.

(i) \bar{e}_{aq} Adducts

The hydrated electron with a redox potential of $\sim 2.7V$ (Baxendale, 1964) reacts with many metal complexes at diffusion controlled rates (characterised by small activation energy of $15 \pm 2 \text{ kJ mol}^{-1}$, Anbar & Hart, 1970) with the ligands acting as bridges for electron transfer to the metal centre.

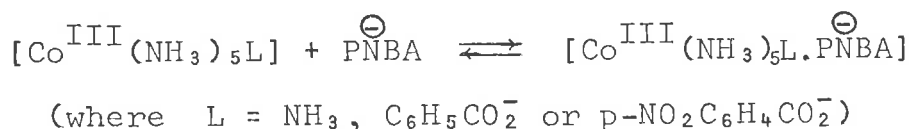
The reduction of $Co(bipy)_3^{3+}$, $Ru(bipy)_3^{3+}$ and $Co(terpy)_3^{3+}$ by \bar{e}_{aq} has been extensively studied (Waltz & Pearson, 1969; Baxendale & Fiti, 1972; Hoffman & Simic 1973). The identity of the weakly absorbing transient ($\epsilon \approx 370 \text{ M}^{-1} \text{ cm}^{-1}$ at $\lambda > 400 \text{ nm}$) has been a matter of conjecture. Hoffman and Simic (1973) detected an intensely absorbing transient species ($\lambda_{max} = 300 \text{ nm}$, $\epsilon_{max} = 4.2 \times 10^4 \text{ M}^{-1} \text{ cm}^{-1}$) following the reduction of $Co(bipy)_3^{3+}$ and $Cr(bipy)_3^{3+}$ with \bar{e}_{aq} . From the similarity of the spectra and chemical beha-

viour with those of the electron adducts of the free ligand ($\lambda_{\text{max}} = 365 \text{ nm}$, $\epsilon_{\text{max}} = 3 \times 10^4 \text{ M}^{-1} \text{ cm}^{-1}$). These authors concluded that the transient absorbance, decaying by a slow unimolecular first order kinetic path, was due to the formation of a coordinated ligand-radical anion. The slower transient decay was due to the intramolecular electron transfer to the metal centre.



Coordinated ligand-radical anions, as transients, have also been observed in the reactions of \bar{e}_{aq} , CO_2^- and $(\text{CH}_3)_2\dot{\text{C}}\text{-OH}$ with p-nitrobenzoatopentamine cobalt(III) complexes (Hoffman & Simic, 1970; Hoffman & Simic, 1972; Simic & Hoffman, 1972). The transient absorbance, prior to $\text{Co}^{2+}(\text{aq})$ formation, was almost identical with the electron adduct of the p-nitrobenzoate free ligand. The electron attachment site is principally the nitro-group (Asmus, Wigger & Henglein, 1966) as no transient coordinated ligand-radical absorbance could be detected for the unsubstituted benzoate ligand or $[\text{Co}(\text{NH}_3)_5\text{BA}]^{2+}$. The results were discussed in terms of steric effects, the overlap of the aromatic π -orbitals with the metal d-orbitals and protonation of the coordinated anion radicals.

In an attempt to assess the significance of the carboxylate group in the intramolecular electron transfer process, Cohen and Meyerstein (1975) have made pulse radiolysis study of a series of reactions of the free ligand radical with Co(III) complexes. The reactions proceed through formation of an outer-sphere complex

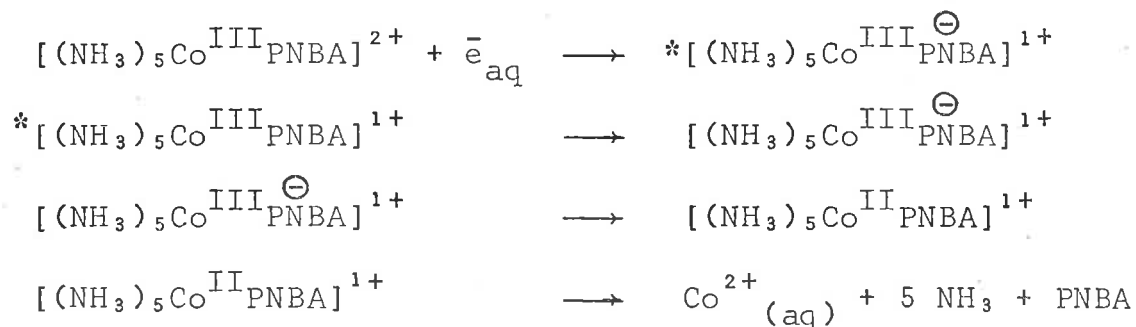


followed by a slow intramolecular electron transfer. They attributed the slowness of the intramolecular step



to the poor 'electron permeability' of the carboxyl group. Recently (Laurence, 1978[†]) it has been found that the electronic effects of the substituents on the aromatic ring and the degree of overlap between the electron attachment site and the π -orbitals are the controlling factors in the rate of the intramolecular electron transfer.

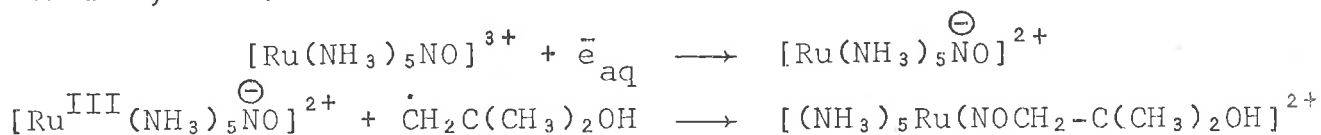
Simic, Hoffman and Brenziak (1977) have invoked an electronically excited species in the initial formation of the Co(III)-ligand-radical and related the rate of intramolecular electron transfer from the radical anion to the electron density at or adjacent to the group bound to the Co(III) centre.



Thornton and Laurence (1978a) have measured the activation parameters for the intramolecular electron transfer process of pentaminebenzoato cobalt(III) complexes.

Hydrogen atom adducts of $[(\text{NH}_3)_5\text{Co}^{\text{III}}\text{NBA}]^{2+}$ are reported (Cohen & Meyerstein, 1971) to be similar to the electron adducts of the same complex.

Co-ordinated ligand radicals have also been observed in the pulse radiolysis of $[\text{Fe}(\text{CN})_5\text{NO}]^{2+}$ (Buxton, Dainton & Kalecinski, 1969; Voorst & Hemmerick, 1966; Bloom, Raynor & Symons, 1971) and $[\text{Ru}(\text{NH}_3)_5\text{NO}]^{3+}$ (Armor & Hoffman, 1975; Armor, Furman & Hoffman, 1975). The coordinated radical



[†] Unpublished results

$[\text{Ru}^{\text{III}}(\text{NH}_3)_5\text{NO}]^{\ominus}$ was found to react with $\dot{\text{C}}\text{H}_2\text{C}(\text{CH}_3)_2\text{OH}$ to give stable product.

(ii) Reactions of Hydroxyl Radical with Metal Complexes

The OH radical is a powerful one electron oxidizing agent, in both acid and



alkaline solution, which may react with metal complexes by (1) addition or adduct formation, (2) hydrogen atom abstraction, (3) displacement and (4) electron transfer to OH.

(a) Hydroxyl Radical Adducts

Hydroxyl radical adducts have been observed in the reactions of OH with $[\text{Co}(\text{NH}_3)_5\text{Py}]^{3+}$ (Hoffman & Kimmel, 1975), $[(\text{NH}_3)_5\text{CoO}_2\text{C}_6\text{H}_5]^{2+}$ (Cohen & Meyerstein, 1971), $[\text{Ru}(\text{bipy})_3]^{3+}$ (Creutz & Sutin, 1975) and $[\text{Fe}(\text{phen})_3]^{2+}$ (Pagsberg & Floryan, 1976). The spectra and kinetic behaviour of the adducts $[\text{Ru}(\text{bipy})_2(\text{bipyOH})]^{2+}$ and $[\text{Fe}(\text{phen})_2(\text{phenOH})]^{2+}$ were found to be similar to those of the free ligand radicals. It was also noted (Creutz & Sutin, 1975) that the spectra and chemical behaviour of a transient absorbance, attributed to $[\text{M}(\text{bipy})_2(\text{bipyOH})]^{2+}$ (M = Fe(II), Os(II), Ru(II) and Cr(III)) with $\lambda_{\text{max}} = 750 - 800 \text{ nm}$ and $\epsilon_{\text{max}} = 0.5 - 2.1 \times 10^3 \text{ M}^{-1} \text{ cm}^{-1}$ were almost independent of the nature of the metal ion in question. Similar results were obtained for $[(\text{NH}_3)_5\text{Co}^{\text{III}}(\text{PyOH})]^{3+}$ and $[(\text{NH}_3)_2\text{Co}^{\text{III}}(\text{O}_2\text{C}_6\text{H}_5\text{OH})]^{2+}$ (Hoffman & Kimmel, 1975; Cohen & Meyerstein, 1971).

(b) Hydrogen Atom Abstraction

Hydrogen atom abstraction from the ligands in the complexes leads to the formation of a carbon radical ($\dot{\text{C}}$); such radicals have been postulated in the γ or X-radiolysis of EDTA complexes of Co(III) (Matsurra et al., 1967), Cu(II) (Bhattacharya & Kundu,

1973), in the reactions of OH radicals with Ni^{II}(EDTA) (Lati & Meyerstein, 1975; Lati, Koresh & Meyerstein, 1975) and en-complexes of Cu(II), Ni(II), Pd(II) and Pt(II) (Anbar, Munoz & Rona, 1963). The reduction of the metal centre caused by OH radical reaction with Co(III), Cu(II) and Fe(III) complexes is believed to proceed via hydrogen atom abstraction followed by intramolecular electron transfer between the ligand radical and the metal. Metal centre reduction can also occur by radical-substrate reaction.

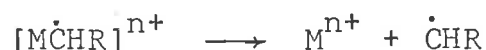
(i) hydrogen atom abstraction



(ii) intramolecular electron transfer



(iii) fragmentation



(iv) radical-substrate reaction



or



(v) disproportionation



Disproportionation seems the most likely path in the decay of the transient where intramolecular electron transfer is energetically unfavourable.

Direct electron transfer by an outer-sphere path occurs in the reactions of OH radicals with Ni^{II}(EDTA) complex where evidence for a relatively long-lived Ni(III) species has been obtained (Lati & Meyerstein, 1971).

Rate constants of co-ordinated ligand-radical for the intramolecular electron transfer reactions are summarized in Table 3.

Table (3)

RATES OF INTRAMOLECULAR ELECTRON TRANSFER

System	Transient	Rate Constant/s ⁻¹	Reference
[Co(bipy) ₃] ³⁺	[Co ^{III} (bipy) ₂ (bipy [⊖])] ²⁺	3.5	1
[Cr(bipy) ₃] ³⁺	[Cr ^{III} (bipy) ₂ (bipy [⊖])] ²⁺	3.5	1
[Co(NH ₃) ₅ (PNBA)] ²⁺	[Co ^{III} (NH ₃) ₅ (PNBA [⊖])] ¹⁺	(2.3 - 2.6) × 10 ³	2,6
[Co(NH ₃) ₅ (MNBA)] ²⁺	[Co ^{III} (NH ₃) ₅ (MNBA [⊖])] ¹⁺	(1.5 - 2.0) × 10 ²	3,6
[Co(NH ₃) ₅ (ONBA)] ²⁺	[Co ^{III} (NH ₃) ₅ (ONBA [⊖])] ¹⁺	(3.0 - 4.0) × 10 ⁵	3,6
	[Co ^{III} (NH ₃) ₅ (ONBAH)] ²⁺	9.5 × 10 ³	3
[Co(NH ₃) ₅ Py] ³⁺	[Co ^{III} (NH ₃) ₅ (PyOH)] ³⁺	6.0	4
[Co(NH ₃) ₅ BA] ²⁺	[Co ^{III} (NH ₃) ₅ (BAOH)] ³⁺	< 10 ⁻²	5
	[Co ^{III} (NH ₃) ₅ (BAH)] ²⁺	< 10 ⁻²	5
[Co(NH ₃) ₅ (NPA)] ²⁺	[Co ^{III} (NH ₃) ₅ (NPA [⊖])] ¹⁺	7 × 10 ^{7*}	6
[Co(NH ₃) ₅ (NCA)] ²⁺	[Co ^{III} (NH ₃) ₅ (NCA [⊖])] ¹⁺	1.4 × 10 ³	6
[Fe(bipy) ₃] ³⁺	[Fe ^{II} (bipy) ₂ (bipy [⊕])] ³⁺	1.12 × 10 ^{2†}	present work
[Fe(phen) ₃] ³⁺	[Fe ^{II} (phen) ₂ (phen [⊕])] ³⁺	0.54 × 10 ^{2†}	present work
[Fe(Me ₄ -phen) ₃] ³⁺	[Fe ^{II} (Me-phen) ₂ (Me ₄ -phen [⊕])] ³⁺	0.53 × 10 ^{2†}	present work
[Ru(bipy) ₃] ³⁺	[Ru ^{II} (bipy) ₂ (bipy [⊕])]	0.29 × 10 ^{2†}	present work

Continued.....

* 2nd order rate constant
† in 10 M HClO₄, $k_1 = k_{\text{obs}}/[\text{Acid}]$

REFERENCES

- (1) Hoffman and Simic, J.C.S., Chem. Comm., 640 (1973).
- (2) Simic and Hoffman, J.A.C.S., 94, 1757 (1972).
- (3) Hoffman and Simic, Proc. 14th Internat. Conf. Coord. Chem., Toronto, 501 (1972).
- (4) Hoffman and Kimmel, J.C.S., Chem. Comm., 549 (1975).
- (5) Cohen and Meyerstein, J.A.C.S., 93, 4179 (1971).
- (6) Thornton and Laurence, 9th AINSE Conf., Lucas Heights, Australia, 25 (1978).

SECTION 4I.4 THERMAL OXIDATION-REDUCTION REACTIONS

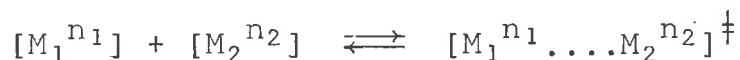
The study of oxidation-reduction photochemistry necessitates an understanding of thermal oxidation-reduction reactions. Such reactions of transition metal complexes are conveniently classified into inner- and outer-sphere mechanisms. This classification is based on the interactions of the reactants in the transition state prior to electron transfer.

Inner-sphere oxidation-reduction reactions, which cannot be faster than ligand substitution reactions, are unlikely to occur within the lifetime of an excited state ($< 10 \mu \text{ sec}$ for transition metal complexes) and have been omitted from this section. No example of an inner-sphere reaction has yet been reported for a photo-induced oxidation-reduction process.

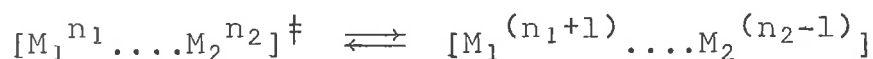
I.4.1 Outer-Sphere Mechanism

An outer-sphere oxidation-reduction process can be visualized as a close approach, without interpenetration, of discrete but flexible reactant spheres in the transition state prior to electron transfer followed by diffusion of the oxidized and reduced species from the solvent cage after reaction.

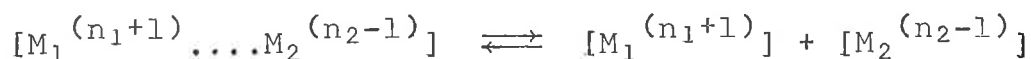
Encounter



Electron transfer



Diffusion from the solvent cage



In an outer-sphere electron transfer process the primary

co-ordination spheres of the reactants and the products retain the ligands originally present.[†] The changes in the oxidation states of the metal centres necessitate some reorganisation of the co-ordination spheres in going from reactants to products. No rearrangement is possible during the electron transfer as this takes place effectively instantaneously (Frank-Condon principle). There are two extreme cases of this reorganization:

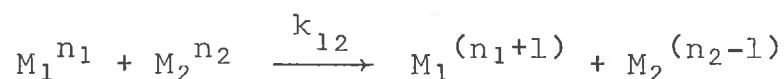
- (1) reorganization prior to electron transfer and
- (2) reorganization subsequent to electron transfer

In any real reaction the mechanism lies between these two extremes.

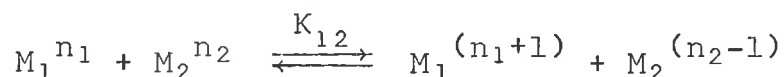
1.4.2 Marcus Theory

The electron transfer is the result of some interaction of the electronic wavefunctions of the reactants. The lack of interpenetration in the outer-sphere transition state suggests that the interaction is small. Marcus (1956, 1963 and 1968) used this assumption to derive a theoretical treatment of outer-sphere electron transfer reaction rates.

The Marcus Theory predicts a simple relationship between the rate constant k_{12}



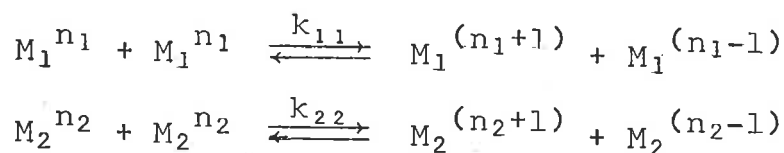
for an electron transfer reaction, K_{12} the equilibrium constant for the reaction



and k_{11} and k_{22} the self exchange rate constants for the reductant

[†] This observation requires the products to be substitutionally inert at the time scale of observation.

and oxidant couples (Marcus, 1959, 1960, 1963).



The relationship is given below

$$k_{12} = (k_{11}k_{22}K_{12}f_{12})^{1/2}$$

or

$$\log f_{12} = \frac{(\log K_{12})^2}{4 \log \left(\frac{k_{11}k_{22}}{Z^2} \right)} \quad (1)$$

where Z is a collision frequency, generally taken as $10^{11} \text{ M}^{-1} \text{ s}^{-1}$. The theory is an adiabatic theory of electron transfer and proceeds from the assumption that within the activated complex for electron transfer the probability of electron transfer is unity. Some additional assumptions in deriving equation (1) are that the work terms for self-exchange and cross-reactions are the same, that the reacting species may be treated as spherical structureless reactants and the motion of the inner-co-ordination shells is harmonic. For $f_{12} = 1$, equation (1) may be simplified to give equation (2).

$$k_{12} \sim (k_{11}k_{22}K_{12})^{1/2} \quad (2)$$

Thus if a series of related reactions with $f_{12} \sim 1$ is studied as a function of K_{12} (i.e. ΔG_{12}°), a plot of $\log k_{12}$ vs. $\log K_{12}$ should be linear with a slope of 0.5 and an intercept of $0.5 \log k_{11}k_{22}$. The rate constants for a number of cross-reactions between transition metal complexes calculated by equation (2) have been found to agree well with the experimental values (Reynold & Lumry, 1966; Basolo & Pearson, 1967; Chou, Creutz & Sutin, 1977). Recently the Marcus relationship has been applied to reactions between metal complexes and organic redox systems (Montasti,

Pelizzetti & Baocchi, 1977) and electron transfer properties of metalloproteins (Creutz & Sutin, 1974).

Current approaches to the theories of electron transfer reactions will be discussed in the chapter entitled "Reactions of ${}^3\text{CuRu}(\text{bipy})_3^{2+}$ with Copper Complexes".

SECTION 5

I.5 REDOX REACTIONS OF POLYPYRIDINE TRANSITION METAL COMPLEXES

The present study involves the photo-induced oxidation-reduction reactions of polypyridine and related complexes. These systems undergo thermal oxidation-reduction processes after the primary photostep. It is therefore relevant to introduce the known redox reactions of polypyridine transition metal complexes in solution.

These redox reactions can be conveniently grouped into outer-sphere and intra-molecular oxidation-reduction reactions.

I.5.1 Outer-Sphere Reactions

Outer-sphere reactions of polypyridine metal complexes have been the subject of several comprehensive reviews (Taube, 1959; Halpern, 1961; Sutin, 1968; Meyer, 1978). No attempt will be made to present a comprehensive review of these outer-sphere reactions here but the behaviour of these complexes towards various types of reductants and oxidants will be summarized.

Electron exchange reactions (Larsen & Wahl, 1965; Dietrich & Wahl, 1963; Meyer & Taube, 1968; Stranks, 1960; Baker, Basolo & Newman, 1959; Zwickel & Taube, 1960; Marcus & Sutin, 1975; Stalnaker, Solenberger & Wahl, 1977) which have no overall free energy change (ΔG^0) and with small barriers to electron transfer have been studied.

The reduction of polypyridine metal complexes by metal aquo ions (Sutin & Gordon, 1961; Ford-Smith & Sutin, 1961; Gordon, William & Sutin, 1961; Davies, Green & Sykes, 1972) have been studied over a wide range of ΔG^0 and the comparison between the experimental and theoretical rate constants (calculated from

Marcus relationship) have been found satisfactory. However, there is evidence that the fit of the experimental data to the Marcus relationship worsens as ΔG° becomes more negative (Chou, Creutz & Sutin, 1977; Hoselton, Lin et al., 1978) and deviates from the relationship (equation (2)) [c.f. Marcus inverted region, page 227]. The reduction rates by Tl(III) (Nord, 1976) were found to be controlled by the type of ligands and not by the overall free energy change (ΔG°).

The oxidations by ClO_3^- , ClO_2 and ClO^- (Shakhashiri & Gordon, 1969), $\text{P}_2\text{O}_8^{2-}$ (Green, Edwards & Jones, 1966) and $\text{S}_2\text{O}_8^{2-}$ (Burgess & Prince, 1966) were found to proceed by outer sphere mechanism via dissociation of the ligand/s. The oxidation of $\text{Fe}(\text{phen})_3^{2+}$ by Cl_2 occurs by the normal outersphere mechanism (Shakhashiri & Gordon, 1968).

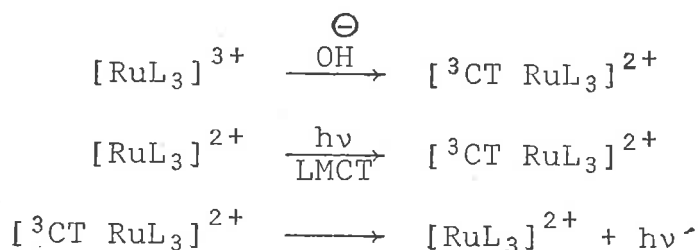
I.5.2 Intramolecular Oxidation-Reduction Reactions

In the reduction of polypyridine metal complexes by strong bases (OH^- , CH_3O^- , EtO^-) "special interactions" of these bases with the ligand have been invoked (Gillard, 1975). Similarly, attack by H_2O on co-ordinated polypyridine ligand-radicals in the photo-reduction of $[\text{ML}_3]^{3+}$ complexes (L = phen, bipy or related ligands) has been postulated (Malik & Laurence, 1978). With a view to bring together the known general reactivity of N-heterocyclic molecules towards strong bases and our knowledge of their metal complexes, the intramolecular oxidation-reduction reactions of polypyridine complexes of transition metals are discussed.

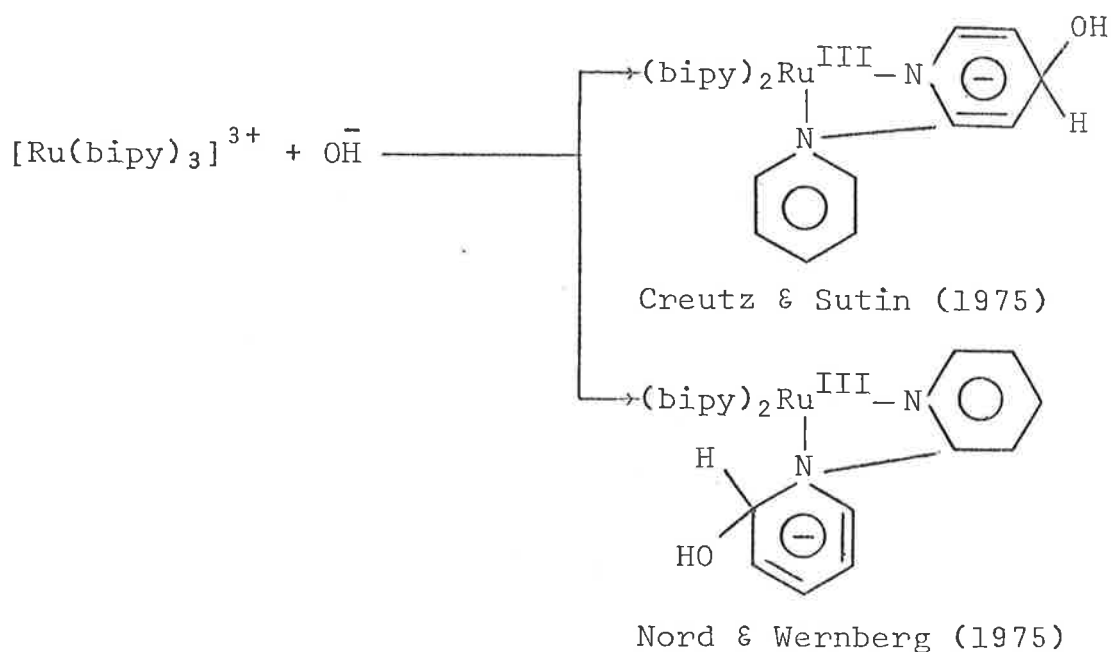
Blau (1898) observed that $[\text{Fe}(\text{bipy})_3]^{3+}$ and $[\text{Os}(\text{bipy})_3]^{3+}$ were instantly reduced to their corresponding M(II) complexes by

hydroxide ion. Dwyer et al., (1952, 1954) found that complexes of the type $[\text{ML}_3]^{3+}$, where L = Fe, Ru or Os and L = phen or bipy, were instantly reduced by OH^- and reduction could be reversed by immediate acidification. On long standing H_2O_2 and O_3 were produced and finally slow degradation of the ligand occurred (Baxendale et al., 1955). To explain this behaviour "special interactions" of OH^- with the complexed ligands were invoked.

Lyttle and Hercules (1966) observed chemiluminescence when acidic solutions of Ru(III) complexes of bipy, DMP, TMP and related ligands were made alkaline with NaOH. The emission spectra were found to be identical with those observed from the corresponding Ru(II) complexes by photoexcitation. It was concluded that a common electronic excited state, $[\text{}^3\text{CT RuL}_3]^{2+}$, was formed in both cases.



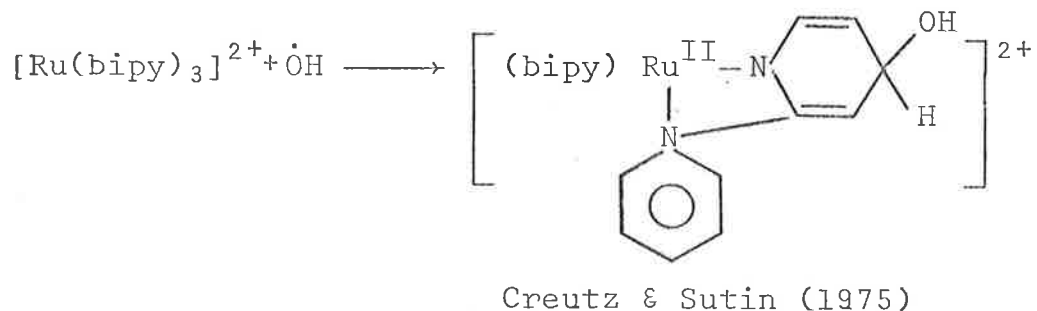
Recently Nord and Wernberg (1972, 1975) and Creutz and Sutin (1975) have re-examined the reduction of Fe(III), Os(III) and Ru(III) complexes of phen and bipy by hydroxide ion. The reduction products were found to be $[\text{ML}_3]^{2+}$ and O_2 and reduction is thought to proceed by the nucleophilic addition of OH^- to the complexed ligand. Nord and Wernberg (1975) have proposed an attack on the 2-(9)-position while according to Creutz and Sutin (1975) addition takes place at the 4-(7)- position to produce a co-ordinated ligand-radical.



The formation and decay of the co-ordinated ligand-radical was found to obey first order kinetics and was independent of the Ru(III) complex concentration. The radical had a broad absorption band ($\lambda_{\text{max}} = 800 \text{ nm}$) and absorbed strongly in the ultraviolet region. Very similar results were obtained for $[\text{Fe}(\text{bipy})_3]^{3+}$. The reduction obeyed the following rate law

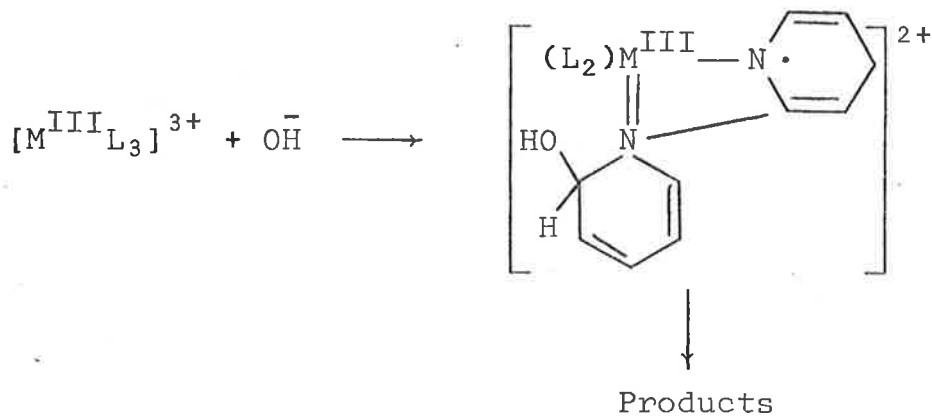
$$k_{(\text{obs})} = k_a[\text{OH}^-] + k_b[\text{OH}^-]^2$$

and the O_2 production was strongly pH-dependent. It was also noted that the spectrum to be similar to that of the species produced by the reaction $[\text{Ru}(\text{bipy})_3]^{2+}$ with $\dot{\text{O}}\text{H}$ studied by pulse radiolysis.

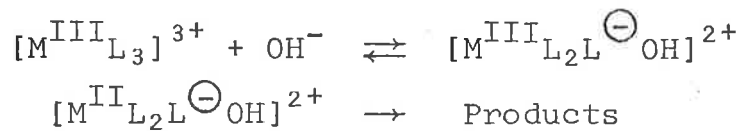


According to Nord and Wernberg (1975) the rate of reduction by OH^- follows the order $\text{Ru} > \text{Fe} > \text{Os}$. From the measurements of

the activation parameters this trend was attributed to the decrease in the enthalpy of the product formation. To explain these results presence of metal-nitrogen double bonding in the reactant and intermediate was invoked.



The mechanism of reduction of $M(III)$ complexes of N-heterocyclic chelates is believed to proceed through a complexed-ligand- $\bar{O}H$ adduct formation and may be written as



EXPERIMENTALII.1 MATERIALSII.1.1 [Fe(phen)₃]³⁺

Tris(1,10-phenanthroline)Iron(III) was prepared by published procedures (Gordon & Sutin, 1961). The method consisted of oxidizing [Fe(phen)₃]²⁺ (prepared from AnalaR ferrous sulphate and 1,10-phenanthroline) with PbO₂ in 0.5 M H₂SO₄. The excess PbO₂ and PbSO₄ was filtered off and Iron(III) perchlorate salt precipitated by the addition of dilute PbSO₄. The precipitate was collected on a sintered glass funnel, washed with dilute HClO₄, recrystallized from diluted HClO₄ and dried under vacuum in the dark.

II.1.2 [Fe(bipy)₃]³⁺

The preparation of tris(2,2'-bipyridine)Iron(III) was followed by Nyholm and Burstall (1952) recipe. 2.0 gm of AnalaR ferrous sulphate heptahydrate (B.D.H.) was dissolved in 150 ml of distilled water and treated with 3.0 gm of bipy. The solution was heated to 50°C till completely dark red solution was obtained. The solution was concentrated to 100 ml, cooled to room temperature and treated with ~ 3 gm of PbO₂ and 10 ml of 10 M H₂SO₄. The solution was stirred with a glass rod till deep blue solution was obtained. The solution was filtered through a sintered glass funnel and the Iron(III) perchlorate salt precipitated by adding dilute HClO₄. The precipitate was washed

with dilute HClO_4 , recrystallized from 1M HClO_4 and dried under vacuum in the dark.

II.1.3 $[\text{Fe}(\text{Me}_4\text{-phen})_3]^{3+}$

Tris(3,4,7,8-tetramethyl-1,10-phenanthroline)Iron(II) salt was prepared by dissolving the appropriate amount of the ligand in absolute alcohol to which an equivalent amount of ferrous sulphate, dissolved in water, was added. The Fe(II) salt was precipitated by the addition of 10% aqueous NaClO_4 solution. The ppt. was collected on a sintered glass funnel, thoroughly washed with distilled water and dried in the air.

The corresponding Fe(III) perchlorate was prepared by suspending the dry Fe(III) salt in 0.5 M HClO_4 and bubbling Cl_2 gas through for ~ two hours while the system was being constantly stirred by a magnetic stirrer to ensure the complete oxidation of the Fe(II) complex. The Fe(III) complex was dried under vacuum in the dark.

II.1.4 $[\text{Co}(\text{phen})_3]^{3+}$

The preparation of $[\text{Co}(\text{phen})_3]^{3+}$ was based on previously described method (Lee, Gorton, Newman & Hunt Jr., 1966), 5.1 gm of phen was dissolved in 500 ml of water by warming to 80°C . To this was added 1.2 gm of $\text{CoCl}_2 \cdot 6\text{H}_2\text{O}$ (in 50 ml of water) and the temperature maintained at 80°C . The solution was cooled at room temperature in air and Cl_2 gas passed for an hour. The solution was chilled in ice to 8°C and Cl_2 passed for a further 10 minutes. It was allowed to warm up to the room temperature and again Cl_2 bubbled through for another 10 minutes after dilution with 100 ml of H_2O . The solution was warmed to 60°C and Cl_2 passed through

for further 5 minutes. The Co(III) perchlorate salt was precipitated by the addition of 20 ml of 70% HClO₄. The addition of HClO₄ not only precipitates the ClO₄-salt but also oxidizes any Co(II) still present in the solution. The ppt. was firstly recrystallized from ethanol and secondly from diluted HClO₄ and dried under vacuum in the dark.

II.1.5 [Co(phen)₂]²⁺

Tris(phen)Co(II) monohydrate was prepared according to the known procedure (Pfeffer & Welderman, 1950). 1.48 gm CoCl₂·6H₂O was dissolved in 80 ml of H₂O to which was added 2.4 gm of phen. H₂O. Then was added 40 ml of methanol and the solution warmed to 68°C. On chilling the solution in ice ochre coloured crystals of Co(phen)₃(ClO₄)₂·H₂O separated which were dried under vacuum.

II.1.6 [Ru(bipy)₃]²⁺

This complex as its chloride salt (Ru(bipy)₃Cl₂) had already been prepared in the laboratory by David Schultz (1975).

II.1.7 [Cu(II) diene]²⁺

The 5,5,7,12,12,14-hexamethyl-1,4,8,11-tetraaza-cyclotetradeca-4,11-diene Copper(II) was prepared by the method of Sadisvian and Endicott (1966) by K. Whitburn (1975).

II.1.8 [Cu(en)₂]²⁺

Cu(en)₂(ClO₄)₂ was prepared (Matheson, 1967) by adding a solution of Cu(ClO₄)₂ in CH₃OH to a slight excess of en. The resulting crystals were filtered, washed, and then recrystallized

twice from hot water containing a trace of en. The product was washed with AR acetone and dried to a constant weight over silica gel in a vacuum dessicator.

II.1.9 [Cu(H₂EDTA)]²⁻

Cupric-EDTA complex was prepared in situ by mixing aqueous solutions of sodium salt of EDTA (one equivalent) with cupric chloride (one equivalent) and finally diluting it to the desired strength.

II.1.10 [Cu(Me₆-tren)(ClO₄)]¹⁺

[Cu(Me₆-tren)(ClO₄)]¹⁺ was prepared according to the published procedures (Ciampolini & Nardi, 1965) by M.M. Hadi.

II.1.11 Copper(II) N-hetrocyclic Diimine Complexes

Copper(II) N-hetrocyclic diimine complexes of the type [CuL₂₋₃]²⁺ (L = phen, bipy, 5-cl-phen, 5-NO₂-phen) were prepared by a modified method described by Faye (1966). The method consisted of mixing CuCl₂ hydrate (in minimum quantity of H₂O) with two or three equivalents of the appropriate ligand (in AR Acetone). The mixture was left for an hour and filtered. The Cu(II) complex was dried by air suction, washed with petroleum ether and finally recrystallized from acetone.

II.1.12 Copper(I) Complexes

All the Copper(I) complexes were prepared in situ by reducing the corresponding Cu(II) complex solution in H₂O either with hydroxylaminehydrochloride or with Na₂SO₃ solution. The pH of the solution was adjusted to 10 with 0.05 M NaOH solution.

The reduction was carried out under anaerobic conditions to avoid any complication arising from the oxidation of the Copper(I) complexes by oxygen.

II.1.13 Other Reagents

Reagent grade HClO_4 (Fluka), H_2SO_4 (B.D.H.), ferrous sulphate (E. Merck or B.D.H.) phen or bipy (Fluka or B.D.H.) were used without any further purification. All other reagents used were of the purest grade available and used without further refining.

II.2 PREPARATION AND STANDARDIZATION OF SOLUTIONS

The glassware was cleaned in Decon-90 solution. Solutions were made up with double distilled water which had been deionized prior to distillation.

The stock solutions of $[\text{Ru}(\text{bipy})_3]^{2+}$, Cu(II)-diene, $[\text{Cu}(\text{Me}_6\text{-tren})]^{2+}$, Cu(II)-phen, bipy or related ligands, $[\text{Cu}(\text{en})_2]^{2+}$, $[\text{Co}(\text{phen})_3]^{3+}$ were prepared by dissolving the solid in the distilled water and diluted to the desired concentration when required.

Stock solutions (1 mM) of $[\text{Fe}(\text{phen})_3]^{3+}$, $[\text{Fe}(\text{Me-phen})_3]^{3+}$ and $[\text{Fe}(\text{bipy})_3]^{3+}$ were prepared by dissolving the solid perchlorate salts in AR HClO_4 (Fluka) or AR H_2SO_4 (B.D.H.). These stock solutions were stored in amber coloured glass stoppered bottles kept under refrigeration. Fresh solutions were prepared by dilution just before the photolysis experiments.

1 mM $\text{Ru}(\text{bipy})_3\text{Cl}_2$ (in H_2O) was oxidized with Cl_2 gas to give apple green $[\text{Ru}(\text{bipy})_3]^{3+}$. The excess Cl_2 was removed by bubbling water-saturated N_2 through the solution and diluted to the desired concentration with distilled water. No stock solution was stored under refrigeration and only fresh solutions were used.

The acidities were adjusted with HClO_4 or H_2SO_4 which were standardized by acid-alkali volumetric titrations owing to the relatively high acidities used in the present work.

The freshly prepared solutions of the complexes were characterized and standardized by UV-visible absorption spectra. Any solution showing deviation from the literature absorption spectrum was rejected. The absorption spectra of the complexes are summarized in table (4).

Table (4)

MOLAR ABSORBANCES USED IN THE STANDARDIZATION OF SOLUTIONS

Complex	Wavelength nm	Molar Absorbance $M^{-1} \text{ cm}^{-1}$	Reference
$[\text{Fe}(\text{phen})_3]^{3+}$	600	870	Ford-Smith & Sutin, 1961
$[\text{Fe}(\text{phen})_3]^{2+}$	510	11,100	Ford-Smith & Sutin, 1961
$[\text{Fe}(\text{Me}_4\text{-phen})_3]^{3+}$	670	1,590	Ford-Smith & Sutin, 1961
$[\text{Fe}(\text{Me}_4\text{-phen})_3]^{2+}$	500	13,800	Ford-Smith & Sutin, 1961
$[\text{Fe}(\text{bipy})_3]^{3+}$	617	320	Ford-Smith & Sutin, 1961
$[\text{Fe}(\text{bipy})_3]^{2+}$	522	8,650	Ford-Smith & Sutin, 1961
$[\text{Co}(\text{phen})_3]^{3+}$	275	79,500	Maki, 1969
$[\text{Cu}(\text{phen})]^{2+}$	670	55	Present work ^b
$[\text{Cu}(\text{phen})]^{1+}$	436	3,500	Present work ^b
$[\text{Cu}(\text{phen})_2]^{2+}$	752	75	Jørgenson, 1955
$[\text{Cu}(\text{phen})_2]^{1+}$	435	7,000	Pflaum & Brandt, 1955b
$[\text{Cu}(5\text{-Cl-phen})_2]^{2+}$	695	35	Pflaum & Brandt, 1955a
$[\text{Cu}(5\text{-Cl-phen})_2]^{1+}$	436	5,000	Present work ^b

Table (4) (Cont...)

$[\text{Cu}(5\text{-NO}_2\text{-phen})_2]^{2+}$	700	40	Present work ^b
$[\text{Cu}(5\text{-NO}_2\text{-phen})_2]^{1+}$	436	6,800	Present work ^b
$[\text{Cu}(\text{dmp})]^{2+}$	740	100	Sundarajan & Wehry, 1972
$[\text{Cu}(\text{dmp})]^{1+}$	450	6,160	Sundarajan & Wehry, 1972
$[\text{Cu}(\text{bipy})_2]^{2+}$	720	90	Jørgensen, 1955
$[\text{Cu}(\text{bipy})_2]^{1+}$	435	4,500	Pflaum & Brandt, 1955b
$[\text{Cu}(\text{bipy})_3]^{2+}$	680	68	Jørgensen, 1955
$[\text{Cu}(\text{bipy})_3]^{1+}$	436	5,000	Present work ^a
$[\text{Cu}(\text{H}_2\text{EDTA})]^{2-}$	745	80	Vogel, 1961
$[\text{Cu}(\text{H}_2\text{EDTA})]^{3-}$	436	950	Present work ^b
$[\text{Cu}(\text{II})\text{diene}]^{2+}$	507	110	Curtis, 1971
$[\text{Cu}(\text{I})\text{diene}]^{1+}$	412	2,000	Palmer, Papaconstantinou & Endicott, 1965
$[\text{Cu}(\text{II})(\text{Me}_6\text{-tren})\text{H}_2\text{O}]^{2+}$	169	725	Lincoln & Hubbard, 1974
$[\text{Cu}(\text{I})(\text{Me}_6\text{-tren})(\text{H}_2\text{O})]^{1+}$	436	8,500	Present work ^a
$[\text{Ru}(\text{bipy})_3]^{3+}$	676	409	Bryant & Fergusson, 1971
$[\text{Ru}(\text{bipy})_3]^{2+}$	453	13,700	Bryant, Fergusson & Powell, 1971
$[\text{Cu}(\text{phen})_3]^{2+}$	680	60	Jørgensen, 1955

Table (4) (Cont...)

$[\text{Cu}(\text{phen})_3]^{1+}$	436	3,700	Present work ^b
$[\text{Cu}(\text{en})_2]^{2+}$	550	65	Pflaum & Brandt, 1955a
$[\text{Cu}(\text{en})_2]^{1+}$	436	6,150	Present work ^a

^a ± 15 - 20%, due to the unstability of the Cu(I) complexes

^b ± 10%

II.3 APPARATUS

A conventional microsecond time-scale flash photolysis was used for absorption and a nanosecond pulsed nitrogen laser (Lambda Physik) used for emission measurements in the present work. A computer-based system for acquisition and treatment of data was employed for both the photolysis apparatuses (Thornton & Laurence, 1978b). The arrangement was such that it allowed the acquisition of data from the two experimental sources and use of commercial interface subsystems simultaneously.

II.3.1 Flash Photolysis Apparatus

The flash photolysis apparatus used was a modification of the previously reported apparatus (Thornton & Laurence, 1973; Falcinella, Felgate & Laurence, 1974; Whitburn, 1976) and the block diagram of the apparatus is shown in Fig. (7).

II.3.1.1 Excitation Source

A Xe-O₂ filled silica flash lamp was used as a source of excitation. The lamp contained 5:1 Xenon-oxygen mixture at a pressure of 2-3 cm of Hg. The flash of light was produced by the discharge of 4.25 μ F high energy storage capacitor across the tungsten electrodes. The discharge was initiated by a mercury ignitron triggered by an SCR circuit controlled by TTL pulses. The maximum energy input by the flash lamp was 1 kJ at 20 kV; in most experiments 0.5 kJ flashes were used. The light flash had a typical width (at the half height) of 10 μ sec with an overall duration of 30 μ sec. The observation of a reaction, during the discharge of the lamp, is difficult because transient species are being formed and the stray light from the flash can

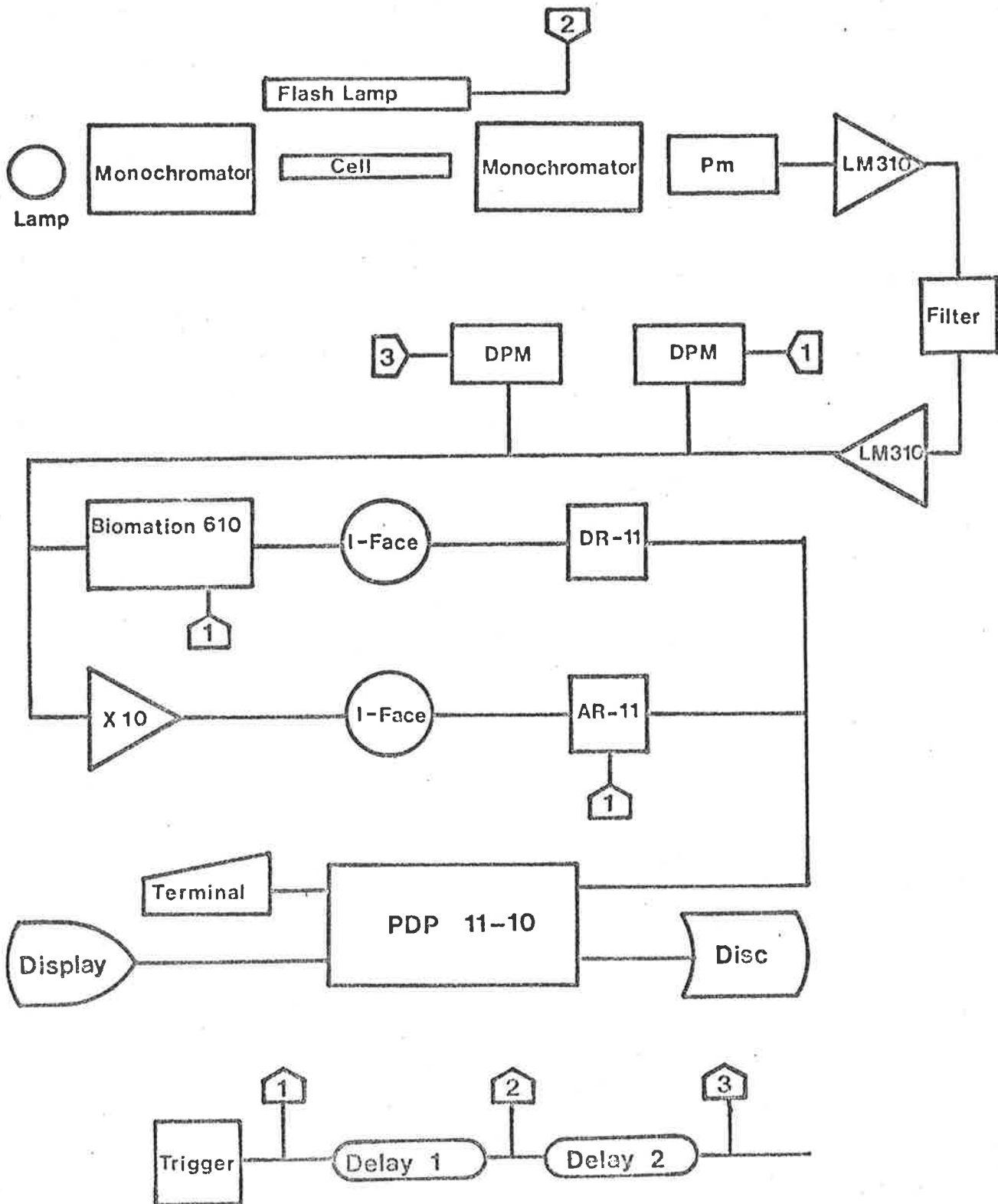


Fig. 7 Block Diagram of Flash Photolysis Apparatus
Reference: Thornton & Laurence, 1978b.

interfere with the monitoring light signal. The emission spectrum of the flash is a continuum over a wide range of the UV-visible spectrum, and is most intense around the 300 nm region. The lamp and the sample cells were enclosed in a polished aluminium reflector.

II.3.1.2 Detection System

Fast spectrophotometric method was used to monitor the absorbance changes in the irradiated solutions at the desired wavelength of observation.

The output of a 75 W Xe or Xe-Hg lamp (Illumination Industries, Inc.) was focussed on to a Bausch and Lomb high intensity monochromator and emergent beam of the desired wavelength passed through the solution cell and then through the inlet collimator of a second monochromator. This collimator contained a series of discs having small concentric holes. These discs greatly reduced the stray light pick-up from the flash into the collecting monochromator. Two sets of monochromators, one each for the UV and visible regions, were used. The stray light pick up could be relatively reduced by working at the wavelength corresponding to the most intense Hg-lines of the monitoring lamp.

The output of the second monochromator was lead into an EMI 9558QB photomultiplier with 100 k Ohm load followed by an integrated circuit voltage follower (LM310) buffer stages. For a background unity absorbance, an absorbance change of 0.02 could be followed with a signal to noise ratio of 10:1 and a response time of 10 μ sec.

The photomultiplier output voltage (the changing transmitted light intensity due to the changing transient concentrations

in the cell) was recorded in one of the several ways.

II.3.1.3 Data Acquisition

Acquisition of data in flashed photolysis experiments utilized either a digital transient recorder (Biomation 610B, Biomation Inc.) or an analog real-time subsystem of the computer (DEC AR-11) together with the three digital voltmeters for recording the initial transmittance, transmittance at a certain delayed time (after the flash) and the integrated flash intensity.

II.3.1.3.1 The Digital Voltmeters

The initial transmittance signal was recorded by a digital voltmeter circuit which sampled and held the value of the signal (normally 10-50 μ sec ahead of the pulse which fired the flash lamp). Another identical meter recorded the signal at an adjustable delay after firing the flash lamp. This facility enabled a method for measuring the transient spectra without using the full data acquisition system. The constancy of the flash output was monitored by the DVM output of a photocell at the end of the perspex 'light-pipe' collecting adjacent to the flash lamp.

II.3.1.3.2 Biomation 610B

The Biomation 610B recorder was used for the transients with a lifetime of less than 1 m sec. The sample intervals ranged from 100 n sec to 50 m sec and the time resolution contained 250 words of information. The usefully employed time interval was from 1 μ sec (time interval $<$ 1 μ sec cannot be used as the system was limited by the flash duration) to 50 m sec.

The 610B converts all the analog input voltage signals to an accuracy of six binary bits which allowed a precision of 0.1% in the final rate constant and an accuracy of 0.04% transmittance change per least significant bit (for an initial 100% transmittance signal of 2 V at the maximum sensitivity). The stored digitized data in the Biomation memory was displayed on an oscilloscope.

The interface between the 610B and the PDP-11/10 computer was through a DEC-11C universal digital input-output board including a 1 k Hz generator. The DR-11C and 610B were connected through a simple interface to make them compatible with each other. If the data generated were satisfactory, and the computer terminal message indicated that the interface is ready to receive the data, they were transmitted to the PDP-11/10 computer on a push-button command for subsequent (kinetic or spectral) analysis. It took 0.25 sec for the transfer of 250 words of information.

II.3.1.3.3 AR-11

To achieve a greater sensitivity in the data storage and for recording transients with lifetimes longer than 1 m sec an analog real-time subsystem, incorporated in a DEC AR-11 subsystem board, was used. This 10 bit converter had a single-ended input with a minimum sample interval of 50 μ sec. The AR-11 module was capable of data storage by setting the time per sample (TPS) and the amplitude specifications. A differential amplifier having fixed gains of one, three and ten was interposed between the photomultiplier and the AR-11 input. An accuracy of 0.025% transmittance change (for an initial 100% transmittance of 2 V at the maximum sensitivity) could be achieved with AR-11. The pro-

programmable clock in the subsystem could be set to cover sample intervals of 50 μ sec to 2 sec. This facility allowed to follow slow reactions ($t_{1/2} \sim 1$ min.). As the data were stored directly in the memory of the computer no data transfer was necessary.

II.3.2 LASER PHOTOLYSIS APPARATUS

Laser photolysis apparatus was used for measuring the lifetime of the emissive excited state of $[\text{Ru}(\text{bipy})_3]^{2+}$ and the block diagram for the laser photolysis arrangement is shown in Fig. (3).

II.3.2.1 Excitation Source

N_2 -laser (Lambda Physik M 100A) was used as a source of excitation and the lifetime of the excited state monitored at the desired wavelength. The N_2 -laser emits an intense pulse at 337.1 nm with a width of ca. 2.5 n sec and consists of three parts: the laser head, the power supply and control unit and the vacuum pump.

The laser head consists of 50 cm long transverse discharge cavity integrated into a special flat-plate transmission of low impedance and equipped with a mirror for amplification of the laser emission.

The power supply and the control unit allowed any pulse repetition frequency between 1-100 Hz. The vacuum pump model VP15 allowed a stream of N_2 gas between pressures of 20-100 Torr to be set up within the laser cavity.

The output power of the laser is strongly dependent on the repetition frequency and the N_2 flow rate. In most of the experiments 50 Hz pulses at a N_2 pressure of 30-40 Torr were employed. The various specifications of the N_2 -laser beam are summarized on the next page.

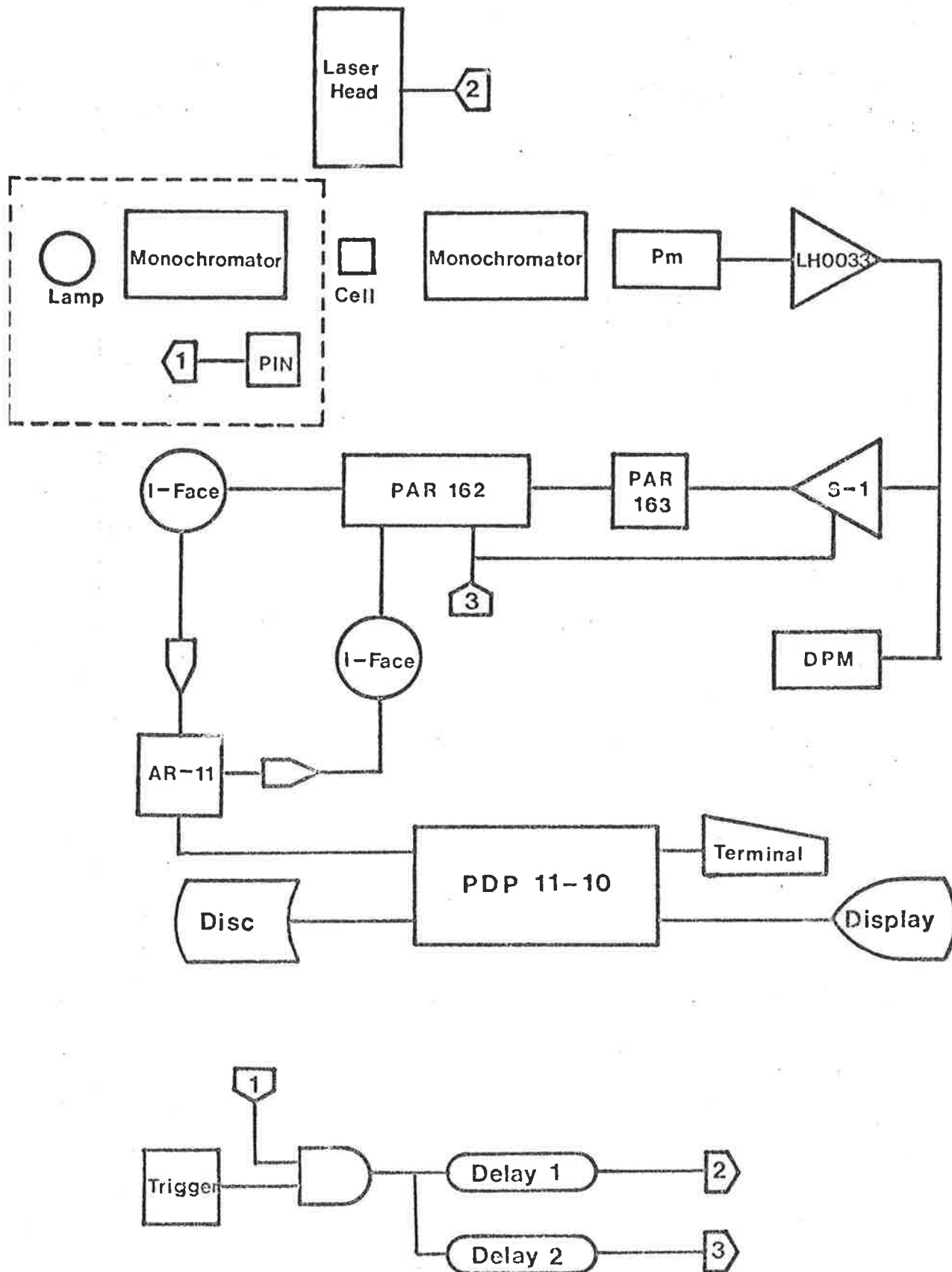


Fig. 8 Block diagram for laser data acquisition. For luminescence measurements, the lamp, monochromator and PIN photodiode sector trigger (inside the dashed lines) are omitted.
Reference: Thornton & Laurence, 1978b

Wavelength	337.1 nm
Peak output power ^c	1 MW
Pulse rise time	2 n sec
Pulse half-width ^b	2.5 n sec
Repetition rate ^a	50 Hz
Pulse energy ^c	2.5 mJ
Beam dimensions	7 mm × 15 mm

The train of pulses, after passing through a focussing lens, was impinged on the sample cell containing the luminescent material.

II.3.2.2 Detection System

The emitted light was monitored perpendicular to the laser beam at 610 nm (for $[\text{Ru}(\text{bipy})_3]^{2+}$) using a Bausch and Lomb high intensity grating monochromator. To reduce the scattered light (from the laser beam) entering the monochromator, a perspex piece was interposed between the cell and the monochromator. The temperature of the cell was maintained by a black metallic thermostatted jacket.

The detection of the signal, coming out of the monochromator, utilized an R 212 UH photomultiplier (Hamamatsu, run at high anode currents of 1-5 A) followed by an integrated-circuit voltage follower (LH 0033) with a 50 Ohm output impedance.

^a At high repetition rate the peak output power is lower

^b Slightly pressure dependent

^c Frequency dependent

II.3.2.3 Data Acquisition

The power of each pulse was sufficiently reproducible to enable the sampling technique to be employed. The signal from the detector was sampled by a sampling head (Tektronix S-1) with a sample gate of width of 300 psec driven by a gated integrator (Princeton Applied Research Type 163) and a boxcar averager (Princeton Applied Research Type 162).

Time scanning of the sampling aperture across the emission decay form was externally controlled by 10-bit digital-to-analog converter, which was a part of the DEC AR-11 subsystem.

The laser pulse was delayed 800 n sec ($\pm 10\%$) with respect to an internal synchronous pulse. This synchronous pulse was also used to trigger the box car averager, after it had been delayed by an appropriate amount before sampling. The lead-in was chosen to be $\approx 10\%$. The total time range scanned was adjusted to ensure that the system reached its initial value.

The transient kinetics were sufficiently defined by a maximum of 250 samples and therefore the delay range was step-scanned. The output of the type 162 integrator representing the sampled signal was digitized by the AR-11 subsystem converter and input to the computer for kinetic analysis. The number of scan steps for the full scan range was entered at the computer terminal while required voltage steps for the scan were set by the program.

II.3.3 Data Processing

(i) Computer System

The DEC PDP-11/10 computer (16k Core memory) and the dual DEC RX-01 floppy disc drive were supported by a fast papertape

reader (Facit) and a teletype printer for a hard copy output. The main terminal, with a limited graphics capability (235 x 512 points resolution), a DEC VT55 was used as the visual display unit (VDU). Data acquisition was controlled by simple assembly language routines accessed by FORTRAN program (KDATAH) as library routines.

(ii) Data Treatment

The digitized voltage output data collected by the biomation or AR-11 peripheral systems were directly amenable to kinetic analysis when transferred to the computer memory. The program KDATAH firstly displayed the raw data on the interfaced terminal (VDU VT55). Since each of the 250 digitized data points was numbered in the memory, the data was accessible to editing routines, including deletion of excessively noisy points, smoothing over noisy sections or actual replacement of the data points as needed.

A signal averaging routine was used to improve signal-to-noise ratios (for noisy traces). This routine allowed two modes of averaging: either a number of samples for each delay value or by repeatedly scanning the total delay range. The choice of mode and the relevant parameters were entered at the control terminal (VT55).

Points on the traces, showing raw data, representing the initial and final absorbance values for the kinetic analysis were chosen and so was the range of points to be covered by the kinetic analysis. The kinetic parameters were entered at the terminal to allow to proceed with the kinetic treatment of the data (1st or 2nd order). The computer subsequently displays $\ln(\Delta A)$ vs time for the first order reaction and $k_2/\epsilon l$ for the

2nd order reaction together with the least-square line of the best fit. For luminescence experiments the display was \ln (integrated intensity) vs time. The display (for absorption or emission experiments) also included the value of the rate constant, and its standard deviation, percentage of the reaction covered, correlation coefficient and the intercept. Data from an experiment can be stored as a file on a floppy disc. The file format included label, comments as well as the information needed to treat the stored data as if it were on line data. Data stored on the disc could be read out for any information or analysis if required subsequently.

The running program, KDATAH, occupied \approx 12 K words of the memory and was fully re-entrant for any set of data. Total clearing of the processed data from the memory allowed new data to be entered.

II.4 EXPERIMENTAL METHODS

This section describes the various experimental techniques used during the course of study.

II.4.1 Flash Photolysis

Flash solutions were contained in a 10 cm × 2 cm quartz cylindrical cell for product analysis. For kinetic runs or spectral measurements thinner, 10 cm × 6 mm, cells were used. In these thinner cells almost homogeneous light absorption could be achieved resulting in higher transient concentration being observable through the middle of the cell, and negligible diffusion effects.

The thinner cell was in the form of a 'flow cell' with an inlet and outlet. The solutions were contained in a 100 ml Quickfit flask equipped with a N₂ inlet to push the solution into the cell, the inlet of the cell being connected through a plastic tubing to one of the openings of the two-way key in the flask's neck. The outlet was connected to another plastic tubing which dropped the out-going solution into a measuring cylinder. As will be shown later on, the photochemical runs for M(III)-polypyridyl species were not affected by oxygen. However, this facility allowed the use of deaerated solutions conveniently whenever necessary. The back diffusion of air through the cell's outlet was quite insignificant. The experiments were carried out at room temperature.

II.4.2 Laser Photolysis

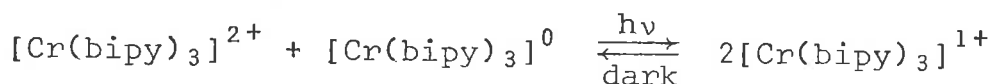
In laser photolysis experiments for measuring the emission lifetime, fluorescence high purity silica cells (1 cm) were used. The cell containing the luminescent material and the quencher was housed in a thermostatted compartment. C.I.G. high purity dry nitrogen or dry argon was used to purge air. For 10-15 minutes a steady stream of the gas was bubbled through and this replacement continued even during the photolysis runs. The temperature control of the thermostat was $\pm 0.2^{\circ}\text{C}$.

LITERATURE SURVEY

There is an increasing interest in the photochemistry of transition metal complexes of polypyridine and related ligands (Balzani & Carassiti, 1970; Adamson & Fleischauer, 1975; Balzani, Laurence et al., 1975) due to the promising properties these complexes possess as possible agents in the photochemically catalysed reduction of water. The survey of the literature presented here includes those systems where permanent or transient photochemical changes have been observed but excludes a discussion of bimolecular electron transfer reactions of the excited states which are discussed in the last chapter. Reports on the luminescence studies (excitation and emission spectra) have also been omitted as such measurements have not been made in the present work. In this survey the metal ions have been arranged in the order of their occurrence in the periodic table.

III.1 CHROMIUM COMPLEXES

$[\text{Cr}(\text{bipy})_3]^{2+}$, which is a low spin and substitutionally inert complex (Basolo & Pearson, 1967), was found to react with $[\text{Cr}(\text{bipy})_3]^0$ under the influence of light to produce $[\text{Cr}(\text{bipy})_3]^{1+}$ (Geiger & Class, 1961) and the reaction could be completely reversed in the dark. Broomhead & Grumley (1968a) reported the photo-

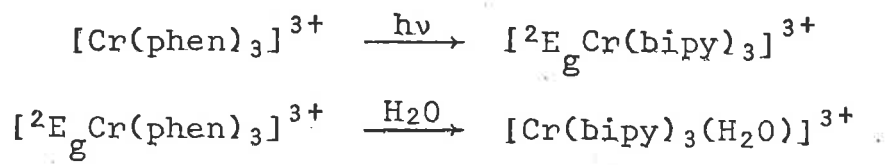


sensitivity of $[\text{Cr}(\text{bipy})_2\text{Cl}_2]^{1+}$. Kirk, Moss and Valentine (1971)

observed the photo solvation of $[\text{CrA}_6]$ ($A = \text{NH}_3$ or X^-) and $[\text{CrL}_3]^{3+}$ ($L = \text{phen}$ or bipy) complexes and proposed that this solvation occurs from the ${}^4\text{T}_{2g}$ state. Arguments have also been presented for a correlation between the quantum yields and the energy gap between the ${}^4\text{T}_{2g}$ and ${}^2\text{E}_g$ states due to the effect on the inter-system crossing rate constant.

The temperature and solvent dependence of the luminescence and photochemistry of Cr(III) complexes with oxygen, nitrogen and carbon donor ligands have been reported (Kane-Maguire & Langford, 1971; Laver & Smith, 1971). Kane-Maguire, Dunlop and Langford (1971) found that racemization is the dominant photoreaction when $[\text{Cr}(\text{phen})_3]^{3+}$ is irradiated ($\lambda \geq 350$ nm) in aqueous solution although phosphorescence was also observed. Iodide ion was found to quench both the phosphorescence and the racemization. Total phosphorescence quenching could be achieved but the photoracemization approached a non-zero limiting value. This remaining unquenchable fraction (0.14) of the reaction was attributed to the direct racemization from the lowest excited quartet state, (${}^4\text{T}_{2g}$), prior to the intersystem crossing to the doublet (${}^2\text{E}_g$). Quenching of the photoracemization and phosphorescence of (+)D- $[\text{Cr}(\text{Phen})_3]^{3+}$ by SCN^- and O_2 was reported and that by iodide ion re-examined by Kane-Maguire and Langford (1976). It was shown that the efficiency for ${}^4\text{T}_{2g} \rightarrow {}^2\text{E}_g$ intersystem crossing is 95% and that the racemization in acidic solution proceeds via thermal population of the ${}^4\text{T}_{2g}$ from the ${}^2\text{E}_g$ state.

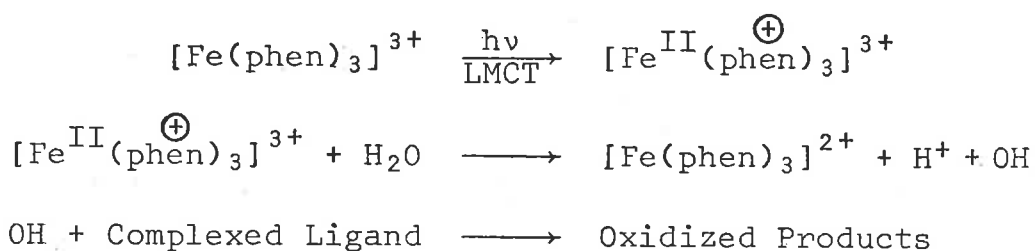
Recently formation of an adduct, $[\text{Cr}(\text{bipy})_3(\text{H}_2\text{O})]^{3+}$, has been proposed in quenching and photosolvation reactions of $\text{Cr}(\text{phen})_3^{3+}$ (Maestri, Bolleta, Manfrin, Moggi & Balzani, 1976; Henry & Hoffman, 1976). The adduct was considered to arise from the reactions of H_2O with the ${}^2\text{E}_g$ state.



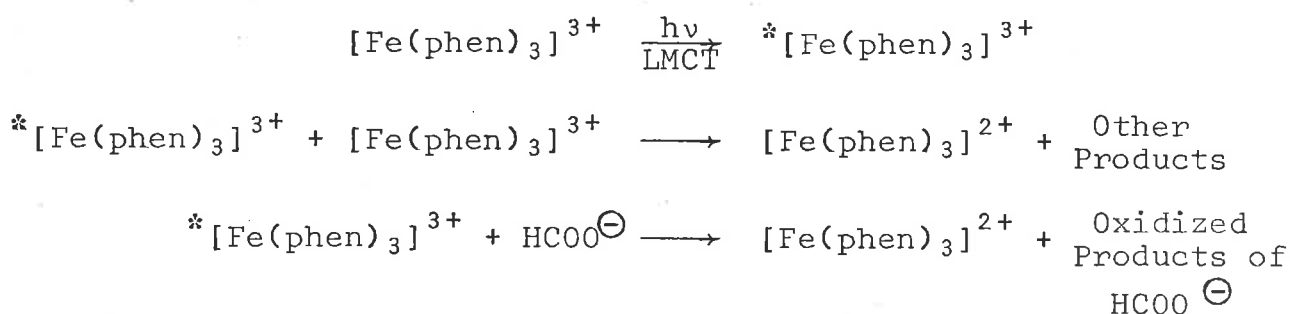
The susceptibility of LF/d-d excited states to such addition reactions requires more detailed experiments before the details of the reactions can be identified.

III.2 IRON COMPLEXES

Blau (1898) was the first to observe the photosensitivity of $[\text{Fe}(\text{phen})_3]^{3+}$. Gilkman and Podlinyaeva (1955) studied the photoreduction of $[\text{Fe}(\text{phen})_3]^{3+}$ and proposed the generation of OH radicals in a secondary thermal process.



In an independent study (Basendale & Bridge, 1955) of the photoreduction of $[\text{Fe}(\text{phen})_3]^{3+}$, in the presence of added HCOOH , an excited state of the Fe(III) complex was proposed as an intermediate:



Measurements of the variation of the quantum yield, $\phi_{-\text{Fe}(\text{phen})_3^{3+}}$, with excitation wavelengths were made in these steady photolysis experiments ($\phi \sim 10^{-2}$ - 10^{-3} for $\lambda_{\text{excitation}} = 365 \text{ nm}$ depending upon the acidity of the medium). The photoreduction was found to be quantitative with the ratio $[\phi_{+\text{Fe}(\text{II})}/\phi_{-\text{Fe}(\text{III})}] = 1.0$. Attempts to follow the photoreduction of $[\text{Fe}(\text{bipy})_3]^{3+}$ failed owing to the poor reproducibility of the system.

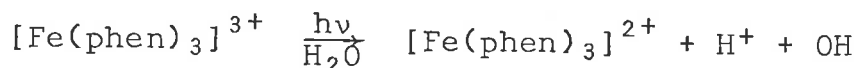
When aqueous solutions of $[\text{Fe}(\text{bipy})_2(\text{CN})_2]^{1+}$ were irradiated ($\lambda = 365 \text{ nm}$) for long period of time the system reached a photo-stationary equilibrium with an increase in pH. However, in acidic

solutions (pH < 3) complete decomposition occurred with $\phi_{-Fe(III)} \sim 1.3 \times 10^{-3}$ (König, 1968; Balzani, Carassiti & Moggi, 1964a). In a similar study on $[Fe(CN)_4(L_2)]^{1-}$ (L = phen or bipy) spectral changes accompanied an increase of pH on irradiation and the photochemical changes could be reversed in the dark (Balzani, Carassiti & Moggi, 1964b). No spectral changes could be detected in the presence of added CN^- ions, while free ligand was found



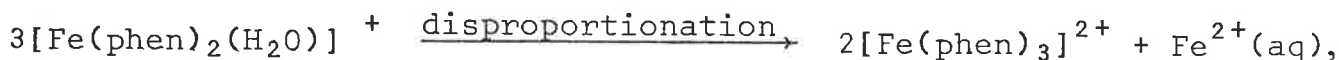
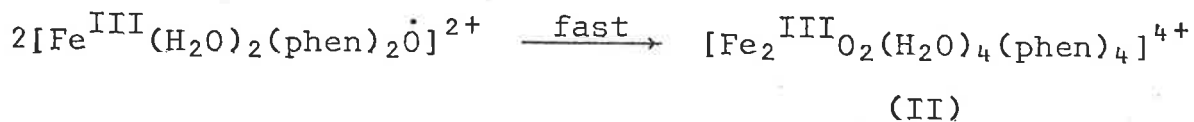
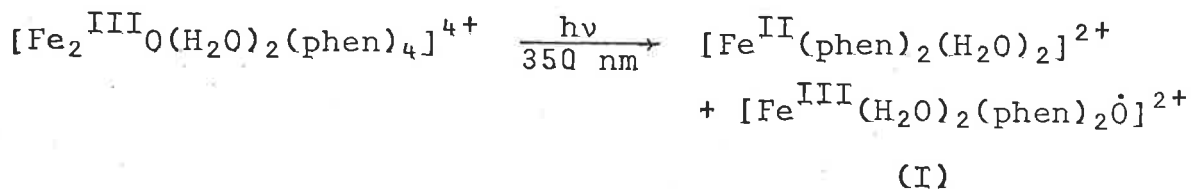
to cause photoreduction and addition of the ligand ($\phi_{+FeL_3^{2+}} \sim 10^{-3}$).

The photoreduction of $[Fe(phen)_3]^{3+}$ in aqueous acidic media was reinvestigated by Wehry and Ward (1971) using steady photolysis techniques. The photoreduction was found to be non-stoichiometric [$\phi_{+FeL_3^{2+}}/\phi_{-FeL_3^{3+}} < 1.0$], in contrast to the previous report (Baxendale & Bridge, 1955) and the present findings (Malik & Laurence, 1978). The primary photostep proposed was the oxidation of H_2O to generate OH radicals. Identification of OH



radicals in the bulk solution seems kinetically and energetically unfavourable (Pagsberg & Floryan, 1976). As will be shown later, no hydroxyl radicals are produced either in the primary photo process or in the secondary thermal reactions.

A number of papers have appeared on the photoreduction of Iron(III) dinuclear species (David, Richardson & Wehry, 1971, 1972 & 1973; David, 1972). Photoreduction of tetrakis(phen)diaquo- μ -oxo-di-iron(III) in aqueous solution produced $[Fe(phen)_3]^{2+}$ and continued after the cessation of irradiation. The proposed mechanism,



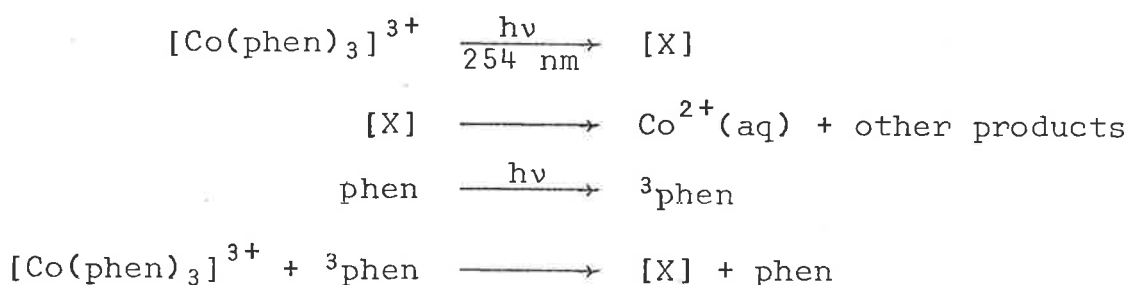
involved the formation of a labile-peroxo-bridged dinuclear species (II) (radical-substrate reaction might explain the reduction of the substrate in the dark). Photoreduction of complexes of the type $[\text{Fe}_2(\text{phen})_4\text{X}_2\text{Y}_2]$ (X or Y = Cl^\ominus , Br^\ominus , SCN^\ominus or ClO_4^\ominus) in aqueous, acetonitrile and methanolic solutions have also been studied (David & Wehry, 1973). The results in CH_3OH solution contrasted with those in H_2O and CH_3CN and different primary photoreactions were postulated in different systems.

An electrochemical probe to estimate the excited state lifetime of the non-luminescent compound, $[\text{Fe}(\text{bipy})_3]^{3+}$, has been described by Langford et al. (1978). The lifetime was estimated to be ca. psec. The photochemical behaviour of Iron(II) diimine complexes in molten salts (AlCl_3 and ethylpyridinium Chloride) has been studied (Chum, et al. 1978). Irradiation with low intensity visible light was found to produce the corresponding Iron(III) complex via an excited state precursor.

III.3 COBALT COMPLEXES

Broomhead, Dwyer and Kane-Maguire (1968) found that $[\text{Co}(\text{phen})_2\text{ox}]^+$, $[\text{Co}(\text{bipy})_2\text{ox}]^{1+}$ and $[\text{Co}(\text{bipy})(\text{ox})_2]^{1-}$ and other N-hetrochelate-oxalato complexes of Co(III) are photosensitive. $[\text{Co}(\text{phen})_2\text{Cl}_2]^{1+}$ was reported to undergo Cl^- release under the sunlight (Broomhead & Grumley, 1968b). Photoactivation of Co(III) and Cu(II) aminates has also been studied (Shagisultanova et al. 1972). The photochemical behaviour of cis-dichlorobis(bipyridyl)-Co(III) has been described by Larsen, Kelm and Wagestian (1972).

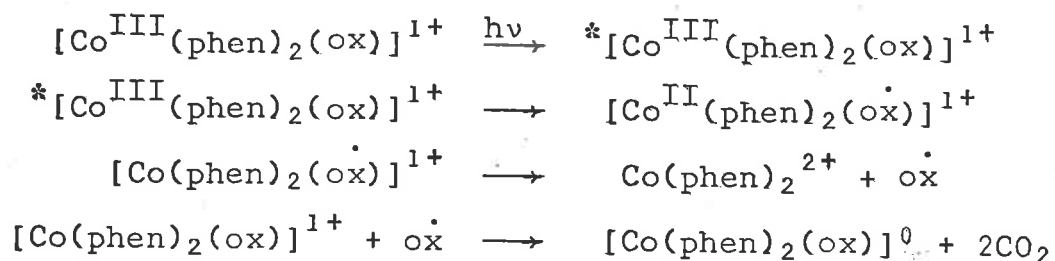
Irradiation of $[\text{Co}(\text{phen})_3]^{3+}$ ($\lambda = 254 \text{ nm}$, LMCT band) causes an oxidation-reduction decomposition (Moggi, Sabbatini & Traverso, 1973). The $1L(\pi \rightarrow \pi^*)$ band at 313 nm was found to be photoinsensitive and the photoreduction was sensitized by the presence of free ligand.



The suggestion that the transient, [X], is a Co(IV) species is unique. The system has been reinvestigated in the present study using flash photolysis and results are discussed elsewhere in this thesis.

Langford, Vuik and Kane-Maguire (1975a & b) studied the photo-reactions of $[\text{Co}(\text{phen})_2\text{ox}]^{1+}$, $[\text{Co}(\text{bipy})_2\text{ox}]^{1+}$ and $[\text{Co}(\text{phen})_3]^{3+}$ in the presence of added oxalate ions. Several other reports on the photochemistry of $[\text{Co}(\text{phen})_2\text{ox}]^{1+}$ and $[\text{Co}(\text{bipy})\text{ox}]^{1+}$ have also appeared (Henning, Jurdeczka & Thomas, 1976; Hennig, Kertscher & Hempel, 1975; Hennig, Hempel, Ackerman & Thomas, 1976).

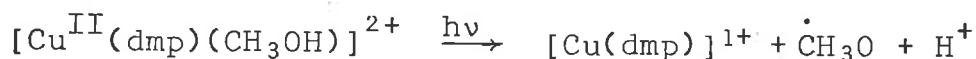
According to Langford and co-workers, the mechanism is:



These authors favoured a ligand field excited state ($^1\text{T}_{1g}$, $^3\text{T}_{1g}$ or $^5\text{T}_{2g}$), as the precursor to the observed photoreaction, although it could not be unambiguously identified. Henning et al. identified oxalate radicals in the system by e.s.r. methods.

III.4 COPPER COMPLEXES

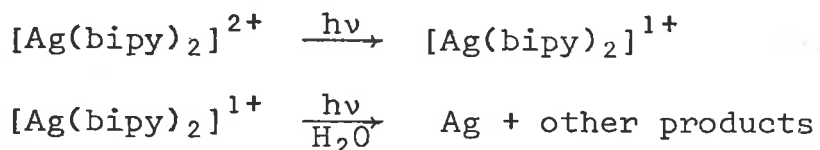
Very little is known about the photochemical behaviour of polypyridine copper complexes. Studies in this field include photoreduction of $[\text{Cu}(\text{dmp})]^{2+}$, $[\text{Cu}(\text{dmp})_2]^{2+}$ in alcoholic solution (Sundarajan & Wehry, 1972a, b & c) and the light induced reactions of $[\text{Cu}(\text{dmp})_2]^{1+}$ in the presence of $\text{K}[\text{Cis-Co}(\text{IDA})]1.5 \text{ H}_2\text{O}$ (McMillin, Buckner & Ahn, 1977). According to Wehry and co-workers the primary photoprocess is the homolytic cleavage of the $\text{Cu}(\text{II})$ -methanol bond and the overall quantum yield for the photoreduction is



affected by the secondary thermal reactions of $\dot{\text{C}}\text{H}_3\text{O}$ or $\dot{\text{C}}\text{H}_2\text{OH}$ radical with the substrate (Sundarajan & Wehry, 1972c). Light induced reactions of $\text{Cu}(\text{dmp})_2^{1+}$ in ethanol-water mixture (30:70) in the presence of $\text{K}[\text{Cis-Co}(\text{IDA})]1.5 \text{ H}_2\text{O}$ were suggested to be due to energy transfer from $[\text{Cu}(\text{dmp})_2]^{1+}$ to the cobalt complex although the possibility of an electron transfer process cannot be ruled out.

III.5 SILVER COMPLEXES

Balzani, Bertoluzza and Carassiti (1962) examined the photochemical behaviour of $[\text{Ag}(\text{bipy})_2]^{2+}$ in the 1L and LMCT bands and the observed photoreaction (production of metallic silver) was explained in terms of a biphotonic process. The second photo-

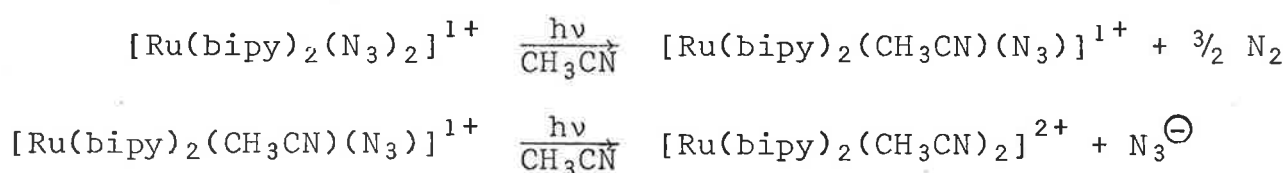


reduction step has been studied in some details (Carassiti, Condorelli & Constanzo, 1964). This is the only example, apart from the photographic materials, of the photochemistry of silver complexes.

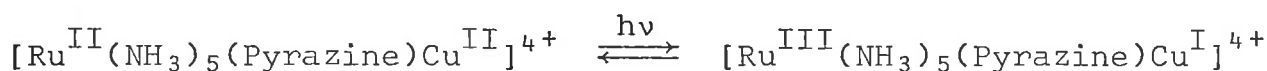
III.6 RUTHENIUM COMPLEXES

It has been reported that no permanent chemical changes are induced by irradiation in $[\text{Ru}(\text{bipy})_3]^{2+}$, although a transient species thought to involve Ru(III) has been observed (Demas & Adamson, 1971; Gafney & Adamson, 1972; Natarajan & Endicott, 1972). The photochemistry of Ru(II) complexes has already been partly discussed in Chapter 1 and additional examples will be given here.

Irradiation of $[\text{Ru}(\text{bipy})_2(\text{N}_3)_2]^{1+}$ in acetonitrile causes photoreduction of the complex (Brown, Callahan & Meyer, 1975). Although the lowest excited state has LMCT character, no free azide radical ($\dot{\text{N}}_3$) could be trapped by acrylamide. In a second light induced step, photosolvolytic of the Ru(II) complex occurred.



Flash photolysis studies (Durrante & Ford, 1975) of $[\text{Ru}^{\text{II}}(\text{NH}_3)_5(\text{Pyrazine})\text{Cu}^{\text{II}}]^{4+}$ have indicated that the complex undergoes photoinduced intramolecular electron transfer followed by



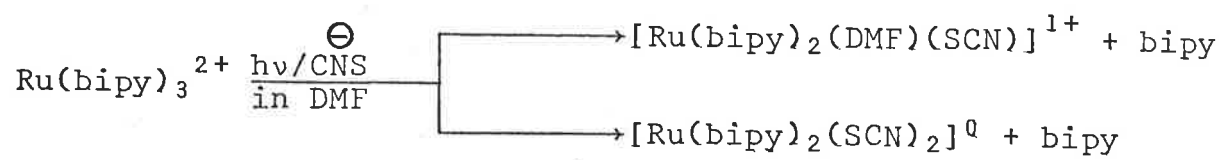
thermal relaxation. Recently Meyer (1978) has reviewed the photoreactions of such dinuclear complexes.

The photo-anation of tris(2,2'-bipyridine)Ru(II) cation by Cl^\ominus and SCN^\ominus have been reported by Gleria et al. (1978) and Hoggard and Porter (1978). In the photolysis of the complex in



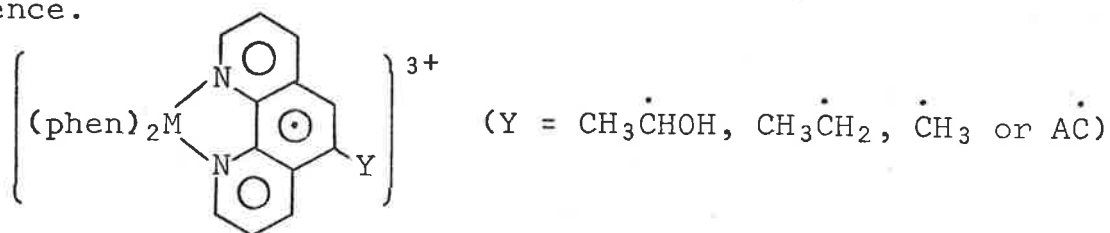
DMF two main products were produced via SCN^\ominus independent and SCN^\ominus

dependent pathways (Hoggard & Porter, 1978).

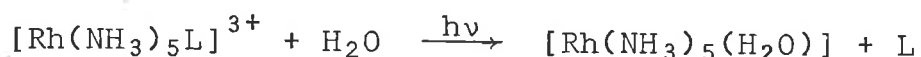


III.7 RHODIUM COMPLEXES

A co-ordinated ligand-radical containing Rh(III) and a solvent radical was identified in the photolysis of $[\text{Rh}(\text{phen})_3]^{3+}$ in ethanol at 77°K (DeArmond & Halper, 1971). The following structure of the metal-chelate radical was proposed on the e.s.r. evidence.



The only photochemical reaction following the LF band excitation of $[\text{Rh}(\text{NH}_3)_5\text{L}]^{3+}$ (L = Py or substituted Py) in aqueous solution at room temperature is the photoaquation (Muir & Huang, 1973a)



The change in photoaquation quantum yield parallels that for the ligand donor ability, without showing any correlation with the absorption maxima in the absorption spectra. The reactive excited state was concluded to be ^3E state. Although photoaquation of X is the usual photoreaction for complexes $[\text{ML}^1_4\text{X}_2]^{1+}$ and $[\text{ML}^2_2\text{X}_2]^{1+}$ ($\text{L}^1 = \text{NH}_3$ or Py; $\text{L}^2 = \text{en}$, bipy or phen; $\text{X} = \text{Cl}^\ominus$, Br^\ominus or I^\ominus ; M = Rh(III) or Ir(III)), amine aquation was also found for pyridine complexes (Muir & Huang, 1973b).

III.8 IRRIDIUM COMPLEXES

Both sunlight and light from the xenon lamp were found to induce aquation of one halide ligand in $\text{cis-}[\text{Ir}(\text{phen})_2\text{Cl}_2]^{1+}$ complex (Broomhead & Grumley, 1968). Chloride aquation also occurred in $[\text{Ir}(\text{phen})\text{Cl}_4]^{1-}$ upon UV-irradiation; the photoaquation product does not seem to be the same isomer as that produced in thermal aquation. The photophysical and photochemical behaviour of Ir(III)-bisphen complexes have been studied by Hoffman, Balzani et al. (1975). In aqueous solution Cl^- aquation (ϕ_{Cl^-} release ≈ 0.05), independent of the excitation wavelength, occurred while in DMF solution a transient species, $[\text{Ir}^{\text{IV}}\text{Cl}_2\text{LL}^\ominus]^{1+}$, was observed.

A report on the photopreparation and characterization of a stable Ir(III) species, $[\text{Ir}(\text{bipy})_2(\text{H}_2\text{O})(\text{bipy})]^{3+}$, containing a monodentate bipy ligand has been published (Watts, Harrington & Van Houten, 1977). Laurence and Thornton (1978), have found no evidence for the occurrence of monodentate-bipy Ir(III) complex.

III.9 PLATINIUM COMPLEXES

Very little attention has been paid to the photochemistry of polypyridine Pt-complexes. Cis and trans-[Pt(Py)₂Cl₂] have been found to isomerize on irradiation ($\lambda = 313 \text{ nm}$) by intra-

cis or trans-[Pt(Py)₂(Cl₂)] $\xrightarrow[313 \text{ nm}]{h\nu}$ trans or cis-[Pt(Py)₂(Cl₂)]

molecular and intermolecular isomerization paths (Moggi, Sabbatini, Varani & Balzani, 1971).

RESULTSSECTION 1IV.1 GENERAL

Transition metal complexes of the type $[M^{III}L_3]^{3+}$ ($M = Fe(III), Co(III)$ and $Ru(III)$; $L = bipy, phen$ or its related ligands) have been studied by the flash photolysis technique. The changes in absorbance following the flash in the wavelength range from 350 nm to 565 nm (where $M(II)$ complexes of phenanthroline, bipyridine and their related ligands absorb more strongly than their corresponding $M(III)$ complexes) occurred in two stages, a fast process (Stage I) followed by a slow process (Stage II), and were dependent upon acid concentration.

(a) Stage I

The initial photoreaction was complete during the light flash ($t_{1/2} < 10 \mu sec$) and lead to an immediate increase in absorbance [Fig. (9)] due to the formation of a $M(II)$ species (Section 2). The quantum yield for the conversion of $[M^{III}L_3]^{3+}$ to $[M^{II}L_3]^{2+}$ by this fast process was independent of the acid concentration (0.5 - 10 M) and the $[M^{III}L_3]^{3+}$ concentration (2.5 - 10 μM) (Section 4).

(b) Stage II

At acid concentration between ca. 0.2 and 2.0 M the initial reaction is followed by another slow reaction which also converts $[M^{III}L_3]^{3+}$ to $[M^{II}L_3]^{2+}$ [Fig. (16)]. The rate of the slow process was dependent upon the initial concentration of the $M(III)$ complex

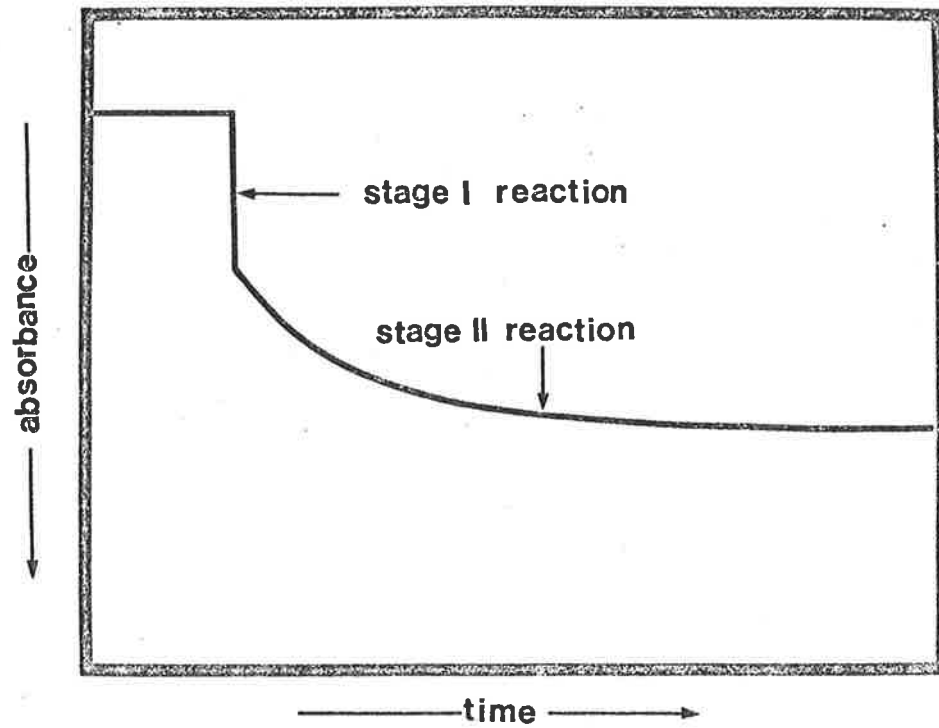


Fig. 9 The Two stages of Photoreduction

[Section 4, Page (120)] and the overall quantum yield for the loss of the M(III) complex is twice the initial quantum yield from the Stage (I).

(c) The effect of Acid Concentration

The quantum yield for the slow reaction decreases with increasing acid concentration [Section 4, Page (113)]. The nature of the reaction changes as the acid concentration increases. Beyond acid concentration ca. 3 M the $[M^{III}L_3]^{3+}$ lost in the initial step [Stage (I), Section 2] is reformed by an acid catalysed path and the overall quantum yield approaches zero [Fig. (12), Section (4), Page (130)] at 10 M $HClO_4$. The rate of reformation of the $[M^{III}L_3]^{3+}$ complex by this reaction was independent of the initial concentration of the $[M^{III}L_3]^{3+}$ complex.

(d) The Photolysis Products

The difference spectra of the photolysis product taken at 1 m sec (at the end of Stage I reaction) and at 1 sec (at the end of the Stage II) after the flash show isosbestic points between 350 nm and 600 nm [Section (3), Page (94)] which are the same as those for the conversion of the $[M^{III}L_3]^{3+}$ to $[M^{II}L_3]^{2+}$ [Chapter 1, Page (5)]. The products of the Stage (I) and Stage (II) are therefore very similar.

(e) The Transient Species

No hydroxyl or other oxidizing radicals are formed as separate species in solution as a result of the photochemical reaction [Section 5, Page (159)]. The primary photochemical reaction produces the $[M^{II}L_2L\cdot]^{\oplus 3+}$ complex [Section (5)]. The M(II)-ligand-radical species then undergoes slow thermal reactions leading to further reduction of $[M^{III}L_3]^{3+}$ [Section (4), Page (114)] or an intramolecular electron transfer to

reform $[M^{III}L_3]^{3+}$ complex [Section (4) Page (137)].

(f) Flash Photolysis of $[Co(phen)_3]^{3+}$

The results of flash photolysis of $[Co(phen)_3]^{3+}$ are discussed in APPENDIX A.

SECTION 2PRELIMINARIESIV.2.1 Thermal Stability Of The Complexes

The thermal stability of the solutions of the complexes was checked before beginning the photochemical experiments. In HClO_4 or H_2SO_4 (0.5 - 1.0 M) all the $[\text{M}^{\text{III}}\text{L}_3]^{3+}$ complexes were found to be stable on the time scale of the photochemical runs. The thermal dark reaction was quite insignificant ($< 0.5\%$ decomposition in ~ 2 hours) compared with the photoreaction (ca. 10-12% per flash).

The Fe(II) complexes in 0.5 M acid (HClO_4 or H_2SO_4) changed in colour from the characteristic red to orange-yellow and finally yellow over two hours probably due to thermal acid hydrolysis (Gillard, 1975; Chagas, Tubino & Vichi, 1978). $[\text{Ru}(\text{bipy})_3]^{2+}$ on the other hand was stable towards thermal acid hydrolysis over two hours under the same conditions.

In concentrated acid (10 M HClO_4 or 18 M H_2SO_4) all the $[\text{ML}_3]^{3+}$ complexes were stable enough to be stored in amber-coloured glass bottles under refrigeration, without any detectable dark reaction (less than 0.5% decomposition) over three months.

IV.2.2 Effect of Monitoring Light

Absorbance changes following the flash were monitored using a Xe:Hg light source [Chapter 2, page (54)]. Although low concentrations of the complexes (normally 5 μM) were used to ensure that the absorption of the light from the flash lamp by the intensely absorbing $[\text{ML}_3]^{3+}$ complexes was uniform, high monitoring light intensities were desirable to obtain good signal to noise ratios (e.g. the absorbance in a 10 cm cell due to 5 μM $[\text{Fe}(\text{phen})_3]^{3+}$ solution was ca. 0.25 at 366 nm). A high monitoring

light intensity may itself produce steady-state photolysis. This was investigated by placing the solution ($5 \mu\text{M} [\text{ML}_3]^{3+}$ in 0.5 M HClO_4 or H_2SO_4) in the cell and following the absorbance changes due to high monitoring light flux. The changes in absorbance were ca. 0.0016 in 15 minutes while the noise level was ca. 0.0011 absorbance units. The results were independent of the monitoring wavelength (350 - 650 nm) and no special precautions against monitoring light photolysis were taken. The optical density changes for different flash photolysis runs under the same experimental conditions, were reproducible to within $\pm 2\%$ for different iris openings of the collimators, which changed the intensity of the monitoring light.

IV.2.3 Oxygen Purging

Molecular oxygen is an excellent scavenger for free radicals and excited triplet states (Golinick, 1968; Kearns, 1971; Foote, 1968; Gijzeman, Kaufman & Porter, 1973) and the effect of O_2 on the flash photolysis experiments was determined. Solutions of $[\text{Fe}(\text{phen})_3]^{3+}$ ($5 \mu\text{M}$) in HClO_4 (0.5 M) were monitored after the flash at 493 nm. The results for the air-saturated ($[\text{O}_2] \approx 10^{-3} \text{ M}$) solutions and for the solutions which had been purged for 15-20 minutes with argon or nitrogen are given in Table (5). The presence of O_2 had no effect on the photolysis quantum yield or on the rate constants for the slow thermal reactions (Stage II) and all further photolysis experiments were carried out with air-saturated solutions. The finding that O_2 had no effect on the photochemistry agreed with the previous steady photolysis results (Baxendale & Bridge, 1955; Wehry & Ward, 1971).

Table (5)

THE EFFECT OF OXYGEN

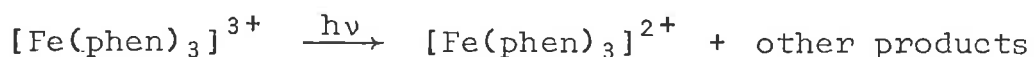
- a. $[ML_3^{3+}] = 5 \mu\text{M}$ in 0.5 M HClO_4 ; b. ± 0.20 ; c. $k_{(\text{obs})}$ is the experimental pseudo-first order rate constant;
 d. 0.5 M H_2SO_4 due to the insolubility of the complex in dilute HClO_4 solution.

Complex ^a	Percentage ^b M(III) Complex lost per flash		Rate Constant ^c ($k_{(\text{obs})}/\text{s}^{-1}$) for Stage II	
	air saturated	Oxygen purged	air saturated	Oxygen purged
$[\text{Fe}(\text{phen})_3]^{3+}$	~ 10%	~ 10%	3.20 ± 0.30	3.10 ± 0.35
$[\text{Fe}(\text{Me}_4\text{-phen})_3]^{3+\text{d}}$	~ 20%	~ 20%	2.49 ± 0.25	2.5 ± 0.26
$[\text{Fe}(\text{bipy})_3]^{3+}$	~ 12%	~ 12%	2.21 ± 0.24	2.3 ± 0.30
$[\text{Ru}(\text{bipy})_3]^{3+}$	~ 11%	~ 11%	4.20 ± 0.50	4.20 ± 0.40

IV.2.4 Photochemical Reactions and Products

Preliminary measurements of the spectra of the solutions after the flash using a recording spectrophotometer showed that $[\text{Fe}(\text{phen})_3]^{3+}$ is photoreduced but the products and stoichiometry of the reaction were uncertain because of the two-step reaction [Section (I), page (84)].

Previous studies (Baxendale & Bridge, 1955; Wehry & Ward, 1971) showed that $[\text{Fe}(\text{phen})_3]^{3+}$ is photoreduced to $[\text{Fe}(\text{phen})_3]^{2+}$. Wehry and Ward (1971) observed that the quantum yield for the loss



of $[\text{Fe}(\text{phen})_3]^{3+}$ ($\phi_{-\text{Fe(III)}}$) was greater than the quantum yield for the production of $[\text{Fe}(\text{phen})_3]^{2+}$ ($\phi_{+\text{Fe(II)}}$) i.e. $\phi_{-\text{Fe(III)}} > \phi_{+\text{Fe(II)}}$.

Differences between $\phi_{-\text{Fe(III)}}$ and $\phi_{+\text{Fe(II)}}$ may occur if photodissociation, leading to loss of the ligand and solvolysis, occurs because the high-spin Fe(II) complex is labile (König, 1968).

To look for possible photodissociation 15 μM solutions of the M(III) complexes in 0.2 M HClO_4 or H_2SO_4 were flashed three times (for a total photoreduction of 30-60%). The photolyte was then reduced with SO_2 and excess SO_2 removed by bubbling N_2 saturated with water vapour through the solution. The concentration of the M(II) complex in the solution was then determined spectrophotometrically using the molar absorbances in Table (4).

Table (6)

LOOKING FOR POSSIBLE PHOTODISSOCIATION

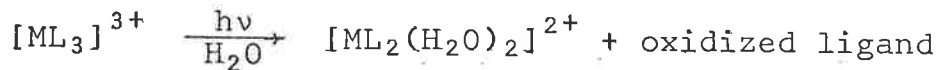
Complex [†]	$\frac{[\text{ACID}]^{\dagger}}{\text{M}}$	Absorbance* in 1 cm cell		$10^5 \times \text{Concentration/M}$	
		Before flashes	After flashes and reduction with SO ₂	Before photolysis	After photolysis and reduction with SO ₂
[Fe(phen) ₃] ³⁺	0.20	0.0130 (600)	0.165 (510)	1.49	1.48
	0.20	0.0131 (600)	0.166 (510)	1.50	1.495
[Fe(Me ₄ -phen) ₃] ³⁺	0.20	0.0238 (600)	0.207 (510)	1.496	1.50
	0.20	0.0240 (600)	0.2071 (510)	1.510	1.50
[Fe(bipy) ₃] ³⁺	0.20	0.0048 (612)	0.139 (520)	1.50	1.50
	0.20	0.0050 (612)	0.139 (520)	1.52	1.50
[Ru(bipy) ₃] ³⁺	0.20	0.0050 (620)	0.027 (454)	1.50	1.50
	0.20	0.0051 (620)	0.027 (454)	1.60	1.50

[†] H₂SO₄

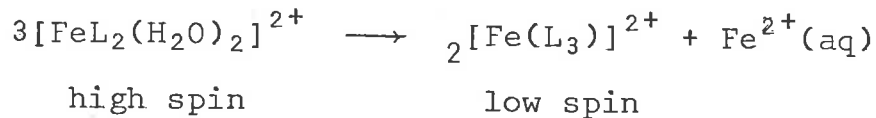
* Numbers in the parentheses refer to the wavelength (nm) of observation

[†] [Complex] = 15 μM

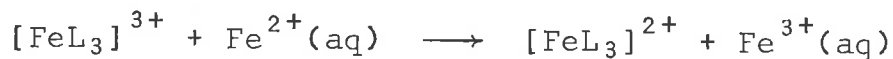
Photodissociation could lead to the formation of high-spin



Fe(II) complexes. The mono- (red) and bis- (blue) Fe(II) N-hetrochelates disproportionate rapidly in aqueous solution (König, 1968; Broomhead et al., 1968) and $\text{Fe}^{3+}(\text{aq})$ and free ligand



would be expected in the solution due to the reaction.



The chelating base is firmly bound in Ru(II) complexes of the type $[\text{RuL}_2\text{X}_2]$ or $[\text{RuLX}_4]^{2-}$ (Dwyer, Goodwin & Gyrafas, 1963). These Ru(II) complexes are low-spin and stable towards disproportionation.

The detection of $\text{Fe}^{3+}(\text{aq})$ and $\text{Fe}^{2+}(\text{aq})$, for the iron complexes was attempted using the thiocyanate and the phenanthroline methods (Vogel, 1961). These colorimetric methods would have easily detected these ions at levels of 5% $\text{Fe}^{3+}(\text{aq})$ and 1-2% $\text{Fe}^{2+}(\text{aq})$ of the yield of $[\text{ML}_3]^{2+}$ complex.

No detectable free ligand ($\leq 10^{-8}$ M, determined by UV absorption) could be extracted from the photolyte with chloroform. The extraction method would have allowed the detection of ca. 10^{-8} M of the free ligand, that is, $\sim 2\%$ of the photochemical yield of the $[\text{ML}_3]^{2+}$ complex.

The lack of free ligand and of aquo ions and the recovery of the M(III) complexes as M(II) complexes (within $> 1\%$ accuracy) in the photolysed solutions shows that no photodissociation occurs and is consistent with the previous findings (Baxendale & Bridge, 1955; Wehry & Ward, 1971) [Table (6)].

SECTION 3STOICHIOMETRY OF THE REACTIONIV.3.1 Difference Spectra(i) $[\text{Fe}(\text{phen})_3]^{3+}$

Difference spectra were taken at 1 m sec (at the end of Stage I) and 1 sec (at the completion of Stage II) after the flash in the photolysis of $[\text{Fe}(\text{phen})_3]^{3+}$ in 0.5 M HClO_4 and are shown in Fig. (10). Both the difference spectra show isosbestic points at 372 ± 3 nm and 573 ± 3 nm. The isosbestic points are the same as those for the reaction:



The isosbestic points for this reaction were obtained by scanning the spectra of $[\text{Fe}(\text{phen})_3]^{3+}$ and $[\text{Fe}(\text{phen})_3]^{2+}$ under the same concentrations. The positions of the absorption bands and the identity of the isosbestic points in the spectra of the initial and final products in the flash photolysis of $[\text{Fe}(\text{phen})_3]^{3+}$ show that these products are very similar to those of Fe(II) low-spin complexes of phen and substituted-phen (Gordon & Sutin, 1961; Ford-Smith & Sutin, 1961) but the visible absorption spectra of phenanthroline and substituted phenanthroline iron(II) complexes are so similar that they do not allow absolute identification of the products, particularly the signal to noise level was equivalent to ca. 0.001 absorbance units while the maximum absorbance changes at 493 nm were ca. 0.02.

(ii) $[\text{Fe}(\text{Me}_4\text{-phen})_3]^{3+}$

The difference spectra for the photolysis of $[\text{Fe}(\text{Me}_4\text{-phen})_3]^{3+}$ in 0.5 M H_2SO_4 taken 1 m sec and 1 sec after the flash showed one isosbestic point at 585 ± 3 nm for both stages of the reaction

Fig. 10 Difference Spectra of the Initial (3) (1msec after the flash), final (2) (1 sec after the flash) Products of Photolysis of $[\text{Fe}(\text{phen})_3]^{3+}$ and that of $[\text{Fe}(\text{phen})_3]^{2+}$ and $[\text{Fe}(\text{phen})_3]^{3+}$ (1) (right ordinate)

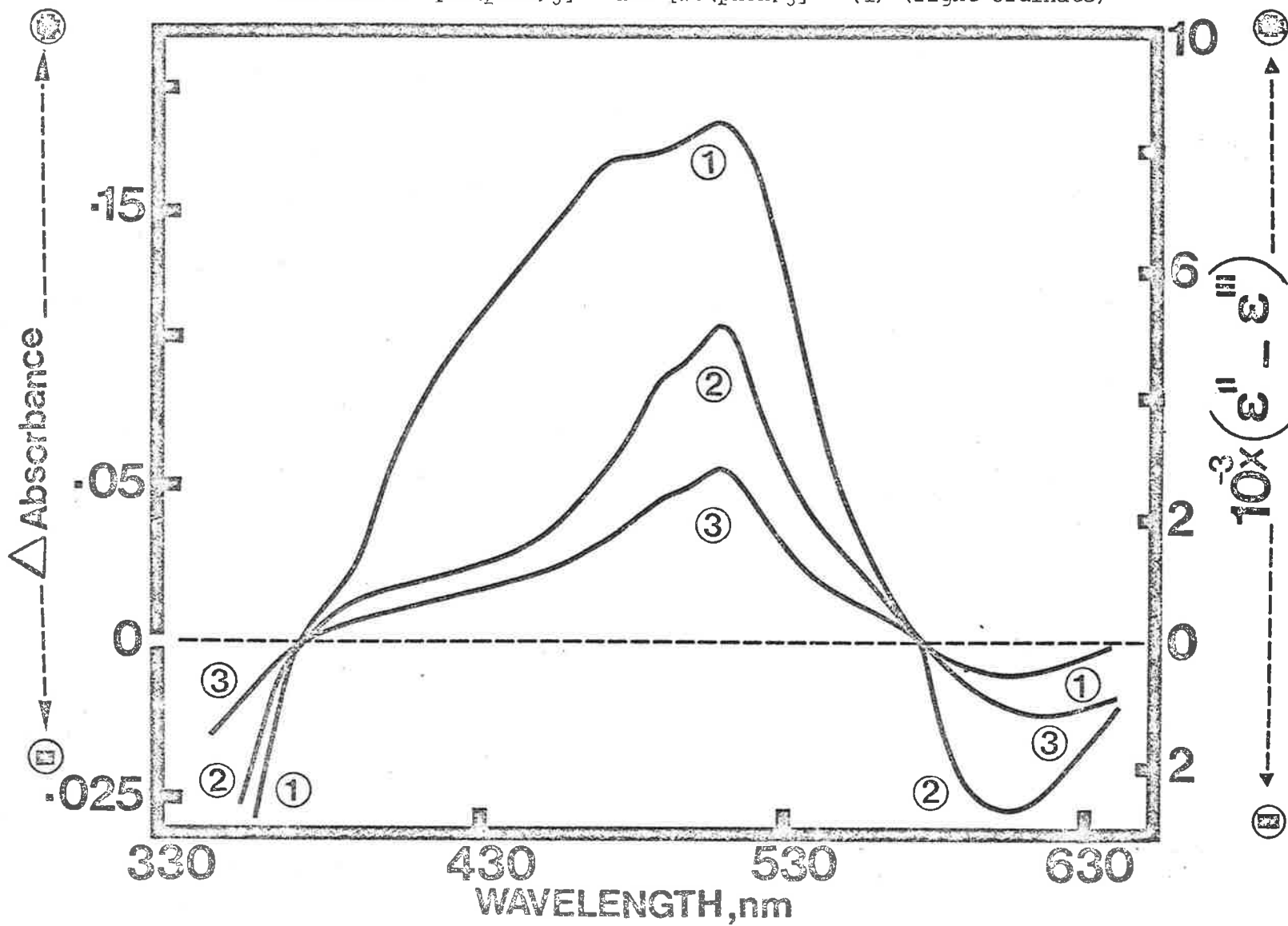


Fig. 11 Difference Spectra of the Initial (1) (1 msec after the flash), final (2) (1 sec after the flash) Products of Photolysis of $[\text{Fe}(\text{Me}_4\text{-phen})_3]^{3+}$ and that of $[\text{Fe}(\text{Me}_4\text{-phen})_3]^{3+}$ and $[\text{Fe}(\text{phen})_3]^{3+}$ (3) (right ordinate).

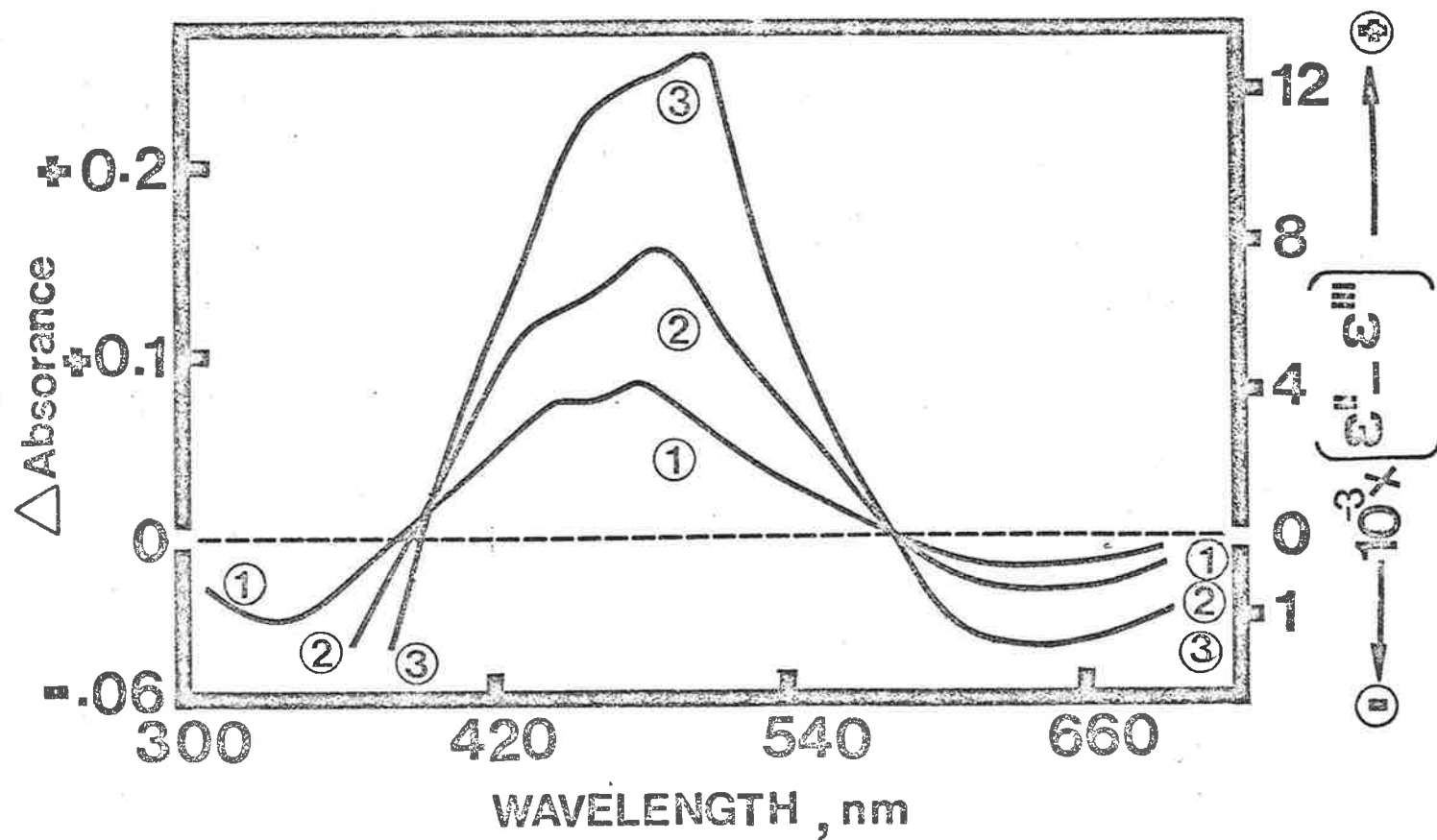
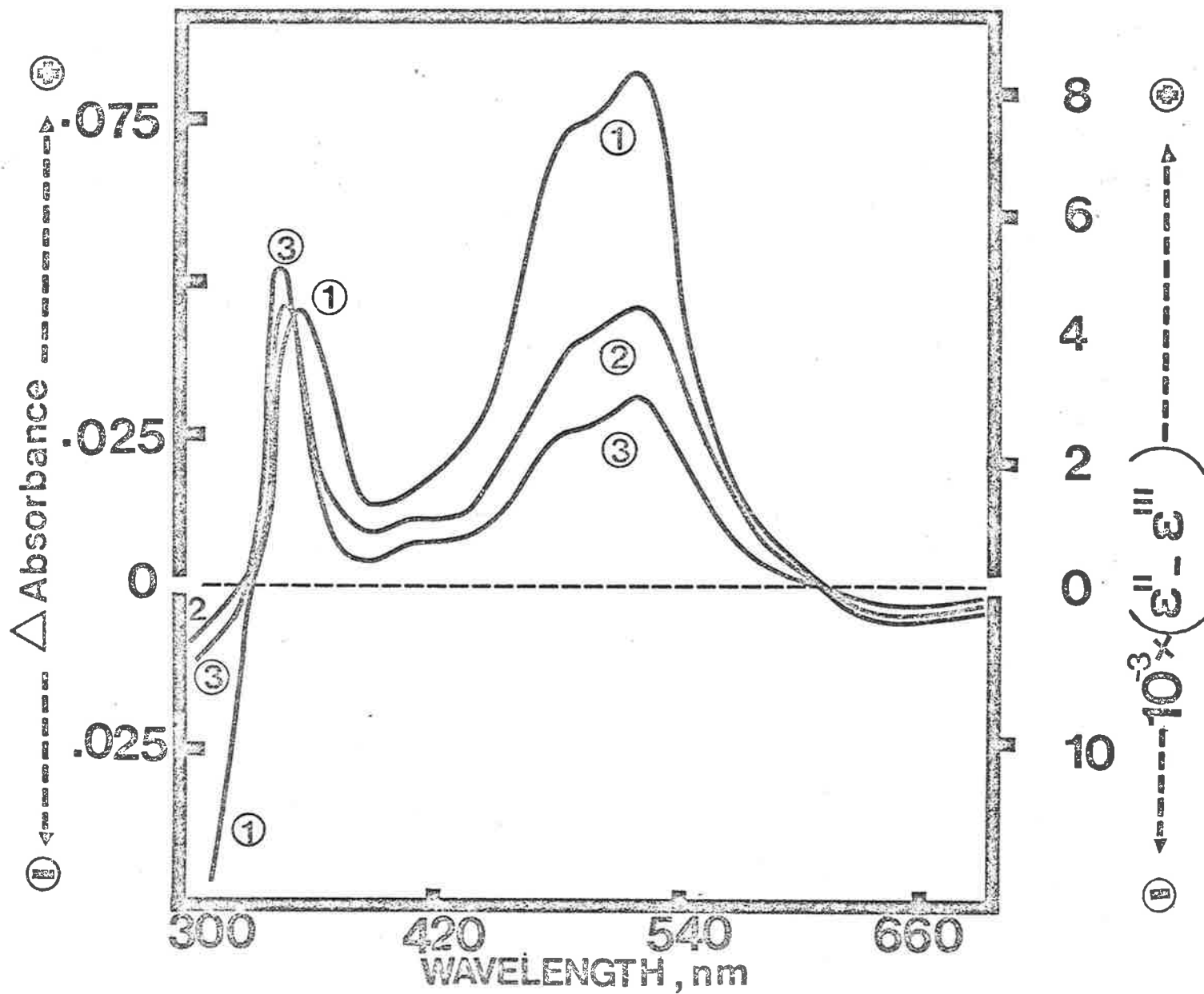
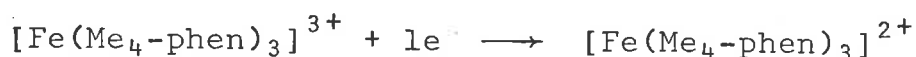


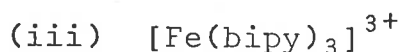
Fig. 12 Difference Spectra of the Initial (3) (1 msec after the flash), final (2) (2.5 sec after the flash) Products of Photolysis of $[\text{Fe}(\text{bipy})_3]^{3+}$ and the Difference Spectra of $[\text{Fe}(\text{bipy})_3]^{2+}$ and $[\text{Fe}(\text{bipy})_3]^{3+}$ (right ordinate)



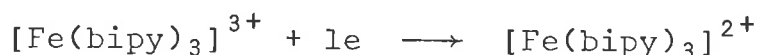
but two different isosbestics at 380 ± 2 nm and 390 ± 2 nm were observed for the initial and final photolysis products [Fig. (11)]. The isosbestic points for the conversion of $[\text{Fe}(\text{Me}_4\text{-phen})_3]^{2+}$ to $[\text{Fe}(\text{Me}_4\text{-phen})_3]^{3+}$ were found to occur at 390 ± 2 nm and 585 ± 2 nm.



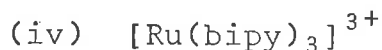
The existence of two different isosbestic points (in the tail of the UV-region) for the initial and final products suggests that the products, though similar, are not identical.



The difference spectra for the photolysis of $[\text{Fe}(\text{bipy})_3]^{3+}$ in 0.5 M HClO_4 taken 1 m sec and 2.5 sec after the flash [Fig. (12)] showed an isosbestic point for the initial (Stage I) and secondary process (Stage II) at 612 ± 2 nm. At the tail of the UV-region two separate isosbestics at 325 ± 2 nm and 336 ± 2 nm were observed for the product formed in Stage (I) and Stage (II) respectively in the flash photolysis of $[\text{Fe}(\text{bipy})_3]^{3+}$. The isosbestic points for the conversion of $[\text{Fe}(\text{bipy})_3]^{3+}$ to $[\text{Fe}(\text{bipy})_3]^{2+}$ were found to be at 330 ± 3 nm and 610 ± 3 nm. Again the initial and

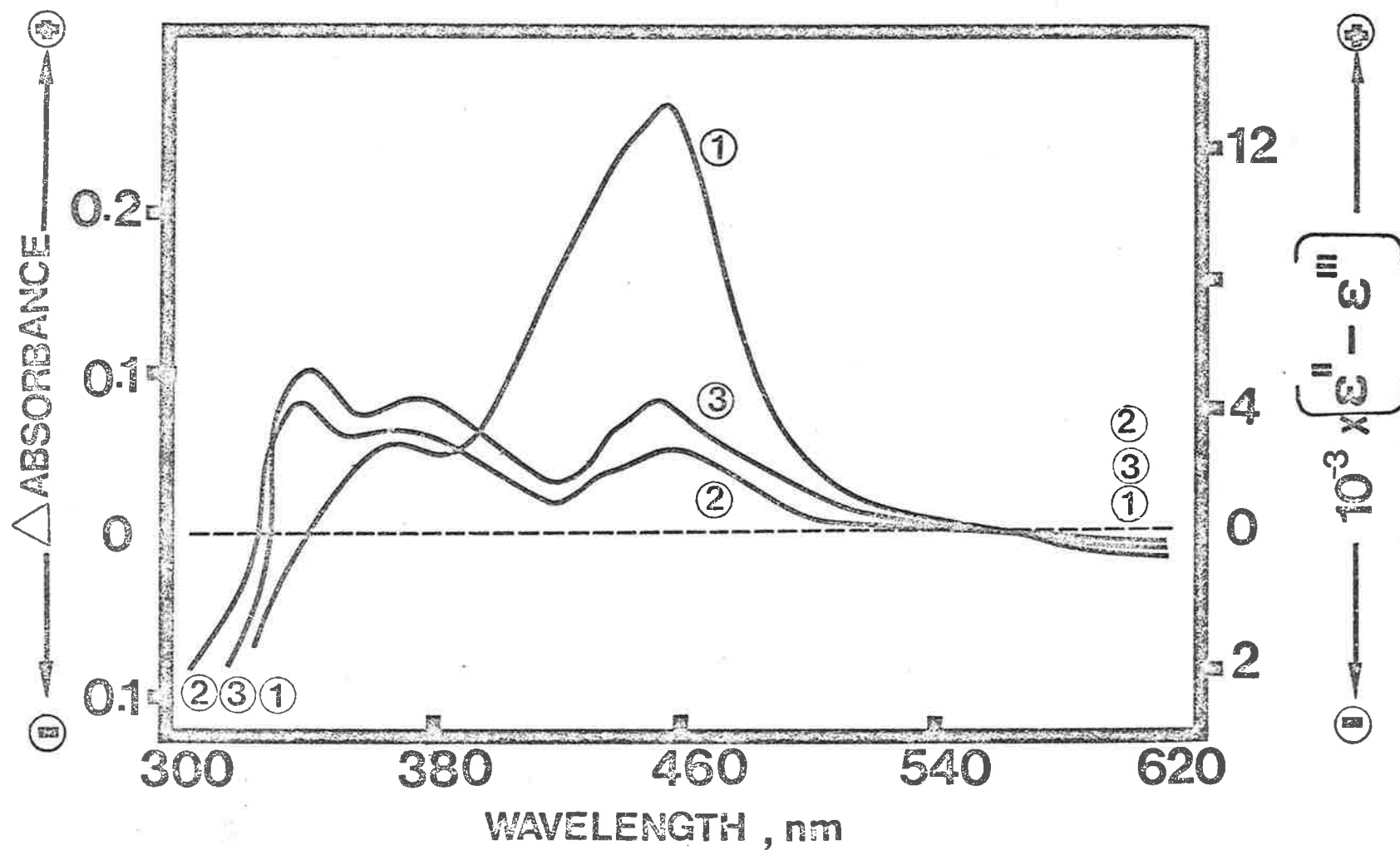


final products are obviously similar but not identical. The difference spectra of the photolysis products and for the tris(bipyridine) Iron(II) and tris(bipyridine) Iron(III) are shown in [Fig. (12)].



For $[\text{Ru}(\text{bipy})_3]^{3+}$ in 0.5 M HClO_4 an isosbestic point at 580 ± 2 nm was observed for both the primary photochemical reaction (Stage I) and secondary thermal process (Stage II) but the difference spectra taken 1 m sec and 1 sec after the flash showed

Fig. 13 Difference Spectra of the Initial (2) (1 msec after the flash), final (3) (1 sec after the flash) Products of Photolysis of $[\text{Ru}(\text{bipy})_3]^{3+}$ including the Difference Spectra of $[\text{Ru}(\text{bipy})_3]^{2+}$ and $[\text{Ru}(\text{bipy})_3]^{3+}$ (1) (right ordinate).



two different isosbestics at 328 ± 2 nm and 335 ± 2 nm for the primary photochemical reaction (Stage I) and the secondary thermal reaction (Stage II) respectively. For the conversion of Ru(III) complex to the corresponding Ru(II) complex there are two isosbestics at 340 ± 3 nm and 580 ± 3 nm. Existence of the two different isosbestic points for the initial and final photoreduction products for $[\text{Ru}(\text{bipy})_3]^{3+}$ further confirms the formation of two different products. Fig. (13) shows the difference spectra for the photolysis products and for the $[\text{Ru}(\text{bipy})_3]^{3+}$ to $[\text{Ru}(\text{bipy})_3]^{2+}$ conversion.

(v) Changes in Intra-Ligand Absorbance

The spectra of the final photoproducts are slightly different (as shown by the isosbestics for the initial and final products) in the tail of the $\pi \rightarrow \pi^*$ intraligand band (300-350 nm). The high intensities of the $\pi \rightarrow \pi^*$ bands ($> 10^4 \text{ M}^{-1} \text{ cm}^{-1}$), the small quantum yields (ca. 0.02) and the concentration of the complexes needed for the flash photolysis runs made it impossible to measure difference spectra at wavelengths below 300 nm with the flash photolysis apparatus. Measurements of the difference spectra below 300 nm for the overall photoreaction products were made by the following procedure.

A solution containing the M(III) complex (10 μM) in 0.2 M H_2SO_4 was divided into two portions. One was used as the reference solution while the other was placed in the photolysis cell and flashed three times. Using the flashed solution as the sample and the original M(III)-complex solution as the reference, the spectra were recorded in the 326 nm to 217 nm range on a Zeiss DMR-10 spectrophotometer by off-setting the base line. Without disturbing the positions of the cells, they were emptied by suction, washed twice with triply distilled water and finally washed

Fig. (14) Difference spectra of the final products of photolysis of M(III) complexes in the intraligand band (325 - 220 nm). For all the spectra (pp. 100 - 103), the concentration of the complex was 10 μ M in 0.2 M H_2SO_4 .

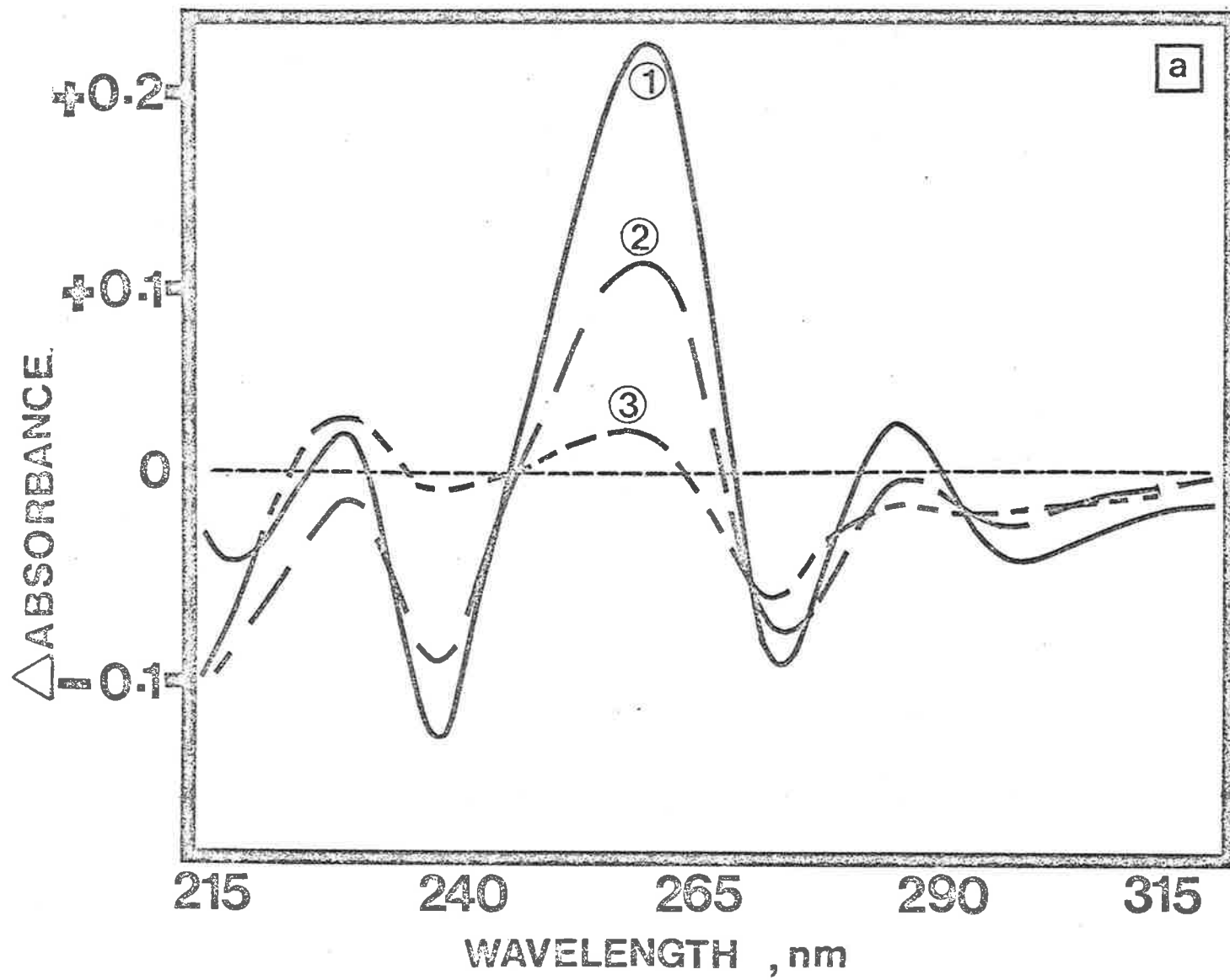
- (1) difference spectra of the original M(III) complex and the flashed solution
- (2) difference spectra of the original M(III) complex - reduced with SO_2 and the flashed solution
- (3) difference spectra of the original M(III)-reduced with SO_2 and the flashed - solution reduced with SO_2 .

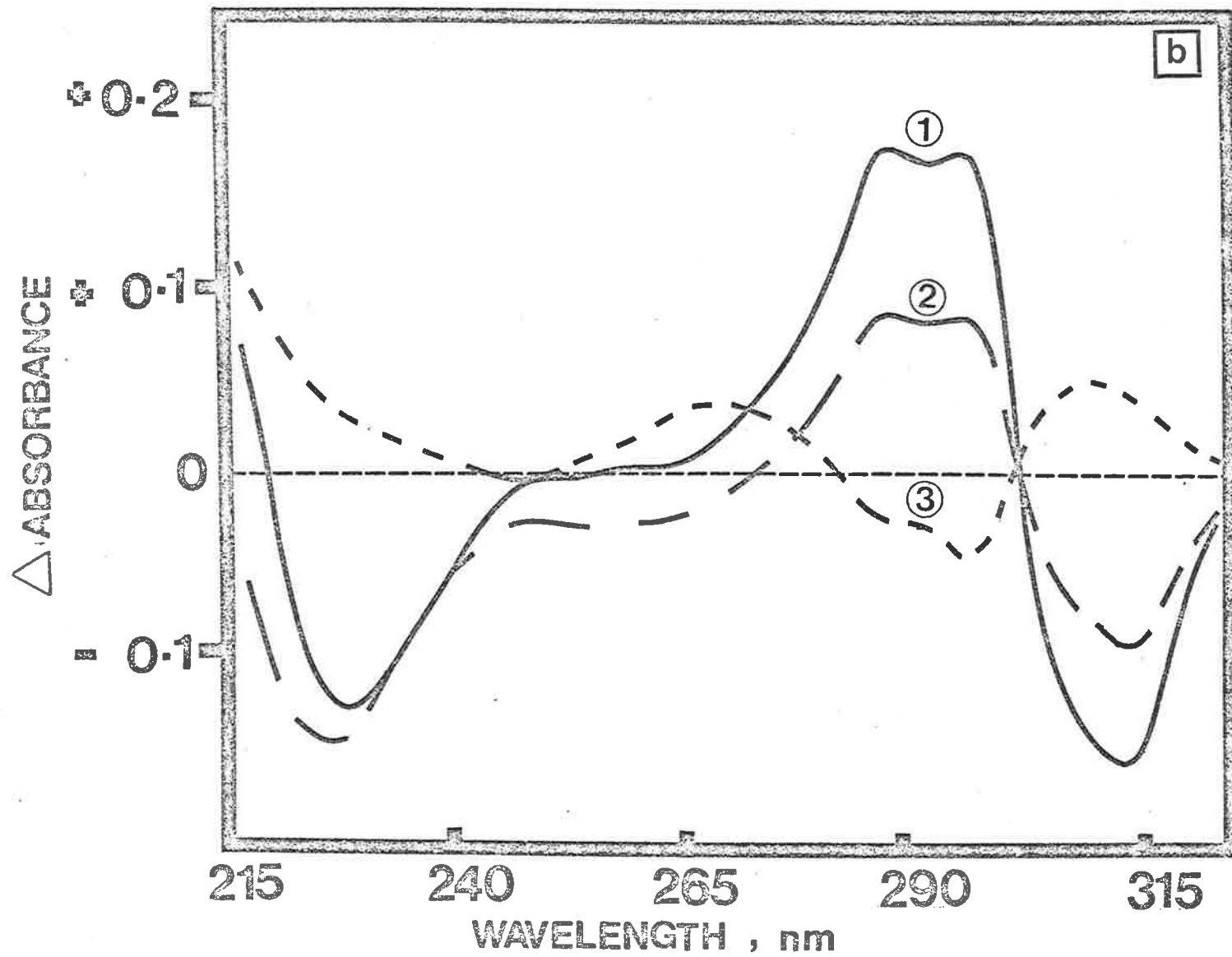
(a) $[Fe(phen)_3]^{3+}$, p. 100

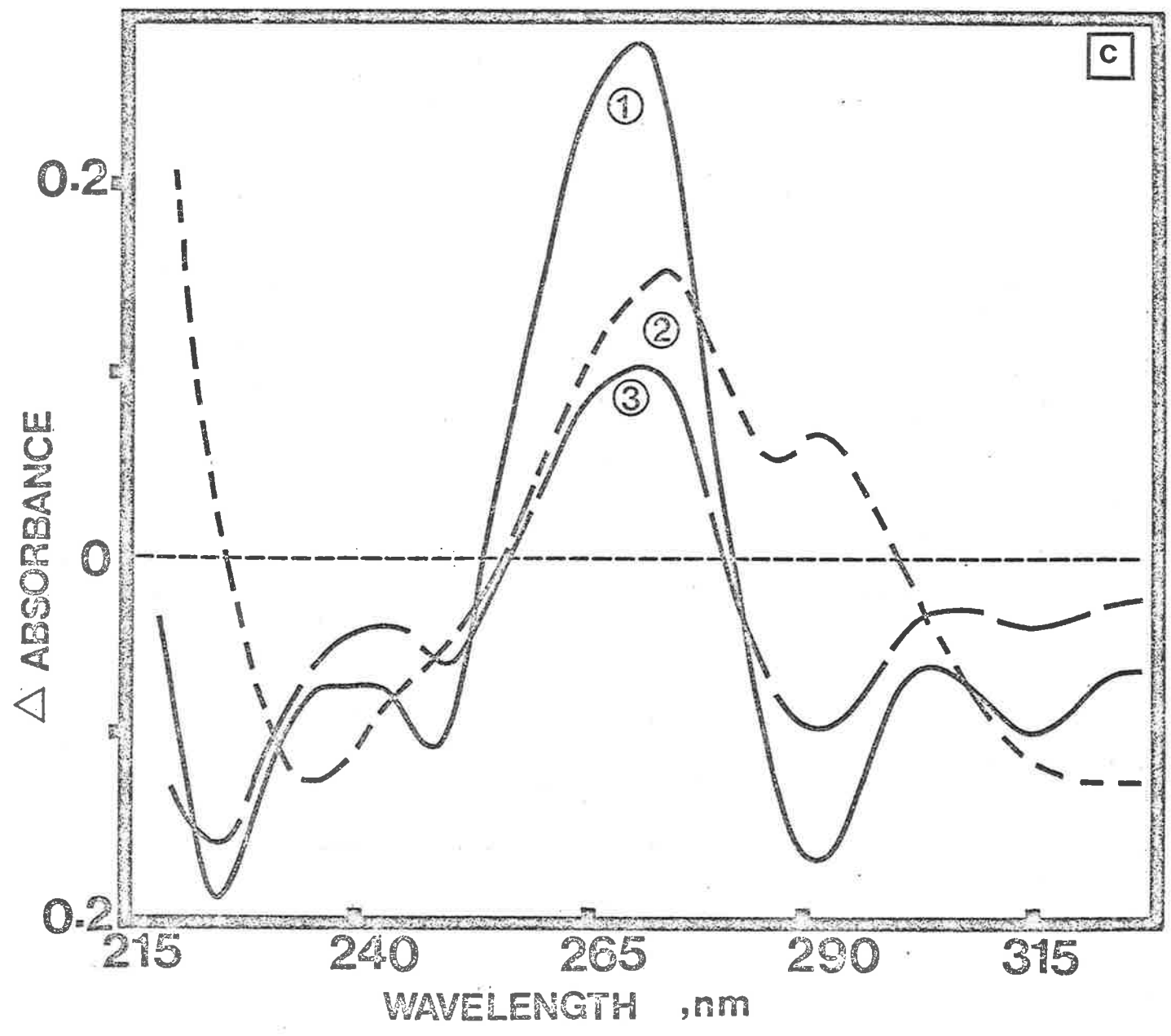
(b) $[Fe(bipy)_3]^{3+}$, p. 101

(c) $[Fe(Me_4-phen)_3]^{3+}$, p. 102

(d) $[Ru(bipy)_3]^{3+}$, p. 103







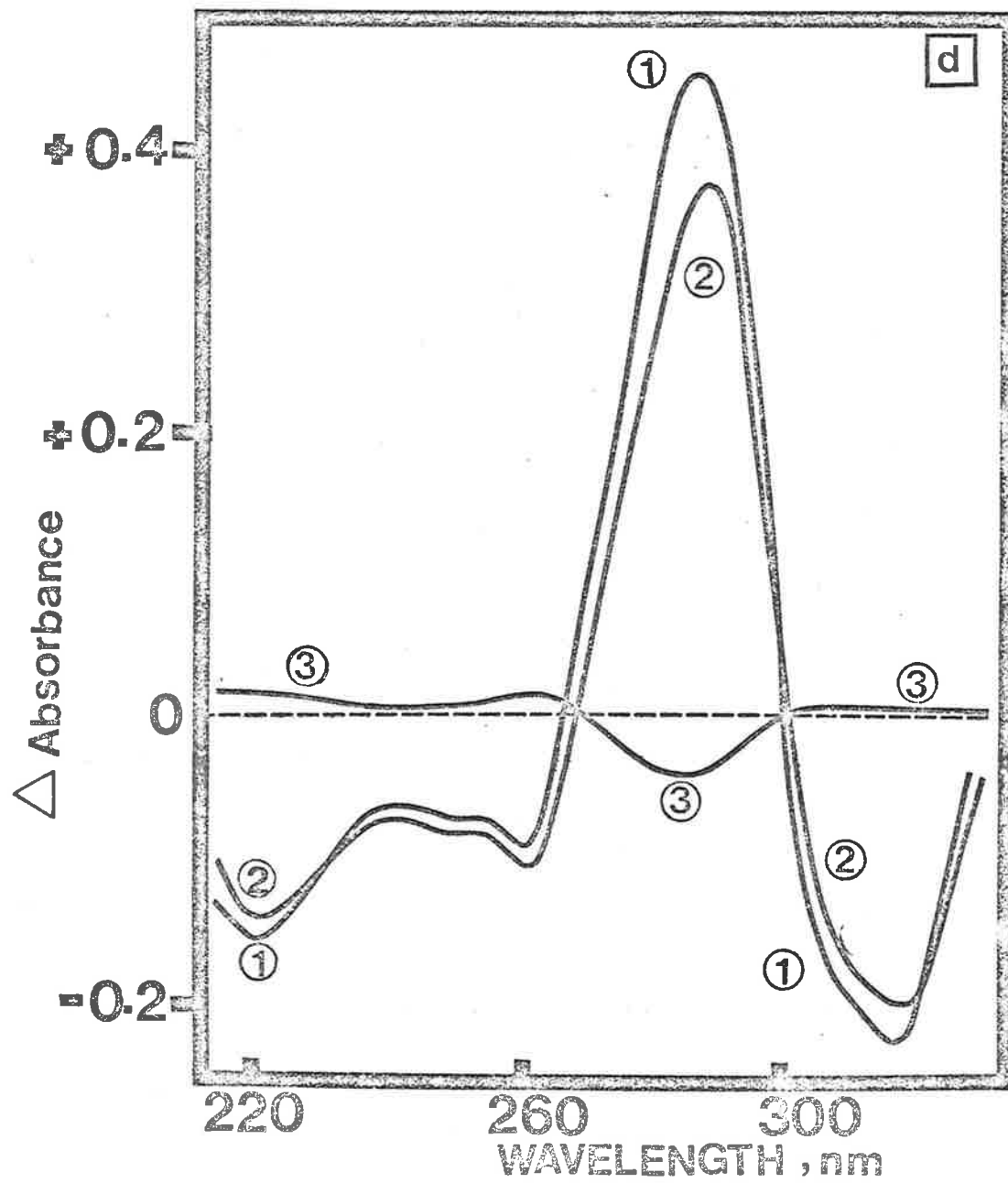


Table (7)

ISOSBESTIC POINTS^a FOR THE DIFFERENCE SPECTRA OF THE FINAL PHOTOLYSIS
PRODUCTS IN THE INTRALIGAND BAND

$[\text{Fe}(\text{phen})_3]^{3+}$	$[\text{Fe}(\text{Me}_4\text{-phen})_3]^{3+}$	$[\text{Fe}(\text{bipy})_3]^{3+}$	$[\text{Ru}(\text{bipy})_3]^{3+}$
225 nm	223 nm	243 nm	270 nm
242 nm	253 nm	249 nm	302 nm
251.5 nm	298 nm	283 nm	
272 nm		303 nm	

^a ± 2 nm

with AR acetone and dried by blowing air through them. During the spectral scans the temperature in the cell compartment was maintained at $25 \pm 0.1^\circ\text{C}$ by a thermostat. The flashed sample was then reduced with SO_2 (AnalaR Grade, B.D.H.) and the excess SO_2 removed by bubbling N_2 (saturated with water vapour) through the solution. Using the original M(III) complex solution as the reference and the flashed-reduced solution as the sample, another set of spectra were recorded. After the same procedure of washing and drying the cells, the spectra of the original solution reduced with SO_2 was recorded against the flashed-reduced, solution for each of the complexes. Fig. 14 (a,b,c,d) shows the three difference spectra for the Fe(III) and Ru(III) complexes. Similar experiments showed no difference between the photolysis products and the M(II) complexes in the visible region from 350 to 700 nm.

The M(II) and M(III) tris-chelates of phen, bipy and their related ligands have D_3 symmetry. The intensity of the intraligand ($\pi \rightarrow \pi^*$) bands in these complexes changes if the symmetry of the molecule falls to C_{2v} (Byrant, Ferguson & Powell, 1971; Bryant & Ferguson, 1971) so that a change in the ligand structure would be reflected in the intensities and probably in the position of the intraligand bands. The difference spectra Fig. 14 (a,b, c and d) suggest that similar structural changes occur in the course of the photolyses for all the ligands. The isosbestic points [Table (7)] between the original solution reduced by SO_2 and the flashed solution reduced by SO_2 clearly show the formation of two different photoreduction products.

IV.3.2 Stoichiometry

For the steady state photolysis of $[\text{Fe}(\text{phen})_3]^{3+}$ (Wehry &

Ward, 1971), the quantum yield for the loss of $[\text{FeL}_3]^{3+}$ ($\phi_{-\text{Fe(III)}}$) and the quantum yield for the production of $[\text{FeL}_3]^{2+}$ ($\phi_{+\text{Fe(II)}}$) were not equal and $[\phi_{+\text{Fe(II)}}/\phi_{-\text{Fe(III)}}] < 1$. In 8.5 M H_2SO_4 the ratio $\phi_{+\text{Fe(II)}}/\phi_{-\text{Fe(III)}}$ was ~ 0.65 and increased as the acid concentration increased, reaching a value of ca. 0.92 in 15 M H_2SO_4 [Fig. (26)].

Baxendale and Bridge (1955) found that $\phi_{+\text{Fe(II)}}/\phi_{-\text{Fe(III)}}$ in the photolysis of $[\text{Fe(phen)}_3]^{3+}$ was 1.0 ± 0.10 . The present results agree with their findings in 0.5 M HClO_4 or H_2SO_4 .

The stoichiometry of the reaction was followed by spectrophotometric measurements. The changes in absorbance (ΔA) were measured on either side of the isosbestic point in the visible region at 493 nm and 630 nm for the Fe(III) complexes and 436 nm and 612 nm for the Ru(III) complex. A 5 μM solution of $[\text{ML}_3]^{3+}$ in 0.2 - 0.5 M HClO_4 or H_2SO_4 was flash photolysed and the absorbance changes (ΔA) measured at both wavelengths for each complex [Table (8)].

For the reaction



at two wavelengths where both $[\text{M}^{\text{III}}\text{L}_3]^{3+}$ and $[\text{M}^{\text{II}}\text{L}_3]^{2+}$ absorb significantly, we have

$$\Delta A(\lambda_1) = \{\epsilon_{\text{II}}[\text{ML}_3^{2+}]_{\text{P}} - \epsilon_{\text{III}}[\text{ML}_3^{3+}]_{\text{C}}\} \ell \quad (1)$$

and

$$\Delta A(\lambda_2) = \{\epsilon'_{\text{II}}[\text{ML}_3^{2+}]_{\text{P}} - \epsilon'_{\text{III}}[\text{ML}_3^{3+}]_{\text{C}}\} \ell \quad (2)$$

where λ_1 and λ_2 = wavelengths of observation

ϵ_{II} and ϵ'_{II} = molar absorbances of M(II) complex at λ_1 and λ_2

ϵ_{III} and ϵ'_{III} = molar absorbances of M(III) complex at λ_1 and λ_2

$[\text{ML}_3^{2+}]_{\text{P}}$ = concentration of M(II) complex produced

Table (8)

DATA FOR STOICHIOMETRY DETERMINING EXPERIMENTS^a $\lambda_1 = 493 \text{ nm}$; $\lambda_2 = 612 \text{ nm}$; $[\text{Fe}(\text{bipy})_3]^{3+}$ ($\lambda_2 = 630 \text{ nm}$) and $[\text{Ru}(\text{bipy})_3]^{3+}$ ($\lambda_1 = 436 \text{ nm}$)

Complex	$\frac{[\text{ML}_3^{3+}]^{3+}}{10^6 \times \text{M}}$	$\frac{[\text{Acid}]}{\text{M}}$	$\Delta\text{O.D.}(\lambda_1)$	$\Delta\text{O.D.}(\lambda_2)$	$\frac{[\text{ML}_3^{3+}]_c}{10^6 \times \text{M}}$	$\frac{[\text{ML}_3^{2+}]_p}{10^6 \times \text{M}}$	$R^e = \frac{[\text{ML}_3^{2+}]_p}{[\text{ML}_3^{3+}]_c}$
$[\text{Fe}(\text{phen})_3]^{3+}$	5.0	0.50 ^b	+0.0522	-0.00291	0.510	0.50	0.980
	20.0	0.20 ^c	+0.759 ^f	-0.090 ^f	8.106	8.106	1.00
	20.0	0.50 ^c	+0.559 ^f	-0.030 ^f	6.70	6.50	0.970
$[\text{Fe}(\text{Me}_4\text{-phen})_3]^{3+}$	5.0	0.5 ^c	+0.14465 ^f	-0.0143 ^f	1.100	1.100	1.00
$[\text{Fe}(\text{bipy})_3]^{3+}$	5.0	0.50 ^b	+0.04213	-0.0011	5.50	5.50	1.00
$[\text{Ru}(\text{bipy})_3]^{3+}$	5.0	0.50 ^b	+0.0722	-0.00182	6.00	6.00	1.00

^a Absorbance changes measured 5 min after the flash. Cell path = 10 cm^b HClO₄^c H₂SO₄^e The ratio R is the mean value of at least three runs^f Absorbance changes measured on Varian Techtron 635 spectrophotometer

$[\text{ML}_3^{3+}]_C$ = concentration of M(III) complex consumed

Solution of the equations (1) and (2) gives

$$[\text{ML}_3^{3+}]_C = \frac{\{\Delta A(\lambda_1) \times \epsilon_{\text{II}}' - \Delta A(\lambda_2) \times \epsilon_{\text{II}}\}}{\{\epsilon_{\text{III}}' \epsilon_{\text{II}} - \epsilon_{\text{III}} \epsilon_{\text{II}}'\} l}$$

and

$$[\text{ML}_3^{2+}]_P = \frac{\{\Delta A(\lambda_1) \times \epsilon_{\text{III}}' - \Delta A(\lambda_2) \times \epsilon_{\text{III}}\}}{\{\epsilon_{\text{III}}' \epsilon_{\text{II}} - \epsilon_{\text{III}} \epsilon_{\text{II}}'\} l}$$

The values of the molar absorbances for the $[\text{M}^{\text{III}}\text{L}_3]^{2+}$ and $[\text{M}^{\text{III}}\text{L}_3]^{3+}$ complexes at the wavelengths of the observations, are given in Table (9).

The ratio $[\text{ML}_3^{2+}]_P / [\text{ML}_3^{3+}]_C$ was found to be very close to unity [1.0 ± 0.03 , Table (8)] proving the equivalence of the production of $[\text{M}^{\text{III}}\text{L}_3]^{2+}$ complex and the loss of $[\text{M}^{\text{III}}\text{L}_3]^{3+}$ complex in the present experiments. This calculation depends upon the validity of the assumption that $\epsilon_{\text{II}}(\text{M}^{\text{II}}(\text{INT})) = \epsilon_{\text{II}}(\text{M}^{\text{II}}(\text{L}_3))$ where $\text{M}^{\text{II}}(\text{X})$ represents both the primary initial photoproduct and the final product.

The difference spectra of the photolysis products [Section 3.1 page (93)], at the end of the primary photochemical reaction (Stage I) and the secondary thermal process (Stage II), Fig. (11), show that the positions of the band maxima and the isosbestic points in the visible region (the charge transfer bands) are the same as those of the low-spin M(II) complexes with the same or related ligands. The spectral differences between the Fe(II)-complexes of phen, bipy and mono-substituted phen or bipy ligands are very small ($\lambda_{\text{max}} = 510-516$ nm, $\epsilon_{\text{max}} = 11,100-11,700$ M⁻¹ cm⁻¹, Gordon, Willian & Sutin, 1961). The assumption that $\epsilon_{\text{II}}(\text{M}^{\text{II}}(\text{INT})) = \epsilon_{\text{II}}(\text{M}^{\text{II}}(\text{L}_3))$ is therefore reasonable, and the values of the ratio $[\text{ML}_3^{2+}]_P / [\text{ML}_3^{3+}]_C$ would be unlikely to be 1.00 ± 0.03 for all the

Table (9)

ABSORPTION SPECTRAL DATA USED IN STOICHIOMETRIC CALCULATIONS

Ligand	Iron(II) Complex		Iron(III) Complex	
	λ/nm	$\epsilon/\text{M}^{-1} \text{ cm}^{-1}$	λ/nm	$\epsilon/\text{M}^{-1} \text{ cm}^{-1}$
phenanthroline	493	10,400	493	251
	510	11,100	510	472
	600	300	600	870
	612	300	612	850
Me ₄ -phenanthroline	493	13,400	493	250
	510	13,000	510	308
	600	300	600	1,280
	612	100	612	1,400
bipyridine	493	7,750	493	90
	520	8,600	520	120
	612	320	612	320
	630	100	630	300
Ligand	Ru(II) Complex		Ru(III) Complex	
	λ/nm	$\epsilon/\text{M}^{-1} \text{ cm}^{-1}$	λ/nm	$\epsilon/\text{M}^{-1} \text{ cm}^{-1}$
bipyridine	436	12,200	436	160
	454	13,800	454	78
	500	2,040	500	90
	612	20	612	316
	620	0	620	320

complexes by chance.

The data for ΔA_0 (at the end of the primary photochemical reaction, Stage I) and ΔA_∞ (at the end of the secondary thermal process, Stage II) [Table (10)] show that the ratio $\frac{\Delta A_\infty}{\Delta A_0}$ is 2.0 (within the experimental error of $\pm 5\%$) suggesting the equal and

Table (10)

RELATIVE CHANGES IN ABSORBANCE FOR STAGE I AND STAGE II

[Complex] ^a	[Acid] ^b /M	$\frac{\Delta A_\infty}{\Delta A_0} = R^c$
[Fe(phen) ₃] ³⁺	0.50	2.0
[Fe(bipy) ₃] ³⁺	0.20	1.99
[Fe(Me ₄ -phen) ₃] ³⁺	0.40 ^d	1.98
[Ru(bipy) ₃] ³⁺	0.50	1.95

(a) 5 μ M solution of the M(III) complex

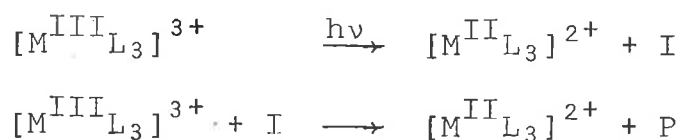
(b) Acid = HClO₄

(c) The value of R is the mean value of at least three runs and refers to at 493 nm for the Fe(III) complexes and at 436 nm for the Ru(III) complex

(d) 0.5 M H₂SO₄ due to the low solubility of the [Fe(Me₄-phen)₃]³⁺ in dilute HClO₄

equivalent production of M(II) complexes for the loss of every molecule of the M(III) complex at each Stage (I and II).

The two reaction stages can therefore be written

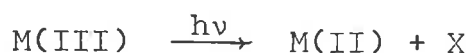


where I and P represent intermediates or final products the nature of which is discussed in Chapter (5).

SECTION 4KINETICS OF THE SECONDARY THERMAL REACTIONSIV.4.1 Introduction

The results of the experiments described in the preceding sections (2 and 3) clearly indicate that

- (i) The primary action of the flash is the reduction of the M(III)-complexes to produce transient low-spin M(II)-species (Stage I)



This reduction of the metal centre requires the equivalent production of an electron deficient species (radical).

- (ii) Following the primary photochemical reaction at low acid concentration (0.5 M) there is a slow reaction which produces a further increase in absorbance (in the wavelength range from 350-550 nm). The ratio of the change in absorbance in the primary photochemical reaction (Stage I) ΔA_0 to that in the secondary thermal process ($\Delta A_\infty - \Delta A_0$) is unity $\left[\frac{\Delta A_0}{\Delta A_\infty - \Delta A_0} = 1.0 \right]$ in 0.5 M acid. This process must be one which produces a stable low-spin M(II) species (Chapter (4) Section (3)) and an obvious reaction is the reduction of another molecule of the M(III)-complex by the intermediate formed in the primary photochemical reaction.



- (iii) No transient absorbance changes were observed which could be attributed to an intermediate formed in the initial step other than a low-spin M(II) complexes

Table (11)

RELATIVE QUANTUM YIELD^a $\left(\frac{\phi_o}{\phi_i}\right)$ WITH INCREASING ACID CONCENTRATION FOR 5 μM $[\text{ML}_3]^{3+}$ SOLUTION

$[\text{Fe}(\text{phen})_3]^{3+}$		$[\text{Fe}(\text{Me}_4\text{-phen})_3]^{3+}$		$[\text{Fe}(\text{bipy})_3]^{3+}$		$[\text{Ru}(\text{bipy})_3]^{3+}$	
$[\text{ACID}]^{\text{b}}/\text{M}$	$\Delta A_{\infty} / \Delta A_0$	$[\text{ACID}]^{\text{c}}/\text{M}$	$\Delta A_{\infty} / \Delta A_0$	$[\text{ACID}]^{\text{b}}/\text{M}$	$\Delta A_{\infty} / \Delta A_0$	$[\text{ACID}]^{\text{b}}/\text{M}$	$\Delta A_{\infty} / \Delta A_0$
0.50	2.0	0.50	1.90	0.50	1.82	0.50	1.94
1.0	1.56	1.0	1.51	1.0	1.22	1.0	1.82
2.0	1.20	1.5	1.22	1.20	1.00	2.0	1.63
3.0	1.00	2.0	1.00	2.0	0.58	3.0	1.40
4.0	0.72	10.0 ^b	0.00	3.0	0.18	5.0	1.00
6.0	0.20			6.0	0.03	6.0	0.51
8.0	0.01			8.0	0.00	8.0	0.08
10.0	0.00			10.0	0.00	10.0	0.00

^a Absorbance changes monitored at 436 nm and 493 nm for the Ru(III) and Fe(III) Complexes respectively.

^b HClO_4

^c 0.5-2.0 M H_2SO_4 used due to the insolubility of the complex in dilute HClO_4

[c.f. the similarity of the spectra of the initial product(s), final product(s) and the normal tris-chelate M(II) complexes].

These observations require the identification of the intermediate products from the primary photochemical reaction and chemical scavenging experiments and kinetic measurements were used.

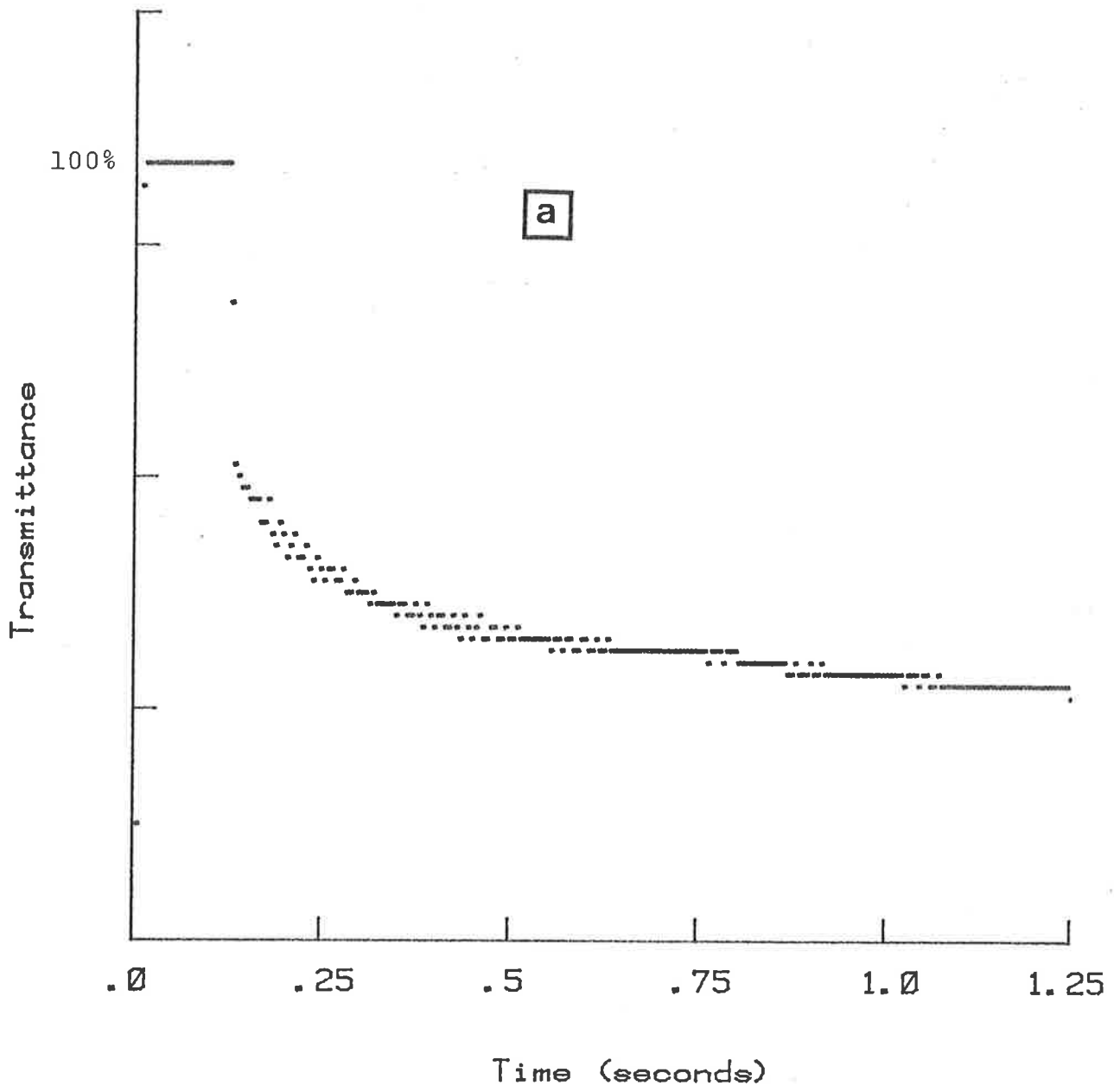
IV.4.2 Kinetics of the Secondary Thermal Reactions at Low Acid Concentration (0.50 - ca. 5 M H⁺)

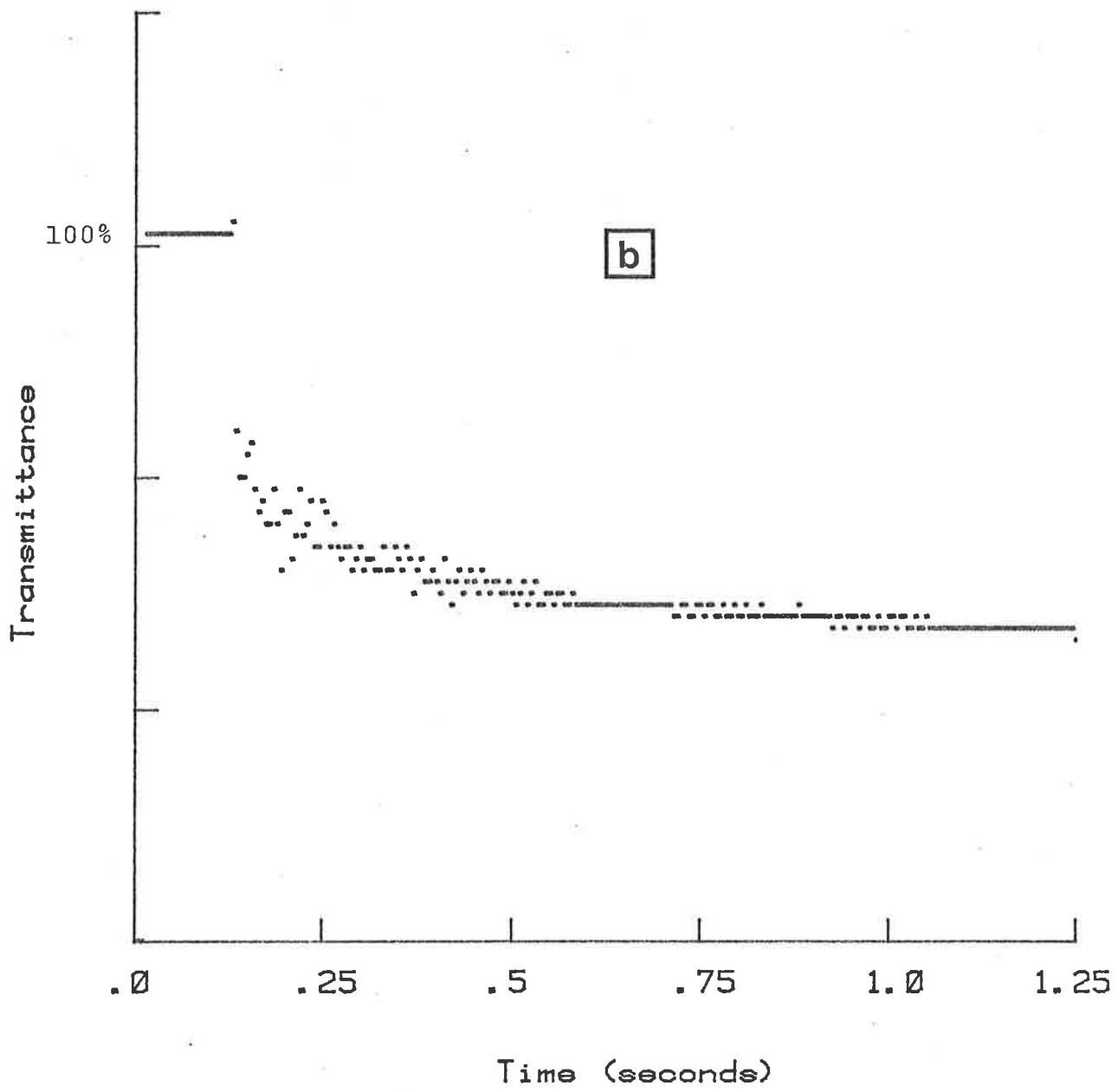
A slow reaction leading to the reduced metal products was observed for all the M(III) complexes in the present study [Fig. 15 (a, b, c and d)]. In each case the reaction was first order for at least two half lives [Page (119)] and the order was independent of the acid concentration. The extent of the reaction $\left(\frac{\Delta A_{\infty}}{\Delta A_0}\right)$, Table (11), and the first order rate constant [Table (12); Fig. (19)] decreased as the acid concentration increased. At a sufficiently high acid concentration (which differed for the different M(III) complexes) the reaction becomes unobservable at wavelengths in the visible region. The first order rate constants below this acid concentration were dependent upon the initial concentration of the M(III) complex[†] [Fig. (16)] and are therefore

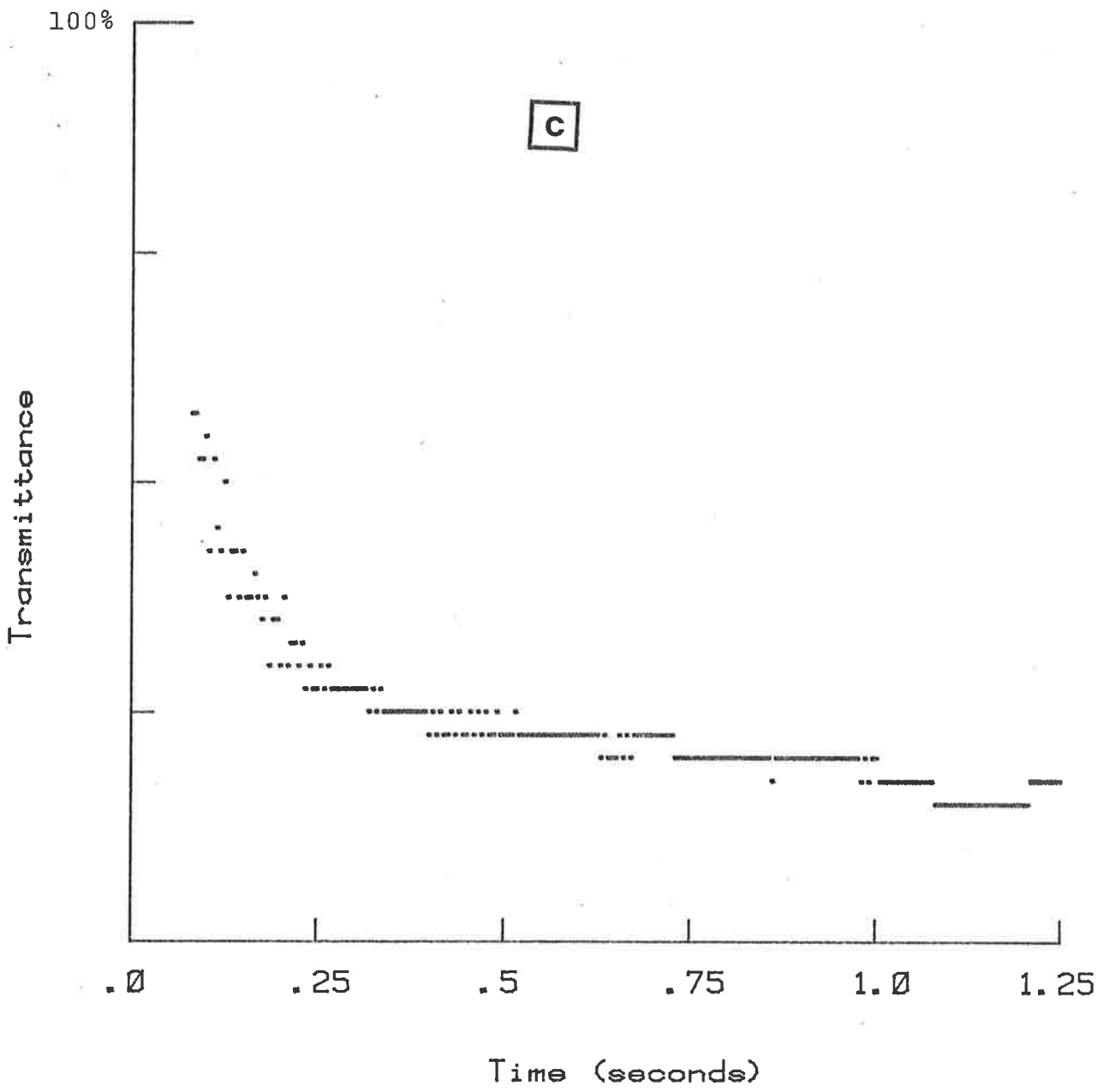
[†] In the flash experiments the concentration of the $[M^{III}L_3]^{3+}$ complex was $\geq 2.5 \mu\text{M}$ and the amount of decomposition in the primary photochemical reaction was ca. $0.25 \mu\text{M}$ for $[\text{Fe}(\text{phen})_3]^{3+}$, $[\text{Fe}(\text{bipy})_3]^{3+}$ and $[\text{Ru}(\text{bipy})_3]^{3+}$ and $0.5 \mu\text{M}$ for $[\text{Fe}(\text{Me}_4\text{-phen})_3]^{3+}$ so that effectively the initial concentration of the $[M^{III}L_3]^{3+}$ was unchanged by the flash, and the initial concentration of $[M^{III}L_3]^{3+}$ could be used in determining the true second order rate constants.

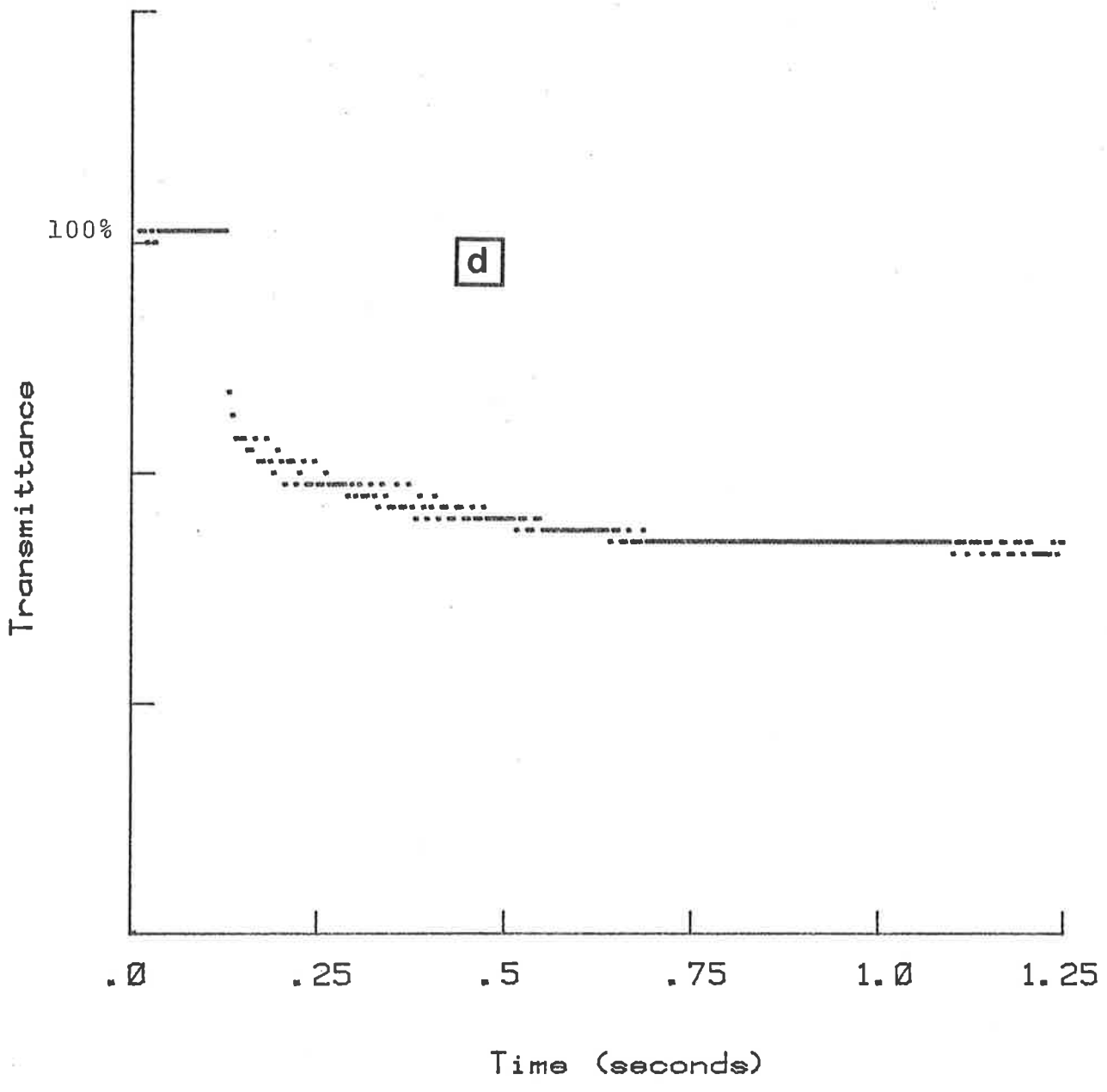
Fig. (15) The slow (Stage II) reaction in the photolysis of $[M^{III}L_3]^{3+}$ complexes. Traces showing changes in absorbance at 493 nm for the Fe(III) and at 436 nm for Ru(III) complexes.

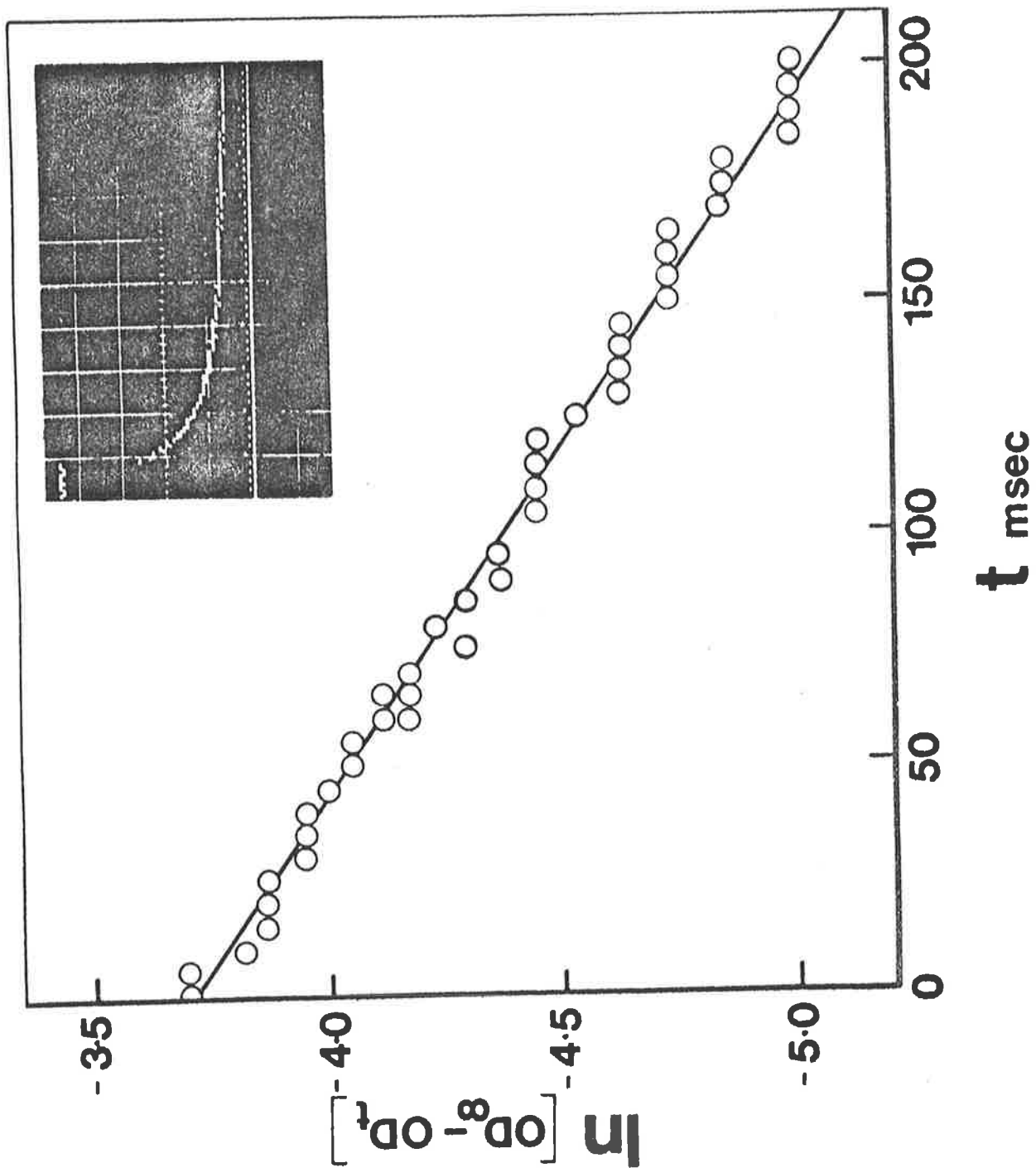
- (a) $[Fe(phen)_3]^{3+}$ (5 μ M) in 0.5 M $HClO_4$, p. 100
- (b) $[Fe(Me_4-phen)_3]^{3+}$ (5 μ M) in 0.5 M H_2SO_4 , p. 101
- (c) $[Fe(bipy)_3]^{3+}$ (5 μ M) in 0.2 M $HClO_4$, p. 102
- (d) $[Ru(bipy)_3]^{3+}$ (5 μ M) in 0.5 $HClO_4$, p. 103











First order plot for the slow formation of iron(II) phenanthroline complexes after the flash. $5 \mu\text{M} [\text{Fe}(\text{phen})_3]^{3+}$ in 0.5 M HClO_4 . The inset shows the original trace of the changes in absorbance at 493 nm , where the fast initial step is followed by the slow step which is plotted in first order form in the figure.

Fig. 16 Plots of Pseudo-first Order Rate Constants versus $[M^{III}L_3]^{3+}$ concentration

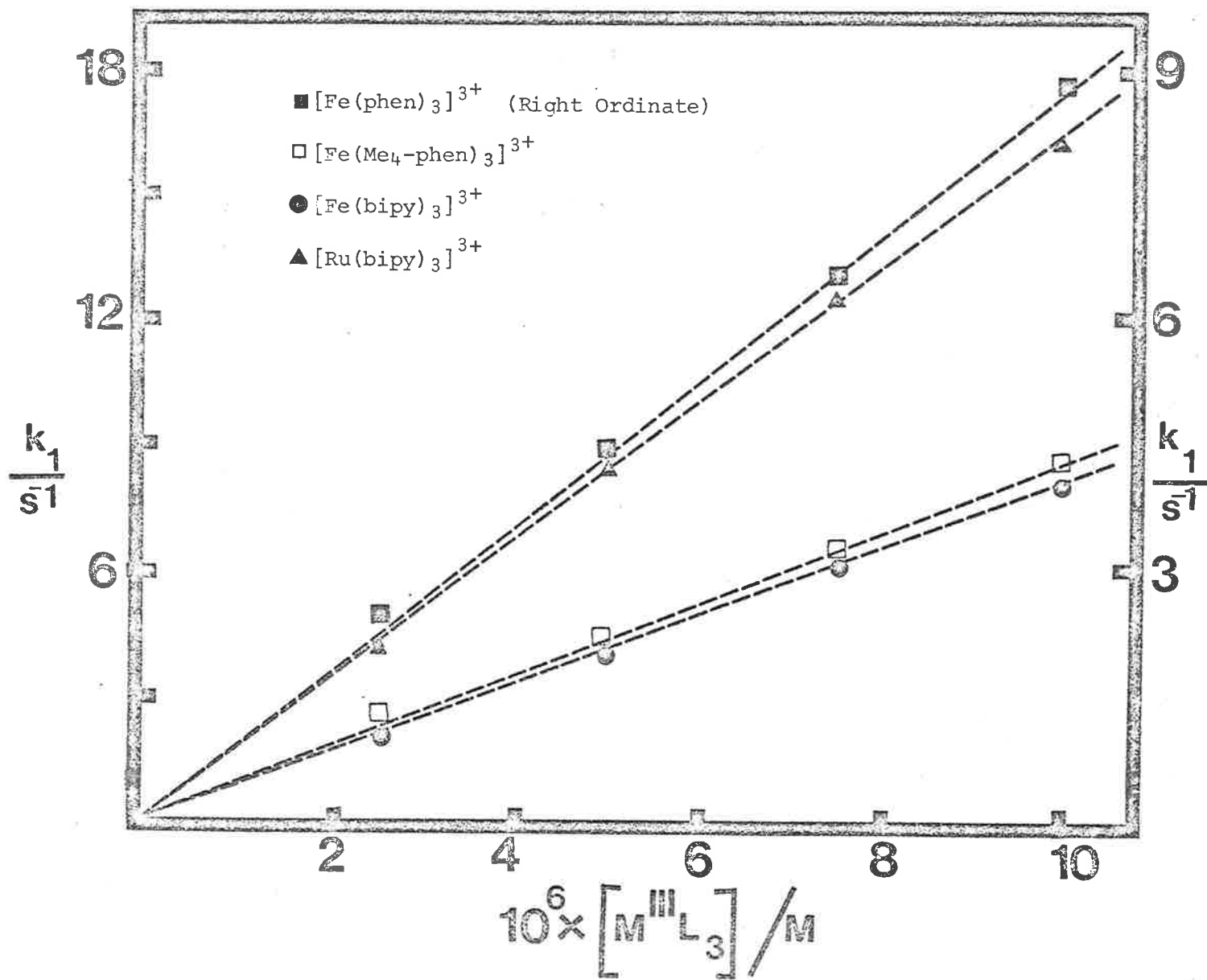


Table (12)

DATA FOR VARIATION OF k_{obs} WITH INCREASING ACID CONCENTRATION

[ACID] /M	$k_{\text{obs}} / \text{s}^{-1}$ ^a FOR SLOW FORMATION (STAGE II) OF M(III) COMPLEXES			
	[Fe(phen) ₃] ³⁺	[Fe(Me ₄ -phen) ₃] ³⁺	[Fe(bipy) ₃] ³⁺	[Ru(bipy) ₃] ³⁺
0.2	-	-	3.90	-
0.5	4.06	4.20 ^b	2.21	4.20
1.0	3.38	2.80 ^b	0.40	3.85
1.20	-	-	Unobservable*	-
1.50	2.51	1.82 ^b	-	2.90
2.0	2.15	Unobservable*	-	2.25
3.0	Unobservable*	-	-	1.35
4.0	-	-	-	0.50
5.0	-	-	-	Unobservable*

^a $k_{(\text{obs})}$ is the experimental pseudo-first order rate constant for 5 μM $[\text{ML}_3]^{3+}$ solution. Kinetic monitored at 493 nm and 436 nm for the Fe(III) and Ru(III) complexes respectively.

^b H_2SO_4 due to insolubility of the complex in dilute HClO_4 solution

* "Kinetic isosbestic effect"

pseudo-first order rate constants. The second order rate constants for the secondary thermal reaction (Stage II) at low acid concentrations were determined from the slopes of straight line plots [Table (13), Fig. (16)] of the pseudo-first order rate constants at $[M^{III}L_3]^{3+}$ concentrations between 2.5 - 10.0 μ M in 0.5 M acid at $22 \pm 2^\circ\text{C}$. The second order rate constants lie in the range $(0.63 - 1.60) \times 10^6 \text{ M}^{-1} \text{ s}^{-1}$ and are summarized in Table (13).

Table (13)
RATE CONSTANTS FOR STAGE II

Complex	$[\text{HClO}_4]/\text{M}$	Bimolecular Rate Constant/ $\text{M}^{-1} \text{ s}^{-1}$ for the reaction $[M^{III}L_3]^{2+} + [\text{Int}] \rightarrow \text{Products}$
$[\text{Fe}(\text{phen})_3]^{3+}$	0.50	$(8.60 \pm 1) \times 10^5$
	0.50 ^a	$(1.30 \pm 0.5) \times 10^6$
$[\text{Fe}(\text{Me}_4\text{-phen})_3]^{3+}$	0.50 ^b	$(8.70 \pm 0.9) \times 10^5$
$[\text{Fe}(\text{bipy})_3]^{3+}$	0.50	$(6.30 \pm 0.8) \times 10^5$
$[\text{Ru}(\text{bipy})_3]^{3+}$	0.50	$(1.60 \pm 0.5) \times 10^6$

^a 0.5M H_2SO_4

^b In 0.5 M H_2SO_4 , due to the insolubility of the $[\text{Fe}(\text{Me}_4\text{-phen})_3]^{3+}$ in dilute HClO_4 solution.

For $[\text{Fe}(\text{phen})_3]^{3+}$, the 2nd order rate constant was dependent of whether H_2SO_4 or HClO_4 was used as the source of H^+ ions. Similar differences in the rate constants in H_2SO_4 and HClO_4 have also been observed for the reduction of transition metal N-hetro-

Table (14)

SECOND ORDER RATE CONSTANTS FOR THE OXIDATION OF $\text{Fe}_{(\text{aq})}^{2+}$ IONS BY VARIOUS
TRANSITION METAL N-HETROCYCLIC COMPLEXES AT 25°C

REFERENCE: Gordon, William and Sutin (1961); Ford-Smith and Sutin (1961).

Complex	$k(0.5 \text{ M HClO}_4)$ $\text{M}^{-1} \text{ s}^{-1}$	$k(0.5 \text{ M H}_2\text{SO}_4)$ $\text{M}^{-1} \text{ s}^{-1}$	$\frac{k(0.5 \text{ M H}_2\text{SO}_4)}{k(0.5 \text{ M HClO}_4)}$
$[\text{Fe}(\text{phen})_3]^{3+}$	3.7×10^4	3.0×10^5	8.1
$[\text{Fe}(5\text{-Me-phen})_3]^{3+}$	2.0×10^4	1.5×10^5	7.5
$[\text{Fe}(5\text{-NO}_2\text{-phen})_3]^{3+}$	1.1×10^6	-	-
$[\text{Fe}(5\text{-Cl-phen})_3]^{3+}$	2.1×10^5	1.5×10^6	7.1
$[\text{Fe}(5\text{-}\phi\text{-phen})_3]^{3+}$	-	3.2×10^6	-
$[\text{Fe}(5,6\text{-Me}_2\text{-phen})_3]^{3+}$	7.8×10^3	6.9×10^4	8.8
$[\text{Fe}(4,7\text{-(C}_6\text{H}_5)_2\text{-phen})_3]^{3+}$	-	3.3×10^4	-
$[\text{Fe}(3,4,7,8\text{-Me}_4\text{-phen})_3]^{3+}$	-	1.9×10^3	-
$[\text{Fe}(\text{bipy})_3]^{3+}$	2.7×10^4	2.2×10^5	8.2
$[\text{Fe}(4,4'\text{-Me}_2\text{-bipy})_3]^{3+}$	6.0×10^2	5.9×10^3	9.8
$[\text{Fe}(\text{terpy})_3]^{3+}$	8.5×10^4	7.4×10^5	8.7
$[\text{Ag}(\text{phen})_2]^{2+}$	-	1.7×10^6	-
$[\text{Ag}(\text{bipy})_2]^{2+}$	-	1.4×10^6	-
$[\text{Ru}(\text{bipy})_3]^{3+}$	2.7×10^4	2.2×10^5	8.2
$[\text{Os}(\text{bipy})_3]^{3+}$	1.43×10^3	1.35×10^4	9.4

cyclic complexes by metal aquo ions (Gordon & Sutin, 1961; Ford-Smith & Sutin, 1961) [Table (14)] and have been attributed to the counter ion effect and to the differences of the hydrogen ion activities for the two acids in aqueous solutions at the same acid concentration.

The reductions of the M(III) N-heterocyclic tris-chelates by the M(II) aquo ions were found to occur by an outer-sphere oxidation-reduction mechanism (Gordon & Sutin, 1961; Ford-Smith & Sutin, 1961; Williams & Sutin, 1961) and the similarities of the data for the secondary thermal reactions (Stage II) suggest that the reactions are also outer-sphere. The rate constants are much higher for the rate constants of the acid hydrolysis of the $[M^{III}L_3]^{3+}$ complexes ($k \sim 10^{-(4-6)} M^{-1} s^{-1}$) (Gillard, Kane-Maguire & Williams, 1977c) and the $[M^{II}L_3]^{2+}$ complexes ($k \sim 2 - 50 s^{-1}$) (Lucie, Stranks & Burgess, 1975; Farrington, Jones & Twigg, 1977; Chagas, Tubino & Vichi, 1978). As the rate constants are greater than the rates of hydrolysis or substitution, an outer-sphere mechanism is indicated.

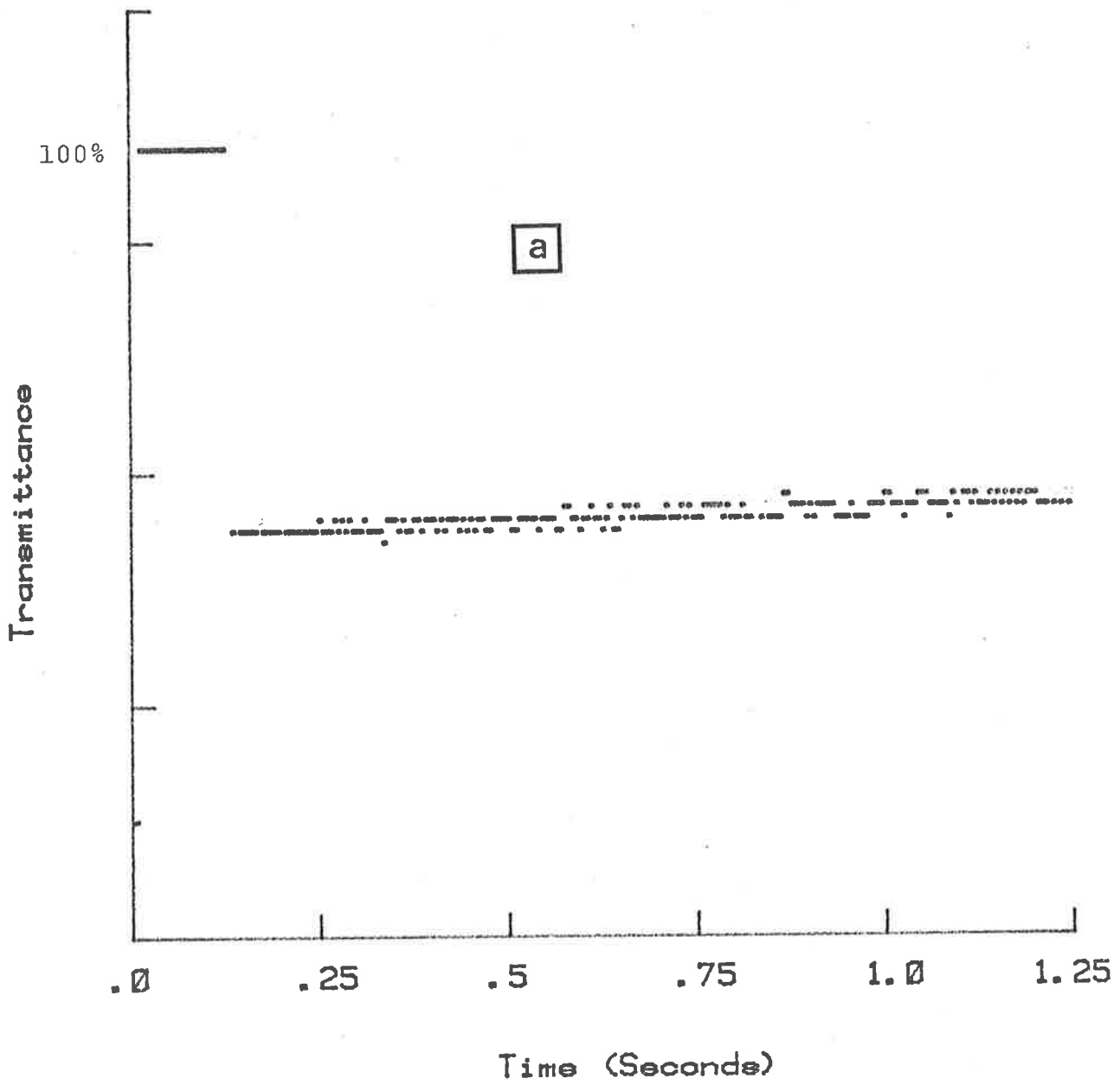
IV.4.3 Kinetics of the Secondary Thermal Reactions at High Acid Concentrations

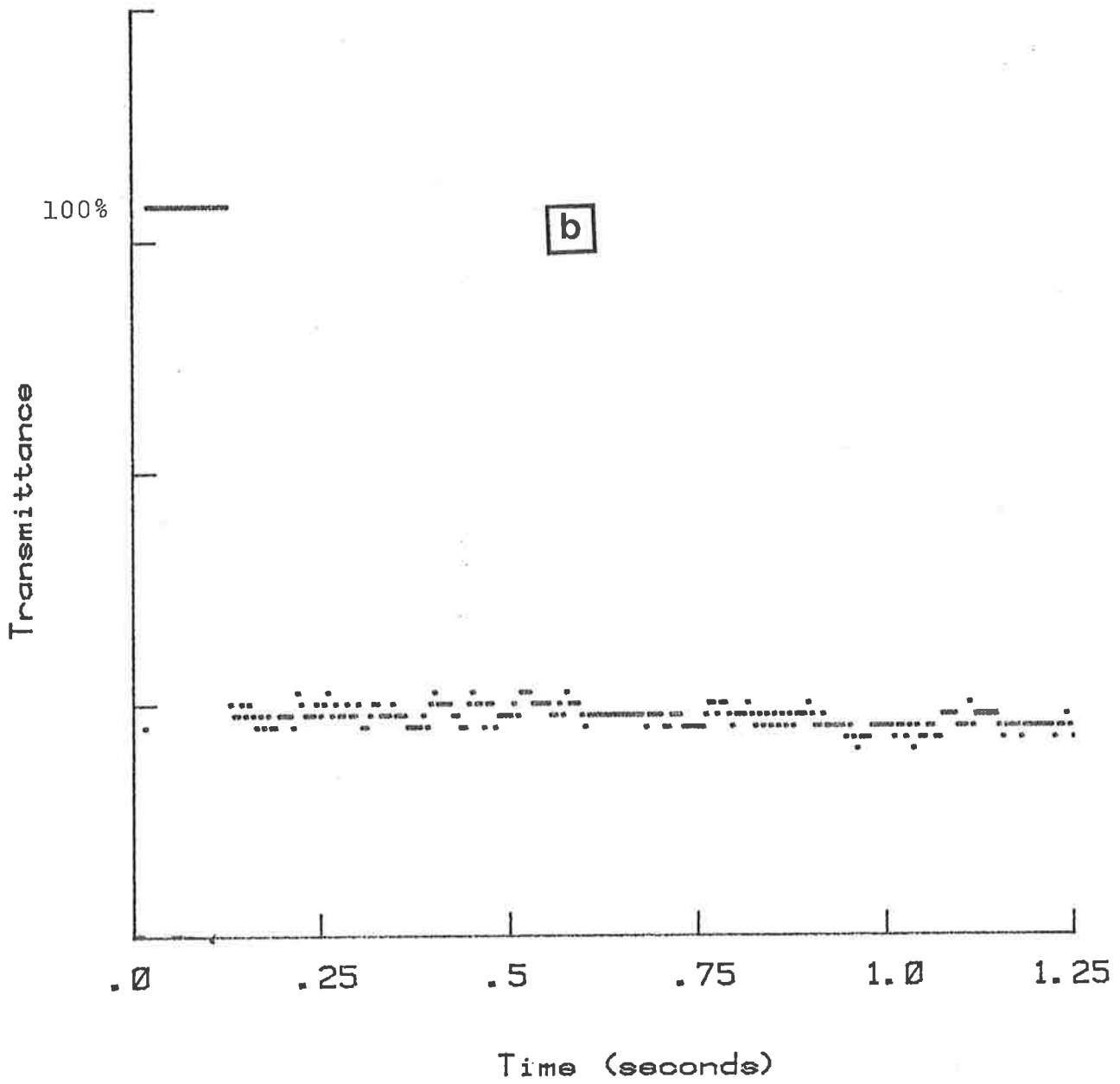
Wehry and Ward (1971) observed in steady-state photolysis experiments that the overall quantum yield[†] for the reduction of $[Fe(phen)_3]^{3+}$ fell with increasing acid concentrations and reached

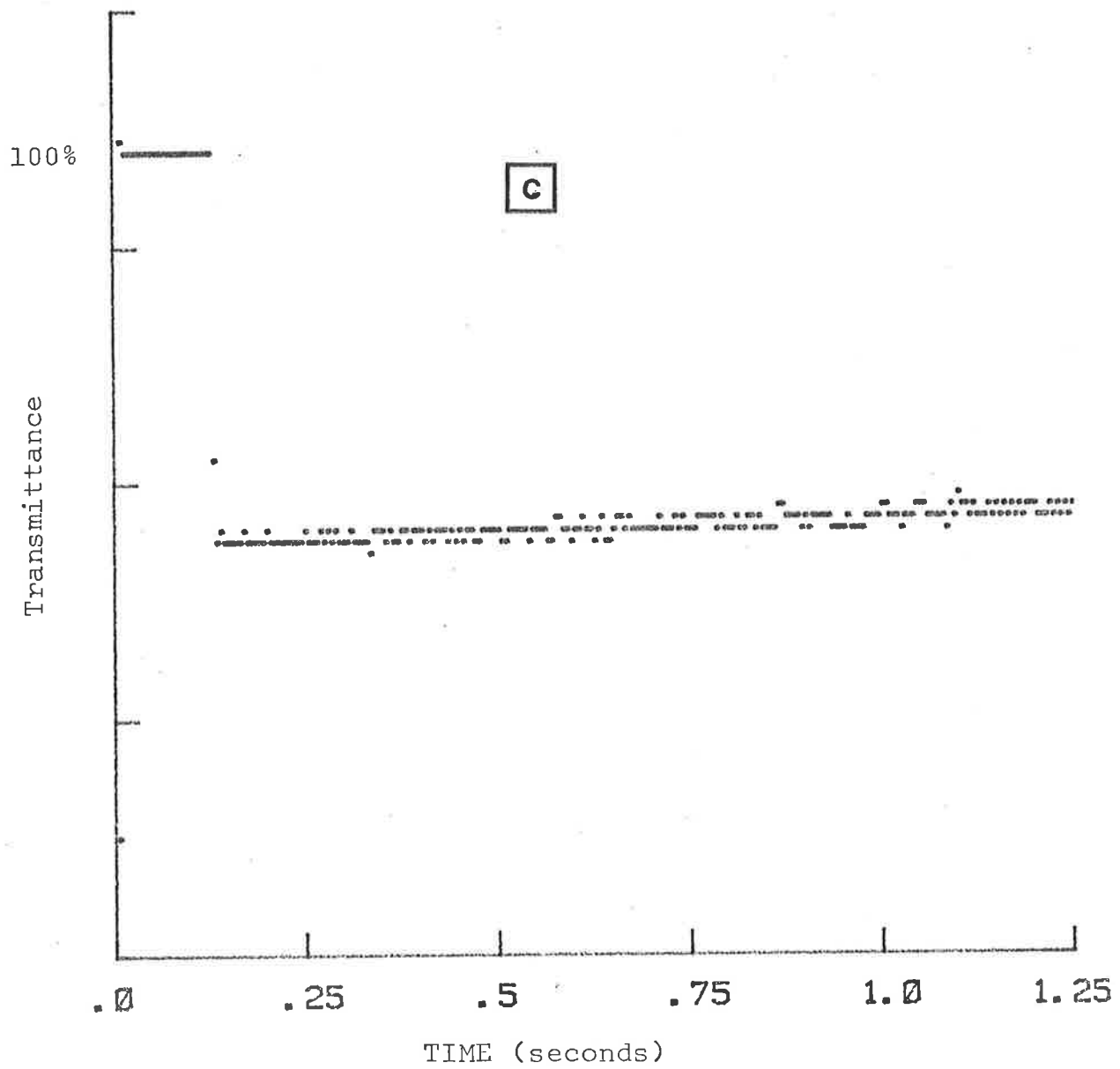
[†] In steady state photolysis experiments the product analyses may be several reaction steps removed from the initial photochemical step and the overall measured quantum yield may well be different from the primary quantum yield due to the presence of secondary thermal reactions.

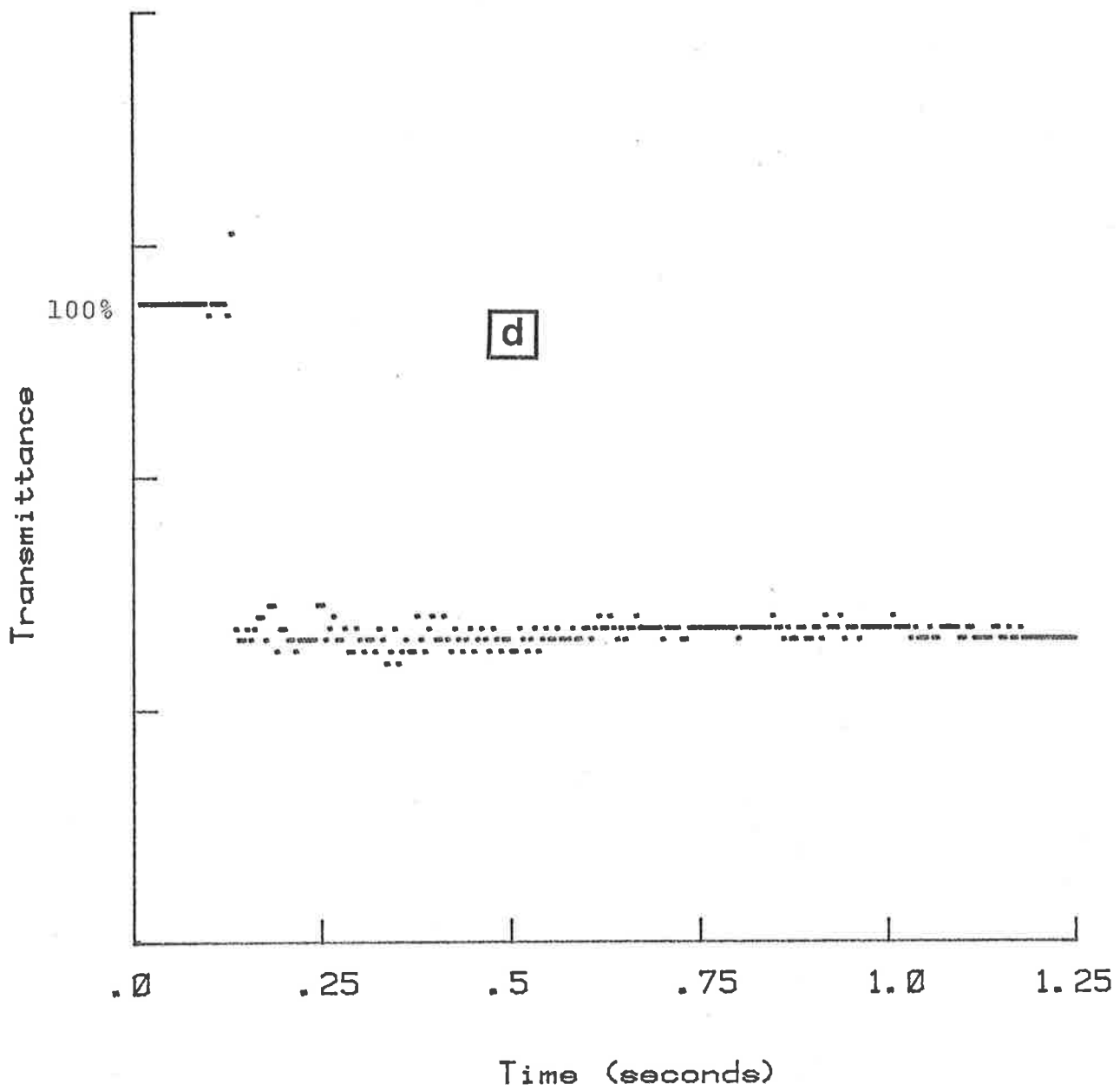
Fig. (17) "Kinetic Isosbestic Effect" in the photolysis of M(III) complexes. Traces showing changes in absorbance at 493 nm for the Fe(III) and at 436 nm for Ru(III) complexes.

- (a) $[\text{Fe}(\text{phen})_3]^{3+}$ (5 μM) in 3.0 M HClO_4 , p. 125
- (b) $[\text{Fe}(\text{Me}_4\text{-phen})_3]^{3+}$ (5 μM) in 2.0 M H_2SO_4 , p. 126
- (c) $[\text{Fe}(\text{bipy})_3]^{3+}$ (5 μM) in 1.2 M HClO_4 , p. 127
- (d) $[\text{Ru}(\text{bipy})_3]^{3+}$ (5 μM) in 5.0 M HClO_4 , p. 128





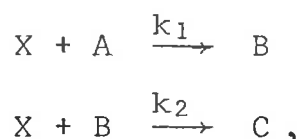




zero in 98% sulphuric acid. Flash photolysis experiments were carried over a wide range of acid concentration (0.5 - 10 M HClO₄) and some experiments were conducted in sulphuric acid (0.5 - 2.0 M, 6.0 M and 15 M).

For the iron and ruthenium complexes studied ($[M^{III}L_3]^{3+}$, L = phen, bipy or their substituted ligand ligands), the pseudo-first order rates for the slow formation of further M(II)-complexes (Stage II) decreased at constant $[M^{III}L_3]^{3+}$ concentration (5 μ M) as the acid concentration increased [Table (12), Fig. (19)]. At the same time $\frac{\Delta A_\infty}{\Delta A_0}$ decreased [Table (11), Fig. (18)]. At an acid concentration in the range 1 - 5 M (the exact value depending on the ligand and the metal) the secondary thermal reaction (Stage II) was unobservable at visible wavelengths. The kinetics were monitored at 493 nm for the Fe(III) complexes and at 436 nm for the Ru(III) complex and there was no further absorbance change after the initial change at this acid concentration [Figure (17)]. This may be termed a "kinetic isosbestic effect".

A "kinetic isosbestic effect" arises from two competing reactions,



for which the rate constants are such that no overall change in the concentration of the species B takes place. For appropriate molar absorbances, at a particular wavelength, no time dependent change in absorbance will be observed. It is this condition which is termed here a "kinetic isosbestic effect". At the acid concentration for which the "kinetic isosbestic effect" was observed, the immediate ($t_{1/2} < 10 \mu$ sec) increase in absorbance at the end of Stage I, was not followed by a further slow increase

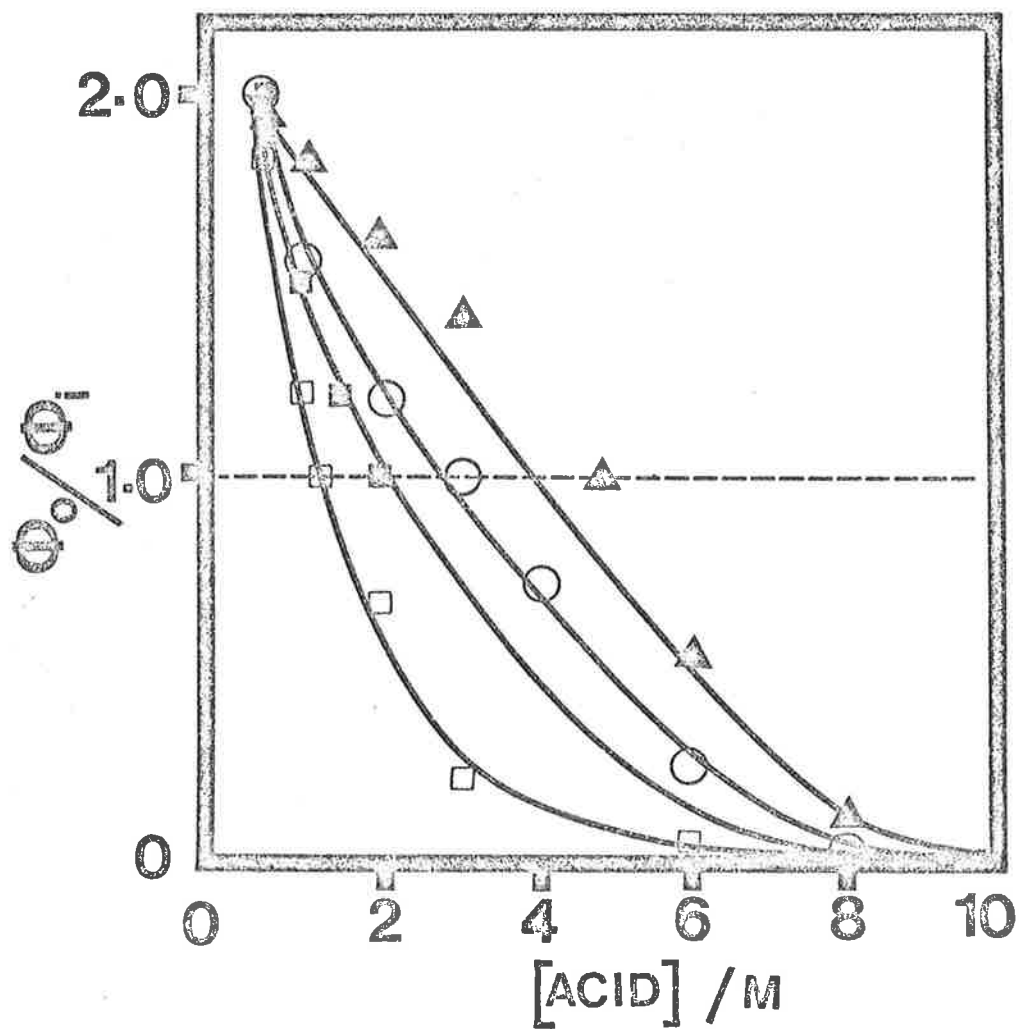
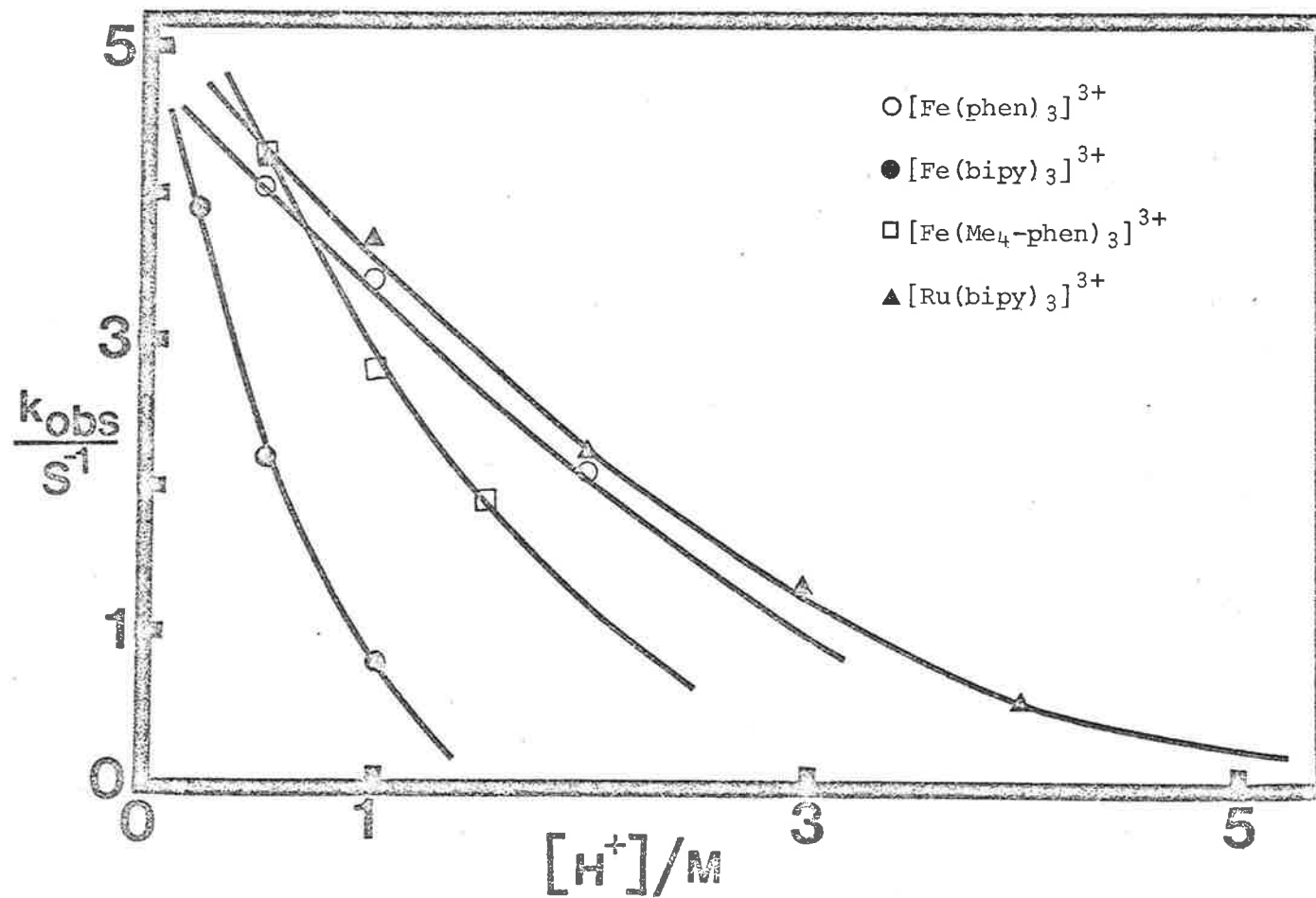


Fig. 18 Plots of Variation of Relative Quantum Yield with Increasing Acid

- O $[\text{Fe}(\text{phen})_3]^{3+}$
- $[\text{Fe}(\text{Me}_4\text{-phen})_3]^{3+}$
- $[\text{Fe}(\text{bipy})_3]^{3+}$
- ▲ $[\text{Ru}(\text{bipy})_3]^{3+}$

Fig. 19 Variation of the Pseudo-first Order Rate Constant (k_{obs}) for the Slow Formation of M(II) Complexes (Stage II) with Increasing Acid Concentration



(Stage II) but stayed constant. The effect of acidity is summarized in Table (12) and Fig. (19) shows the variation of the pseudo-first order rate constants for the slow formation of M(II) complexes with increasing acid concentration (0.5 - ca. 5 M).

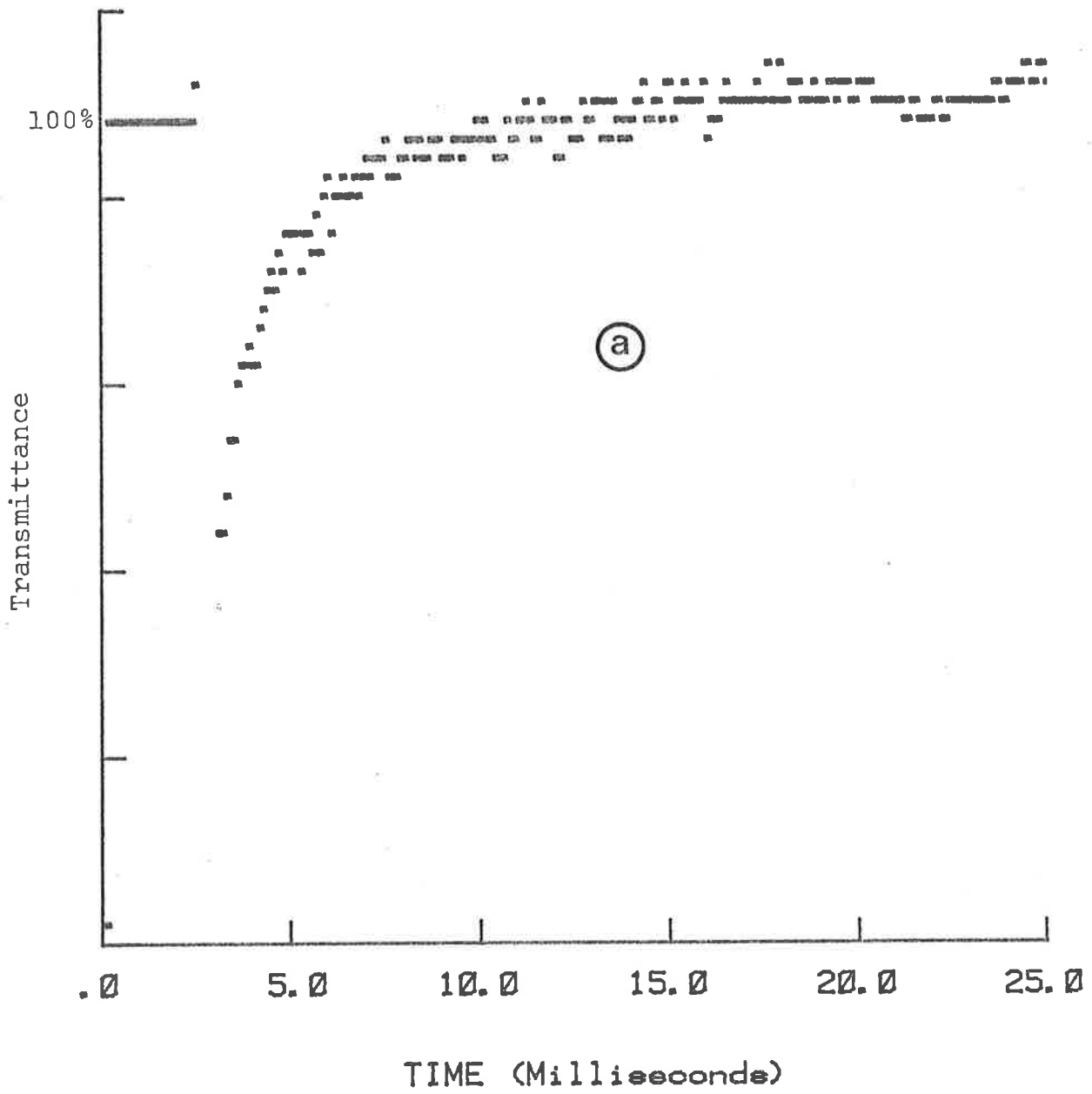
When the acid concentration was increased above that at which the "kinetic isosbestic effect" was observed the initial increase in absorbance (Stage I) was followed by a decay of the absorbance in which the M(III)-complexes were regenerated [Fig. 20 (a, b, c and d)]. The extent of this reaction, measured by ΔA_{∞} , increased with the acid concentration.

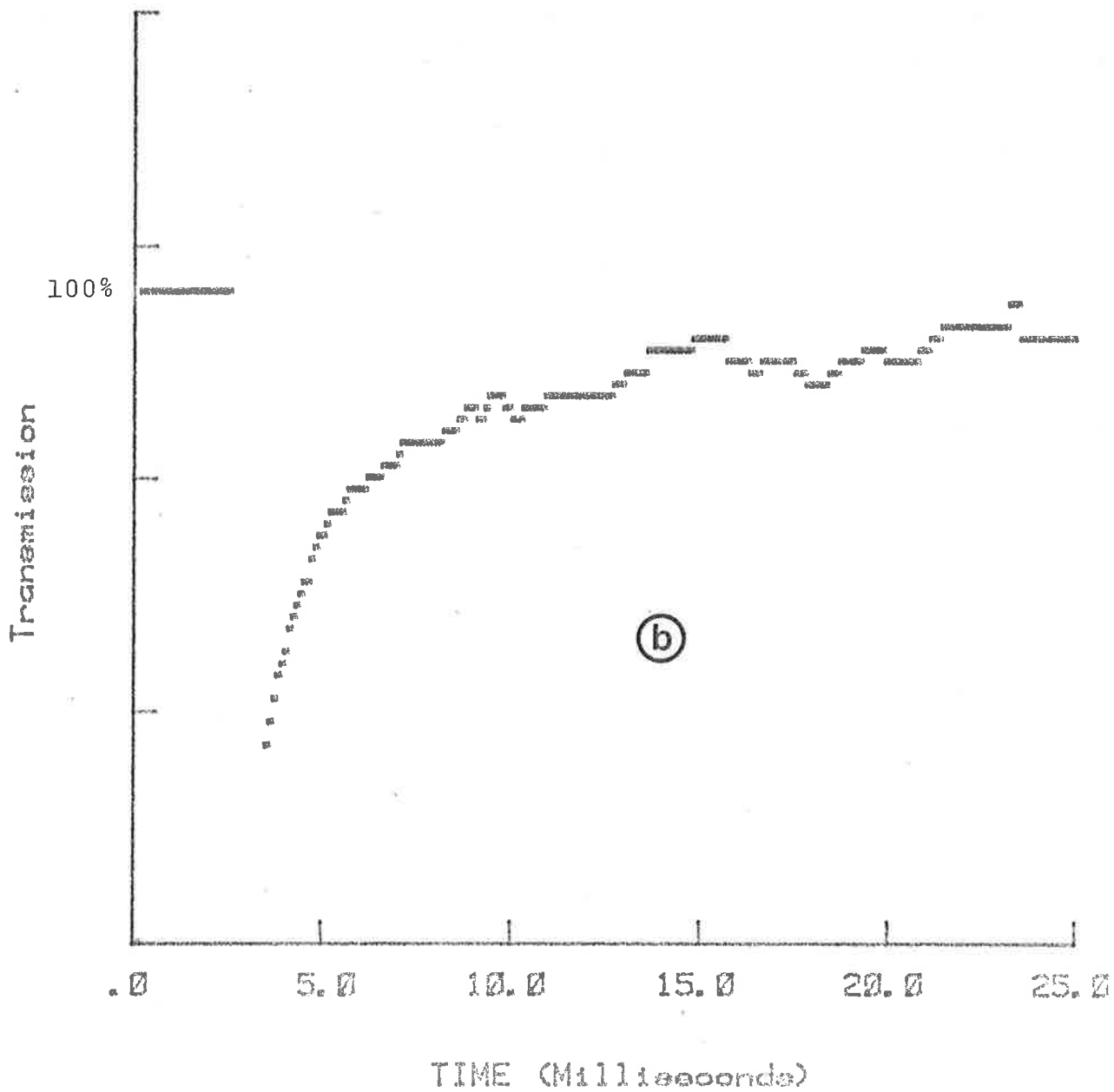
In 10 M HClO₄ or 15 M H₂SO₄ the absorbance at the end of this secondary reaction was that before the flash (within $\pm 0.1\%$) at all wavelengths. The effect is therefore that the overall quantum yield falls to zero at the highest acid concentrations although the initial quantum yield measured immediately after the flash (ΔA_0) is acid independent [Table (17)]. The rate of decay of the initial increase in absorbance (ΔA_0 at 493 nm for Fe(III) complexes and at 436 nm for the Ru(III) complex) was first order in all cases and was independent of the concentration of the M(III) complex. The first order rate constant for the decay of the transient absorbance to reform M(III) complex increased as the acid concentration increased. The dependence of the rate constant on the acid concentration for this decay was greater than first order. Neither the plot of $k_{1st}(\text{obs})$ vs $[\text{Acid}]^{\dagger}$ nor $k_{\text{obs}}/\text{Acid}$ vs $a_{\text{H}_2\text{O}}$ was linear [Fig. (21 and 22)], suggesting a complex acid dependence for the rate of regeneration of the

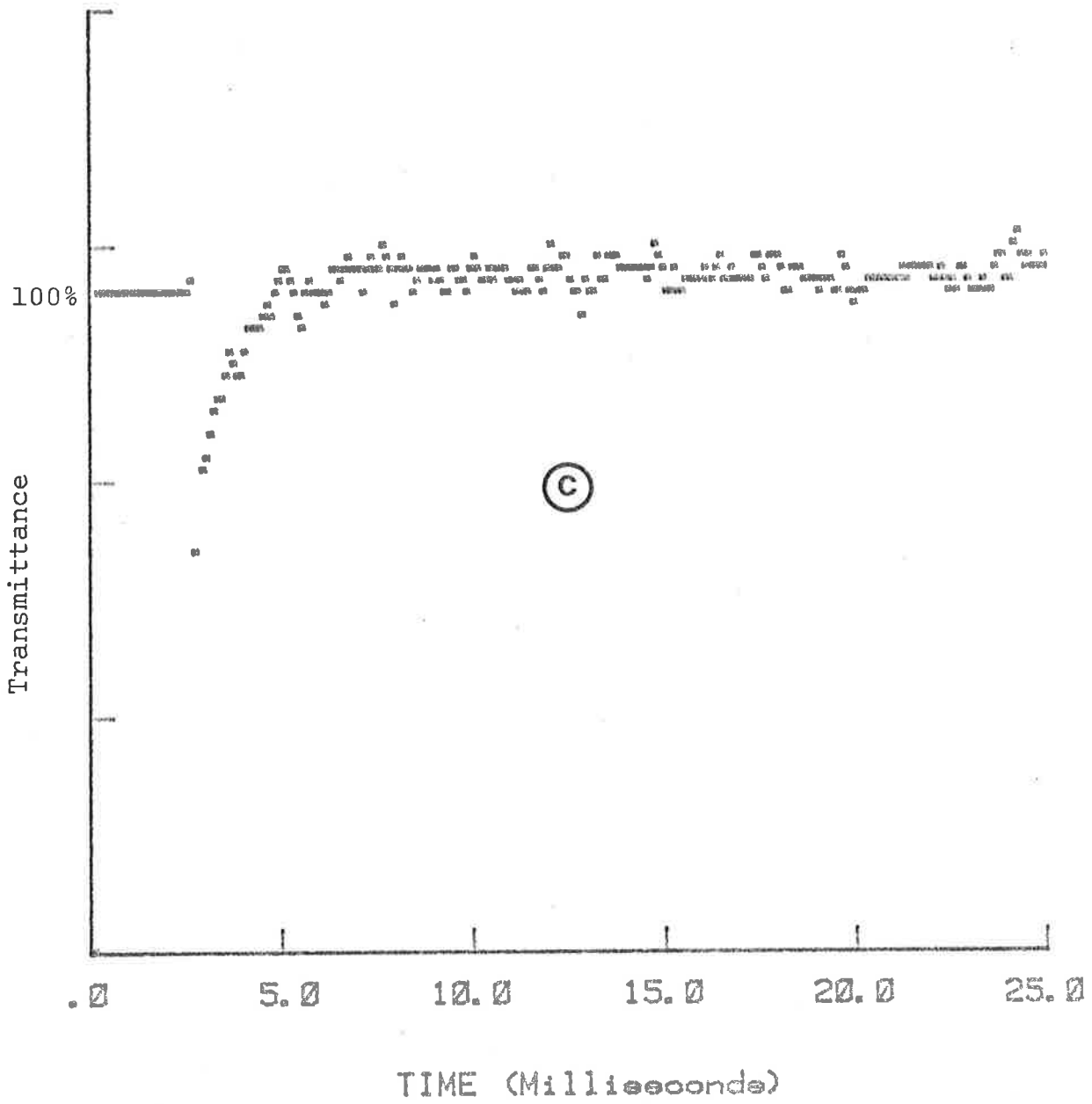
[†] At acid concentrations ≥ 6.0 M HClO₄ k_{1st} vs $[\text{H}^{\dagger}]$ would be meaningless as nothing is known about the $[\text{H}^{\dagger}]$ in such high acidities (Bunnet, 1961).

Fig. (20) Decay of the transient absorbance (Stage I) to reform M(III) complexes. Traces showing changes in absorbance at 493 nm for the Fe(III) and at 436 nm for Ru(III) complexes. For all the traces the initial concentration of the M(III) complex was 5 μ M in 10 M HClO₄.

- (a) [Fe(phen)₃]³⁺, p. 133
- (b) [Fe(Me₄-phen)₃]³⁺, p. 134
- (c) [Fe(bipy)₃]³⁺, p. 135
- (d) [Ru(bipy)₃]³⁺, p. 136







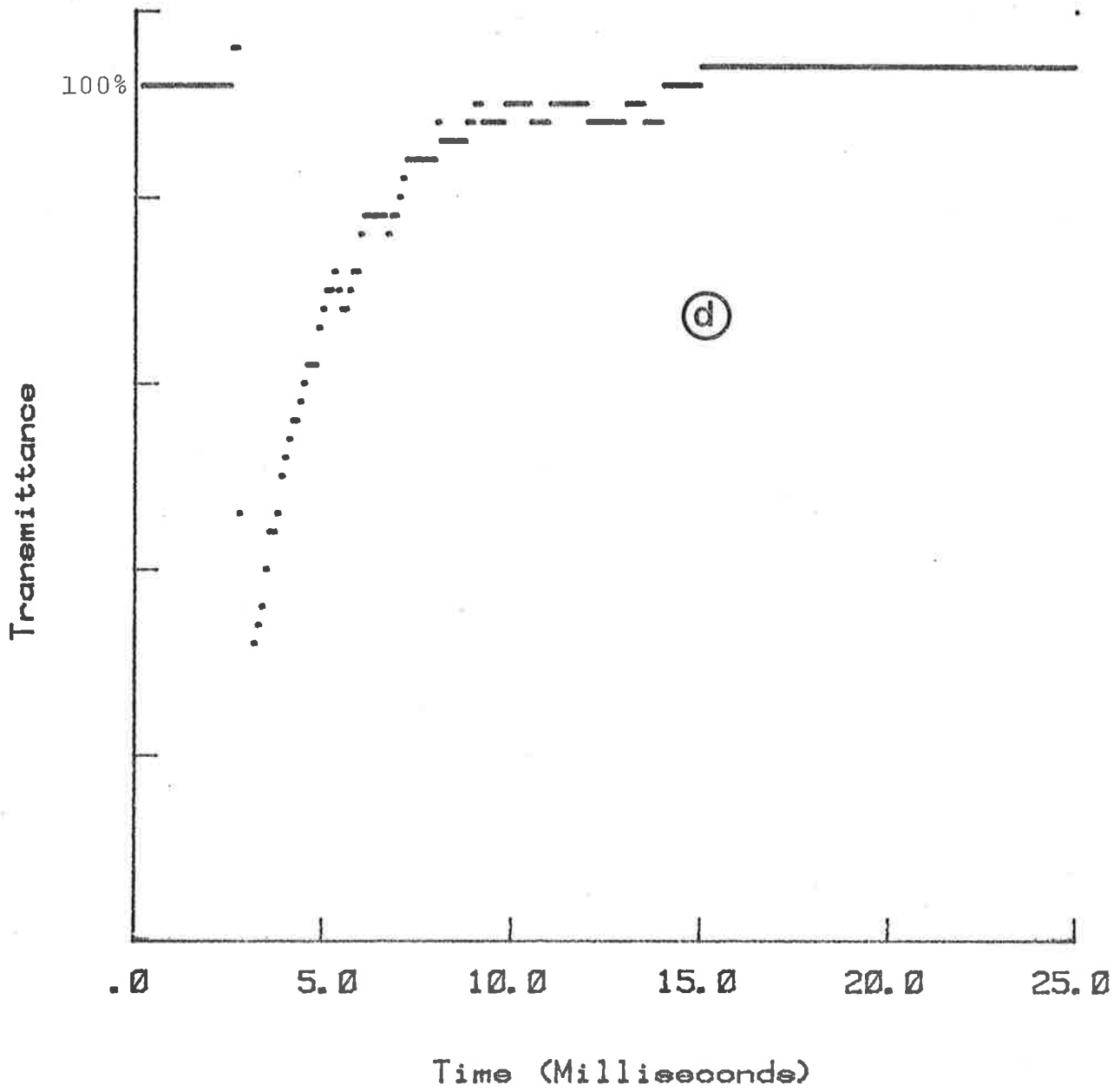


Table (15)

DATA FOR k_{obs} WITH INCREASING ACID CONCENTRATION

$\frac{[\text{ACID}]^a}{\text{M}}$	$k_{\text{obs}}^b / \text{s}^{-1}$ FOR THE TRANSIENT DECAY TO REFORM $[\text{M}^{\text{III}}\text{L}_3]^{3+}$			
	$[\text{Fe}(\text{phen})_3]^{3+}$	$[\text{Fe}(\text{Me}_4\text{-phen})_3]^{3+}$	$[\text{Fe}(\text{bipy})_3]^{3+}$	$[\text{Ru}(\text{bipy})_3]^{3+}$
3.0	-	-	0.136	-
4.0	0.65	-	0.25	-
5.0	-	-	1.00	-
6.0	35.30	-	32.20	19.30
7.0	-	-	165.30	-
8.0	272.20	230.30	360.50	153.50
9.0	-	327.51	487.80	-
10.0	540.10	-	-	-
10.00	482.46 ^c	525.0	1175.50	286.40

^a HClO_4 ^b $k_{(\text{obs})}$ is the pseudo-first order rate constant (k_{expt}) for $5 \mu\text{M}$ $[\text{ML}_3]^{3+}$ solution. ^c $10 \mu\text{M}$ $[\text{Fe}(\text{phen})]^{3+}$.^b Kinetics monitored at 493 nm and 436 nm for the Fe(III) and Ru(III) complexes respectively.

Fig. 21 Plots of $k_{(obs)}$ Versus Acid Concentration

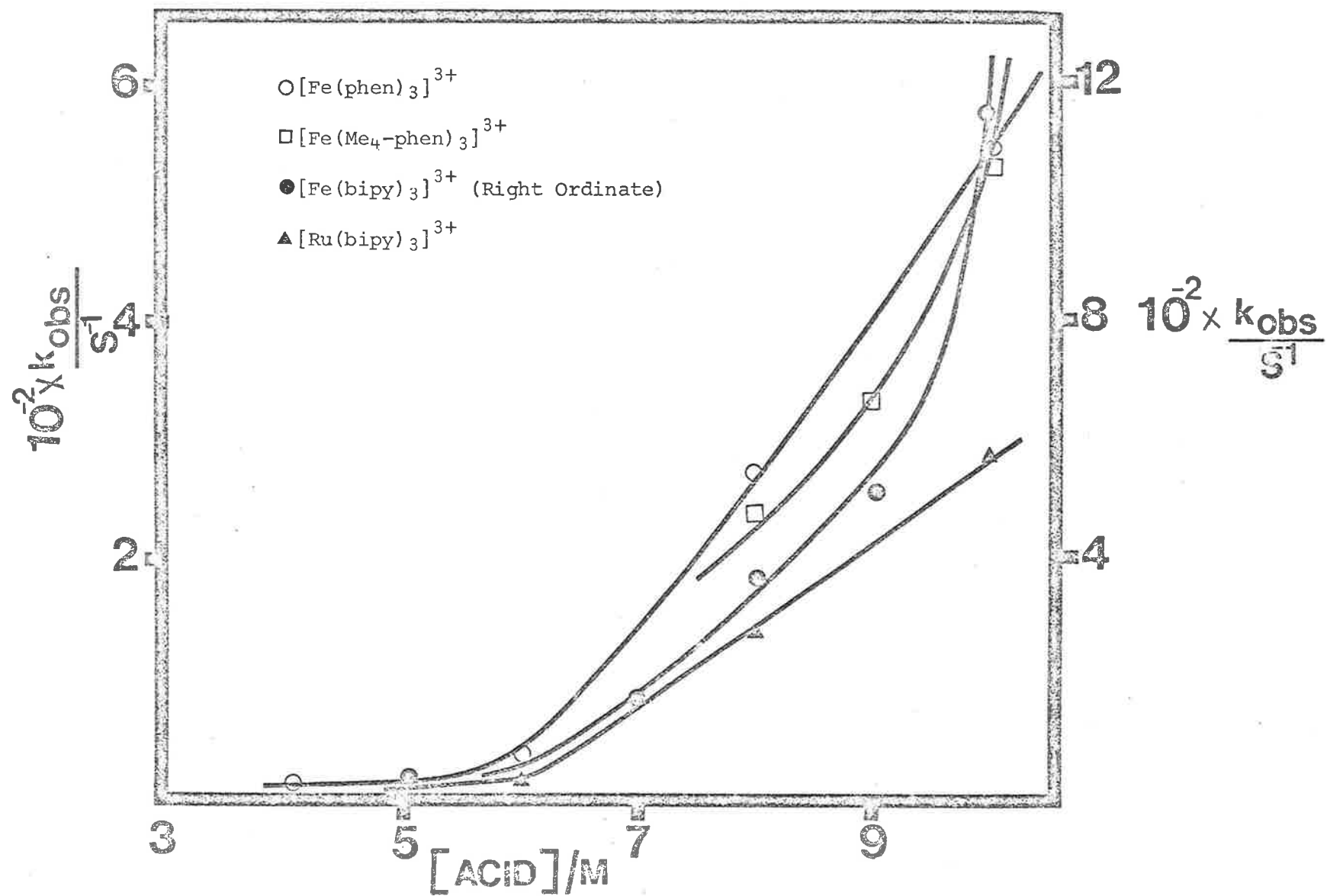


Table (16)

EFFECT OF THE ACTIVITY OF WATER ON THE DECAY OF
THE TRANSIENT TO REFORM $[M^{III}L_3]^{3+}$ COMPLEX

Complex ^a	$\frac{[Acid]^b}{M}$	a_{H_2O}	$k_{obs}^c = \frac{k_1}{[Acid]}$
$[Fe(phen)_3]^{3+}$	4.0	0.733	0.16
	6.0	0.47	6.0
	8.0	0.193	34.0
	10.0	-	54.0
$[Fe(Me_4-phen)_3]^{3+}$	8.0 ^d	0.193	34.0
	9.0 ^d	0.100	40.0
	10.0 ^d	-	53.80
$[Fe(bipy)_3]^{3+}$	3.0	0.83	0.45
	4.0	0.733	0.625
	6.0	0.470	6.4
	7.0	0.32	33.0
	8.0	0.193	44.0
	9.0	0.104	50.8
	10.0	-	118.0
$[Ru(bipy)_3]^{3+}$	6.0	0.470	3.8
	8.0	0.193	19.2
	10.0	-	28.6

^a $[Complex] = 5.0 \times 10^{-6} M$

^b $HClO_4$

^c Kinetics monitored at 493 nm for the Fe(III) Complexes and at 436 nm for the Ru(III) Complex. $k_1 = k_{expt}$ (pseudo-first order)

^d Lower $HClO_4$ concentrations not possible due to the insolubility of the Complex.

Fig. 22 Graphs Showing the Effect of Water Activity. Plots of $k_{(obs)}/[Acid]$ versus a_{H_2O}

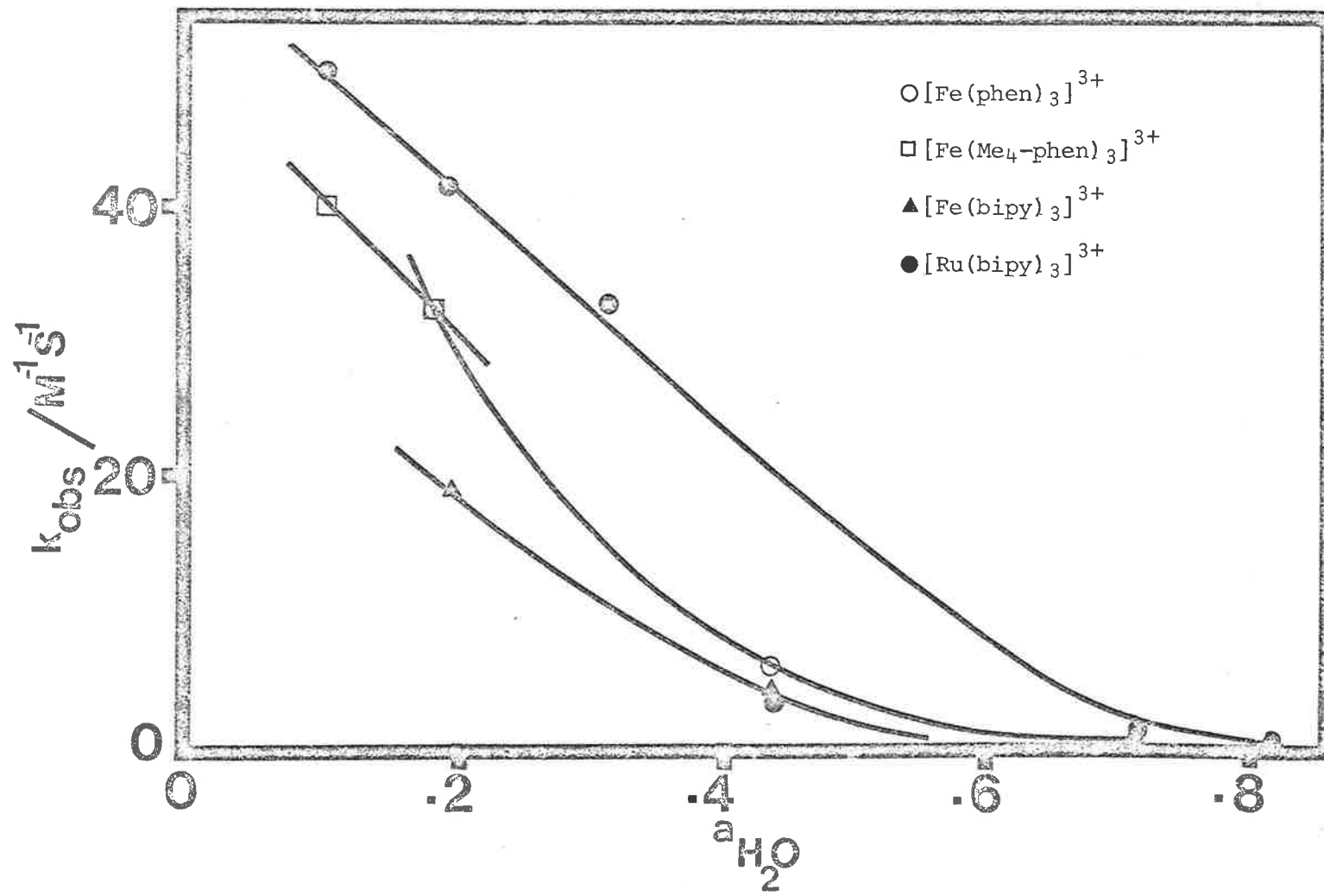


Table (17)
PRIMARY QUANTUM YIELDS^a

$[\text{Fe}(\text{phen})_3]^{3+}$		$[\text{Fe}(\text{Me}_4\text{-phen})_3]^{3+}$		$[\text{Fe}(\text{bipy})_3]^{3+}$		$[\text{Ru}(\text{bipy})]^{3+}$	
$[\text{Acid}]^c/\text{M}$	$10^2 \times \Delta A_0$	$[\text{Acid}]^b/\text{M}$	$10^2 \times \Delta A_0$	$[\text{Acid}]^c/\text{M}$	$10^2 \times \Delta A_0$	$[\text{Acid}]^c/\text{M}$	$10^2 \times \Delta A_0$
0.50	2.97	0.50	7.67	0.2	3.20	0.5	3.22
1.00	2.51	1.0	8.00	0.5	2.98	1.0	3.41
2.00	2.58	1.50	7.80	1.0	2.86	2.0	3.30
3.00	2.66	2.00	7.43	3.0	2.79	3.0	3.25
6.00	2.56	10.00 ^c	7.02	5.0	2.94	8.0	3.90
8.00	2.35			10.00	3.10	10.0	3.60
10.00	2.21						

^a The yields per flash measured for 5 μM $[\text{ML}_3]^{3+}$ solutions. The variations in the yields for different runs may be attributed to the flash lamp output and the EHT needed for the back off voltages. The absolute values are also dependent upon the voltage level for the 100% transmittance. Error = $\pm 15\%$.

^b H_2SO_4 due to the insolubility of the Complex

^c HClO_4

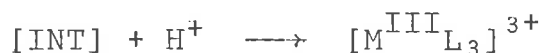
M(III) complex. This may reflect changes in the water activity in the solution which falls rapidly at high acid concentration as well as changes in the hydrogen ion activity [Table (18)] and the ionic strength dependence of the reaction.

The immediate absorbance (ΔA_0) and the final absorbance change at infinite time ΔA_∞ (both ΔA 's refer to the absorbance changes in the range of 350 - 500 nm) after the end of the thermal reaction are proportional to the primary quantum yield (ϕ_i) and overall quantum yield (ϕ_0) respectively and the ratio $\frac{\Delta A_\infty}{\Delta A_0}$ is the ratio of the quantum yields (ϕ_0/ϕ_i) of the overall and the primary photochemical processes. The variations of the quantum yields for the various $[ML_3]^{3+}$ complexes with acid concentration are given in Table (11) and Fig. (18) shows the plots of ϕ_0/ϕ_i versus acid concentration.

IV.4.4 Summary of the Effect of Acidity

The effects of acidity (0.5 - 10 M HClO₄) on the rate constants and relative quantum yields suggests the existence of two competing secondary thermal processes for the decay of an initial reactive intermediate [INT].

(a) An acid catalysed path to regenerate the original M(III) complex (dominant at high acid concentration)



and (b) A reaction with another molecule of $[M^{III}L_3]^{3+}$ at low acid concentration to produce more M(II) species. This reaction is a dominant one at 0.5 M HClO₄ and observable at 0.5 - 4.0 M (depending upon the complex).



Table (18)

THE ACTIVITY OF WATER IN DIFFERENT ACIDS AT 25°C

REFERENCE: Bunnet, (1961)

Molarity of Acid	Activity of H ₂ O		
	HCl	HClO ₄	H ₂ SO ₄
0.5	0.982	0.982	0.982
1.0	0.962	0.959	0.960
1.5	0.940	0.933	0.933
2.0	0.914	0.906	0.906
2.5	0.885	0.871	0.865
3.0	0.851	0.830	0.822
3.5	0.818	0.783	0.775
4.0	0.782	0.733	0.721
4.5	0.753	0.673	0.667
5.0	0.700	0.610	0.604
5.5	0.659	0.536	0.541
6.0	0.615	0.468	0.479
6.5	0.570	0.388	0.420
7.0	0.527	0.319	0.364
7.5	0.481	0.250	0.309
8.0	0.439	0.193	0.259
8.5	0.399	0.144	0.214
9.0	0.360	0.100	0.173
9.5	0.324	0.071	0.138
10.0	0.289	-	0.108
10.5	0.256	-	0.0828

Table (19)

ACTIVITY COEFFICIENTS OF ACIDS AT 25°C

Reference: Robinson and Stokes (1959)
 "Electrolyte Solutions",
 Butterworths, London, 2nd ed.

Molarity	HCl	HBr	HI	HClO ₄	HNO ₃
0.1	0.796	0.805	0.818	0.803	0.791
0.2	0.767	0.782	0.807	0.778	0.754
0.3	0.756	0.777	0.811	0.768	0.735
0.4	0.755	0.781	0.823	0.766	0.725
0.5	0.757	0.789	0.839	0.769	0.720
0.6	0.763	0.801	0.860	0.776	0.717
0.7	0.772	0.815	0.883	0.785	0.717
0.8	0.783	0.832	0.908	0.795	0.718
0.9	0.795	0.850	0.935	0.808	0.721
1.0	0.809	0.871	0.963	0.823	0.724
1.2	0.840	0.917	1.027	0.858	0.734
1.4	0.876	0.969	1.098	0.900	0.745
1.6	0.916	1.029	1.175	0.947	0.758
1.8	0.960	1.094	1.260	0.998	0.775
2.0	1.009	1.168	1.356	1.055	0.793
2.5	1.147	1.389	1.641	1.227	0.846
3.0	1.316	1.674	2.015	1.448	0.909
3.5	1.518	-	-	1.726	-
4.0	1.762	-	-	2.08	-
4.5	2.04	-	-	2.53	-
5.0	2.38	-	-	3.11	-
5.5	2.77	-	-	3.83	-
6.0	3.22	-	-	4.76	-

IV.4.5 The Effect of the Concentration of $[M^{III}L_3]^{3+}$ at Constant Acid Concentration

Since the rate of decay of the initial transient absorbance (Stage I) to form the original M(III) complex is independent of the concentration of $[ML_3]^{3+}$ and rate of slow increase in absorbance (from 350 nm to 550 nm range) to further produce M(II)-species (Stage II) is a linear function of the $[ML_3]^{3+}$ concentration Fig. (16) and both these processes have the same rate at the "kinetic isosbestic acid concentration" this effect should be dependent upon the concentration of the $[ML_3]^{3+}$. An increase in $[ML_3]^{3+}$ concentration will favour the slow formation of the increased absorbance (Stage II, at 493 nm for the Fe(III) complexes and at 436 nm for the Ru(III) complex) due to the M(II) species while the decay of the initial transient absorbance to reform the original complex will be favoured by decreasing the $[ML_3]^{3+}$ concentration. This effect was observed for $[Fe(phen)_3]^{3+}$.

At a $[Fe(phen)_3]^{3+}$ concentration of 5 μ M in 3.0 M HClO₄ no change in absorbance was observed after the primary photochemical reaction ("kinetic isosbestic point") while slow formation occurred for 10 μ M $[Fe(phen)_3]^{3+}$ in 3.0 M HClO₄. On the other hand decay of the initial transient absorbance towards the original complex was observed for 2.5 μ M $[Fe(phen)_3]^{3+}$ [Fig. (23)]. Close to 3.0 M HClO₄, the changes in absorbances were too small for the rate constants to be measured accurately. However, the effects of the $[Fe(phen)_3]^{3+}$ concentrations shown in Fig. (23) at acid concentrations close to that at which no secondary thermal process followed the initial photochemical reaction confirmed the reaction scheme involving two competing processes.

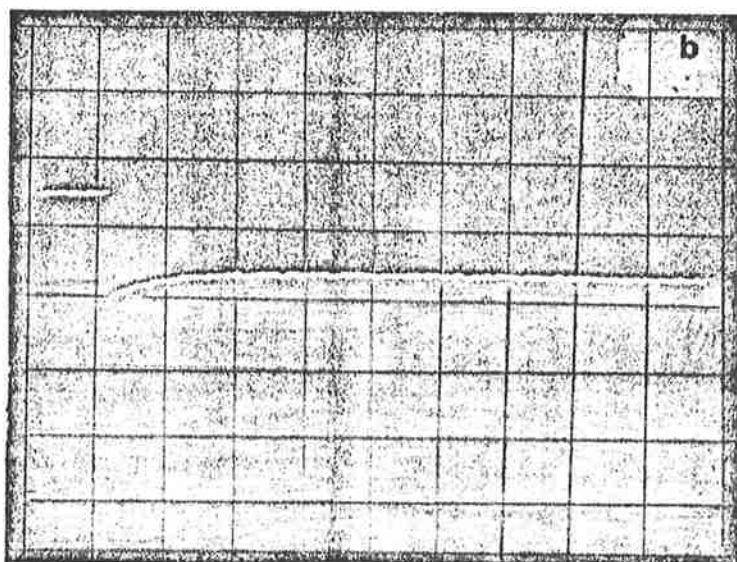
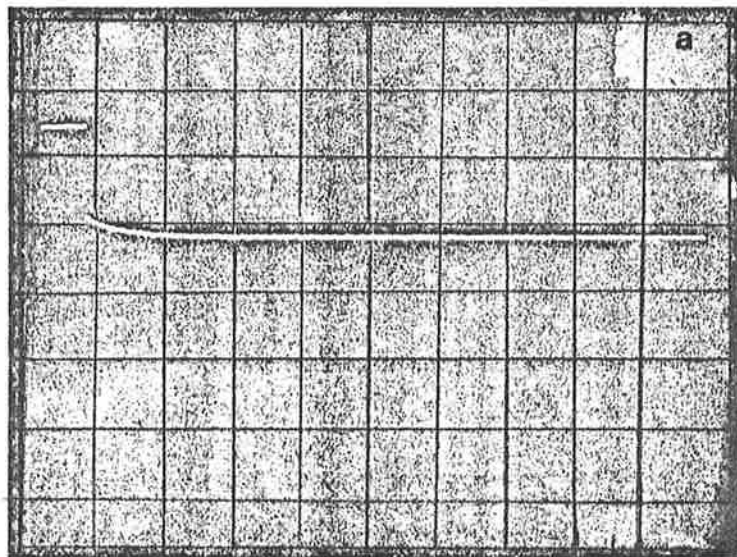


Fig. (23) Flash pictures showing the effect of $[\text{Fe}(\text{phen})_3]^{3+}$ concentration (a = 10 μM ; b = 2.5 μM) at 3 M HClO_4 on the photolysis of $[\text{Fe}(\text{phen})_3]^{3+}$ ion. For both the flash pictures vertical full scale = 0.5 V and the horizontal scale = 125 m sec/division

IV.4.6 Influence of Ionic Strength

The effect of increasing the acid concentration in decreasing the quantum yield for the overall process [$\phi_0 \rightarrow 0$ at 10 M HClO_4 , Table (11), Fig. (18)] was due to the relative effects of the acid concentration on the two reactions which competed for the intermediate produced in the primary photochemical process. Because of the large changes in ionic strength between 0.5-10 M HClO_4 it was not immediately apparent that the effect was primarily due to the change in acid concentration or to the change in the ionic strength.

Photolysis of a 5 μM solution of $[\text{Fe}(\text{phen})_3]^{3+}$ in 0.5 M HClO_4 were carried out at different ionic strengths [Table (20)]. NaClO_4 was used to adjust the ionic strengths. Fig. (28) shows the changes in absorbance after the flash at $I = 5.0$ M, $[\text{H}^+] = 0.5$ M.

Table (20)
EFFECT OF IONIC STRENGTH

$[\text{Fe}(\text{phen})_3^{3+}]$ μM	$[\text{HClO}_4]$ M	ionic strength (I) M	k_{obs} s^{-1}	$\frac{\Delta A_{\infty}}{\Delta A_0} = R$
5.0	0.5	2.0	$(3.7 \pm 0.5) \times 10^{-1}$	1.40
5.0	0.5	3.0	$(1.06 \pm 0.2) \times 10^{-1}$	1.00
5.0	0.5	4.0	$(0.79 \pm 0.1) \times 10^{-1}$	0.03
5.0	0.5	5.0	$(0.81 \pm 0.09) \times 10^{-1}$	0.02

At ionic strengths > 3 M the transient absorbance decays to reform the original M(III) complex [Fig. (24)]. The extent of the decay increased with increasing ionic strength (the value

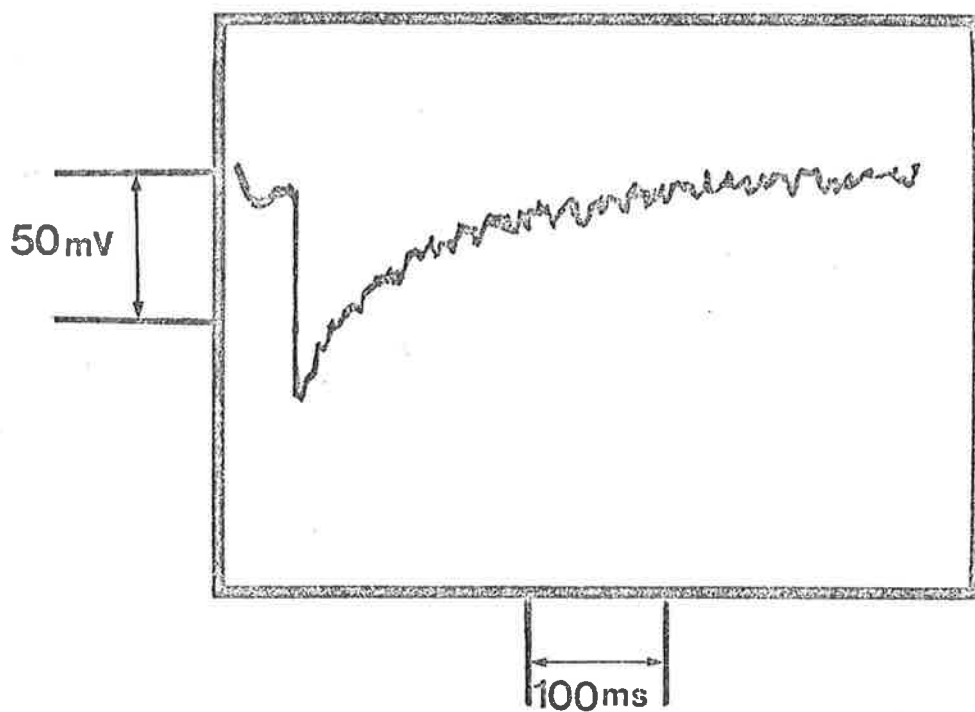


Fig. 24 Flash Picture Showing the Effect of Ionic Strength (5.5 M) on the Photolysis of $[\text{Fe}(\text{phen})_3]^{3+}$

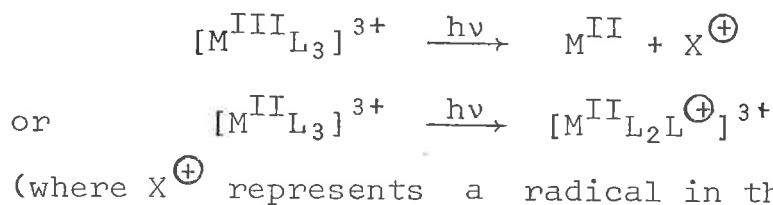
of $\Delta A_{\infty}/\Delta A_0$ decreases[†]). The decay was first order even at $I = 5.0$ M and was independent of ionic strength between 4.0 and 5.0 M. The effect of increasing ionic strength parallels that of increasing acid concentration [Fig. (18), Table (15)].

[†] The kinetics and the absorbance changes were monitored at 493 nm. $k(\text{obs})$ is the pseudo-first order rate constant.

SECTION 5 THE NATURE OF THE INTERMEDIATE SPECIES

IV.5.1 Chemical Scavenging Experiments

The primary photochemical reaction produces an M(II) low-spin species [Section (3) Page (93)] and it must involve an electron transfer to produce an equivalent one electron deficient species (radical). Two possible reactions to produce an oxidized ligand and a reduced metal centre are:



Wehry and Ward (1971) suggested that hydroxyl radicals are produced in the photolysis of $[Fe(phen)_3]^{3+}$ in aqueous solution and proposed the reaction,



as the primary photoreaction. They found that methylmethacrylate (MMA), in the solution of $[Fe(phen)_3]^{3+}$, was polymerized during the photolysis. Attempts have therefore been made to identify hydroxyl radicals in the flash photolysis of the $[M^{III}L_3]^{3+}$ complexes.

Hydroxyl radical is a weakly absorbing species ($\epsilon_{max} \sim 10^3$ $M^{-1} cm^{-1}$, $\lambda_{max} \sim 200$ nm, Matheson & Dorfman, 1969) and therefore the direct detection of the hydroxyl radical is difficult in strongly absorbing solutions of the metal(III) and metal(II) complexes. Experiments with well-known hydroxyl radical scavengers (alcohols, halide ions) and $Cu^{2+}(aq)$ ions were carried out in order to determine the possible role of hydroxyl radicals in the photochemical reductions and to determine the nature of the intermediate species.

IV.5.2 Scavenging of Hydroxyl Radicals(i) Alcohol Scavengers

Methanol, ethanol and t-butanol are known to scavenge hydroxyl radicals at nearly diffusion controlled rates (ca. $10^9 \text{ M}^{-1} \text{ s}^{-1}$, Asmus, Moeckel & Henglein, 1973). If the secondary thermal



reaction at low acid concentrations, which produces further M(II) species (Stage II), involves a reaction between hydroxyl radicals and the M(III) complex then the extent of the reaction ($\Delta A_\infty - \Delta A_0$) and the rate constant for Stage (II) would be expected to decrease in the presence of hydroxyl radical scavengers. R^\bulletO radicals produced in this way might themselves react with $[\text{M}^{\text{III}}\text{L}_3]^{3+}$ to produce $[\text{M}^{\text{II}}\text{L}_3]^{2+}$.



However alkoxy radicals are much less reactive than OH radicals and in this case rate constants for the slow thermal production of $[\text{M}^{\text{II}}\text{L}_3]^{2+}$ (Stage II) would be expected to be much smaller.

The effect of hydroxyl radical scavengers on the secondary thermal reaction (Stage II) for $[\text{Fe}(\text{phen})_3]^{3+}$ is summarized in Table (21).

Table (21)

EFFECT OF ALCOHOL SCAVENGERS ON $k_{1\text{st}}$ (STAGE II)

Scavenger	Concentration of the Scavenger/M	k^a (Stage II)/ s^{-1}	$(\Delta A_\infty - \Delta A_0)^b$
none	0	3.91 ± 0.4	1.01
CH_3OH	0.10	4.02 ± 0.3	1.12
$\text{CH}_3\text{CH}_2\text{OH}$	0.10	4.15 ± 0.5	1.05
$(\text{CH}_3)_3\text{COH}$	0.10	3.95 ± 0.5	1.03

^a k_{1st} (Stage II) is the observed pseudo-first order rate constant.

^b The kinetics monitored at 493 nm for $5 \mu\text{M}$ $[\text{Fe}(\text{phen})_3]^{3+}$ in 0.5 M HClO_4 .

The data in Table (21) clearly indicate that the slow increase in absorbance (k (Stage II)) is unaffected by the addition of MeOH, EtOH and t-butanol in concentrations up to 0.1 M . Under these conditions hydroxyl radicals react with the alcohols in $\leq 0.01 \mu\text{sec}$ and effectively all the hydroxyl radicals are scavenged.

Table (22)

SUMMARY OF RATE CONSTANTS FOR REACTIONS
OF OH RADICALS WITH $[\text{ML}_3]$ COMPLEXES

Complex	Rate Constant $\text{M}^{-1} \text{ s}^{-1}$	Reference
$[\text{Fe}(\text{phen})_3]^{2+}$	$\sim 10^{10}$	Pagsberg & Floryan, 1976
$[\text{Fe}(\text{phen})_3]^{3+}$	$(0.6 - 2.0) \times 10^{10}$	Creutz & Sutin, 1975
$[\text{Ru}(\text{bipy})_3]^{2+}$		
$[\text{Ru}(\text{bipy})_3]^{3+}$		

The lack of decrease in the rate constant or the extent ($\Delta A_\infty - \Delta A_0$) of the slow formation of the M(II) complexes (Stage II) cannot be due to the competitive scavenging of the hydroxyl radicals by the $[\text{Fe}(\text{phen})_3]^{3+}$. The concentration of $[\text{Fe}(\text{phen})_3]^{3+}$ was $5 \mu\text{M}$ and such scavenging would require a rate constant of $> 10^{11} \text{ M}^{-1} \text{ s}^{-1}$ for the reaction



The reaction between the hydroxyl radical and the Fe(II) low-spin complex, produced in the primary photochemical reaction,



would be even less favourable due to its lower concentration (ca. 0.25 μM). The rate constant for the reaction,



is $\sim 10^{10} \text{ M}^{-1} \text{ s}^{-1}$ (Pagsberg & Floryan, 1976).

The hydroxyl radical is a strongly oxidizing species [Chapter I, Page (32)] and it is difficult to see how a low-spin M(II) complex (primary photoproduct) could, by reacting with hydroxyl radicals, produce M(II) species (i.e. cause the 'Stage II reaction'). The reaction of OH radicals with $[\text{Fe(phen)}_3]^{2+}$ produces a ligand hydroxy-adduct (Pagsberg & Floryan, 1976) and the generation of



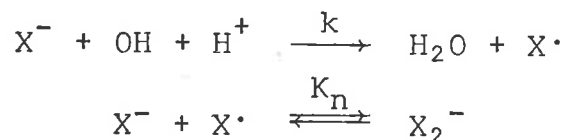
OH radicals in the bulk solution (Wehry & Ward, 1971) seems kinetically and energetically unfavourable. The rate constants of hydroxyl radicals with the scavengers used are summarized below.

SUMMARY OF RATE CONSTANTS OF OH RADICALS WITH
ALCOHOL AND HALIDE ION SCAVENGERS

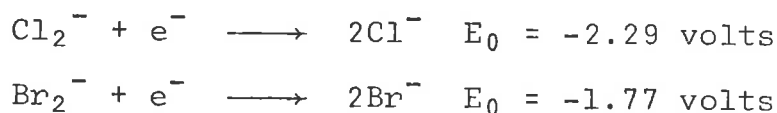
Scavenger	Rate Constant $\text{M}^{-1} \text{ s}^{-1}$	Reference
MeOH	8.3×10^8	Neta & Dorfman, 1968
EtOH	1.1×10^9	Rabani & Stein, 1962
t-But OH	5.2×10^8	Wilson et al., 1971
Cl^-	3.5×10^9	Thornton & Laurence, 1973
Br^-	2×10^9	Thornton & Laurence, 1974

(ii) Halide Ion Scavengers

Hydroxyl radicals react with halide ions (X^-) to give halogen radical anions (X_2^-) (Thornton & Laurence, 1973, 1974).

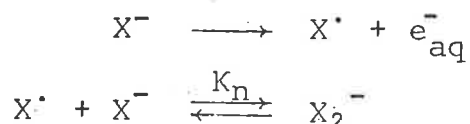


The pseudo-second order rate constants for the reactions of halide ions with hydroxyl radicals in 0.5 M H^+ are ca. $3.5 \times 10^9 \text{ M}^{-1} \text{ s}^{-1}$ and $2 \times 10^9 \text{ M}^{-1} \text{ s}^{-1}$ for Cl^- and Br^- respectively (Thornton & Laurence, 1973, 1974) and the equilibrium constant (K_n) is $\geq 10^5 \text{ M}^{-1}$ ($X = Cl, Br$) (Thornton & Laurence, 1973, 1974). The halogen radical anions are strong oxidizing agents (Thornton & Laurence, 1973, 1974) and absorb at 370 nm ($\epsilon \sim 8 \times 10^3 \text{ M}^{-1} \text{ cm}^{-1}$



where there is isosbestic point for the photochemical reduction of $[Fe(phen)_3]^{3+}$, Fig. (10). Detection of halogen radical anions is therefore relatively simple at 370 nm.

Flash photolysis of solutions containing $5 \mu\text{M } [Fe(phen)_3]^{3+}$ and 0.5 M $HClO_4$ was carried out in the presence (10^{-2} M) and absence of Cl^- and Br^- ions. The monitoring wavelength was 372 nm. The results are summarized in Table (23). In the presence of $10^{-2} \text{ M } X^-$ ($X = Br, Cl$), the change in absorbance after the flash at 372 nm corresponded to the production of X_2^- species in less than 3% of the yield of Fe(II) complex under the same conditions. The presence of $10^{-2} \text{ M } X^-$ did not change the transient absorbances seen at 493 nm. The small yield of X_2^- can be fully accounted for by the absorption of light in the halide ion. The photolysis



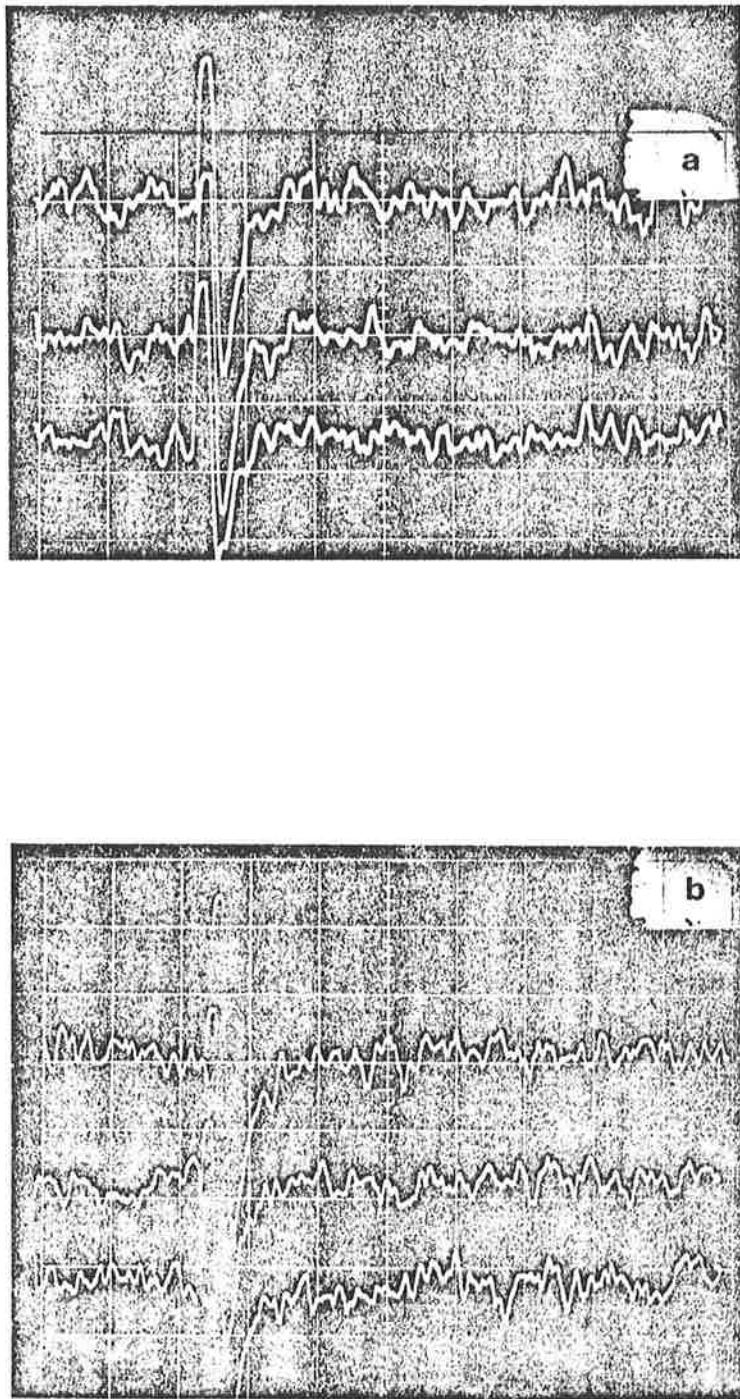


Fig. (25) Traces showing the changes in absorbance at 273 nm in the absence (a) and presence (b) (10^{-3} M Cl^-) in the photolysis of $[\text{Fe}(\text{phen})_3]^{3+}$ ($5 \mu\text{M}$) in 0.5 M HClO_4 . For both the flash pictures vertical scale = 40 mV/division and horizontal scale = 125 μ sec/division

Table (23)

DATA FOR FLASH PHOTOLYSIS^a OF $[\text{Fe}(\text{phen})_3]^{3+}$. A SEARCH FOR HYDROXY RADICALS

$\frac{[\text{Fe}(\text{phen})_3]^{3+}}{10^6 \times \text{M}}$	$\frac{[\text{HClO}_4]}{\text{M}}$	$\frac{[\text{NaCl}]}{\text{M}}$	$\frac{\text{Wavelength}}{\text{n.m.}}$	ΔA_0	Yield of the transients $10^7 \times \Delta C/\text{M}$
5.0	0.50	10^{-4}	493 ^e	0.0246 ^b	2.47
5.0	0.50	0.00	372	0.00156 ^c	0.65
5.0	0.50	10^{-4}	372	0.00146 ^c	0.61
5.0	0.50	0.00	372	0.00152 ^d	0.64
5.0	0.50	10^{-4}	372	0.00163 ^d	0.68

^a Light from the flash lamp filtered with a silica filter with a low wavelength cut-off of < 220 nm.

^b The absorbance change measured 500 μ sec and 1 sec after the flash.

^c The change in absorbance measured 100 μ sec after the flash.

^d The change in absorbance measured 500 μ sec after the flash.

^e Without silica filter

of X^- requires a wavelength < 230 nm (Thornton & Laurence, 1973) and when the light from the flash lamp was filtered with a silica filter with a low wavelength cut-off of 220 nm the yield of X_2^- was effectively reduced to zero [Fig. (25)].

In 0.5 M H^+ , for 10^{-2} M X^- , the effective half-life for the production of halogen radical anions from OH radicals is ca. 0.04 μ sec. This is much shorter than the half-life ($t_{1/2} \sim 0.2$ sec) of the secondary thermal reaction (Stage II) for 5 μ M $[Fe(phen)_3]^{3+}$ in 0.5 M $HClO_4$. The rate constant for the reaction of OH radicals with $[Fe(phen)_3]^{3+}$ has been estimated to be ca. 6×10^9 $M^{-1} s^{-1}$ (Creutz & Sutin, 1975) so that $t_{1/2}$ for the reaction

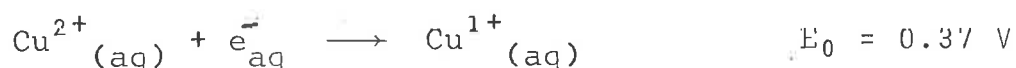
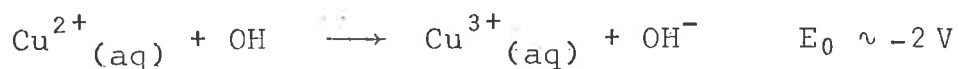


is ~ 25 μ sec for 5 μ M $[Fe(phen)_3]^{3+}$. The failure to detect X_2^- radicals is therefore due to the absence of photochemically produced OH radicals and not to the competitive scavenging of hydroxyl radicals by $[Fe(phen)_3]^{3+}$ or by the primary photoproduct, Fe(II) low-spin species, for the same reasons as those discussed for the alcohol scavengers.

No evidence was obtained for the production of hydroxyl radicals in the photo-reduction of $[Fe(phen)_3]^{3+}$ in aqueous acidic media, and in view of the unfavourable thermodynamic and kinetic parameters for any reaction likely to produce OH radicals in these experiments, it must be concluded that Wehry and Ward (1971) were mistaken in attributing the polymerization of methyl methacrylate in their systems to OH production.

IV.5.3 $Cu^{2+}(aq)$ Scavengers

$Cu^{2+}(aq)$ ions react rapidly with powerful oxidizing species such as OH radicals to give $Cu^{3+}(aq)$ (Meyerstein, 1971a & b) and with reductants (e.g. \bar{e}_{aq}) to give $Cu^I(aq)$ (Meyerstein, 1978)



and therefore are useful scavengers of both oxidizing and reducing species.

When solutions containing $5 \mu\text{M}$ $[\text{Fe}(\text{phen})_3]^{3+}$ and HClO_4 (0.5 M) were photolysed in the presence of $\text{Cu}^{2+}(\text{aq})$ ions (10^{-2} M) the secondary thermal slow process (Stage II) was effectively reduced to zero [Table (24)] although the primary quantum yield was unaffected. The results of these experiments are summarized in Table (24).

Table (24)
EFFECT OF $\text{Cu}^{2+}(\text{aq})$ AS SCAVENGER

$\frac{[\text{Fe}(\text{phen})_3]^{3+}}{\text{M}}$	$\frac{[\text{HClO}_4]}{\text{M}}$	$\frac{[\text{Cu}^{2+}(\text{aq})]}{\text{M}}$	$\frac{k^a(\text{Stage II})}{\text{s}^{-1}}$	$(\Delta A_\infty - \Delta A_0)^b$
5×10^{-6}	0.50	0	4.1 ± 0.3	0.026
5×10^{-6}	0.50	10^{-3}	0.9 ± 0.5	0.007
5×10^{-6}	0.50	10^{-2}	unobservable	1.01

^a k represents the pseudo-first order rate constant for Stage II reaction.

^b The kinetics and absorbance changes monitored at 493 nm.

As there was no evidence for the generation of OH or other strongly oxidizing radicals in the photoreduction of $[\text{Fe}(\text{phen})_3]^{3+}$, the reduced yield of the secondary thermal reaction by $\text{Cu}^{2+}(\text{aq})$ ions is probably due to the reducing nature of the intermediate species formed in the primary photochemical reaction.

IV.5.4 The Intermediate

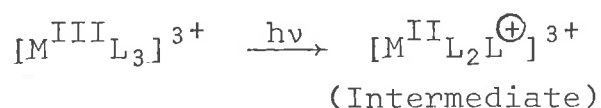
The experimental evidence for the nature of the intermediate can be summarized at this point:

- (1) The initial photochemical reaction produces a low-spin M(II) species and a reactive intermediate [Page (142)].
- (2) The reactive intermediate is not the hydroxyl radical as proposed by Wehry and Ward (1971) [Page (157)].
- (3) The reactive intermediate is capable of reducing the original $[ML_3]^{3+}$ complex and $Cu^{2+}_{(aq)}$ ions [Page (158)].

The experimental evidence leads to the conclusion that in the case of $[Fe(phen)_3]^{3+}$, the intermediate is a Fe(II)-ligand-radical complex [Chapter (5), Page (164)].



Chemical scavenging experiments were carried out only for the $[Fe(phen)_3]^{3+}$ system but the similarities in the photochemical behaviour of all the $[ML_3]^{3+}$ complexes studied allow the conclusion that the primary photochemical reaction is the production of the M(II)-ligand-radical species in which the radical is still bound to the metal centre. Therefore for all the M(III) complexes the initial photochemical act may be written as



Discussion of the details of the reduction of another molecule of the $[M^{III}L_3]^{3+}$ complex by the $[M^{II}L_2L^{\oplus}]^{3+}$ species is given in Chapter (5).

DISCUSSIONV.1 THE PHOTOCHEMICAL AND THERMAL REACTIONS

The amounts of the M(II) complexes produced by the photolysis of the M(III) complexes at the completion of the thermal reactions are equivalent to the amounts of the M(III) complexes lost and hydroxyl radicals are not produced either during the photolysis or in the secondary thermal reactions. The overall quantum yield (ϕ_0) for $[\text{Fe}(\text{phen})_3]^{3+}$ is zero in 98% sulphuric acid. Wehry and Ward (1971) interpreted the fall in the quantum yield as being due to the failure of a primary charge transfer from the solvent (CTFS) at the very low water concentration present in 16-18M



sulphuric acid. The flash photolysis of the M(III) complexes shows [Chapter (4), Section (4), Page (141)] that the true primary quantum yield ($\phi_{\dot{1}}$) is independent of the acid concentration and ionic strength and is the same in 0.5 M HClO_4 as in 10 M HClO_4 or 15 M H_2SO_4 where the concentration of water is very small. The primary photochemical reaction cannot therefore involve charge transfer from the solvent water. The isosbestic points and the difference spectra taken immediately after the flash clearly show that the primary photoproduct is a low-spin M(II) complex very similar to the equivalent $[\text{ML}_3]^{2+}$ complex. It must therefore be concluded that the ligand is the electron donor, the primary photochemical reaction producing a reduced metal centre and oxidized ligand. The secondary thermal reactions then involve the



reduced metal species and the ligand radical. The fact that the ligand is the electron donor can explain the variation of quantum yield for $[Fe(phen)_3]^{3+}$ with the wavelength of irradiation[†] (Wehry & Ward, 1971) in particular the rise in the quantum yield in the intraligand $\pi\pi^*$ band of the complexes.

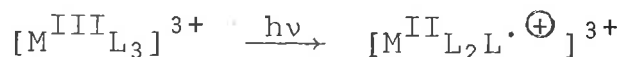
At the acid concentrations above the "kinetic isosbestic point" for each complex the intermediate species reforms the original $[M^{III}L_3]^{3+}$ complex by a first order or pseudo-first order process with an acid dependent rate constant. The rate of this process is independent of the initial concentration of the original complex. The first order kinetics eliminate the possibility that this thermal back reaction is one between $[ML_3]^{2+}$ and a radical in solution for both would be formed in equal concentration in the primary photochemical reaction that is, the thermal back reaction at high acid concentrations cannot be of the type



In this case the back reaction would show second order kinetics even if it were acid dependent. We must conclude from this experimental evidence, together with absence of any transient absorbance which could be expected if independent radical species

[†] Wehry and Ward (1971) estimated $\phi \leq 10^{-4}$ in the charge transfer band (350-700 nm) and 2.5×10^{-2} at 254 nm. The maximum $\phi = 0.14$ was observed for 240 nm. The results in the present study agreed that no detectable photoreaction could be observed when light from the flash lamp was filtered with a glass filter ($\lambda > 350$ nm).

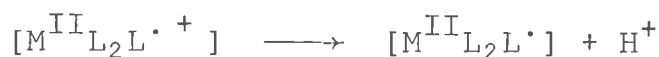
of the type $(L \cdot^+)$ were produced, that while the primary photochemical reaction involves the production of $(L \cdot^+)$, this remains bound to the metal centre. The thermal back reaction seen at



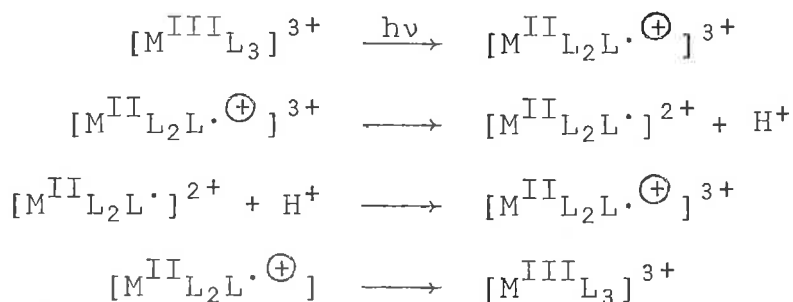
high acid concentrations is then



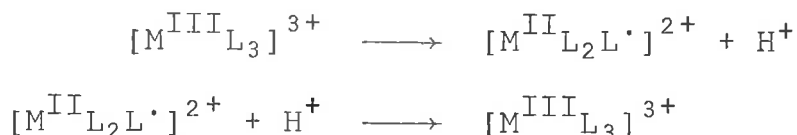
and is an intramolecular electron transfer. The overall acid dependence of this reaction suggests that while $[M^{II}L_2L \cdot^{\oplus}]^{3+}$ may be the initial photochemical product, this is stabilized by rapid deprotonation.



The overall sequence is then



However the relative rates of the individual steps are not known and the overall effect is

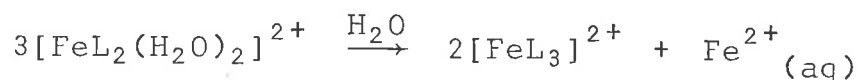


The thermal back electron transfer competes with a reaction which is first order in the concentration of $[M^{III}L_3]^{3+}$ and produces further M(II) low-spin species (Stage II) and this reaction is the dominant one below the acid concentration at which "kinetic isosbestic effect" is observed for each complex and is the only observable thermal reaction in 0.5 M HClO₄ where $\phi_o/\phi_i = \frac{\Delta A_\infty}{\Delta A_0}$ is

2.0: The bimolecular rate constants for this reaction are summarized in Table (13). This reaction cannot be the reduction of the $[M^{III}L_3]^{3+}$ complex by M^{II} -aquo ions as this occurs with both iron and ruthenium complexes. Even for the iron complex, where $Fe^{2+}_{(aq)}$ ions are stable and the reaction is possible



because $Fe^{2+}_{(aq)}$ ions would be produced in the photolysis only if photodissociation leading to the disproportionation of the Fe(II)



high-spin had occurred (König, 1968) but neither $Fe^{2+}_{(aq)}$ nor $Fe^{3+}_{(aq)}$ were detected. The rate constants for the reduction of $[FeL_3]^{3+}$ complexes by $Fe^{2+}_{(aq)}$ [Table (14)] are ca. $10^4 M^{-1} s^{-1}$ (Gordon & Sutin, 1961; Ford-Smith & Sutin, 1961) and are two orders of magnitude smaller than those for the thermal reactions ($\sim 10^6 M^{-1} s^{-1}$). For the ruthenium complex the relative stabilities of Ru(III) and Ru(II) complexes (Dwyer, Goodwin & Gyrafas, 1963) make a reaction of this type impossible.

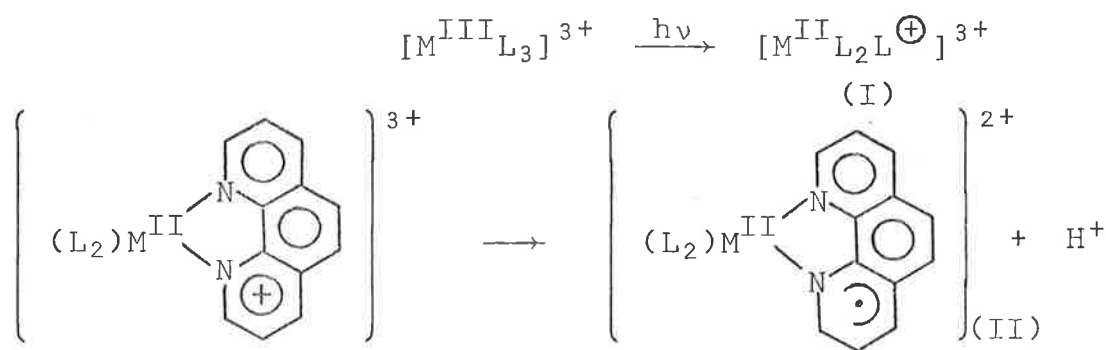
V.2 TRANSIENT SPECIES AND PHOTOCHEMICAL PRODUCTS

The identification of the primary photoproduct as a low-spin M(II) species containing a ligand-radical is not surprising in view of the relative inertness of low-spin iron(II) and ruthenium(II) complexes of N-heterocyclic ligands, and may be contrasted with the observations on $[\text{Co}(\text{phen})_3]^{3+}$ where the labile cobalt(II) species loses the ligand radical by solvolysis [Appendix (A)]. Electron transfer from the ligand to metal in systems such as $[\text{FeCl}]^{2+}$ or $[\text{Co}(\text{NH}_3)_5\text{X}]^{2+}$ produces labile high-spin Fe(II) or Co(II) and the ligand free radicals have been identified as separate species [Table (1), Page (14)]. In these cases it is possible for the radical to subsequently re-oxidize the metal centre by bimolecular reaction in solution, such as



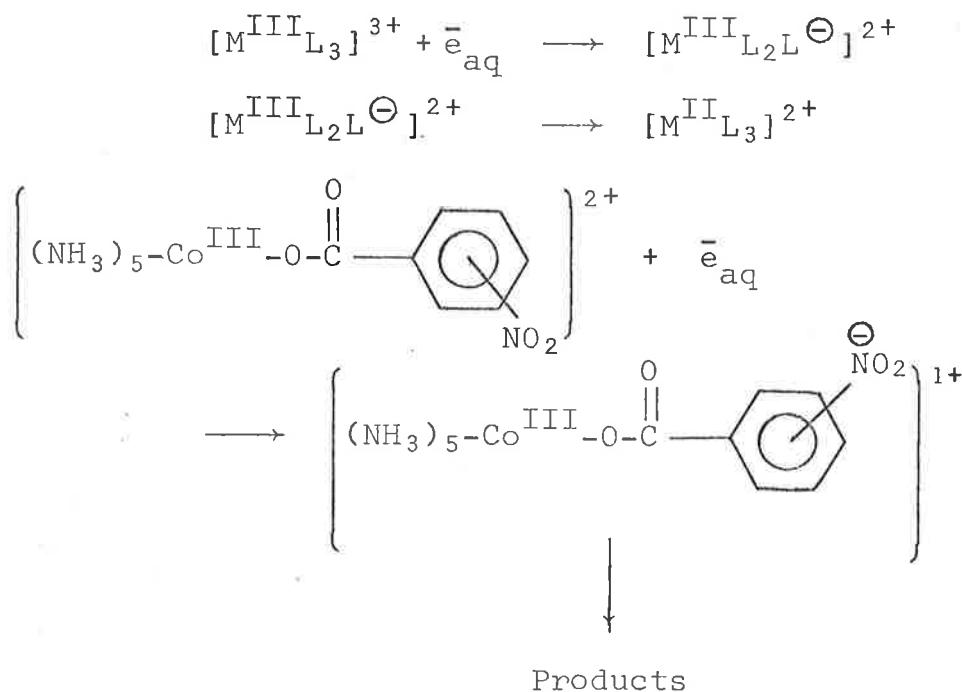
In the present case, the re-oxidation can take place by an intramolecular electron transfer to reform the original complex and this path is favoured by high acid concentrations.

The initially formed radical-cation species (I) will tend to be stabilized by the loss of a proton (either as a part of the primary photochemical act or subsequently) to form the $[\text{M}^{\text{II}}\text{L}_2\text{L}^\cdot]^{2+}$ complex (II)



Ligand-radical complexes of the type $[\text{M}^{\text{III}}\text{L}_2\text{L}^\ominus]^{2+}$ have been observed in the reactions of M(III)-complexes of phen, bipy,

typ and py with \bar{e}_{aq} and ligand-radical complexes of nitro-benzoato-cobalt(III), such as $[(\text{NH}_3)_5\text{Co}^{\text{III}}-\text{OCO}-\text{C}_6\text{H}_4-\text{pNO}_2]^{1+}$, are also produced by reaction with \bar{e}_{aq} and CO_2^{\ominus} . Intramolecular electron transfer reactions then lead to metal reduction. The chemistry

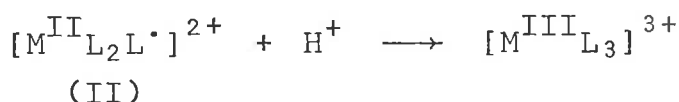


of coordinated ligand-radicals has been reviewed in Chapter 1, Page (26) .

In the reactions of the complexes $[\text{M}^{\text{III}}\text{L}_3]^{3+}$ ($\text{M} = \text{Fe}, \text{Ru}$ or Os and $\text{L} = \text{phen}$ or bipy) with OH^- [Chapter (I), page (43)] an intermediate, possibly $[\text{M}^{\text{III}}\text{L}_2\text{LOH}]^{2+}$, ($\lambda_{\text{max}} = 700 - 800 \text{ nm}$) was detected which decayed with first order kinetics. The spectra and kinetic behaviour of the $[\text{M}^{\text{III}}\text{L}_2\text{LOH}]^{2+}$ transients were essentially independent of the complex (Creutz & Sutin, 1975; Nord & Wernberg, 1975).

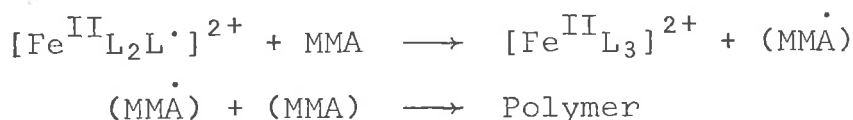
Creutz and Sutin (1975) observed an absorbance with $\lambda_{\text{max}} > 800 \text{ nm}$, which they attributed to the species $[\text{M}^{\text{II}}\text{L}_2\text{LOH}]^{2+}$, in the oxidation of $[\text{M}^{\text{II}}\text{L}_3]^{2+}$ complexes by hydroxyl radicals but no such absorbance was observed in the present study.

The $[M^{II}L_2L\cdot]^{2+}$ ligand-radical complex decays by competitive oxidation by another molecule of $[M^{III}L_3]^{3+}$ complex and by reformation of the original complex (by an acid catalysed path) and this accounts for the dependence of quantum yield on



the acid concentration [Chapter (4), Page (130)] and on the concentration of the radical scavengers [Chapter (4), Page (158)].

Wehry and Ward (1971) found $\phi_{-[Fe(phen)_3]^{3+}}$ in 8.5 M sulphuric acid to be 2.5×10^{-2} . The quantum yield was reduced to a limiting value of 1.3×10^{-2} in the presence of 10^{-2} M methyl-methacrylate [Fig. (26)]. That is $\phi_{(\text{absence of MMA})} / \phi_{(\text{presence of MMA})} = 2$. Scavenging of the $[M^{II}L_2L\cdot]^{2+}$ intermediate (species III) by MMA would prevent the reduction of another



molecule of $[M^{III}L_3]^{3+}$ and reduce the quantum yield to one half the value in the absence of the scavenger.

Electrophillic substitution reactions are the most favoured reactions for benzene and similar aromatic hydrocarbons (Gould, 1959) while N-hetrocyclic aromatics like pyridine or phenanthroline favour nucleophillic substitution reactions. The formation of pyridine N-oxides and N-alkylated pyridines are the most common examples. The oxidation of the $[M^{II}L_2L\cdot]^{2+}$ complex by another molecule of $[M^{III}L_3]^{3+}$ will produce a two electron deficient

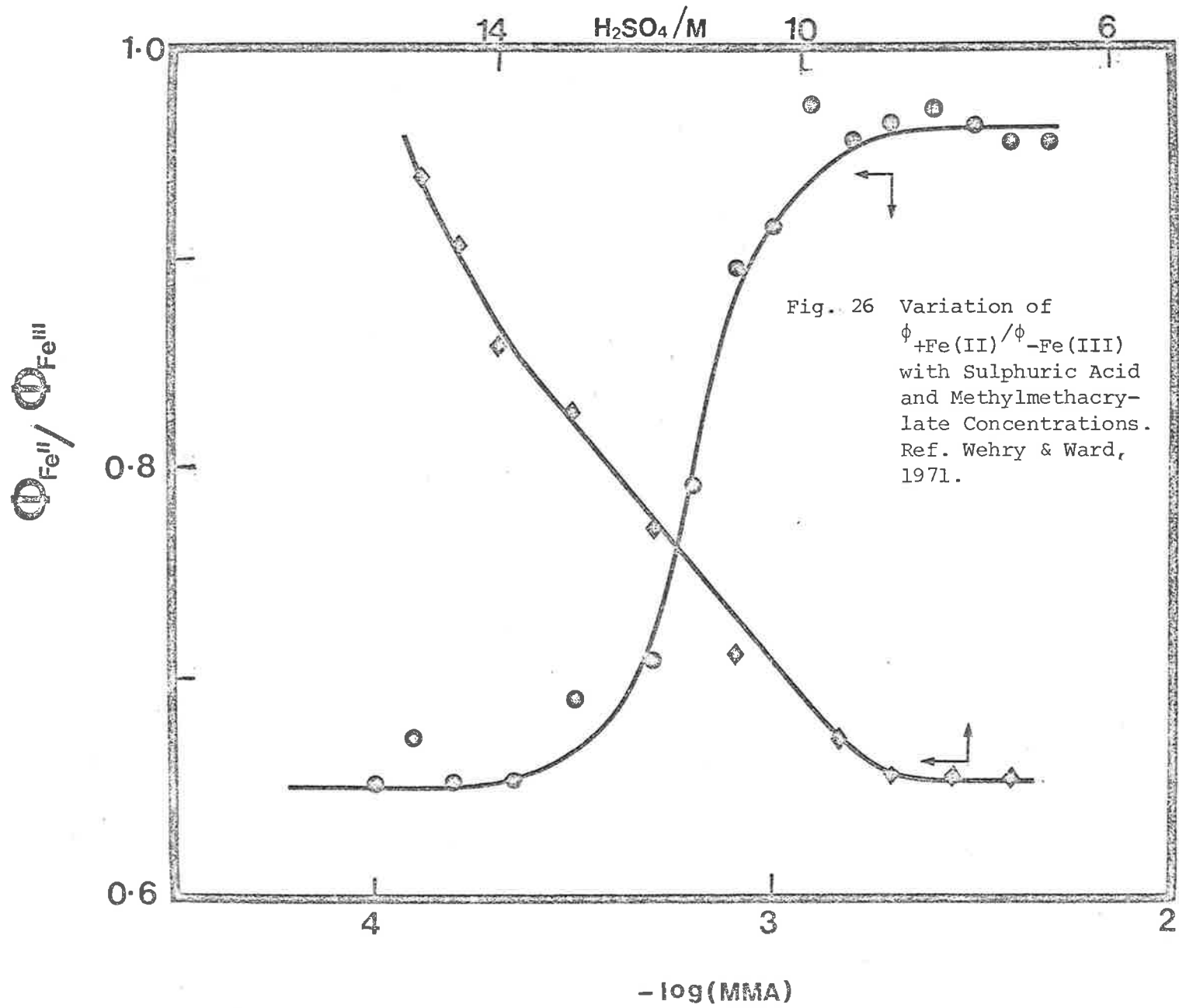
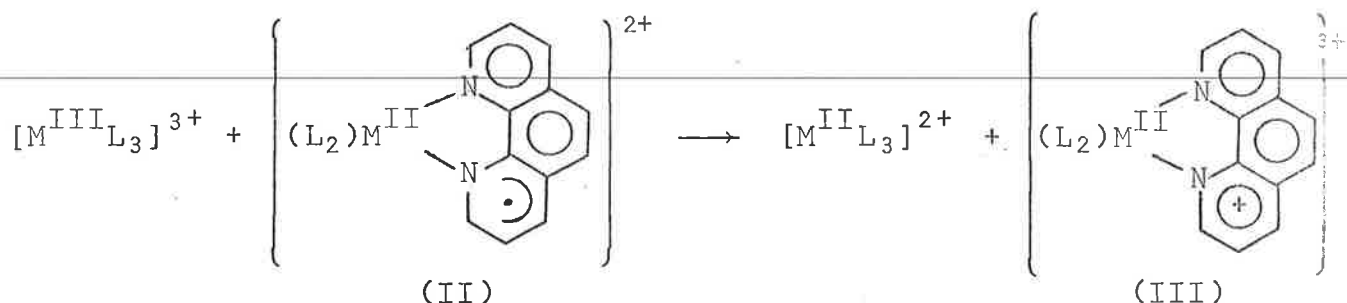


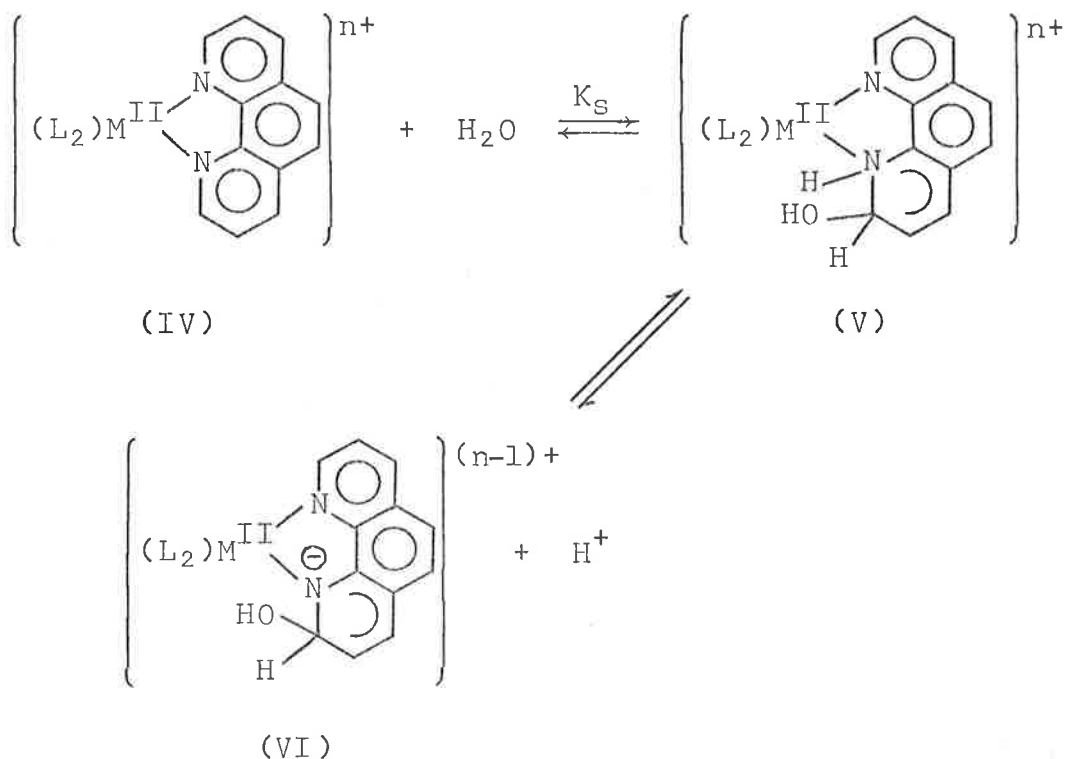
Fig. 26 Variation of $\phi_{+\text{Fe(II)}} / \phi_{-\text{Fe(III)}}$ with Sulphuric Acid and Methylmethacrylate Concentrations. Ref. Wehry & Ward, 1971.

species(III) still bound to the M(II) ion.

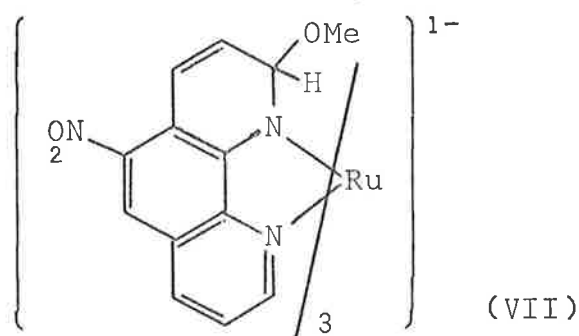


Species (III) is expected to be relatively more susceptible towards the nucleophilic attack especially by small molecules like H₂O to form an adduct such as $[M^{II}L_2(L^{\oplus}H_2O)]^{3+}$.

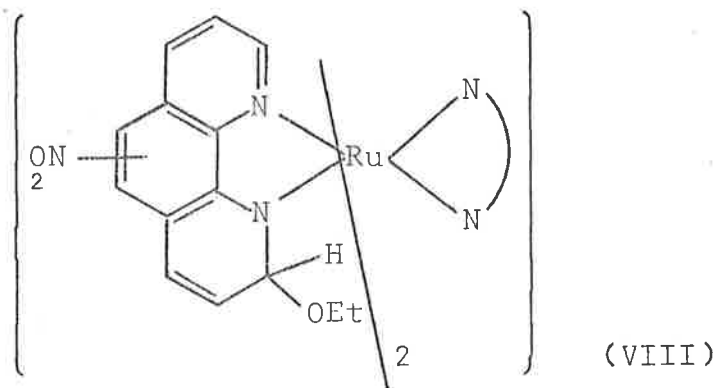
Complexing of metals by phen, bipy and related ligands may be analogous to quarternization (Gillard, 1975) making the 2-(9)-position accessible to nucleophilic attack while the 4-(7)-position is favoured for the free ligands. Gillard and his co-workers (Gillard, Hughes & Williams, 1976; Beilli, Gillard & James, 1976; Gillard & Williams, 1977; Gillard, 1975; Gillard & Lyones, 1973) have elegantly demonstrated the co-existence of covalent hydrate (V), its pseudo-base (VI) and the $[ML_3]^{n+}$ complex (IV)



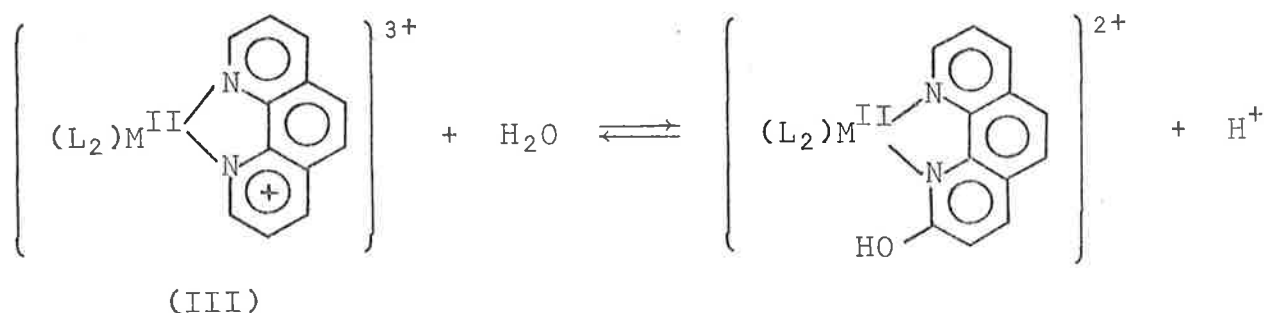
They observed a number of (at least initially) reversible changes in the spectra of $[ML_x]^{n+}$ complexes on the addition of base. The complexes included $[ML_2]^{2+}$ ($M = Pd, Pt$ and $L = bipy$ or 5,5'-dimethyl-bipy) and $[M(5-NO_2-phen)_3]^{3+}$ ($M = Fe(III)$ and $Ru(III)$). The nature of species (V) in basic solutions for $Pt(bipy)_2^{2+}$, (Gillard & Lyones, 1973) was confirmed by the 1H n.m.r. spectrum assigned by reference to the spectra of phen and its methyl substituted derivatives, both complexed to $Pt(II)$ and as the free ligands. Recent spectroscopic studies (Gillard, Hughes & Williams, 1976; Gillard, Kane-Maguire & Williams, 1977a & b) have shown that methoxide ion (MeO^-) reacts reversibly with methanolic solutions of the tris(5- NO_2 -phen) $Ru(II)$ cation, $[RuL_3]^{2+}$, via addition to the 2-position of each heterocyclic ligand to give species (VII).



An analogous addition occurs with ethoxide ion (EtO^-) in ethanol, except that with excess ethoxide the diethoxy adduct, Species (VIII), precipitates.



The existence of the covalent hydrate, Species (VIII), has been established unequivocally and attack by nucleophiles such as H_2O , on the $M(II)$ ligand-radical species (III) to establish an acid-base equilibrium is highly favourable due to the electron deficient nature of one of the aromatic rings.

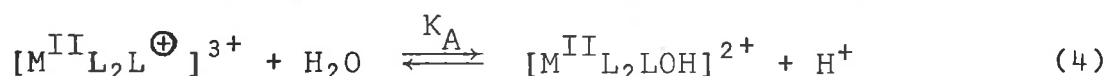
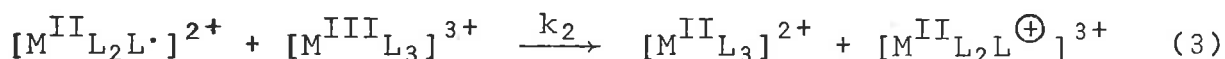
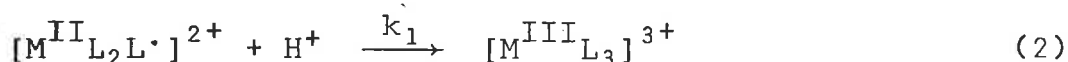
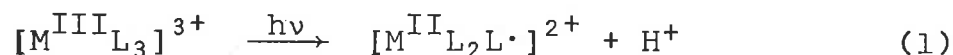


The final products in the photolysis of the $M(III)$ complexes are therefore probably $[ML_3]^{2+}$ and $[ML_2LOH]^{2+}$.

These two products of the photolysis cannot be easily distinguished even after continuous photolysis as the spectral differences between $Fe(II)$ complexes of phen, bipy and their mono-substituted ligands are very small ($\lambda_{\max} = 510 - 516 \text{ nm}$, $\epsilon_{\max} = 11,100 - 11,700 \text{ M}^{-1} \text{ cm}^{-1}$) and the same is probably true for the $Ru(II)$ complexes. However, the occurrence of two separate isobestic points for $[Fe(\text{Me}_4\text{-phen})_3]^{3+}$, $[Fe(\text{bipy})_3]^{3+}$ and $[Ru(\text{bipy})_3]^{3+}$ in the tail of the $1L(\pi \rightarrow \pi^*)$ transition band and the difference spectra in the $1L(\pi \rightarrow \pi^*)$ absorption band clearly show that the two final photolysis products differ in the molecular structure of the ligand.

V.3 KINETIC ANALYSIS

The reaction scheme



can account for the observations in the photolysis of the M(III) complexes. The decay of the transient $[M^{II}L_2L\cdot]^{2+}$ by the two competitive processes [(2) and (3)] may be written as

$$\frac{d[M^{II}L_2L\cdot]}{dt} = -\{k_1[H^+] + k_2[M^{III}L_3]\}[M^{II}L_2L\cdot] \quad (5)$$

and the integrated rate expression is given by

$$\ln \frac{[M^{II}L_2L\cdot]}{[M^{II}L_2L\cdot]_0} = -\{k_1[H^+] + k_2[M^{III}L_3]\}t \quad (6)$$

where $t = 0$ refers to the time at the end of the light flash. For a given run, the experimentally observed pseudo-first order rate constant will be given by

$$k_{\text{expt.}} = k_1[H^+] + k_2[M^{III}L_3]$$

Assuming $[M^{III}L_3]^{3+}$ to be practically transparent at the wavelength of the observation and that the molar absorbances (ϵ^{II}) of $[M^{II}L_2L\cdot]^{2+}$, $[M^{II}L_3]^{2+}$, $[M^{II}L_2LOH]^{2+}$ and $[M^{II}L_2L^{\oplus}]^{3+}$ are the same, the changes in absorbance with time following the flash, can be expressed as

$$(A_t - A_\infty) = \epsilon^{II} [M^{II}L_2L\cdot] \times \frac{k_2[M^{III}L_3] - k_1[H^+]}{k_1[H^+] + k_2[M^{III}L_3]} \quad (7)$$

Equations [(6) and (7)] describe the complex acid dependence for the $[M^{II}L_2L\cdot]^{2+}$ intermediate due to the two [eqns. (2)

and (3)] secondary thermal reactions. With an increase in the acid concentration the term $k_2[M^{III}L_3]$ decreases while $k_1[H^+]$ increases. At the acid concentration for which the "kinetic isobestic effect" is observed, the reaction (3) becomes unobservable.[†] At this stage no change in absorbance is seen after the initial photochemical reaction and from equation (7), when $k_2[M^{III}L_3] = k_1[H^+]$ the term $(A_t - A_\infty)$ becomes zero. Equation (7) also accounts for the change in the sign of absorbance i.e. the change over from the formation $((A_t - A_\infty)$ is positive for $k_1[H^+] \ll k_2[M^{III}L_3]$) to the decay of the transient absorbance $((A_t - A_\infty)$ is negative for $k_1[H^+] \gg k_2[M^{III}L_3]$) to regenerate the original $[M^{III}L_3]^{3+}$ complex as the acid concentration is increased.

The relative stoichiometry of the production of M(II) low-spin complexes in the initial photochemical reaction [eqn. (1)] and the secondary thermal reaction [eqn. (3)] and the relative quantum yield for the final and initial photoreductions is given by

$$\frac{\Delta A_\infty}{\Delta A_t} = \frac{\phi_o}{\phi_i} = \frac{2k_2[M^{III}L_3]}{k_1[H^+] + k_2[M^{III}L_3]} \quad (8)$$

The fall in overall quantum yield (ϕ_o) (although the primary quantum yield, ϕ_i ($\Delta A_o \propto \phi_i$), remains constant) is due to the competition between the thermal back electron transfer [eqn. (2)] and the reduction of another molecule of $[M^{III}L_3]^{3+}$ by the ligand-radical complex (species II) (eqn. 3). In dilute acid solutions $k_2[M^{III}L_3] \gg k_1[H^+]$ and the ratio ϕ_o/ϕ_i approaches the limiting

[†] The reaction becomes unobservable due to the changes in absorbance caused by the reactions (2) and (3) but it should be kept in mind that the $k_{obs} = k_1[H^+] + k_2[M^{III}L_3]$ and $\frac{k_{obs}}{k_{obs}}$ is not zero.

value of 2.0. When the rate of the back electron transfer [eqn. (2)] is equal to the rate of slow formation of M(II) complexes (Stage II) ($k_1[H^+] = k_2[M^{III}L_3]$) there will be no change in absorbance after the primary photochemical act and the ratio ϕ_o/ϕ_i is unity. In concentrated acid solutions (10 M HClO₄) $k_1[H^+] \gg k_2[M^{III}L_3]$ and the ratio ϕ_o/ϕ_i is close to zero. The equations therefore account for the experimental observations and can also explain the equivalent production of M(II) complex for the loss of every molecule of M(III) complex at each stage (I and II).

The observed rate constant, $k_{(obs)} = k_1[H^+] + k_2[M^{III}L_3]$, in relation to the absorbance changes in the integrated rate equation takes the form

$$\ln(A_t - A_\infty) = -k_{(obs)} \times t + \ln \left\{ \epsilon^{II} [M^{II}L_2L\cdot] \times \frac{k_2[M^{III}L_3] - k_1[H^+]}{k_1[H^+] + k_2[M^{III}L_3]} \right\} \quad (9)$$

so that a plot of $\ln(A_t - A_\infty)$ against t should be a straight line with a slope of $-k_{(obs)} = k_1[H^+] + k_2[M^{III}L_3]$. This is, of course, the form of the first order plots obtained experimentally. The second term on the right hand side of eqn. (9) gives the intercept of

$$\ln \left\{ \epsilon^{II} [M^{II}L_2L\cdot] \times \frac{k_2[M^{III}L_3] - k_1[H^+]}{k_1[H^+] + k_2[M^{III}L_3]} \right\}$$

This intercept will be constant for any particular set of acid and $[M^{III}L_3]^{3+}$ concentrations, as both these concentrations are much higher than the concentrations of $[M^{II}L_2L\cdot]^{2+}$ species produced by the flash.

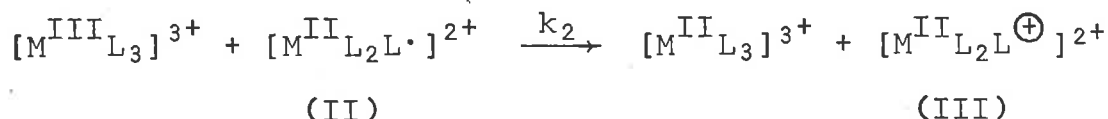
The plot of k_{obs} ($\approx k_{expt.}$) versus acid concentration[†] for

[†] At high acid concentrations $k_{obs} = k_1[H^+]$

the decay of the transient to reform the original M(III) complex (eqn. (2)) should be a straight line but Fig. (21) does not show such a relationship. The differences are due to the other properties of the medium changing as the acid concentration increases at the high acid concentrations, and ionic strength [Chapter (4), Page (148)] has been shown to have an effect similar to that of the acid.

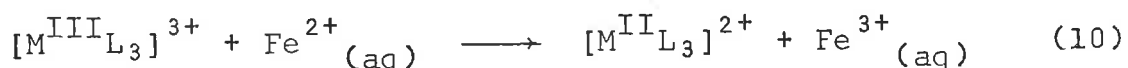
V.4 THERMAL INTRAMOLECULAR AND INTERMOLECULAR ELECTRON TRANSFERS

The values of the rate constants, k_2 , for the reaction (3) vary only by a factor of two in going from the Fe(III) to Ru(III)

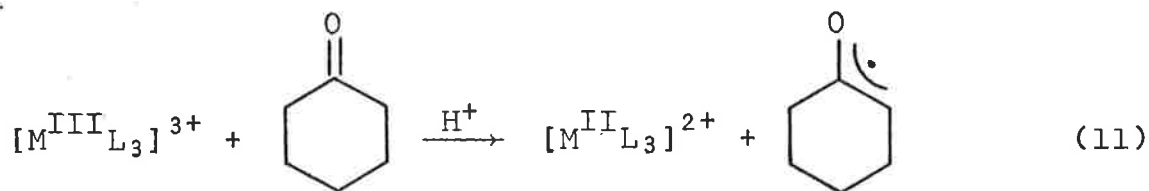


complexes. The electron transfer in equation (3) must occur by outer-sphere mechanism as the rate constants ($\sim 10^6 \text{ M}^{-1}\text{s}^{-1}$) for the electron transfer reactions are much higher than for the substitution reactions ($10^{-(4-6)} \text{ M}^{-1} \text{ s}^{-1}$) for the $[M^{III}L_3]^{3+}$ complexes (Gillard, Kane-Maguire & Williams, 1977c) and also ($2 - 50 \text{ s}^{-1}$) for the $[M^{III}L_3]^{2+}$ complexes (Lucie, Stanks & Burgess, 1975; Farrington, Jones & Twigg, 1977; Chagas, Tubino & Vichi, 1978).

For the electron transfer direct to the M(III) centre, the rate for the Ru(III) complex might be expected to be much higher than for the Fe(III) complexes due to the fact that in ruthenium the metal d-orbitals are spatially more diffused. The fact that the differences in the rate constants (k_2) are trivial [Table (13)] suggests that the electron transfer from the radical-ligand complex (Species II) to the $[ML_3]^{3+}$ occurs via the periphery of the polypyridine rings and that the small differences in k_2 may be attributed to the degree of overlap between the ligand π -orbitals and the metal d-orbitals. Similar arguments have been advanced for the outer-sphere reduction of M(III) polypyridine transition metal complexes by $\text{Fe}^{2+}(\text{aq})$ ions (Sutin & Gordon, 1961; Ford-Smith &

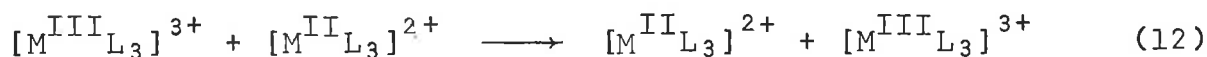


Gordon, 1961), by cyclohexanone (T. Ng. & Henry, 1976) in aqueous



acidic media and in the thiocyanate catalysed reduction of cytochrome c by chromous ions (Yandell, Fay & Sutin, 1973).

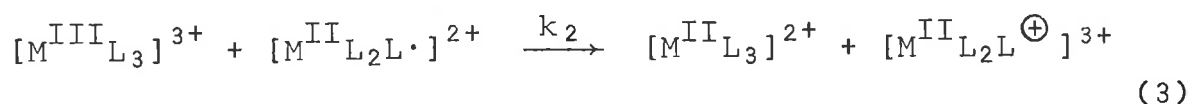
Electron transfer in reaction (3) by an outersphere mechanism via the periphery of the polypyridine rings is also supported by the self-exchange data for M(II)/M(III) (M = Fe, Ru and Os) polypyridine complexes (Solenberger, 1969; Ruff & Zimonyi, 1973; Chan & Wahl, 1974; Young, Richard Keene & Meyer, 1977). Differential excitation flash photolysis studies (Young, Richard Keene & Meyer, 1977) have shown that the self-exchange rates for the reaction



where M = Ru and L = bipy or phen, to be $2.0 \times 10^9 \text{ M}^{-1} \text{ s}^{-1}$, while the rate constant for the electron transfer between $\text{Ru}(\text{bipy})_3^{2+}$ and $\text{Ru}(\text{phen})_3^{3+}$ was estimated ca. $1.2 \times 10^9 \text{ M}^{-1} \text{ s}^{-1}$. Ruff and



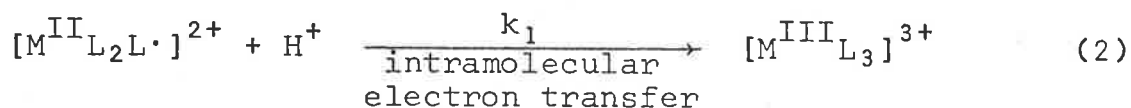
Zimonyi (1973) have reported the self exchange rate between $[\text{Fe}(\text{phen})_3]^{2+}$ and $[\text{Fe}(\text{phen})_3]^{3+}$ to be $(3.3 \pm 1.4) \times 10^8 \text{ M}^{-1} \text{ s}^{-1}$. It is clear from the self-exchange rate data that the differences in the rates of intermolecular outer-sphere electron transfers are as small as those for the reaction (3) in the present study.



The complexes with lower values of k_2 are expected to

approach the maximum overall quantum yield (ϕ_0) at relatively lower acid concentrations while reverse is true for the complexes with higher values of k_2 . This is evident from the plots of $\Delta A_\infty/\Delta A_0$ versus acid concentration [Fig. (18)].

The thermal intramolecular back electron transfer to rege-

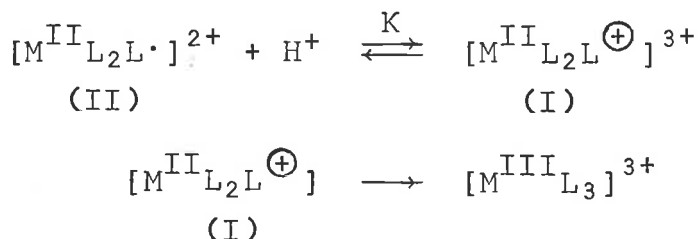


nerate the original $[M^{III}_{L_3}]^{3+}$ complex is acid catalysed. It is not known if the intramolecular electron transfer accompanies the protonation step or if it takes place subsequently to the protonation, and the significance of concentration of protons in concentrated acid (where $a_{H^+} \ll [H^+]$) is doubtful. However within an order of magnitude k_1 can be estimated to lie in the range 50-100 s^{-1} [Table (3)]. The rate of the intramolecular electron transfer can be no smaller than the observed rate.

As most protonation reactions take place at diffusion con-



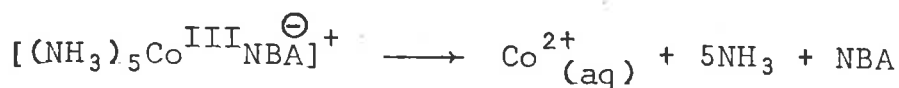
trolled rates (10^{10} - 10^{11} $M^{-1} s^{-1}$) the slowness of reaction (2) can be attributed to the slowness of the intramolecular electron transfer, but the division of the overall reaction into two steps



While mechanistically probable, does not allow the separate estimation of K and k because

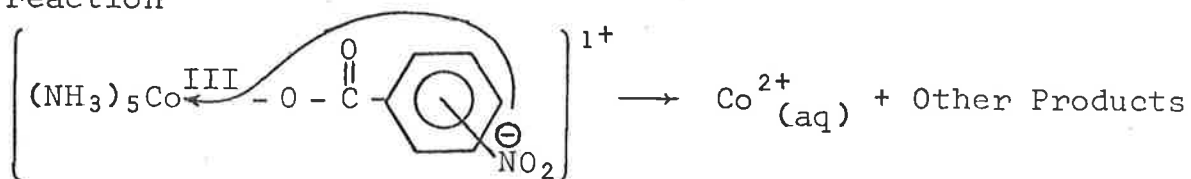
$$k_1 = kK$$

Intramolecular electron transfer reactions of the type

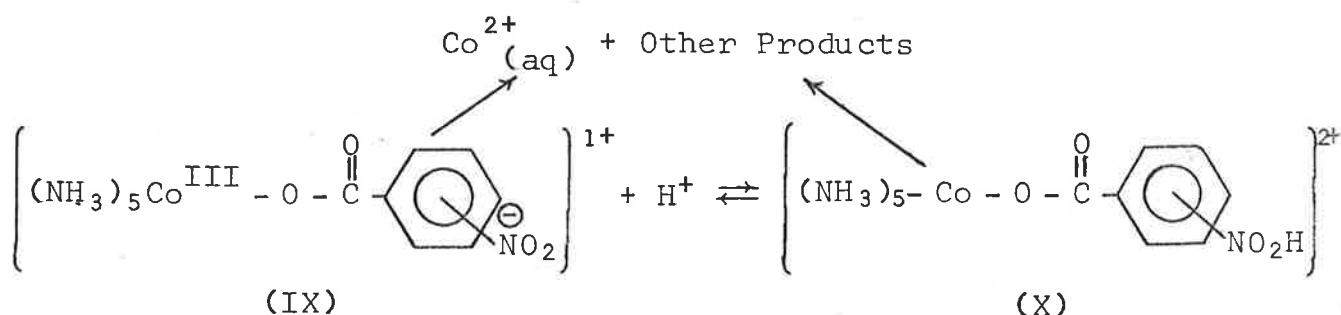


have rate constants in the range 10^2 – 10^5 s⁻¹.

The rates of intramolecular electron transfer for the reaction



were found to decrease (Cohen & Meyerstein, 1975; Hoffman & Simic, 1972) as the acidity of the medium was increased (pH = 6.7 to 2.0) and the effect was attributed to the acid-base reaction.

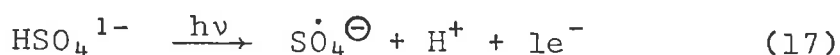
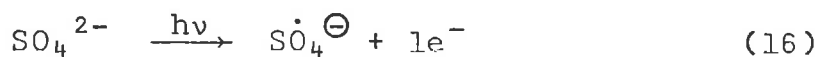


The protonated species (X) reduces the metal centre (Co^{III}) at a lower rate than species (IX) due to the decreased electronic charge density on the benzoato ligand. In the present work k_1 increases due to the protonation of the species $[\text{M}^{\text{II}}\text{L}_2\text{L}]^{2+}$ increasing the positive charge on the ligand, $[\text{M}^{\text{II}}\text{L}_2\text{L}^{\oplus}]^{3+}$, thus facilitating the intramolecular electron transfer from the reduced metal centre (M^{II}) to the ligand.

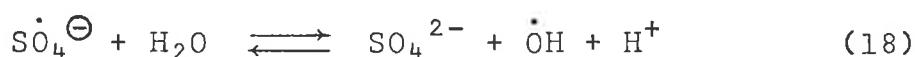
V.5 DIFFERENCES BETWEEN THE STEADY STATE AND FLASH PHOTOLYSIS
OF [Fe(phen)₃]³⁺

The observation of Wehry and Ward (1971) that the photo-reduction of [Fe(phen)₃]³⁺ was non-equivalent [$\phi_{+Fe(II)}/\phi_{-Fe(III)} < 1$] may be attributed to three reasons: (a) thermal reactions of the transients formed by the inadvertant photolysis of H₂SO₄ (8.5 - 18 M) with the photolysis products or with the complex (b) secondary photolysis of the photoproducts and (c) thermal acid hydrolysis of Fe(II) complexes produced by the photolysis of [Fe(phen)₃]³⁺. The non-equivalence was not observed in the flash photolysis experiments [Chapter (4), Page (107)] where much reduced photolysis time (30 μ s) and overall time of observations (1 - 2.5 sec maximum) reduces the effects of secondary photolysis and competing thermal reactions.

(A). Sulphate and bisulphate ions are known to be photolysed and flash photolysis produces $\dot{S}O_4^\ominus$ radical (Hayon & McGarvey, 1967; Dogliotti & Hayon, 1967). These sulphate radicals absorb weakly



in the visible region ($\lambda_{max} = 455 \text{ nm}$, $\epsilon_{max} = 460 \text{ M}^{-1} \text{ cm}^{-1}$) and decay by second order kinetics with a rate constant of $4.2 \times 10^8 \text{ M}^{-1} \text{ s}^{-1}$. The pseudo-first order rate constant for the decay is dependent on the concentration of hydroxide ions. No transient absorbance corresponding to $\dot{S}O_4^\ominus$ radicals could be detected at $\text{pH} \geq 10.4$. These observations were interpreted in terms of conversion to hydroxyl radicals (Hayon & Dogliotti, 1967).

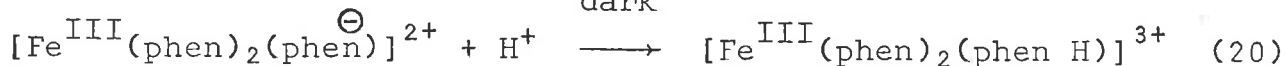
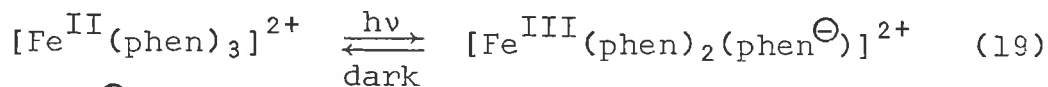


The photolysis products of [Fe(phen)₃]³⁺ will be quite

susceptible to attack by SO_4^{\ominus} as similar reactions of SO_4^{\ominus} with aromatic compounds have been observed (Chawla & Fessenden, 1975; Zemel & Fessenden, 1975; O'Neill, Schulte-Frohlinde, 1977; Sekested, Holeman & Hart, 1977; Neta, Madhavan, Zemel & Fessenden, 1977). The photolytic generation of SO_4^{\ominus} from H_2SO_4 has also been observed (at $[\text{H}_2\text{SO}_4] \geq 2.5 \text{ M}$) in the present study and the results are in agreement with the previous findings.

Reactions (16), (17) and (18) may become significant in 8 - 18 M H_2SO_4 under stationary state photolysis especially where light intensities of ca. 2×10^{16} quanta s^{-1} at 253.7 nm were employed for irradiation times of ~ 3 hours (Wehry & Ward, 1971) and would lower the quantum yield for the production of Fe(II) complexes. The reactions of SO_4^{\ominus} with the solvent may also explain their indirect detection of hydroxyl radicals by standard methods (Gosh, Mukerjee & Palit, 1964; Palit & Mukerjee, 1962).

(B). Picosecond flash photolysis has shown that $[\text{Fe}(\text{phen})_3]^{2+}$ undergoes transient bleaching (Kirk, Hoggard, Porter, Rockley & Windsor, 1976) with sub-microsecond recovery times (Street, Goodall & Greenhow, 1978). Some of the Fe(II) complex is destroyed, forming non-absorbing species. In acidic solutions, which tend to stabilize the Fe(III) complex and labilize the Fe(II) complex, the recovery time is expected to increase significantly and a



disproportionation reaction of the type



may lead to the reduction of $\phi_{+\text{Fe}(\text{II})}$. Similar disproportionation reactions have been observed in the reactions of hydroxyl radicals

with $[\text{Fe}(\text{phen})_3]^{2+}$ and free phen ligand (Pagsberg & Floryan, 1976)



(C). $[\text{Fe}(\text{phen})_3]^{2+}$ is much less stable than $[\text{Fe}(\text{phen})_3]^{3+}$ in acidic solutions [Chapter (4), Page (87)] and thermal acid hydrolysis of the photoreduction products may be partially responsible for the non-quantitative equivalence in the steady state photolysis experiments of Wehry and Ward (1971). These authors rule out this possibility because the equivalence discrepancy became smaller as the sulphuric acid concentration was increased from 7 to 16 M (Fig. (26)).

The rate of dissociation of $[\text{Fe}(\text{bipy})_3]^{2+}$ in aqueous acidic media is reduced by ca. 10% on the addition of 1 M chloride, nitrate or bisulphate, and sodium lauryl sulphate reduces the rate greatly (Gillard, 1975). The rates of racemization of $[\text{Fe}(\text{phen})_3]^{3+}$ and $[\text{Fe}(\text{bipy})_3]^{3+}$ were found to be zero in 100% H_2SO_4 , an effect attributed to the absence of water (Gillard, Kane-Maguire & Williams, 1977c). Recently Chagas, Tubino and Vichi (1978) have demonstrated that the hydration of the added cations, which also affects the water activity, is an important factor in retarding the dissociation of $[\text{Fe}(\text{phen})_3]^{3+}$ and $[\text{Fe}(\text{bipy})]^{3+}$.

In the present study it was observed that $[\text{Fe}(\text{phen})_3]^{2+}$ dissolved in 98% H_2SO_4 produces $[\text{Fe}(\text{phen})_3]^{3+}$ quantitatively ($\pm 5\%$ uncertainty) in room light (in ≤ 10 minutes) showing that the thermal acid hydrolysis is effectively zero as the water activity approaches zero. Another anomalous behaviour of the M(III) N-heterocyclic complexes, which can be related to the water activity, is that they can be precipitated from the dilute perchloric acid solution by the addition of solid NaClO_4 but not

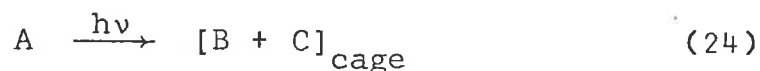
from the concentrated perchloric acid (10 M) solution. In 15 M H_2SO_4 , where the water activity is \sim zero (Bunnett, 1961), the decrease in the equivalent discrepancy (Wehry & Ward, 1971) may reflect the effect of the decrease in water activity on the thermal acid hydrolysis of the photoproducts which can be important at 8.5 M H_2SO_4 [Fig. (26)].

V.6 THE EFFECTS OF VISCOSITY, IONIC STRENGTH AND WATER ACTIVITY

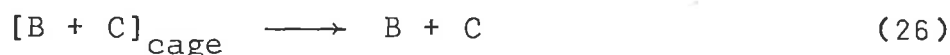
In view of the large changes in both hydrogen ion activity and water activity with changes in the acid concentration and ionic strength between 0.5 - 10 M, and the marked increase in the viscosity of the solutions, as well as the presence of equilibria involving covalent hydrates of the phen and bipy ligands, a quantitative interpretation of the effects of viscosity, ionic strength and water activity has not been undertaken. However, the experimental data do allow a qualitative discussion of the effects in relation to the primary quantum yield, the secondary thermal reactions and the photolysis products.

V.6.1 Effect of Viscosity

For a photochemical reaction leading to the production of



the species B and C in a viscous medium, the efficiencies of the primary cage recombination, equation (25), and the secondary recombination process, equation (27), after escape from the solvent

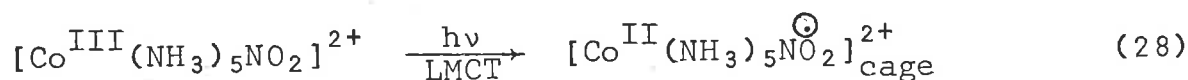


cage, equation (26), may be significantly affected by the solvent viscosity. Scandola et al. (1973) have studied the effect of viscosity on the photolysis of $[\text{Co}(\text{NH}_3)_5\text{NO}_2]^{2+}$. They found that the ratio[†] of the isomerization product $[\text{Co}(\text{NH}_3)_5\text{ONO}]^{2+}$ to the

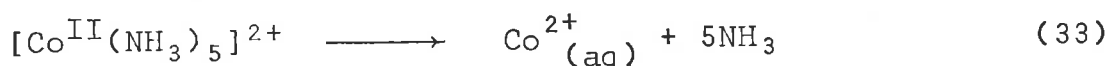
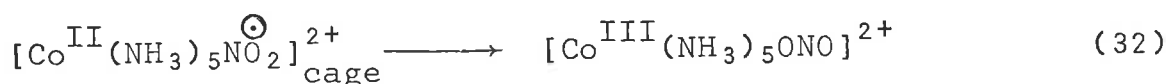
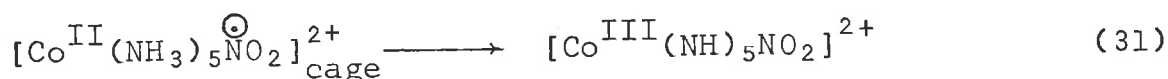
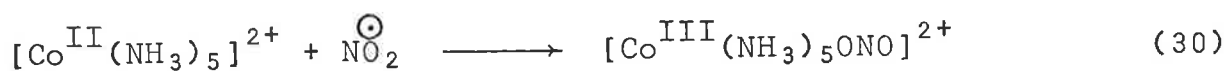
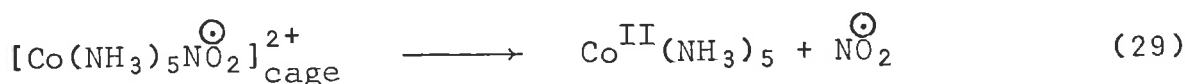
[†]The quantum yields for the isomerization product, $[\text{Co}(\text{NH}_3)_5\text{ONO}]^{2+}$, and $\text{Co}^{2+}_{(\text{aq})}$ were based on the steady state illumination experiments and are the overall quantum yields. It is not always possible to measure the primary quantum yields in steady state photolyses.

photoreduction product, $\text{Co}^{2+}_{(\text{aq})}$, increased as the viscosity of the medium was increased, due to the trapping of the primary photoproducts in the solvent cage:

primary photoreaction



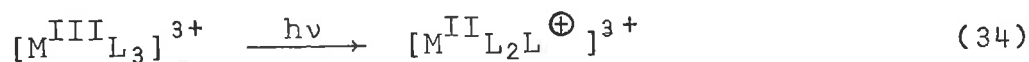
secondary thermal reactions



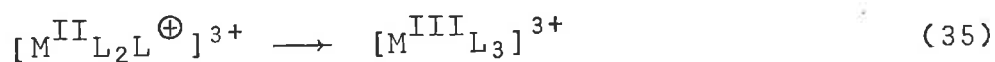
Similar effects have been observed in the photolysis of $[\text{Co}(\text{NH}_3)_5\text{CNS}]^{2+}$ (Endicott & Ferrandi, 1974), $[\text{Co}(\text{NH}_3)_5\text{Br}]^{2+}$ (Endicott, Ferrandi & Barber, 1975) and $\text{Trans-}[\text{Cr}(\text{NH}_3)_2(\text{CNS})_4]^{1-}$ (Gutierrez & Adamson, 1978).

(i) Effect of Viscosity on Primary Quantum Yield

In the present study the primary photochemical reaction produces a M(II) low-spin ligand-radical complex $[\text{M}^{\text{II}}\text{L}_2\overset{\oplus}{\text{L}}]^{2+}$,



so no primary bimolecular recombination reaction in the solvent cage is possible. The primary recombination is the unimolecular intramolecular back electron transfer from the reduced metal centre to the oxidized ligand and therefore no effect of viscosity on

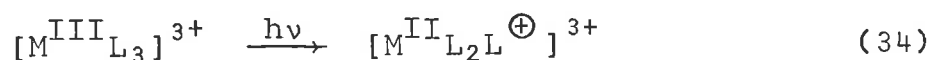


the primary recombination and hence on the primary quantum yield is expected. The present results show that the primary quantum yield under all medium conditions is the same [Table (17)].

(ii) Effect of Viscosity on the Photophysics

The electronic absorption spectra of the transition metal complexes are perturbed by changes in the solvent composition (Jørgensen, 1955) and a photoreactive state which changes the charge density near the metal centre, the likely precursor to a redox process, would be affected by the change in the solvent due to changes in the solvent-excited state interactions. In the present case the primary quantum yields are constant [Table (17)] for all the complexes at all ionic strengths and acid concentrations.

A photochemical reaction of the type



will cause some electrostrictive relaxation of the solvent molecules owing to the change in the charge distribution between the ground state and the excited electronic state. This necessitates the reorientation of the solvent molecules and it has been suggested (Endicott, Barber & Ferrandi, 1975) that the rates of electronic and vibrational relaxation of the vibrationally excited electronic states are higher than or at least comparable with the rates of dielectric relaxation. A molecule such as $[M^{II}L_2L^{\oplus}]^{2+}$ (Species II) generated in the primary photochemical reaction would be expected to cause a relatively small reorientation of the solvent molecules[†] with no significant change in the solvent-

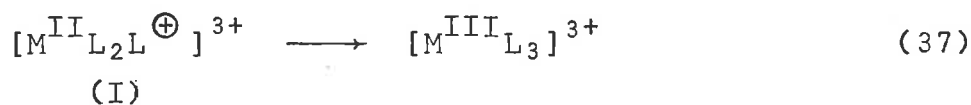
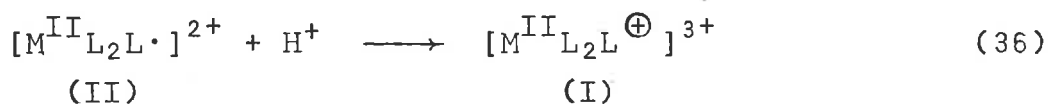
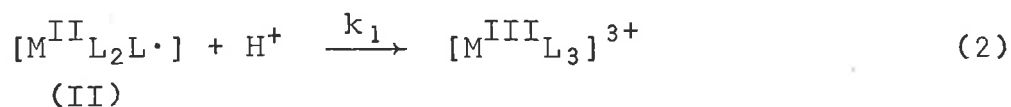
[†]A vibrationally excited electronic state of the type $[M^{\oplus} - L^{\ominus}]$ or $[M^{\ominus} - L^{\oplus}]$ would probably require more reorganization of the dielectric compared to $[M^{II} - L^{\oplus}]^{3+}$.

excited state energetics. This is probably why the primary quantum yield remains constant in all the media used.

(iii) Effect of viscosity on the secondary thermal reactions

The rates of intermolecular electron transfer (k_2) between the M(II) ligand-radical complex (Species II) and the $[M^{III}L_3]^{3+}$ complex are well below ($k_2 \sim 10^6 \text{ M}^{-1} \text{ s}^{-1}$) the diffusion controlled limits. Therefore the direct effect of viscosity on the efficiency of the reaction is expected to be small.

On the other hand the acid catalysed intramolecular electron transfer (equation (2)) is basically a two step process.



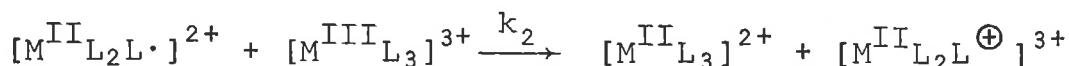
Protonation reactions are in general diffusion controlled and reaction (36) may be viscosity dependent but the unimolecular act of actual electron transfer from the metal centre to the ligand (equation (37)) is viscosity independent. This complex viscosity dependence of the rate of the overall reduction (equation (2))



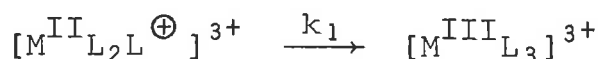
may be partially responsible for the non-linearity of the plot of k_{obs} versus acid concentration [Fig. (21)], but activity effects are likely to be much greater.

V.6.2 Effects of the Ionic Strength and Water Activity

~~An increase in the ionic strength of the medium will increase~~
the rate of thermal production of the M(II) complexes as these
are the reactions for which $Z_1Z_2 = +6$,



while the rate of intramolecular electron transfer (k_1) would remain



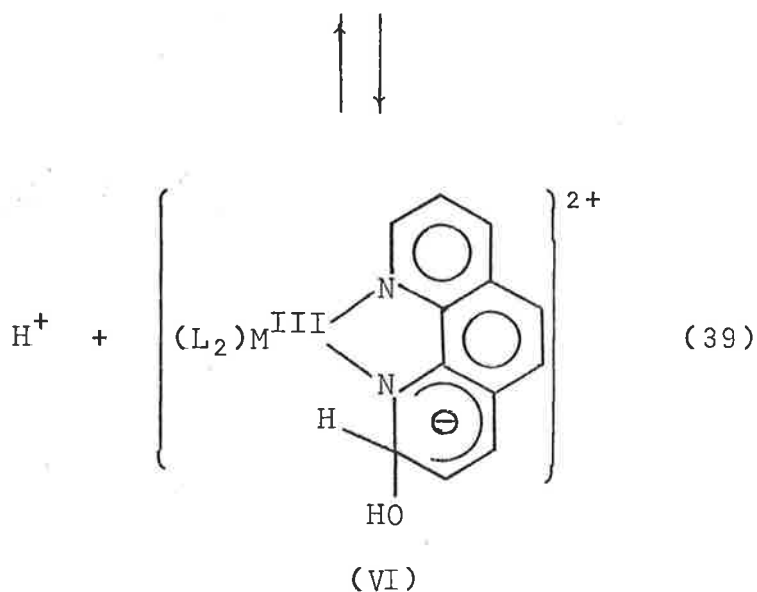
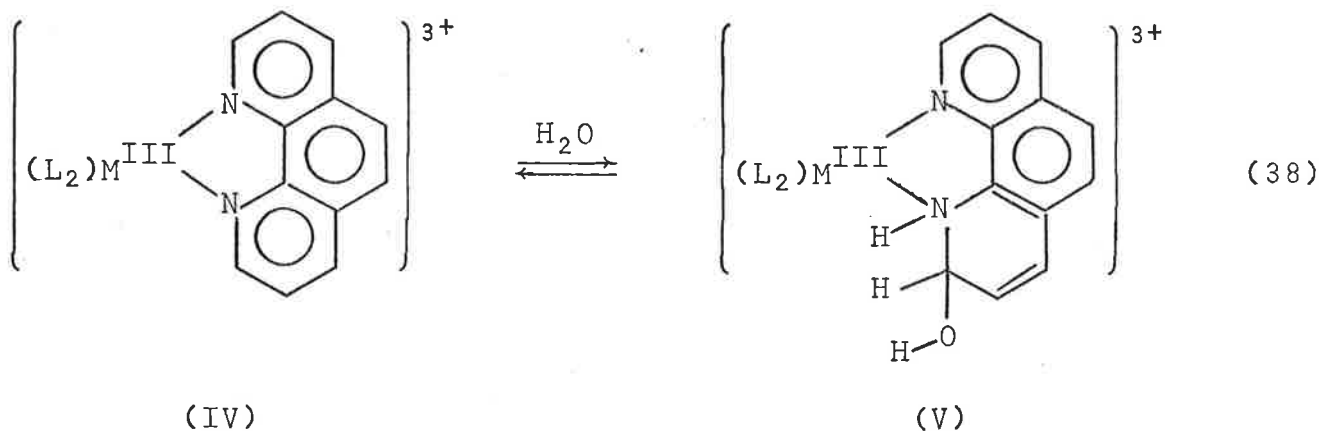
almost unaffected. The effect of ionic strength on the kinetics
of the secondary thermal reactions is summarized in Table (20)
and parallels the effect of the acidity of the medium.

It has been observed (Richard, Ridd & Tobe, 1963; Shakhshiri
& Gordon, 1969; Wehry & Ward, 1971) that both photochemical and
thermal stabilities of $[Fe(phen)_3]^{3+}$ in aqueous acidic media increase
as the acid concentration is increased and reach a maximum in 98%
 H_2SO_4 . According to Tobe et al. (1963) the critical variable
with respect to thermal stability of $[Fe(phen)_3]^{3+}$ in aqueous H_2SO_4
is the concentration of "free" water and suggested that thermal
decomposition of $[Fe(phen)_3]^{3+}$ proceeds by a substitution reaction
in which one or more water molecules is weakly bound to iron in
the transition state.

The important role of water activity in the thermal electron
transfer reactions of M(III) N-heterocyclic complexes is emphasized
by the present observations that the overall quantum yield approach-
es zero in 10 M $HClO_4$ or 15 M H_2SO_4 , where activity is effectively
zero (Bunnett, 1961), although the primary quantum yield is
constant.

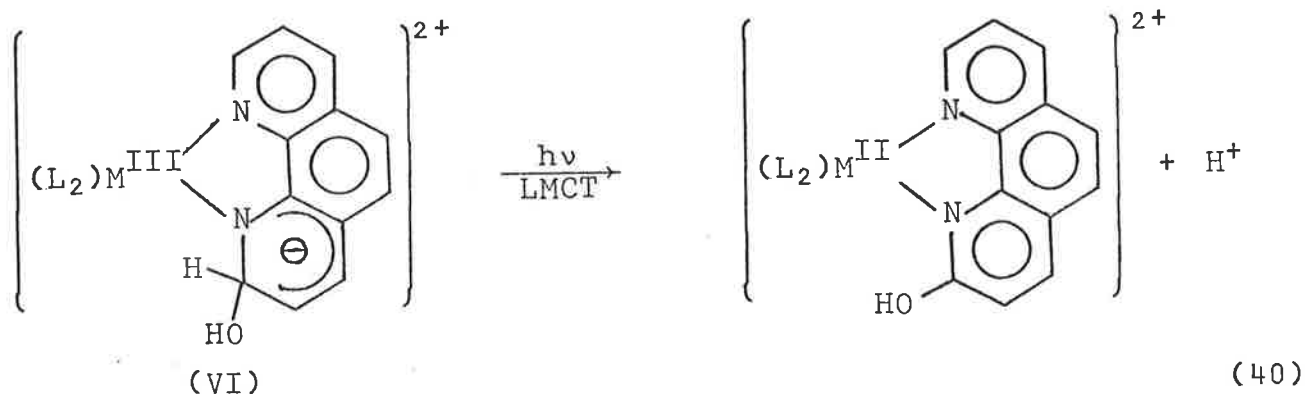
The water activity falls by a factor of ~ 60 as the acid

concentration is increased from 0.5-9.50 M HClO₄ [Table (18)]. The proportion of the covalent hydrate (IV), which is dominant in dilute acid solution, or its pseudo-base (V) would be significantly decreased (probably to zero) in concentrated acid solution (Gillard, 1975; Gillard et al., 1977). The pseudo-base (VI) is expected to offer resistance to the intramolecular electron transfer from the metal centre to the ring due to the increased



electron density on the ligand and may account for the fact that the decay of the transient absorbance to reform the original M(III) complex is unobservable in dilute acid solution. As the acid concentration is increased the activity of water falls and so does the amount of covalent hydrate or its pseudo-base in

solution. This may partially be responsible for the rapid increase in the rate of thermal back-electron transfer (k_1) with the increasing acid concentration. In dilute acidic solutions the pseudo-base of the covalent hydrate (VI) may lead to the formation of $[M^{II}L_2LOH]^{2+}$ in the primary photo-induced LMCT step.



The overall quantum yield for the photoreduction of the $[ML_3]^{3+}$ complexes approaches zero in concentrated acidic solutions (10 M $HClO_4$ or 18 M H_2SO_4) due to the increase in viscosity of the solution, fall in the water activity and increase in the ionic strength.

V.7 THE PRIMARY PHOTOCHEMISTRY OF $[ML_3]^{3+}$ COMPLEXES

The photochemistry of the $[ML_3]^{3+}$ complexes of phenanthroline and bipyridine ligands is not only related to the photophysics of the complexes but also to the photophysics of the ligands because of the reactivity of the intense intra-ligand (IL) absorption bands at wavelengths below 300 nm.

V.7.1 Photophysics of Phenanthroline and Bipyridine ligands

The photophysics and photochemistry of the free ligands (phen and bipy) have been extensively studied (Brinen, Rosebrook & Hirt, 1963; Perkampus et al., 1968; Rabold & Piette, 1968; Bandyopadhyay & Harriman, 1977; Harriman, 1978; Schulman, Tidwell, Cetorelli & Winefordner, 1971) and the energy level diagrams for the various excited states of phenanthroline and bipyridine in water are shown in Fig. (27). Table (25) summarizes the photophysical properties of the free ligands.

The fluorescence maximum is shifted towards lower energies due to an increased contribution from an $n \rightarrow \pi^*$ state (Bandyopadhyay & Harriman, 1977; Harriman, 1978) probably because of the hydrogen bonding of the lone pair of electrons on the nitrogen atom. The phosphorescence efficiency and the lifetime of the $^3\pi\pi^*$ -state[†] is independent of the polarity of the solvent [Table (25)]. The phosphorescent state is probably the lowest triplet state in water at $22,200 \text{ cm}^{-1}$ (450 nm, $\sim 2.7V$) for phenanthroline and at $\sim 23,300 \text{ cm}^{-1}$ (429 nm, $\sim 2.83V$) for bipyridine. For subs-

[†] There are two triplet states in the free ligands namely $^3n\pi^*$ and $^3\pi\pi^*$ -states reached by intersystem crossing from the $^1n\pi^*$ and $^1\pi\pi^*$ states respectively.

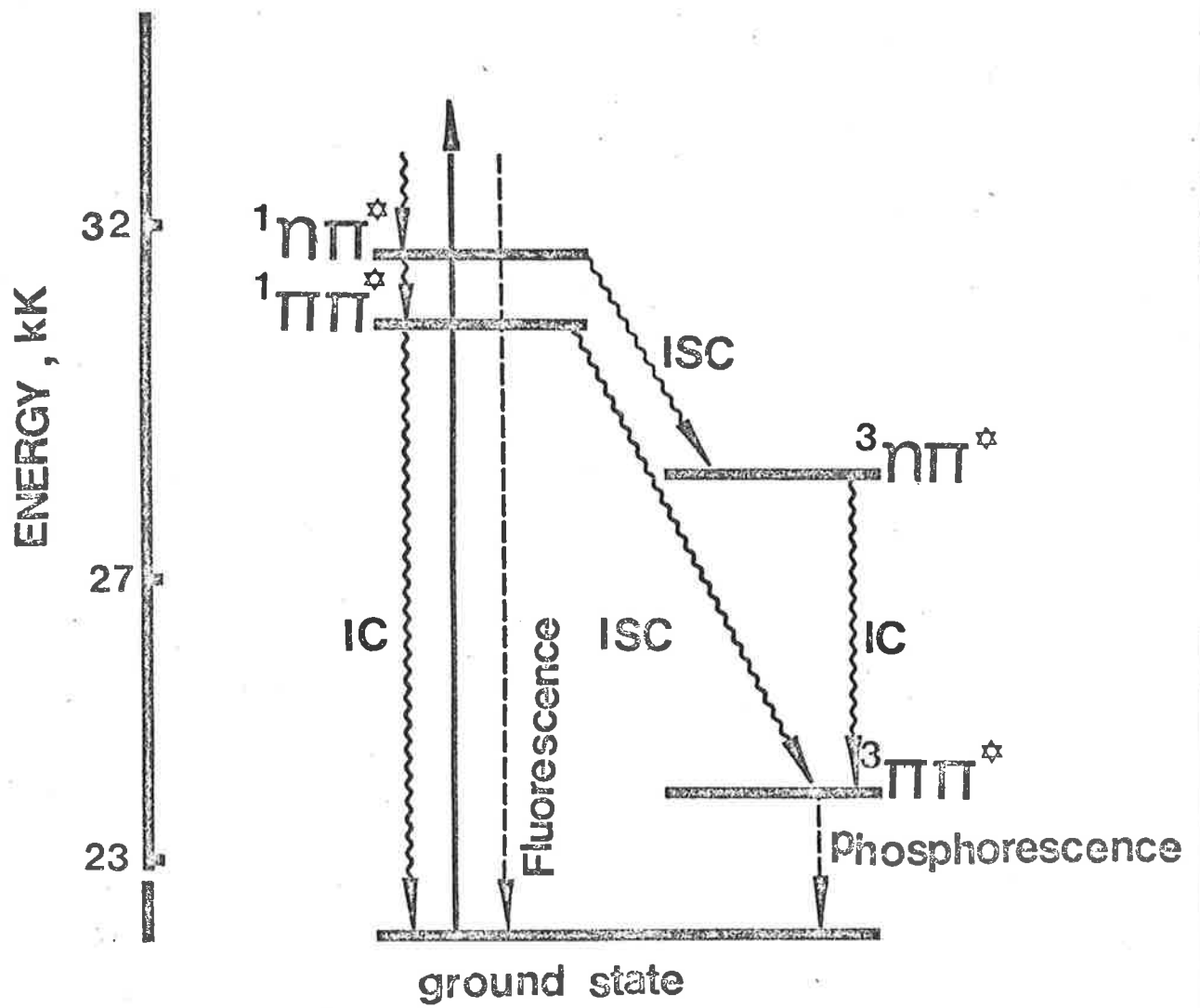


Fig. 27a Diagram for the Photophysics of Bipyridine Ligand

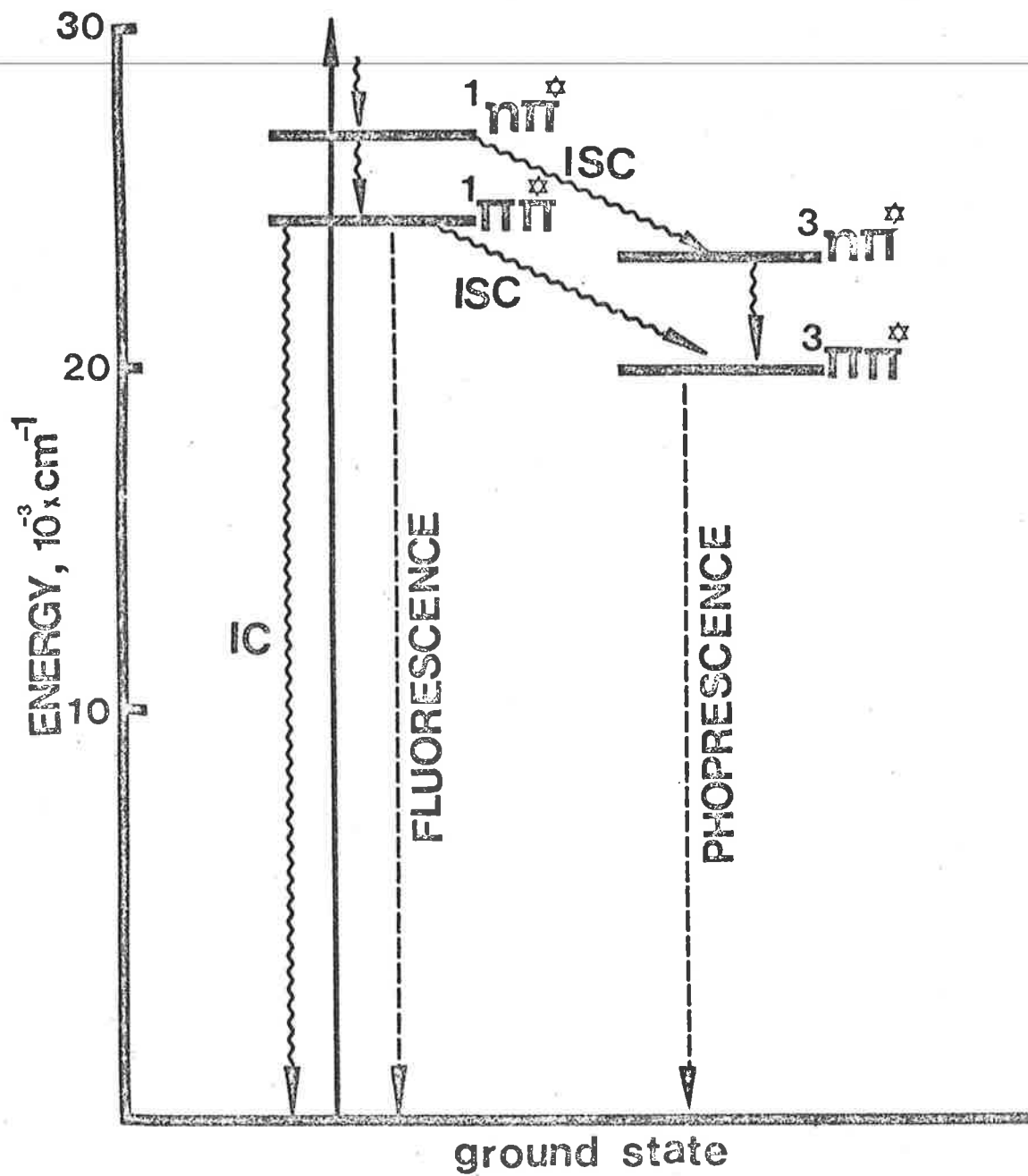


Fig. 27b Diagram for the Photophysics of Phenanthroline Ligand

Table (25)

PHOTOPHYSICAL PROPERTIES OF 1,10-PHENANTHROLINE AND 2,2'-BIPYRIDINE LIGANDS

REFERENCE: Harriman, 1978; Harriman & Bandyopadhyay, 1977.

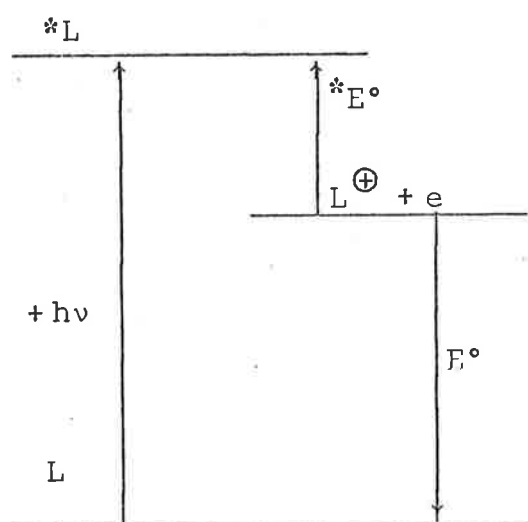
Ligand	Solvent	λ_F /nm	ϕ_F^a	τ_S /ns ^b	τ_P /ns ^a	τ_T /μs ^a	λ_T /nm
1,10-phenanthroline	water	360	0.010	7.00	1.52	42	450 425
	methanol	367	0.004	2.04	-	-	-
	ethanol	366	0.004	2.10	1.41	35	445 425
	propan-2-ol	-	-	-	-	33	445 422
	cyclohexane	378	0.001	< 1.0	-	26	442 422
	heptane	380	0.001	-	1.50	19	440 420
	2-methylbutane	378	0.001	< 1.0	1.46	17	440 420
2,2'-bipyridine	cyclohexane	-	0.005	< 1.0	1.02	86	-
	ethanol	-	0.009	2.0	0.95	78	-
	water	-	0.018	7.1	0.95	75	-

λ_F = wavelength maximum for fluorescence; ϕ_F = efficiency of fluorescence; τ_S = lifetime of the singlet excited state ($^1\pi\pi^*$); τ_P = lifetime of the phosphorescence emission; τ_T = lifetime of the triplet excited state ($^3\pi\pi^*$); λ_T = wavelength maximum for phosphorescence.

^a $\pm 10\%$; ^b ± 0.05 ns; ^c ± 0.05 s.

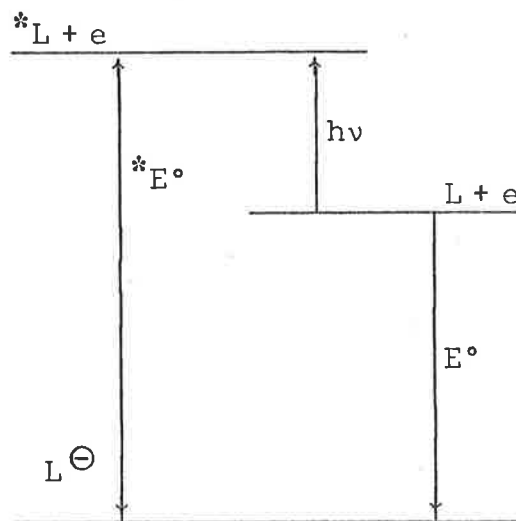
tituted phenanthrolines and bipyridines the efficiencies and intensities of the fluorescent and phosphorescent states are expected to change but the ordering of the energy levels of the excited states remains the same (Crasby, Watts & Carstens, 1970; Hagar, Watts & Crosby, 1975; Hagar & Crosby, 1975).

One of the most important consequences of the absorption of light leading to electronic excitation is that of increasing the electronic affinity and decreasing the ionization potential of the molecule, thus making it a better reductant and/or oxidant. The ordering of the excited state of the ligand ($*L$) compared to the oxidized ligand (L^{\oplus}), reduced ligand (L^{\ominus}) and the ground state ligand (L) may be represented as:



$*L$ better reductant than L

(a)



$*L$ better oxidant than L

(b)

The fact that the excited ligand state is both a better oxidant and a better reductant than the ligand in the ground state will be of obvious importance for the electron transfer reactions of the excited states of the $[ML_3]^{3+}$ complexes.

V.7.2 Energy levels of the $[ML_3]^{3+}$ Complexes

The spectra of the $[ML_3]^{3+}$ [Figs. (3 & 4)] have been discussed in Chapter (I) [Page (8)]. The various assigned excited states of Ru(III) and Fe(III) complexes of bipyridine are summarized in Table (26).

TABLE (26)

SPECTRA OF Fe(III) AND Ru(III) COMPLEXES OF BIPYRIDINE
 ν , band energy in cm^{-1} ; ϵ , molar absorbance in $\text{M}^{-1} \text{cm}^{-1}$;
 δ , half-band width in cm^{-1} ; a, vibrational structure.

REFERENCE: Bryant and Fergusson, 1971.

Complex	Characteristics	Assignments		
		$\pi \rightarrow \pi^*(2)$	$\pi \rightarrow \pi^*(1)$	$\pi \rightarrow t_2$
$[\text{Fe}(\text{bipy})_3]^{3+}$ in $\text{H}_2\text{O}/\text{Cl}_2$	ν	-	32870, 31730, 25910 ^a	16310
	ϵ	-	34100, 34000, < 100	289
	δ	-	730	1240
$[\text{Ru}(\text{bipy})_3]^{3+}$ in $\text{H}_2\text{O}/\text{Ce}^{4+}$	ν	-	-	14790
	ϵ	-	-	409
	δ	-	-	1240

A high energy MLCT corresponding to $e \rightarrow \pi$ transition has been assigned in the spectrum of $[\text{Ru}(\text{bipy})_3]^{2+}$ (Lyttle & Hercules, 1969) but the assignment of the LMCT band ($\pi \rightarrow e$ transition) in $[\text{M}^{\text{III}}\text{L}_3]^{3+}$ complexes has not been made due to the high intensities ($> 10^4 \text{ M}^{-1} \text{cm}^{-1}$) of the intraligand ($\pi \rightarrow \pi^*$) bands. However, recent molecular orbital calculations (Mayoh & Day, 1978) have

shown that all the calculated states below 29,000 cm^{-1} are overwhelmingly $\pi \rightarrow \text{M}^{\text{III}}$ charge transfer type for the $[\text{Ru}(\text{bipy})_3]^{3+}$, $[\text{Ru}(\text{phen})_3]^{3+}$ and $[\text{Fe}(\text{phen})_3]^{3+}$ complexes. It is much harder (Mayoh & Day, 1978) to distinguish between the LMCT and intraligand ($\pi \rightarrow \pi^*$) states in the UV-region, not only because of the small energy differences between $\pi \rightarrow \text{M}^{\text{III}}$ and the $\pi \rightarrow \pi^*$ states, but also because the intraligand states have considerable LMCT character. The mixture of orbital contribution to the wave functions for these states (LMCT and 1L) is very important in understanding the nature of the primary photochemical act. Although labels such as " $\pi \rightarrow \pi^*$ intraligand transition" are obviously largely meaningless in these circumstances, they will be used here as traditional designations for the states and transitions, but it must be remembered that considerable metal character is present.

V.7.3 The Primary Photochemical Reaction

The findings in the present study agree with those of Baxendal and Bridge (1955) and Wehry and Ward (1971) that $[\text{Fe}(\text{phen})_3]^{3+}$ is photochemically inert in the wavelength range of 300-650 nm ($\phi_{-\text{Fe}(\text{III})} \leq 10^{-4}$) but the quantum yield rises in the $\pi \rightarrow \pi^*/1\text{L}$ transition region ($\phi_{-\text{Fe}(\text{III})} = 0.14$ at 240 nm, Wehry & Ward, 1971) suggesting that the 1L ($\pi \rightarrow \pi^*$) excited state is photochemically active. This is consistent with the conclusion that ligand is the electron donor in the primary photochemical reaction.

Two alternate explanations can be put forward to explain the observed photoreduction of the transition metal N-heterocyclic complexes by photoexcitation in the $\pi\pi^*/1\text{L}$ band.

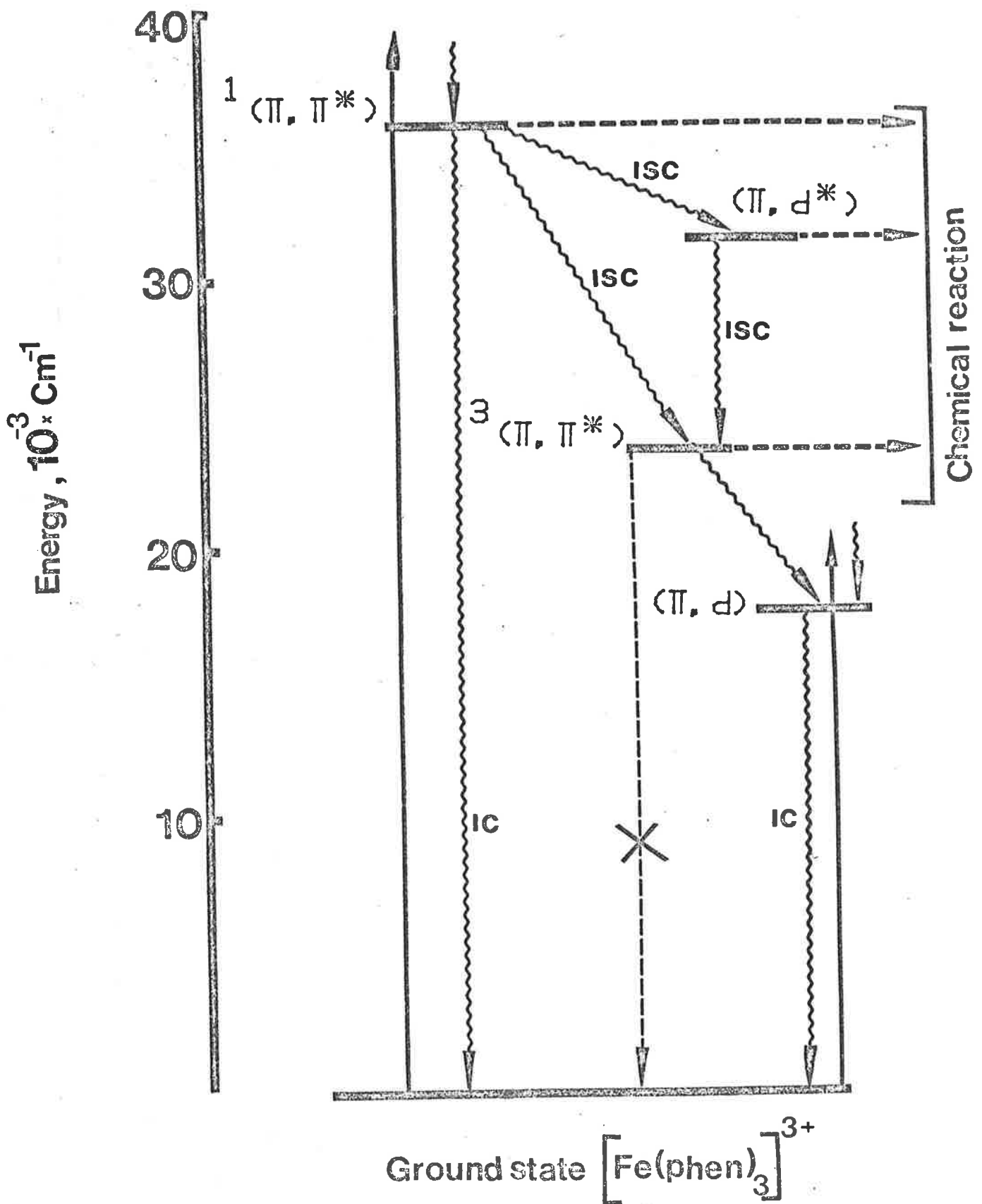


Fig. 28 An unlikely Hypothetical Diagram to Explain the Photochemical Reaction of $[\text{Fe}(\text{phen})_3]^{3+}$ by Excitation in the Intraligand ($\pi \rightarrow \pi^*$) band. Spin labels for the Excited States are traditional and largely meaningless.

(A). The overlap between the $\pi \rightarrow \pi^*$ transition and the π -e absorption band (Mayoh & Day, 1978) may lead to the photo-reduction of the complex. A photoreactive state, precursor to the observed photoredox process, may not be populated from the ground state because of the spin selection rules and may be populated from an excited ligand state (π^*) by a non-radiative process [Fig. (28)]. This explanation is unlikely in view of the predicted small energy gap between LMCT and $\pi\pi^*$ energy levels (Mayoh & Day, 1978) and low quantum yield of ca. 0.14 at 240 nm (Wehry & Ward, 1971). An intersystem crossing from a triplet ligand state ($^3\pi^*$) to the charge transfer doublet (^2CT) or quartet (^4CT) should be highly unfavourable. However even with a relatively light element as iron some breakdown of the strict spin-selection rules (because of spin-orbit coupling) may occur and this is more true for ruthenium.

(B). The luminescence of the free ligands (phenanthroline, bipyridine) is completely quenched in the $[\text{M}^{\text{III}}\text{L}_3]^{3+}$ complexes. Quenching of the luminescence of inorganic complexes (Gafney & Adamson, 1972; Balzani, Laurence et al., 1975) and of organic compounds (Rehm & Weller, 1970) by electron transfer is well established and is known to compete efficiently with the natural decay of the excited states although intermolecular electron transfer quenching of the luminescence involves the formation of a collision-encounter complex. If a luminescent excited state contains both the reducing ($^3\pi^*$ state) and the oxidizing M(III) sites, internal quenching by an intramolecular electron transfer from the excited ligand state to the M(III) central atom may efficiently compete with the internal conversion and natural decay of the excited ligand state ($^1\pi\pi^*$ and/or $^3\pi\pi^*$). The photoreduction of the transition metal N-heterocyclic complexes in the

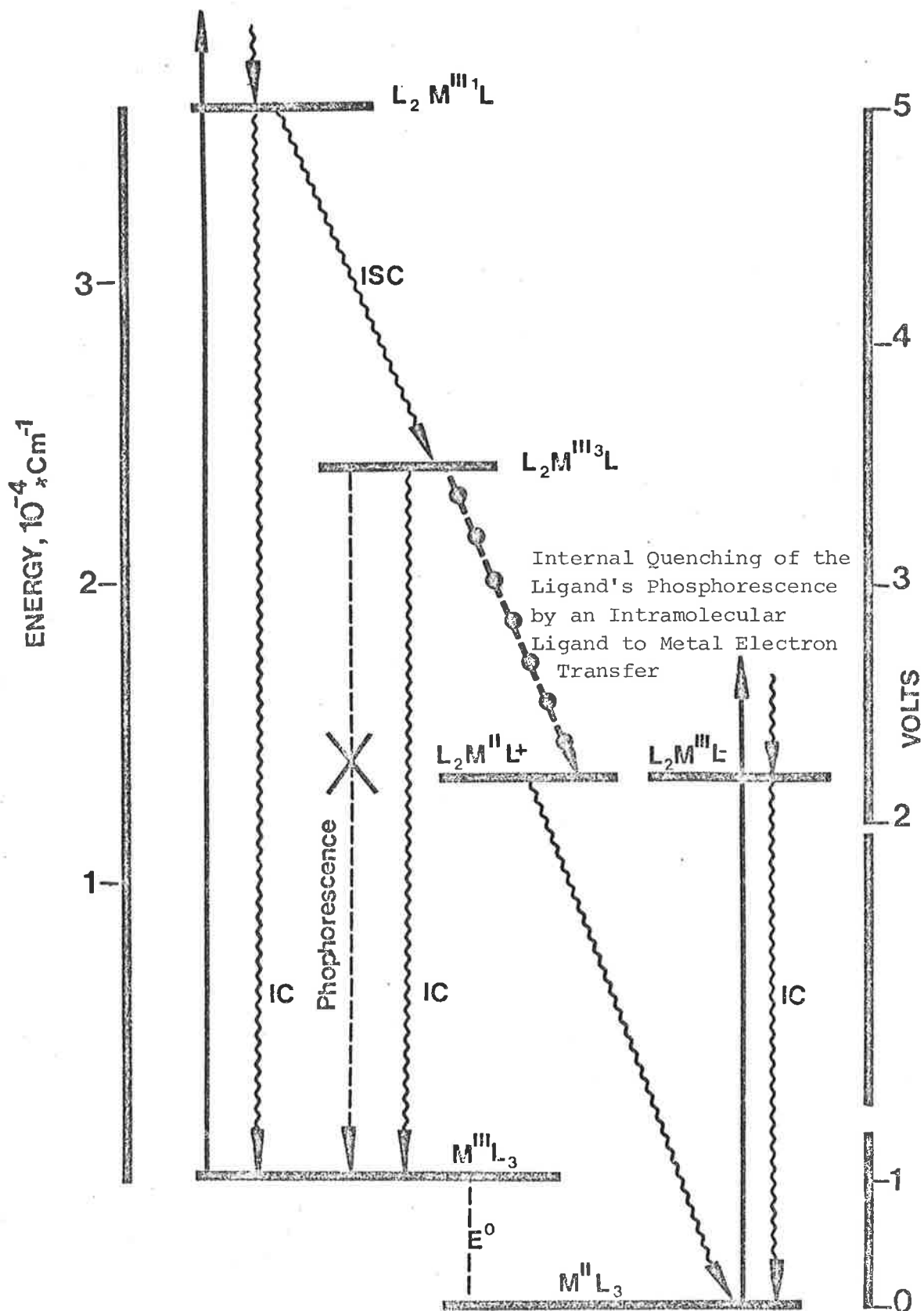


Fig. 29 The Proposed Diagram for the Photoreduction of $[\text{Fe}(\text{phen})_3]^{3+}$ by Excitation in the Intraligand ($\pi \rightarrow \pi^*$) band by Internal Quenching of the Ligand's Phosphorescence by an Intramolecular Ligand to Metal Electron Transfer - An Exemplary Case for M(III) Complexes. For comment on Spin labels see Fig. 28.

present study may therefore be due to the internal quenching of the $^3\pi^*$ luminescence by an intramolecular electron transfer process [Fig. (29)]. Consistent with this view is the observation (Rabold & Piette, 1968) that the phosphorescent half-lives of the phenanthroline complexes of Zn(II) and Cd(II) complexes are 2.05 sec and 1.40 sec respectively while the Hg(II), Fe(III) and Ru(III) complexes are completely quenched. The internal quenching of the ligand phosphorescence can probably explain the fact that the primary quantum yield (ϕ_i) remains constant under all acidities (0.5 M to 10 M HClO₄) because the phosphorescence efficiency is not expected to be changed by the change in the polarity of the solvent (Bandyopadhyay & Harriman, 1977; Harriman, 1978).

All the observations are equally consistent with the state(s) responsible for the high absorption and the photochemical quantum yields (at $\lambda < 300$ nm) being those for which the wavefunctions contains appreciable intraligand ($\pi \rightarrow \pi^*$) and LMCT ($\pi \rightarrow e$) character (Mayoh & Day, 1978). For such an excited state, involving mixing of metal and ligand orbitals, the partial LMCT character provides a simple and direct path to the M(II) ligand-radical intermediate.

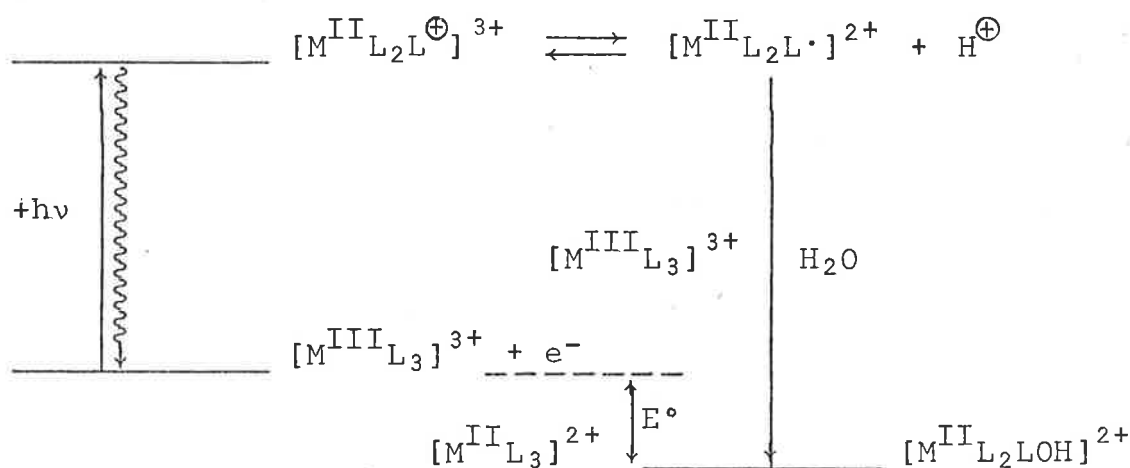


Table (27)

REDOX POTENTIALS FOR THE $[ML_3]^{3+}$ COMPLEXES AND
 pK_a VALUES OF THE LIGANDS

Complex	E° of Complex Volts ^a	pK_a of ligand
$[Fe(phen)_3]^{3+}$	1.06 ^b	4.86 ^f
$[Fe(Me_4-phen)_3]^{3+}$	0.81 ^c	6.31 ^g
$[Fe(bipy)_3]^{3+}$	0.97 ^b	4.34 ^h
$[Co(phen)_3]^{3+}$	0.370 ^d	4.86 ^f
$[Ru(bipy)_3]^{3+}$	1.29 ^e	4.34 ^h

^a The formal oxidation potentials of the complexes are in 1M H_2SO_4

^b Smith & Ritcher, Ind. Eng. Chem., Anal. Ed., 16, 580 (1944).

^c Brandt & Smith, Anal. Chem., 21, 1313 (1949).

^d Chou, Creutz & Sutin, J.A.C.S., 99, 5615 (1977).

^e Young, Nagle, Meyer & Whitten, J.A.C.S., 100, 4773 (1978).

^f Smith & Banick, Talana, 2, 348 (1959).

^g Schilt & Smith, J. Phys. Chem., 60, 1546 (1956).

^h Baxendale & George, Trans. Faraday Soc., 46, 55 (1950).

V.7.4 Conclusion

The observations that

- (1) the complexes are photoreduced by absorption of light in the intraligand absorption band
- (2) the complexes undergo two step process (Stage I and Stage II) except $[\text{Co}(\text{phen})_3]^{3+}$ which produces $\text{Co}(\text{II})$, a high-spin labile species.
- (3) the order of magnitude of the thermal intramolecular and intermolecular electron transfer rates are the same
- (4) the change of ligands, which affects the electron donating ability measured by $\text{p}K_a$ values [Table (27)], has no effect on the photochemical behaviour of the complexes
- (5) the photochemical behaviour remains the same in going from $\text{Fe}(\text{III})$ to $\text{Ru}(\text{III})$ although it is accompanied by significant changes in the reduction potentials of the complexes [Table (27)].

lead to the conclusion that the photochemistry of transition metal N-heterocyclic complexes is governed by the ligand and is essentially independent of the metal centre in question.

PART II

OXIDATION-REDUCTION REACTIONS
OF COPPER COMPLEXES

REACTIONS OF EXCITED $[\text{Ru}(\text{bipy})_3]^{2+}$ WITH COPPER COMPLEXESSECTION 1VI.1 INTRODUCTION(a) Electron Transfer Reactions of $*[\text{Ru}(\text{bipy})_3]^{2+}$

The photoemissive state of $[\text{Ru}(\text{bipy})_3]^{2+}$ is predominantly charge transfer in character ($*\text{CT}[\text{Ru}(\text{bipy})_3]^{2+}$) [Chapter 1, Page 4]. Gafney and Adamson (1972) suggested that the excited state $*[\text{Ru}(\text{bipy})_3]^{2+}$ could be quenched by electron transfer processes:



Definite evidence for electron transfer quenching of $*[\text{Ru}(\text{bipy})_3]^{2+}$ was first obtained in 1974 (Breck & Wan, 1973; Bock, Meyer & Whitten, 1974; Navon & Sutin, 1974; Laurence & Balzani, 1974). Recently the thermodynamic and kinetic aspects of bimolecular electron transfer reactions of excited states of inorganic complexes have been extensively reviewed (Balzani, Laurence et al. 1975; Balzani, Bolleta & Moggi, 1978; Balzani, Bolleta, Gandolfi & Maestri, 1979). The excited states of transition metal complexes have enabled electron transfer reactions to be tested over wide ranges of standard free energy change and can simplify the experimental measurements of very fast electron transfer reactions (Young, Keene & Meyer, 1977; Meyer, 1978).

Table (28)

STEREOCHEMISTRY OF COPPER COMPLEXES

Complex	Geometry	Reference
CuCl ₂ (gaseous)	Linear	1
[Cr(NH ₃) ₆ CuCl ₅]	Trigonal-bipyramidal	1
[Cu(1,3-pn) ₂ (H ₂ O)]SO ₄	Square-pyramidal	1
[Cu(diene)(NO ₃) ₂]	Compressed rhombic-octahedral	1
[Cu(H ₂ O) ₄ (HCOO) ₂]	Elongated tetragonal-octahedral	1
[Cu(Me-acac) ₂]	Square coplanar	1
K ₂ [PbCu(NO ₂) ₅]	Octahedral	1
Ba ₂ [CuF ₆]	Compressed tetragonal-octahedral	1
Cs ₂ [CuCl ₄]	Compressed tetrahedral	1
[Cu(bipy) ₂ (ONO)]NO ₃	Cis-distorted octahedral	1
[Cu(en) ₃ SO ₄]	Trigonal octahedral	1
Cu(en) ₂ (BF ₄) ₂	Elongated rhombic octahedral	1
[Cu(dmp) ₂] ²⁺	Distorted tetrahedral	2
[Cu(Me ₆ -tren)(H ₂ O)] ²⁺	Trigonal bipyramidal	3
[Cu(bipy) ₂ I] ¹⁺	Trigonal bipyramidal	1
[Cu(phen)] ²⁺	Pseudo-octahedral	4
[Cu(phen) ₂] ²⁺	Trigonal bipyramidal	4
[Cu(phen) ₃] ²⁺	Tetragonal	4
K ₂ [Cu(H ₂ EDTA)]	Distorted octahedral	1

Table (28) Cont....

REFERENCES:

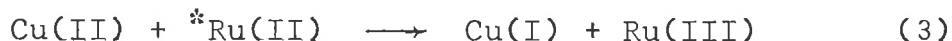
- (1) Hathaway & Billing, *Coord. Chem. Rev.*, 5, 143 (1970).
- (2) Sundararajan & Wehry, *J. Phys. Chem.*, 76, 1528 (1972).
- (3) Ciampolini & Nardi, *Inorg. Chem.*, 5, 41 (1966).
- (4) Fay, *Canad. J. Chem.*, 44, 2165 (1966).

(b) Electron Transfer Reactions of Cu(II) Species

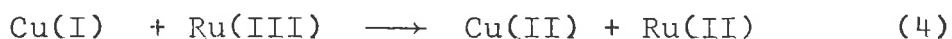
The $3d^9$ Cu(II) ion lacks cubic symmetry and Jahn-Teller effects yield distorted forms of the basic stereochemistries (Sidwick, 1950; Wells, 1962; Schunn, 1966; Furlani, 1968; Billing & Hathaway, 1970; Cotton & Wilkinson, 1972). The range of stereochemistries which have been identified in solution and/or the solid state are summarized in Table (28).

Oxidation-reduction reactions of Cu(I) and Cu(II) ions are of interest because of suggestions that these reactions show a preference for inner-sphere mechanisms. This preference is attributed to the expected high ligand reorganization energy requirements for the outersphere mechanism for the tetragonal Cu(II) ion changing to the tetrahedral Cu(I) ion. Outer-sphere redox reactions of copper-containing proteins have been reported in many cases to occur extremely rapid because of the presumed stereochemistry (between square planar and tetrahedral) of the copper site in these proteins (Holwerda, Wherland & Gray, 1976; Siiman, Young & Carey, 1976). To test the existence of special structural barriers in the outer-sphere electron transfer reactions of copper complexes the reactions of the excited state of $[\text{Ru}(\text{bipy})_3]^{2+}$ with copper complexes have been studied. Advantage has been taken of:

- (i) The large free energy changes which accompany these reactions [Page (244)].
- (ii) The possibility of studying both the reduction reaction



and the reverse oxidation reaction

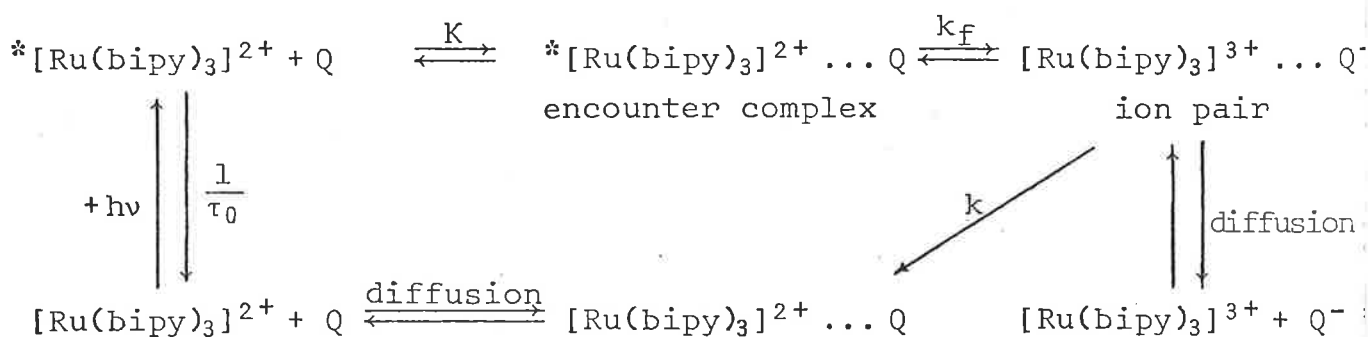


These reaction pairs [eqn. (3) and (4)] involve the same electron exchange reaction for the copper complexes and therefore are particularly relevant to current theories of electron transfer reactions.

SECTION 2

VI.2 REDOX PROPERTIES OF $^*[\text{Ru}(\text{bipy})_3]^{2+}$

The formal reduction potential of the excited state - Ru(III) couple, $[\text{Ru}(\text{bipy})_3]^{3+/2+^*}$, was estimated to be 0.81 V (in 0.1 M $[\text{N}(\text{C}_2\text{H}_5)_4](\text{ClO}_4)$) from measurements of the quenching by a series of nitrobenzenes (Bock, Meyer & Whitten, 1975). The observed bimolecular quenching rate constant, k_q^{obs} , was expressed in terms of the equilibrium constant, K , for encounter complex formation,



the free energy change, (ΔG_r^0) , for the electron transfer step (k_f) and the composite rate constant, k , for all the processes by which the radical pair can disappear to form the ground state products (Rehm & Weller, 1970).

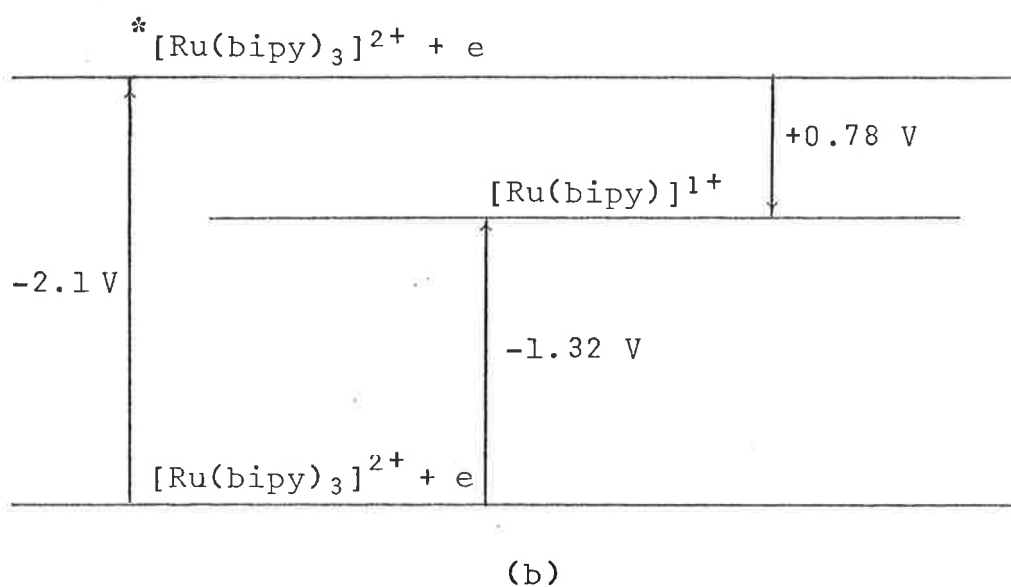
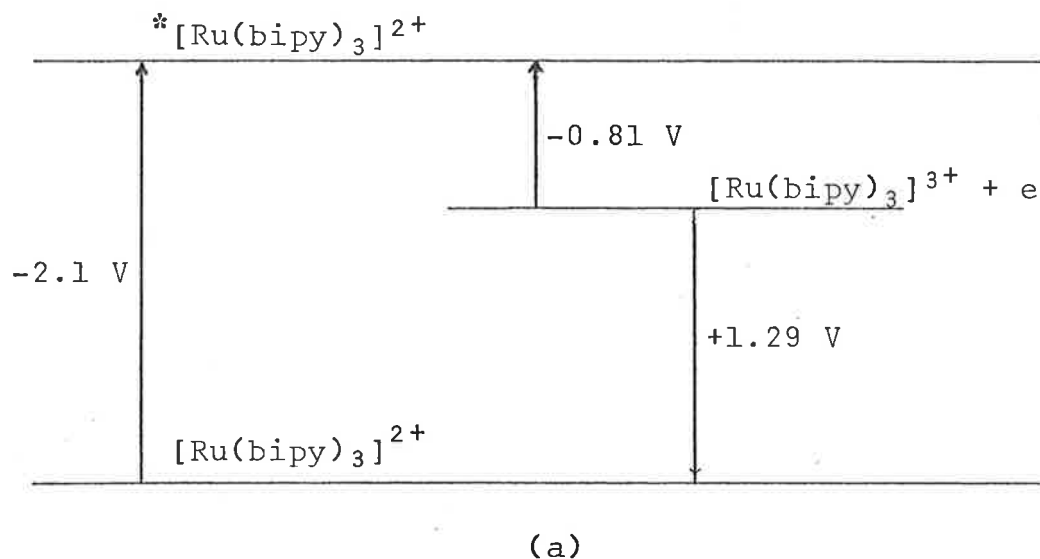
$$k_q^{\text{obs}} = \frac{K k}{2} e^{-(\Delta G_r^0/RT)} \quad (5)$$

$$\begin{aligned}
 \text{and} \quad \Delta G_r^0 &= E_{1/2}([\text{Ru}(\text{bipy})_3]^{3+}/^*[\text{Ru}(\text{bipy})]^{2+}) \\
 &\quad - E_{1/2}[\text{Q}/\text{Q}^-] + w_p - w_r \quad (6)
 \end{aligned}$$

where w_p and w_r represent the work required to bring the product ions ($[\text{Ru}(\text{bipy})_3]^{3+}$ and Q^-) and reactants ($^*[\text{Ru}(\text{bipy})_3]^{2+}$ and Q) together to form an ion pair and encounter complex respectively. From the extrapolation of the two linear portions of the plot of k_q^{obs} vs. $E_{1/2}$, the value of $-(0.81 \pm 0.02)$ V for E^0 for $[\text{Ru}(\text{bipy})_3]^{3+}/^*[\text{Ru}(\text{bipy})_3]^{2+}$ was obtained. The potentials of the ground state

couples $[\text{Ru}(\text{bipy})_3]^{3+/2+}$ (1.29 V; Anderson, Salmon, Meyer & Young, 1977) and $[\text{Ru}(\text{bipy})_3]^{2+/1+}$ (-1.33 V; Saji & Aoyagui, 1975) are also known. The excited state $^*[\text{Ru}(\text{bipy})_3]^{2+}$ has the emission maximum at 610 nm (in H_2O) (Lyttle & Hercules, 1969), i.e. the excited state is ca. 2.03 V above the ground state.

The effects of the photoexcitation on the redox potentials are shown in the diagrams:



The oxidizing



and reducing



potentials of $[\text{Ru}(\text{bipy})_3]^{2+}$ are enhanced by the excitation and $^*[\text{Ru}(\text{bipy})_3]^{2+}$ is an intermediate in a number of photochemical electron transfer reactions of $[\text{Ru}(\text{bipy})_3]^{2+}$ (Balzani, Laurence et al., 1975; Meyer, 1978; Balzani, Bolleta, Gandolfi & Maestri, 1979).

SECTION 3VI.3 OXIDATION-REDUCTION REACTIONS OF COPPER COMPLEXES

This section outlines general pattern of the reactivity of copper complexes towards different oxidants and reductants. No attempt is made to present a comprehensive review of the subject. Recently, the redox reactions of the 'blue' copper proteins have been reviewed (Holwerda, Wherland & Gray, 1976).

The oxidation-reduction reactions of copper complexes can be divided into: (1) reductions of Cu(II) Complexes, (2) oxidations of Cu(I) Complexes and (3) Cu(I)-Cu(II) self exchange rates.

VI.3.1 Reductions of Cu(II) Complexes

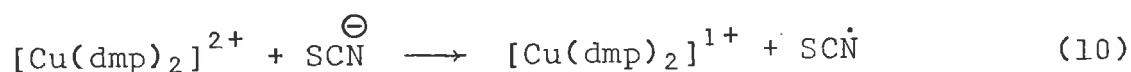
Careful quantitative measurements of the rates of reduction of Cu(II) complexes in reactions for which all the ancillary data needed to apply theoretical treatments of the electron transfer reactions (E^0 values, self exchange rates etc.) exist, are rare. The most useful are the reductions by metal aquo ions (Shaw & Espenson, 1968; Parker & Espenson, 1969a), reductions of copper blue proteins (Holwerda, Wherland & Gray, 1976) and the reductions of Cu(II) N-heterocyclic complexes by ferrocyanide (Augustin & Yandell, 1978).

Reduction by metal aquo ions is believed to occur principally by inner-sphere mechanism. Chromium(II) reduces $\text{Cu}_{(\text{aq})}^{2+}$ ion (Shaw & Espenson, 1968) in HClO_4 solution, forming Cu(I) which decomposes to the copper metal only slowly. On the basis of the similarity of the reduction to that by OH^\ominus ion the inner-sphere mechanism was postulated. The rate law was

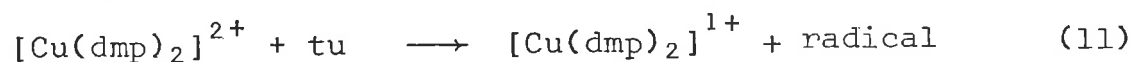
$$+ \frac{d[\text{Cu(I)}]}{dt} = \left(a + \frac{b}{[\text{H}^+]} \right) [\text{Cu(II)}][\text{Cr(II)}] \quad (9)$$

with $a = 0.17 \text{ M}^{-1} \text{ s}^{-1}$ and $b = 0.587 \text{ s}^{-1}$. The rate constant, for the reduction of $\text{Cu}_{(\text{aq})}^{2+}$ by V^{2+} (Parker & Espenson, 1969a), $26.6 \text{ M}^{-1} \text{ s}^{-1}$ at 25°C lies in the same range as those found for the inner-sphere oxidations of V^{2+} by other reactants (Dodel & Taube, 1965; Zwinckel & Taube, 1961; Baker, Orhanovic & Sutin, 1967; Malin & Swinehart, 1968; Espenson, 1967; Price & Taube, 1968; Newton & Baker, 1964, 1965).

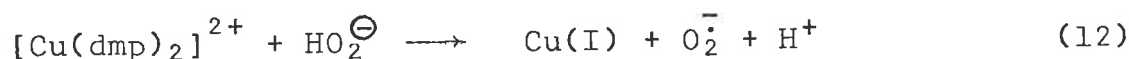
The reduction of $[\text{Cu}(\text{dmp})_2]^{2+}$ by thiocyanate ion, thiourea and hydrogen peroxide in aqueous HClO_4 and in methanolic solutions is believed to occur by both the inner-sphere and outer-sphere mechanisms (Davies & Loose, 1976a, b). The rates of outer-sphere reduction by SCN^- ion



by thiourea,

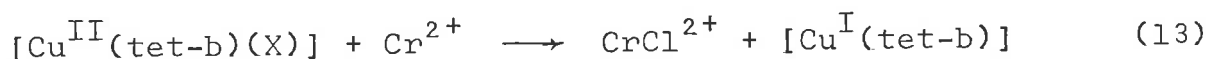


and by HO_2^-



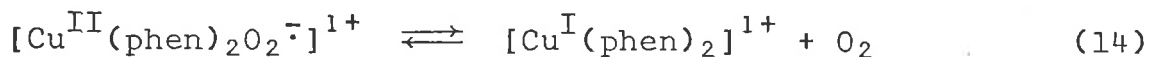
are $72 \pm 2 \text{ M}^{-1} \text{ s}^{-1}$, $(5.2 \pm 0.6) \times 10^3 \text{ M}^{-1} \text{ s}^{-1}$ and $1.2 \times 10^6 \text{ M}^{-1} \text{ s}^{-1}$ respectively. The rates of reduction of Cu(II) bis-complexes with imidazole (Im), ethylenediamine (en) and 1,3-diaminopropane by HO_2^- were estimated to be ca. $10^{-3} \text{ M}^{-1} \text{ s}^{-1}$ (Sharma & Schubert, 1971).

Cu(II) complexes of the saturated macrocyclic ligand (tet), $[\text{Cu}^{\text{II}}(\text{tet-b})(\text{X})]$ ($\text{X} = \text{Cl}^-$, Br^- or tu) are reduced by Cr^{2+} , V^{2+} and $[\text{Ru}(\text{NH}_3)_6]^{2+}$ (Al-Shatti, Segal & Sykes, 1977). The rates of the inner-sphere reduction for the various complexes were



found to lie in the range $80 \text{ M}^{-1} \text{ s}^{-1}$ to $< 10^{-2} \text{ M}^{-1} \text{ s}^{-1}$.

Reduction of $\text{Cu}_{(\text{aq})}^{2+}$ by HO_2^\cdot and O_2^- radicals proceeds by an inner-sphere path with preliminary formation of a $[\text{Cu}^{\text{II}}-\text{HO}_2]$ or $[\text{Cu}^{\text{II}}-\text{O}_2^-]$ complex (Rabani, Klug-Roth & Lilie, 1973; Meisel, Laynon & Czapski, 1974; Kozlov & Berdnikov, 1973). The catalytic oxidation of organic substrates (methanol, cumene) in an organic media by Cu(II) phen-complexes has been attributed to the formation of a copper-oxygen complex.



In nearly all cases of oxidation of organic or main-group substrates by Cu(II) species an inner sphere mechanism seems favoured and the data are of little relevance to outer sphere electron transfers.

The oxidation of ferrocytochrome c by a number of Cu(II) complexes of N-heterocyclic ligands has been studied recently (Augustin & Yandell, 1978). These presumably five- or six-coordinate complexes (including coordinated water molecules) were found to oxidize ferrocytochrome c at rates from $10^6 \text{ M}^{-1} \text{ s}^{-1}$ to $< 1 \text{ M}^{-1} \text{ s}^{-1}$. The rates of outer sphere reduction of Cu(II) complexes by ferrocytochrome c are presented in Table (29). The differences in the rates were attributed to special structural barriers to the outer-sphere electron transfer process arising from the stereochemical changes between Cu(I) and Cu(II) species.

Table (29)

RATES OF REDUCTION OF Cu(II) N-HETEROCYCLIC COMPLEXES
BY FERROCYTOCHROME C

Reference: Augustin & Yandell, 1978

Complex	$k/\text{M}^{-1} \text{ s}^{-1}$
$[\text{Cu}(\text{dmp})_2]^{2+}$	$(1.00 \pm 0.04) \times 10^6$
$[\text{Cu}(\text{phen})_2]^{2+}$	$(2.72 \pm 0.26) \times 10$
$[\text{Cu}(\text{phen})_3]^{2+}$	< 0.2
$[\text{Cu}(\text{NO}_2\text{-phen})_2]^{2+}$	$(1.5 \pm 0.06) \times 10^2$
$[\text{Cu}(\text{bipy})_3]^{2+}$	< 0.5

VI.3.2 Oxidations of Copper(I) Complexes

Studies of the oxidation of copper(I) complexes mainly consists of data for the rate of oxygen uptake by Cu(I) complexes of N-heterocyclic ligands and for reactions of Cu(I) species with $\text{Fe}_{(\text{aq})}^{3+}$ and $\text{V}_{(\text{aq})}^{3+}$ ions. Recently the kinetics of oxidation of Cu(I) Complexes by Co(III)-EDTA Complexes and by pentaminepyridine ruthenium(III) Complexes have been reported.

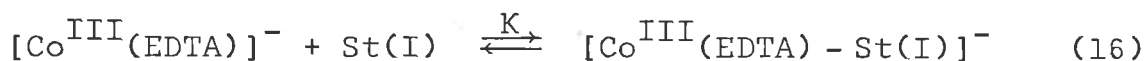
The oxidation of Cu(I) Complexes by dioxygen are presumably inner-sphere and for a wide range of Cu(I) Complexes the rate constants lie between 10^2 - $10^4 \text{ M}^{-1} \text{ s}^{-1}$ (Zuberhüler, 1967, 1969, 1970; Petch & Anbar, 1970; Arce, Spodine & Zamudio, 1975; Crumbliss & Gestant, 1976).

The reduction of $\text{Fe}_{(\text{aq})}^{3+}$ by $\text{Cu}_{(\text{aq})}^{1+}$ is believed to proceed by an inner-sphere mechanism with

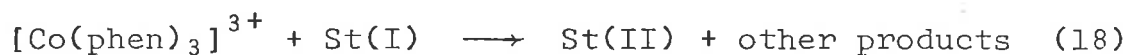
$$-\frac{d[\text{Fe(III)}]}{dT} = \frac{k_{\text{obs}} [\text{Fe(III)}][\text{Cu(I)}]}{[\text{H}^+]} \quad (15)$$

$k_{\text{obs}} \approx 2.5 \times 10^4 \text{ M}^{-1} \text{ s}^{-1}$ at 2°C (Parker & Espenson, 1969) but in striking contrast, the reaction of Cu_{aq}^+ with $[\text{FeN}_3]^{2+}$ and $[\text{FeF}]^{2+}$ were too fast for stopped-flow studies ($k_{\text{FeN}_3^{2+}} \geq 10^8 \text{ M}^{-1} \text{ s}^{-1}$, $k_{[\text{FeF}_2]^+} = 5 \times 10^6 \text{ M}^{-1} \text{ s}^{-1}$; Parker & Espenson, 1969b). $\text{Cu}_{(\text{aq})}^+$ ions (d^{10}) show no ligand field effects and while the rate constants for water exchange have not been measured, the electrostatic field suggests a rate of water exchange approximating that for a Group I ion of about the same ionic radius ($r_{\text{Cu}^+} = 0.96 \text{ \AA}$, $r_{\text{Na}^+} = 0.95 \text{ \AA}$; Cotton & Wilkinson, 1972), i.e. ca. 10^9 s^{-1} , so that in most cases the rate of substitution would not limit the rate of inner-sphere electron transfers. Very rapid oxidations of the equally labile $\text{Cr}_{(\text{aq})}^{2+}$ ion (Thornton & Laurence, 1974) have also been shown to have an appreciable inner-sphere character.

The oxidation of cuprous stellacyanin, St(I), by $[\text{Co}(\text{EDTA})]^-$ at pH = 7 is believed (Holwerda et al., 1977) to proceed through the formation of a transient complex followed by an intramolecular electron transfer with $K = 149 \text{ M}^{-1}$ and $k = 0.169 \text{ s}^{-1}$ at 25.1°C



and an ionic strength of 0.5 M, but the reduction of $[\text{Co}(\text{phen})_3]^{3+}$ by St(I) was found to occur by an outer-sphere mechanism with a rate constant of $1.8 \times 10^5 \text{ M}^{-1} \text{ s}^{-1}$ (McArdle et al., 1974).

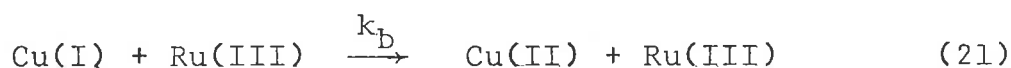
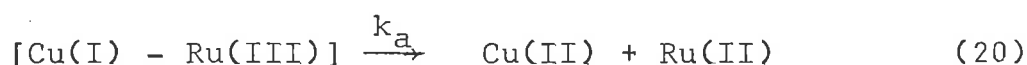
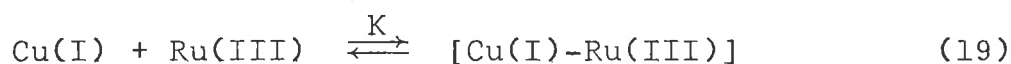


The rate constants for the outer-sphere oxidation of $[\text{Cu}(\text{phen})_2]^+$ and $[\text{Cu}(\text{bipy})_2]^+$ by $[\text{Co}(\text{EDTA})]^-$, $[\text{Co}(\text{PDTA})]^-$ and $[\text{Co}(\text{CyDTA})]^-$ were found to be remarkably similar (ca. $3 \times 10^3 \text{ M}^{-1} \text{ s}^{-1}$; Holwerda et al., 1977) with the order

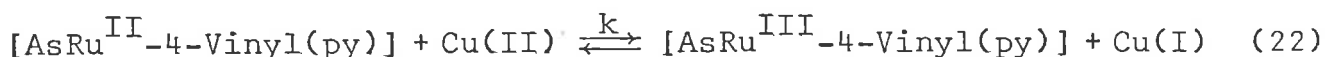


The activation parameters were claimed to be typical of those for outer-sphere processes with similar reactants (Wilkins & Yelin, 1968; Grossman & Wilkins, 1967).

The oxidation of $\text{Cu}_{(\text{aq})}^{\text{I}}$ by $[\text{AsRu}^{\text{III}}\text{-4-Vinyl(py)}]$ was found (Hurst, 1976; Norton Jr. & Hurst, 1978) to occur by both intermolecular (k_{b}) and intramolecular (k_{a}) pathways with the rate constants of $1.4 \times 10^3 \text{ M}^{-1} \text{ s}^{-1}$ and ca. $10^{-2} \text{ M}^{-1} \text{ s}^{-1}$ respectively.



Cupric ion is an effective catalyst for the oxidation of [AsRu^{II}-4-Vinyl(py)] by dioxygen with a rate constant (k) of $34 \pm 0.6 \text{ M}^{-1} \text{ s}^{-1}$.



No evidence is available on the effects of complex geometry on the rate constants for the oxidation of Cu(I) complexes and most of the studied reactions are inner-sphere. Despite the number of systems studied, the data as yet do not form a basis for a discussion of the intimate mechanism of electron transfer reactions of Cu(I) and Cu(II) complexes.

VI.3.3 The Self Exchange Rates of Cu(I) and Cu(II) Complexes

The self exchange rates of copper complexes are largely a matter of conjecture. The self exchange rates have been estimated for Cu(I) complexes of N-heterocyclic ligands, Cu(I)-chloro complexes and copper blue proteins on the basis of the Marcus theory of electron transfer reactions but these estimates are not beyond criticism.

The exchange rates for the presumably tetrahedral chloro-complexes present in concentrated (12 M) HCl are high, ca. 2×10^8 (McConnell & Weaver, 1956). Valee and Williams (1968) found that the electron transfer and self exchange rate for 'blue' copper proteins are comparatively fast (ca. $2 \times 10^5 \text{ M}^{-1} \text{ s}^{-1}$). It was suggested that the geometry of the copper ion in these enzymes is intermediate between square planar and tetrahedral so facilitating the electron transfer by reducing the reorganizational barrier but the existence of a large reorganizational barrier to

self exchange between normal Cu(I) and Cu(II) systems is largely conjectural, and in many cases the direct application of the Marcus theory is hampered by the lack of free energy data.

Recent estimates of the self exchange rates of bis-phen and -bipy complexes fall in the range $10^2 \text{ M}^{-1} \text{ s}^{-1}$ to $10^4 \text{ M}^{-1} \text{ s}^{-1}$ (Augustin & Yandell, 1978). The available data on self exchange rates are summarized in Table (30).

Table (30)

RATE CONSTANTS FOR SELF EXCHANGE OF COPPER COMPLEXES

System	Self Exchange Rate/ $\text{M}^{-1} \text{ s}^{-1}$	Reference
$[\text{CuCl}]^{0,1+}$	5×10^8	McConnell & Weaver, 1956
$[\text{St(I)}]/[\text{St(II)}]$	2×10^5	Valee & Williams, 1968
$[\text{Cu(bipy)}_2]^{1+,2+}$	4×10^6	Holwerda et al., 1977
$[\text{Cu(phen)}_2]^{1+,2+}$	5×10^7	
$[\text{Cu(dmp)}_2]^{1+,2+}$	1.8×10^4	Augustin & Yandell, 1978
$[\text{Cu(phen)}_2]^{1+,2+}$	7.4×10	
$[\text{Cu(NO}_2\text{-phen)}_2]^{1+,2+}$	1.0×10^2	

SECTION 4VI.4 EXPERIMENTALVI.4.1 Solutions and Apparatus

The preparation, characterization and standardization of the solutions of the copper complexes and the data acquisition and treatment in the laser excitation and flash photolysis experiments have been described in Chapter 2.

VI.4.2 Laser Excitation - Measurements of the Quenching Rate Constants

The quenching rate constants, k_q , for the quenching of the luminescence of $^*[Ru(bipy)_3]^{2+}$ by the copper complexes, $Cu^{II}L_n$ (L = bipy, phen or its related ligands, diene, en, Me₆-tren, EDTA, viol) were obtained from the Stern-Volmer plots (Eqn. 24) of the excited state lifetimes in the presence of varying con-

$$\tau_0/\tau = 1 + k_q [Cu(II)] \quad (24)$$

centrations (1.0 - 10.0 mM) of the quenchers. A pulsed N₂ laser (Lambda Physik; $\lambda_{excitation} = 337.1$ nm; energy/pulse = 2.5 mJ) was used as the excitation source and the excited state emission was monitored at 610 nm (Lyttle & Hercules, 1969). The experiments were carried out at the natural pH of the solutions at $25 \pm 0.2^\circ C$.

VI.4.3 Flash Photolysis - Measurements of the Thermal Back Electron Transfer Rates

The mechanism of quenching was determined by flash photolysis experiments. Solutions of $[Ru(bipy)_3]^{2+}$ (10 μM) and the copper complex (4 mM) were flashed using visible light from the flash lamp. UV-light from the flash lamp was excluded by a glass

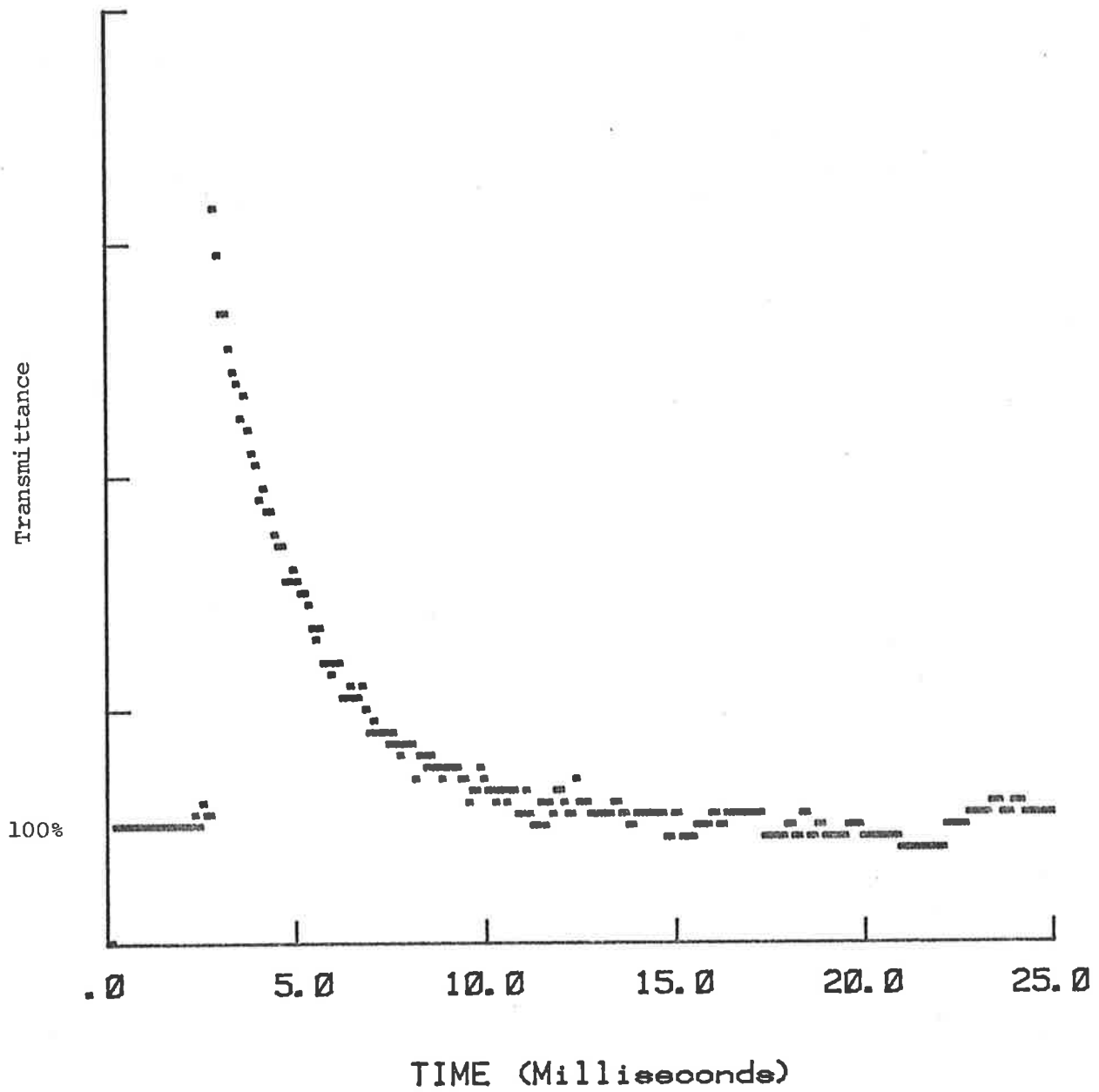


Fig. (30) Absorbance changes at 436 nm in the photolysis of $[\text{Ru}(\text{bipy})_3]^{2+}$ ($10 \mu\text{M}$) and $[\text{Cu}(\text{Me}_6\text{-tren})(\text{H}_2\text{O})]^{2+}$ (4 mM) at the natural pH.

filter.

Absorbance changes following the flash occurred in two stages [Fig. (30)]. The first stage took place during the light flash and caused an immediate ($t_{1/2} < 10 \mu\text{sec}$) decrease in the absorbance at 436 nm. This change in absorbance corresponds to the formation of $[\text{Ru}(\text{bipy})_3]^{3+}$ ($\epsilon_{\text{Ru(II)}}^{436} = 1.2 \times 10^4 \text{ M}^{-1} \text{ cm}^{-1}$; $\epsilon_{\text{Ru(III)}}^{436} \approx 2 \times 10^2 \text{ M}^{-1} \text{ cm}^{-1}$). The second stage lasted 0.5 to 500 m sec (dependent upon the copper(II) complex) and corresponds to the return of the system to its original state before the flash. Fig. (30) shows typical absorbance changes for a solution 10 μM in $[\text{Ru}(\text{bipy})_3]^{2+}$ and 4 mM in $[\text{Cu}(\text{Me}_6\text{-tren})(\text{H}_2\text{O})]^{2+}$.

VI.4.4 Measurements of the Activation Energies for the Quenching Rate Constants

The activation energies were measured for the $\text{Cu}_{(\text{aq})}^{2+}$ $[\text{Cu}(\text{phen})_2]^{2+}$ and $[\text{Cu}(\text{bipy})_2]^{2+}$ quenchers. These measurements were made by Ms. P. Ashwood, Mr. R.J. Thomas and Dr. G.S. Laurence (Department of Physical and Inorganic Chemistry, University of Adelaide). The experiments were carried out over the temperature range 287°K to 309°K at a constant ionic strength of 0.50 M. The ionic strength was adjusted with NaClO_4 (AnalaR, B.D.H.).

SECTION 5VI.5 RESULTS

A series of copper complexes $\text{Cu}^{\text{II}}\text{L}_n$ ($\text{L} = \text{bipy}, \text{phen}$ or its related ligands, EDTA, en, diene, $\text{Me}_6\text{-tren}$, viol; $n = 1\text{-}3$) were used as quenchers. The bimolecular quenching rate constants, k_q , and the rate constants, k_{th} , for the thermal reactions of the photolysis products to reform $[\text{Ru}(\text{bipy})_3]^{2+}$ and the copper(II) complexes, where this data is available, are given in Table (31). The values of k_q and k_{th} fall in the ranges $\sim 10^7 - 10^9 \text{ M}^{-1} \text{ s}^{-1}$ and $\sim 10^8 - 10^9 \text{ M}^{-1} \text{ s}^{-1}$ respectively, and are of the order of rates of reactions of $\text{Cu}^{2+}_{(\text{aq})}$ ion with excited Ru(II) complexes of N-hetrocyclic ligands (Hoselton et al., 1978).

The absorbance changes following the flash are consistent with reactions (25), (26), (27) and (28).



The decrease in absorbance at 436 nm during the light flash represents photoexcitation and quenching and is due to the conversion of $[\text{Ru}(\text{bipy})_3]^{2+}$ to $[\text{Ru}(\text{bipy})_3]^{3+}$ (reactions (25) and (27)). No transient absorbance other than Ru(III) formation could be detected in the flash photolysis experiments. Reaction (27) results in the formation of equal concentrations of $[\text{Ru}(\text{bipy})_3]^{3+}$ and $\text{Cu}^{\text{I}}\text{L}_n$ and for equal concentrations second order kinetics would be expected for the thermal oxidation reaction (28) between $[\text{Ru}(\text{bipy})_3]^{3+}$ and $\text{Cu}^{\text{I}}\text{L}_n$. Second order kinetics were indeed observed for the return of the system to the original

Table (31)
 QUENCHING AND THERMAL ELECTRON TRANSFER
 RATE DATA

^aJame & Williams, 1961; ^bPalmer, Papaconstantinou & Endicott, 1969.

Quencher	$\frac{E^0}{\text{Volts}^a}$	$10^{-8} \times k_q / M^{-1} s^{-1}$	$10^{-8} \times k_{th} / M^{-1} s^{-1}$
$\text{Cu}_{(\text{aq})}^{2+}$	+0.176	0.50	2.6
$[\text{Cu}(\text{phen})]^{2+}$	-	3.27	1.823
$[\text{Cu}(\text{phen})_2]^{2+}$	0.1740	7.50	3.36
$[\text{Cu}(\text{phen})_3]^{2+}$	-	3.94	23.3
$[\text{Cu}(\text{Me}_4\text{-phen})_3]^{2+}$	0.268	1.46	32.0
$[\text{Cu}(\text{NO}_2\text{-phen})_3]^{2+}$	0.379	3.65	5.7
$[\text{Cu}(\text{Cl-phen})_2]^{2+}$	0.400	9.20	17.3
$[\text{Cu}(\text{bipy})_2]^{2+}$	0.120	3.41	≥ 20
$[\text{Cu}(\text{bipy})_3]^{2+}$	-	7.77	27.7
$[\text{Cu}(\text{viol}^*)_2]^{2+}$	-	33.6	-
$[\text{Cu}(\text{H}_2\text{EDTA})]^{2-}$	-	2.6	3.7
$[\text{Cu}(\text{en})_2]^{2+}$	-0.360	0.31	83.4
$[\text{Cu}^{\text{II}}(\text{diene})]^{2+}$	-0.490 ^b	0.353	-
$[\text{Cu}^{\text{II}}(\text{Me}_6\text{-tren})]^{2+}$	-	2.30	65.1

* 1,3-dimethylviolurate

state and the observed rate constants were converted to the true

$$k_{\text{obs}} = \frac{k_{\text{th}}}{\Delta \epsilon l} \quad (29)$$

second order rate constant (k_{th}) using

$$\Delta \epsilon_{436} = \epsilon_{\text{Ru(II)}}^{436} - \epsilon_{\text{Ru(III)}}^{436} - \epsilon_{\text{Cu(I)}}^{436} \quad (30)$$

The second order plots were linear for at least two half lives.

The activation parameters for the quenching by $\text{Cu}_{(\text{aq})}^{2+}$, $[\text{Cu}(\text{phen})_2]^{2+}$ and $[\text{Cu}(\text{bipy})_2]^{2+}$ are summarized in Table (32).

Table (32)

ACTIVATION PARAMETERS FOR QUENCHING BY COPPER COMPLEXES

Quencher	$\Delta H^\ddagger / \text{kJ mol}^{-1}$	$\Delta S^\ddagger / \text{J K}^{-1} \text{ mol}^{-1}$
$\text{Cu}_{(\text{aq})}^{2+}$	13.81	-54.2
$[\text{Cu}(\text{phen})_2]^{2+}$	21.95	-4.4
$[\text{Cu}(\text{bipy})_2]^{2+}$	17.20	-17.8

The quenching of $^*[\text{Ru}(\text{bipy})_3]^{2+}$ by $\text{Cu}^{\text{II}}\text{L}_n$ complexes is clearly due to electron transfer from the flash photolysis experiments. Direct evidence from flash photolysis experiments could not be obtained for $[\text{Cu}^{\text{II}}(\text{diene})]^{2+}$ and $[\text{Cu}(\text{viol})_2]^0$ due to the strong absorbance by these complexes at wavelengths between 300 nm and 500 nm, so that inner filter effect prevented excitation of the $[\text{Ru}(\text{bipy})_3]^{2+}$ by the light from the flash. However, the values of k_q [Table (31)] are not inconsistent with the view that all of the Cu(II) complexes investigated quench $[\text{Ru}(\text{bipy})_3]^{2+}$ by an electron transfer mechanism.

It is obvious that the rates of both the reduction of Cu(II) by $^*[\text{Ru}(\text{bipy})_3]^{2+}$ and oxidation of Cu(I) by $[\text{Ru}(\text{bipy})_3]^{3+}$ are much greater than for most of the redox reactions of copper complexes discussed in section VI.3 (pp. (212)-(218)).

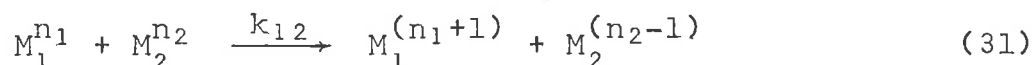
SECTION 6DISCUSSIONVI.6.1 General Observations

The dynamic bimolecular quenching of the excited states involves the formation of a collision encounter complex and it has been reported that the quenching efficiency in the collision encounter is affected by the charge on the complex (Wagastian & Hamond, 1971; Pfeil, 1971; Demas & Adamson, 1971; Fujita & Kobayashi, 1972; Bolleta, Maestri & Moggi, 1973), by the geometry of the complex (Adamczyk & Wilkinson, 1972; Maestri, Moggi & Balzani, 1973) and by the nature of the ligands (Linschitz & Pekarinen, 1960; Steel & Linschitz, 1962; Banfield & Hussain, 1969; Ohno & Kato, 1969).

But over the range of Cu(II) complexes in Table (31) the rates are insensitive to these factors, although they are below the diffusion controlled limit for ionic charge product of +4 and encounter distances between 5 Å and 10 Å at the ionic strengths used. The reactions are undoubtedly outer-sphere, as both $[\text{Ru}(\text{bipy})_3]^{2+}$ and $[\text{Ru}(\text{bipy})_3]^{3+}$ are very inert and the flash photolysis experiments show clearly the immediate, direct, formation of $[\text{Ru}(\text{bipy})_3]^{3+}$.

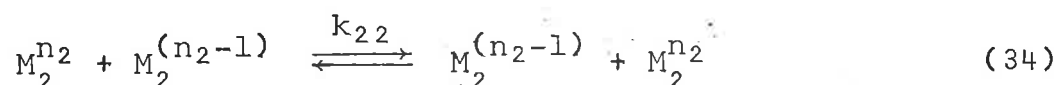
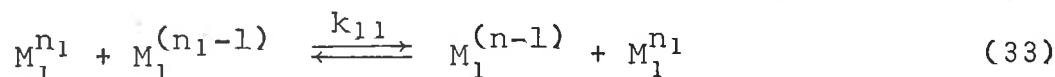
VI.6.2 Current Approaches to Theories of Electron Transfer Rates(i) The Marcus Theory

Marcus (1956, 1965, 1968) and Marcus and Sutin (1975) have shown that the free energy of activation (ΔG_{12}^{**}) for the electron transfer reaction (36) can be written as



$$\Delta G_{12}^{**} = \left(\frac{\Delta G_{11}^{**} + \Delta G_{22}^{**}}{2} \right) + \left(\frac{\Delta Gr^0}{2} \right) + \frac{(\Delta Gr^0)^2}{8(\Delta G_{11}^{**} + \Delta G_{22}^{**})} \quad (32)$$

where ΔG_{22}^{**} and ΔG_{22}^{**} refer to the free energies for the self exchange reactions (33) and (34)



and ΔGr^0 is the overall free energy change for the cross reaction (31). Equation (32) can be written in terms of a reorganizational parameter λ_{12} , where

$$\lambda_{12} = 2(\Delta G_{11}^{**} + \Delta G_{22}^{**}) \quad (35)$$

$$\begin{aligned} \therefore \Delta G_{12}^{**} &= \left(\frac{\Delta G_{11}^{**} + \Delta G_{22}^{**}}{2} \right) + \left(\frac{\Delta Gr^0}{2} \right) \\ &= \left(\frac{\lambda_{12}}{4} \right) + \left(\frac{\Delta Gr^0}{2} \right) \end{aligned} \quad (36)$$

$$\text{when } 8(\Delta G_{11}^{**} + \Delta G_{22}^{**}) \gg \Delta Gr^0 \quad (37)$$

For equation (36), ΔG_{12}^{**} will reach a minimum when $\Delta Gr^0 = -\lambda_{12}$ and increase again as ΔGr^0 becomes large and negative i.e. the rate constant for the cross reaction (31) between a single reductant $M_1^{n_1}$ and a homogenous series of oxidants ($M_{2a}^{n_2}$, $M_{2b}^{n_2}$,) should increase[†] up to maximum as the reduction potential of the oxidant increases [Fig. (31), Page (227)]. The region in which the rate constant (k_{12}) decreases with increasing $|\Delta Gr^0|$ is called the "abnormal" or the "Marcus inverted" region. Creutz and Sutin (1977) found 'vestiges' of the inverted region in the

[†] Assuming that the self exchange rates (k_{22}) for the series of oxidants do not change to any significant extent.

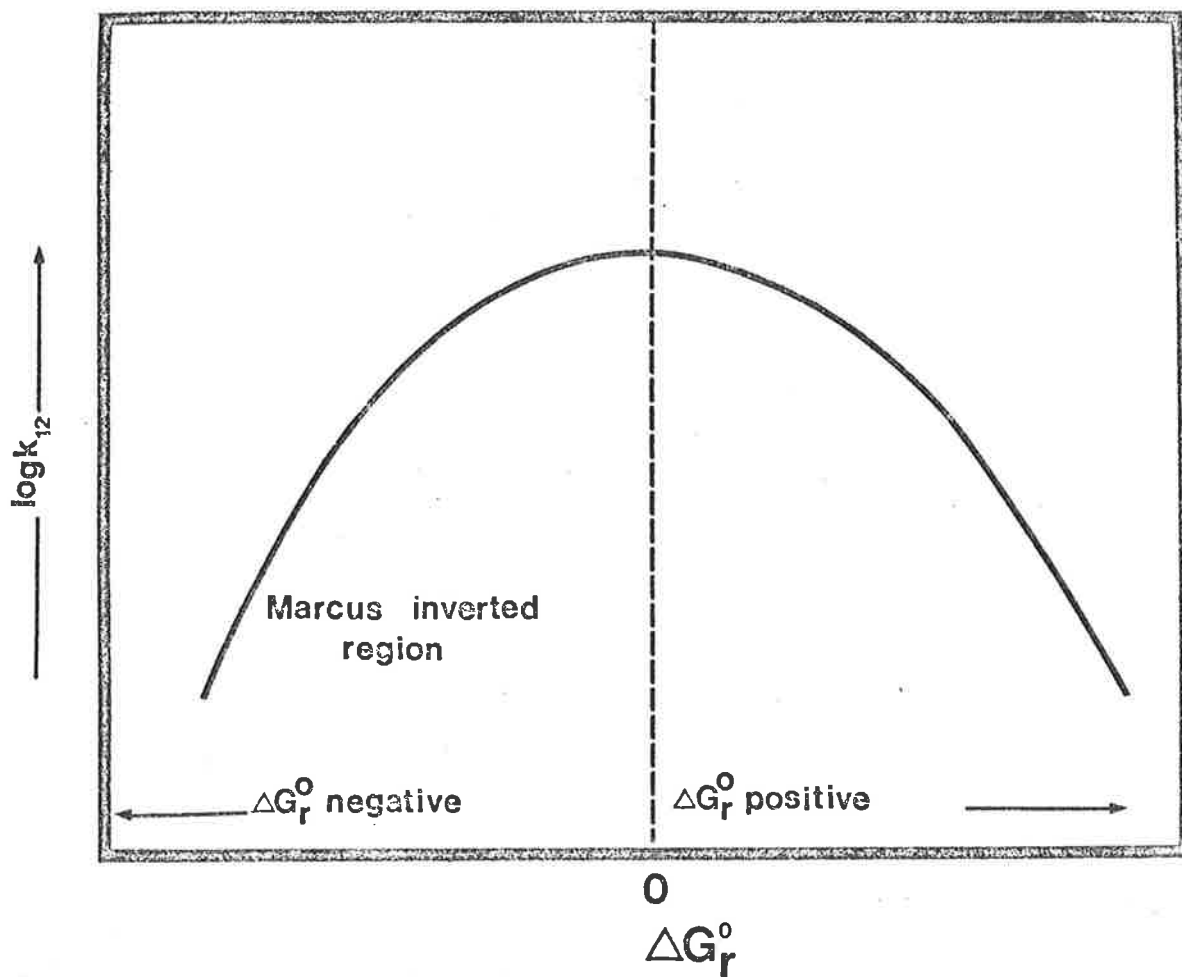
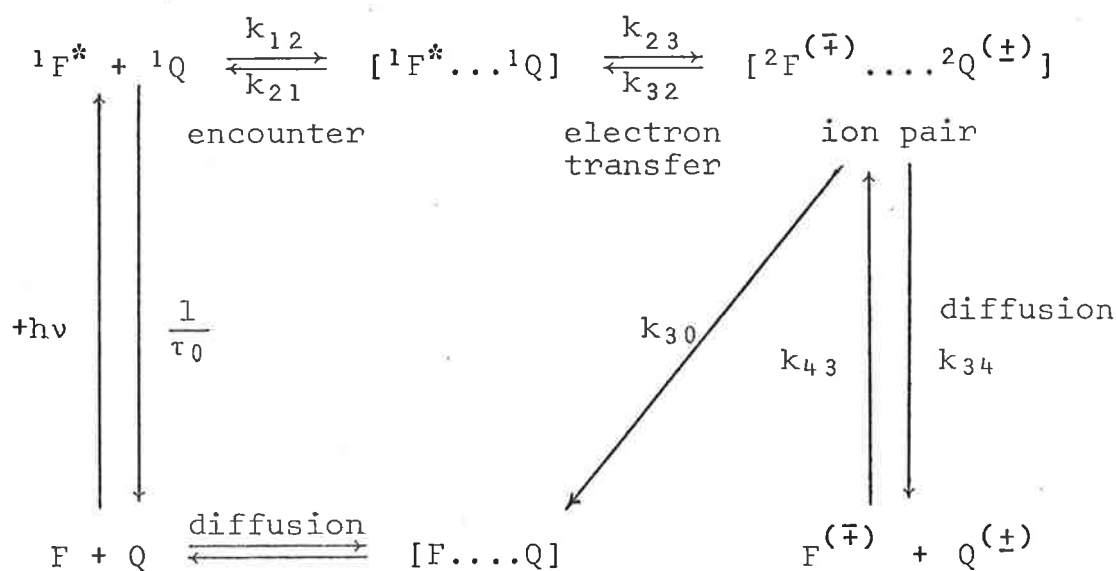


Fig. 31 The Marcus Theory's Predicted Behaviour of $\log k_{12}$ versus ΔG_r°

quenching of the luminescence of Ru(II) complexes $[\text{RuL}_3]^{2+}$ (L = bipy, dmb) by trivalent polypyridine metal complexes $[\text{ML}_3]^{3+}$ (M = Cr(III), Ru(III), Os(III); L = bipy, dmb). The quenching rate constants decreased from $2.7 \times 10^9 \text{ M}^{-1} \text{ s}^{-1}$ to $1.5 \times 10^9 \text{ M}^{-1} \text{ s}^{-1}$ as the reduction potential of the oxidant ($E_{1/2}^\circ$) increased from 0.5 V to 2.1 V. However the rate constants are close to diffusion controlled and the evidence for the existence of the inverted region was slight.

(ii) The Rehm-Weller Treatment

Rehm and Weller (1969, 1970) could not find any evidence of the "inverted" region in their study of the electron transfer quenching of the fluorescence of pyrene-3-carboxylic acid, Benz(-c)-acridine, Ben(a)anthracene and pyrene-4-carboxylic acid by anilines, substituted anilines and methoxy substituted benzenes. The rate constants for the electron transfer step were found to increase



from $10^6 \text{ M}^{-1} \text{ s}^{-1}$ to a limiting value of $2 \times 10^{10} \text{ M}^{-1} \text{ s}^{-1}$ over a range of ΔG^0 from $+15 \text{ K cal mol}^{-1}$ to $-60 \text{ K cal mol}^{-1}$. In fact the limiting value was reached at $-15 \text{ K cal mol}^{-1}$. Large deviation from the relationship given in equation (36) (the Marcus

theory) occurred for $|\Delta Gr^0| > 15 \text{ K Cal mol}^{-1}$. These deviations may be accounted for within the framework of the Marcus theory

by assuming:

- (1) that all the three electron transfer processes (k_{23} , k_{32} and k_{30}) occur by normal outer-sphere mechanisms which involve solvational changes before and after the electron transfer (k_{23}) so that their rates can be written as

$$k_{ij} = k^0 e^{-(\Delta G_{ij}^\ddagger)} \quad (38)$$

- (2) that $k^0 \sim \frac{1}{\tau_\epsilon}$, where τ_ϵ is the dielectric relaxation time of the solvent

- (3) that the electron transfer steps differ in ΔG_{ij}^\ddagger

- (4) that $\Delta G_{30}^\ddagger \approx \text{zero}$ so that $k_{30} \approx k^0$ and the rate of electron transfer step (k_{23}) can be written as

$$k_{23} = k_{30} e^{-(\Delta G_{23}^\ddagger)/RT} \quad (39)$$

and including

- (i) The alternate pathways by which the ion pair can disappear (represented by the composite rate constant k_{30}), in particular the back electron transfer leading to the formation of an excited state of different multiplicity from that of the radical pair or ground state (Weller, 1967; Knibe, Rehm & Weller, 1968).
- (ii) The assumption that ΔG_{12}^{**} is a monotonic function of ΔGr^0 , expressed as

$$\Delta G_{12}^{**} = \left(\frac{\Delta Gr^0}{2} \right) + \left[\left(\frac{\Delta Gr^0}{2} \right)^2 + \left(\frac{\lambda_{12}}{4} \right)^2 \right]^{1/2} \quad (40)$$

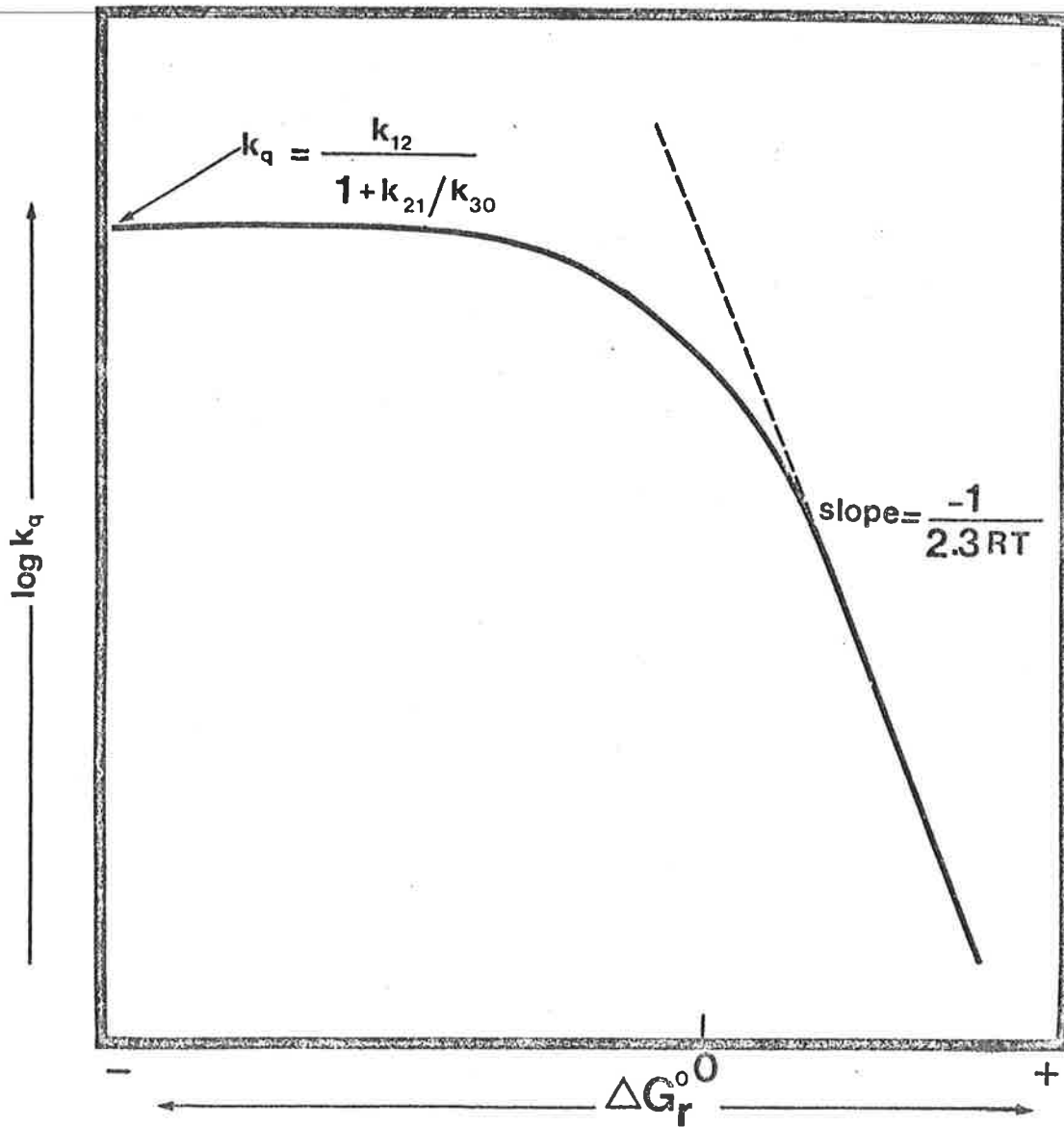


Fig. 32 The Rehm-Weller Treatment's Predicted Behaviour of $\log k_q$ versus ΔG_r^0

The bimolecular quenching rate constant k_q , for the reaction scheme, can then be written as

$$k_q = \frac{k_{12}}{1 + \frac{k_{21}}{k_{23}} + \frac{k_{21}}{k_{30}} \times e^{(\Delta Gr^\circ/RT)}} \quad (41)$$

where $K_{23} = e^{-(\Delta Gr^\circ/RT)}$ (42)

From equation (41) k_q increases as $-\Delta Gr^\circ$ becomes more negative until it reaches the diffusion controlled limit [Fig. (31)].

The value of the limit for large $|\Delta Gr^\circ|$ is given by

$$k_q = \frac{k_{12}}{1 + \frac{k_{21}}{k_{30}}} \quad (43)$$

and the slope of the linear relation for large $|\Delta Gr^\circ|$ is

$$\frac{1}{2.3 RT} \text{ [Fig. (32)].}$$

The experimental results agree with the predictions of the Rehm-Weller equation for the electron transfer quenching of fluorescent aromatic molecules (Rehm & Weller, 1969; 1970), thionine and lamiflavin acid (Vogelman et al., 1975), the duroquinone triplet (Scheerer & Gratzel, 1977), the lowest excited states of $[\text{Cr}(\text{bipy})_3]^{2+}$ and $[\text{Ir}(\text{Me}_2\text{-phen})_2\text{Cl}_2]^{1+}$ (Ballardini et al., 1978) and cyano-substituted anthracenes (Eriksen & Foote, 1978).

The controversy over whether the Marcus theory or the Rehm-Weller treatment is the better description of electron transfer reactions for which $|\Delta Gr^\circ|$ is large, is undecided. The near diffusion controlled rate constants for many of the systems studied make interpretation of the results difficult at the detailed level required to distinguish the treatments.

VI.6.3 Rate Constants, Activation Parameters and the Marcus theory

For the quenchers used the rate constants (k_q and k_{th}) and the activation parameters (E_a , ΔH_{12}^\ddagger and ΔS_{12}^\ddagger) were expected to vary significantly for the copper complexes in going from pseudo-octahedral complexes such as $[\text{Cu}(\text{H}_2\text{O})_6]^{2+}$ to the trigonal bipyramidal Cu(II) bis-polypyridine complexes due to the existence of possible structural barriers as suggested by Augustin and Yandell (1978). The fact, that the differences in the rate constants ($k_q \sim 10^7 - 10^9 \text{ M}^{-1} \text{ s}^{-1}$ and $k_{th} \sim 10^8 - 10^9 \text{ M}^{-1} \text{ s}^{-1}$) and activation energies (ca. 16 - 25 kJ mol^{-1}) are not great, does not confirm this expectation. Chou, Creutz and Sutin (1977) have reported the rate constants for the thermal outer-sphere electron reactions and their activation energies. The values of ΔH_{12}^\ddagger were found to range from $\sim -16 \text{ kJ mol}^{-1}$ to $\sim +53 \text{ kJ mol}^{-1}$ while the entropy of activation (ΔS_{12}^\ddagger) fell in the range $\sim -(46-175) \text{ JK}^{-1} \text{ mol}^{-1}$ for the observed rate constants ($k_{12}^{obs} \sim 10^4 - 10^7 \text{ M}^{-1} \text{ s}^{-1}$). Recent studies of the reduction of Ru(III) amine complexes by $[\text{TiOH}]^{2+}$ ($\Delta H_{12}^\ddagger \approx 15 - 35 \text{ kJ mol}^{-1}$; $\Delta S_{12}^\ddagger \approx 95 - 12 \text{ JK}^{-1} \text{ mol}^{-1}$; Davies & Earley, 1978) and reduction of Os(III) tris-polypyridine complexes by iodide and thiocyanate ions ($\Delta H_{12}^\ddagger \approx 8 - 17.5 \text{ kJ mol}^{-1}$; $\Delta S_{12}^\ddagger \approx 4 - 18 \text{ JK}^{-1} \text{ mol}^{-1}$; Nord, Pederson & Farver, 1978) and the estimates of Chou, Creutz and Sutin (1977) show that orders of magnitude of the activation parameters for the thermal outer-sphere electron transfer reactions to be as small as in the present study [Table (32)].

The Marcus theory (eqn. 36) predicts that the plot of $\log k_{12}$ versus $\log K_{12}$ should be linear for similar systems, provided the range of K_{12} values is small enough but the plot is non-linear in the present case [Fig. (33)].

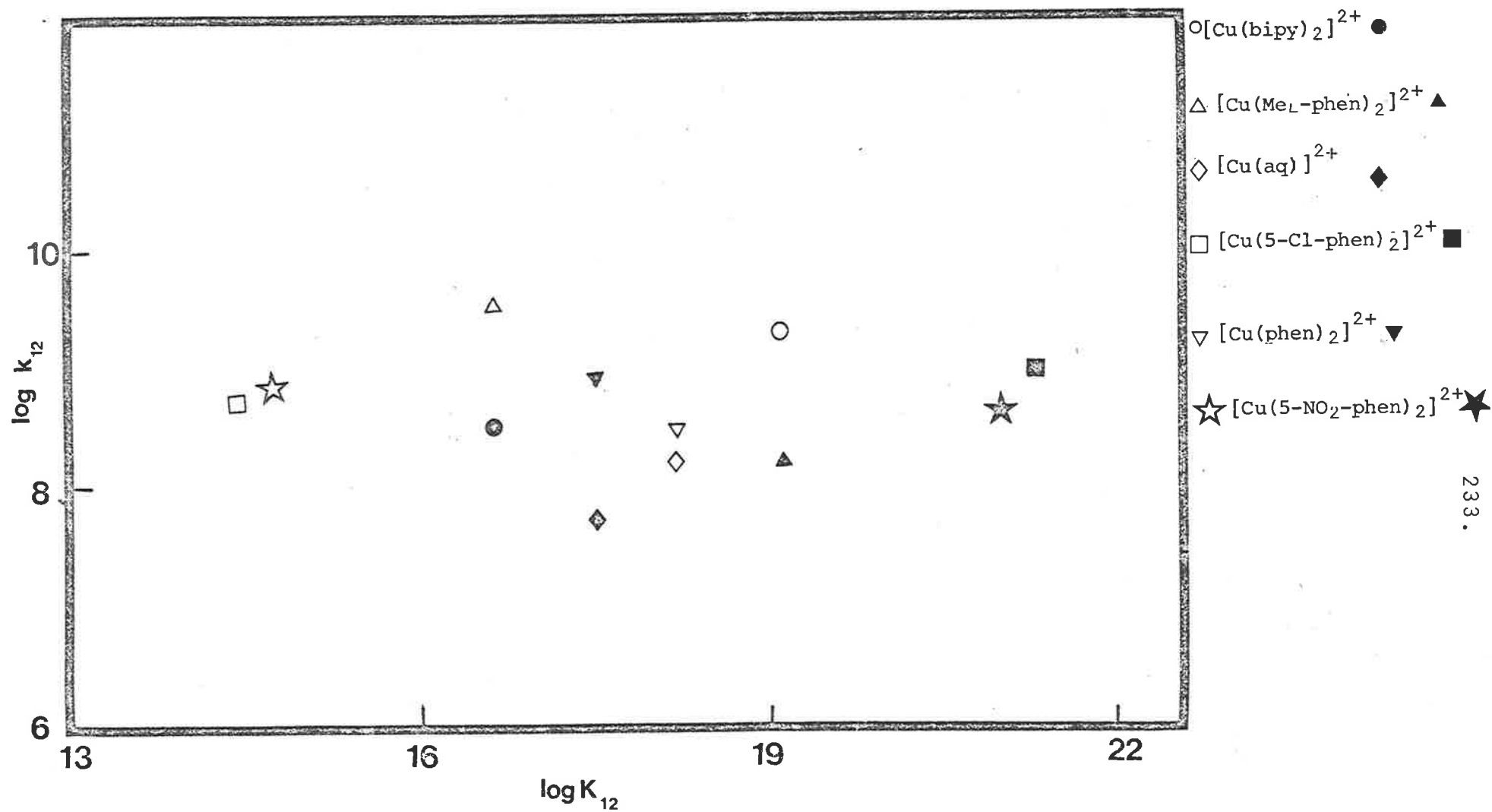
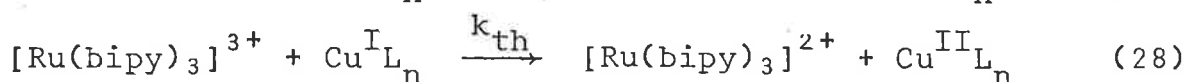
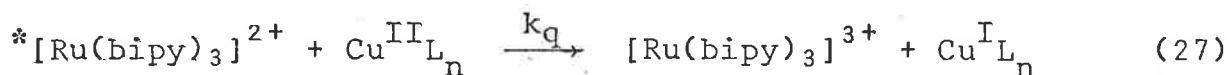


Fig. (33) Plot of $\log k_{12}$ versus $\log K_{12}$ for the copper complexes used as quenchers. The hollow points and full points refer to the thermal and photochemical processes respectively.

From the rates of the photochemical reductions (k_q) of Cu(II) complexes and the thermal reoxidation (k_{th}) of the Cu(I) complexes



it was possible to estimate photochemical (k_{ex}^ϕ) and thermal (k_{ex}^{th}) exchange rates. The self exchange rate data, based on the values of $2 \times 10^9 \text{ M}^{-1} \text{ s}^{-1}$ for the thermal exchange rate of $[\text{Ru}(\text{bipy})_3]^{2+,3+}$ and $3 \times 10^9 \text{ M}^{-1} \text{ s}^{-1}$ for $[\text{Ru}(\text{bipy})_3]^{*2+,3+}$ are summarized in Table (33).

Surprisingly, the exchange rates estimated on the basis of the photochemical (k_q) and thermal reactions (k_{th}) do not agree probably because the ΔG^0 values for the photochemical and thermal reactions differ in some cases by 84 kJ mol^{-1} . The values are also at variance with previous estimates. The estimates of the calculated self-exchange rates can be compared with those of Holwerda et al. (1977) and Augustin and Yandell (1978), Table (30).

Flash photolysis experiments clearly show the quenching to be by an outer-sphere electron transfer mechanism. The possibility of quenching by an energy transfer process can be ruled out because of the magnitude of the quenching rate constants (k_q). Quenching by an energy transfer process only leads to the electron-transfer products



if oxidation of $[\text{Ru}(\text{bipy})_3]^{2+}$ by the excited $^*\text{Cu}(\text{II})$ species occurs before these species diffuse from the cage in which they are formed. This requires that the electron transfer between $[\text{Ru}(\text{bipy})_3]^{2+}$ and $^*\text{Cu}(\text{II})$ to be diffusion controlled but the quenching rate constants (k_q) are below the diffusion controlled limit.

Notice that

- (1) no linear relationship exists between $\log k_{12}$ and $\log K_{12}$
- (2) the Cu(I)-Cu(II) exchange rates* (k_{ex}^ϕ and $k_{\text{ex}}^{\text{th}}$) are different
- (3) the estimated exchange rates for the copper complexes in this work are different from the previously reported values estimated from different cross reactions

These observations raise the question of whether the Marcus theory is applicable to these oxidation-reduction reactions involving copper complexes and ruthenium tris-bipyridine complexes.

* The exchange rates estimated on the basis of the quenching rate constants (k_q) and thermal reaction rates (k_{th}) are termed here as photochemical (k_{ex}^ϕ) and thermal ($k_{\text{ex}}^{\text{th}}$) exchange rates.

VI.6.4 The Relationship between k_{12} and K_{12}

This is shown in Fig. (33) [$\log k_{12}$ versus $\log K_{12}$] and Fig. (34) [ΔG_{12}^\ddagger versus ΔG^0]. Deviations from linearity are expected for $|\Delta G^0|$ far from zero (eqn. (36)) and cannot be taken to imply that the Marcus relationship is inapplicable, as the Cu(I)-Cu(II) exchange rates are unknown so that a test of the complete equation (36) cannot be made.

For a series of polypyridine ruthenium complexes, Hoselton et al. (1978) measured the rates of reaction with $\text{Cu}_{(\text{aq})}^{2+}$ ions. They estimated k_{ex} for $\text{Cu}_{(\text{aq})}^+ - \text{Cu}_{(\text{aq})}^{2+}$ as $10^{-5} \text{ M}^{-1} \text{ s}^{-1}$, and as the self exchange rates for the ruthenium complexes are all expected to be close to $2 \times 10^9 \text{ M}^{-1} \text{ s}^{-1}$, the value for $[\text{Ru}(\text{bipy})_3]^{2+} - [\text{Ru}(\text{bipy})_3]^{3+}$ (Young, Keene & Meyer, 1977), were able to calculate the expected dependence of ΔG_{12}^\ddagger on ΔG^0 for these systems. For $\Delta G^0 < \sim -40 \text{ kJ mol}^{-1}$, the observed ΔG_{12}^\ddagger values deviated from the Marcus relationship in the sense that the observed cross-reaction rate constants at large negative values of ΔG^0 were less than expected. This deviation was attributed to the shapes of the potential surfaces, in departures from adiabaticity, and in nuclear funnelling and other quantum mechanical contributions.

Some of the reactions in Table (33) have $\Delta G^0 < -125 \text{ kJ mol}^{-1}$ and may well show deviations of this kind, but the self exchange rates of Cu(I)-Cu(II) complexes are not known. An examination of the trends in the self exchange rates estimated from the Marcus relationship suggests however that other factors may be involved.

VI.6.5 Estimation of Cu(I)-Cu(II) Self Exchange Rates

The Marcus equation (36) was solved for the cross reactions

Fig. (34) Plots of ΔG_{12}^\ddagger versus ΔG_{12}^0 . The values of energy changes are shown as hollow points and full points for the thermal and photochemical processes respectively.

1. $[\text{Cu}(\text{phen})_2]^{2+}$
2. $[\text{Cu}(\text{aq})]^{2+}$
3. $[\text{Cu}(\text{bipy})_2]^{2+}$
4. $[\text{Cu}(\text{H}_2\text{EDTA})]^{2-}$
5. $[\text{Cu}(5\text{-Cl-phen})_2]^{2+}$
6. $[\text{Cu}(\text{Me}_4\text{-phen})_2]^{2+}$
7. $[\text{Cu}(5\text{-NO}_2\text{-phen})_2]^{2+}$
8. $[\text{Cu}(\text{diene})]^{2+}$

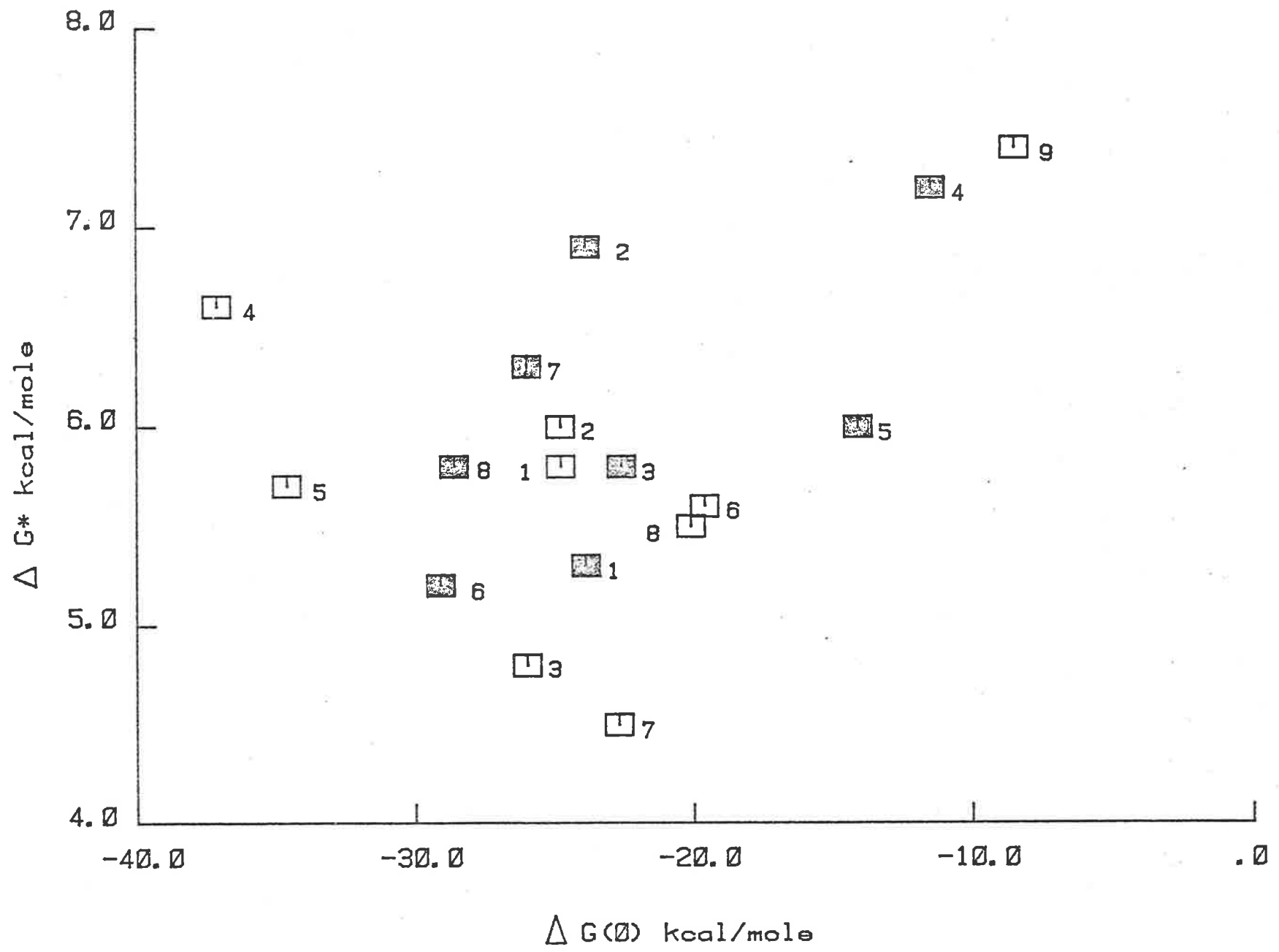


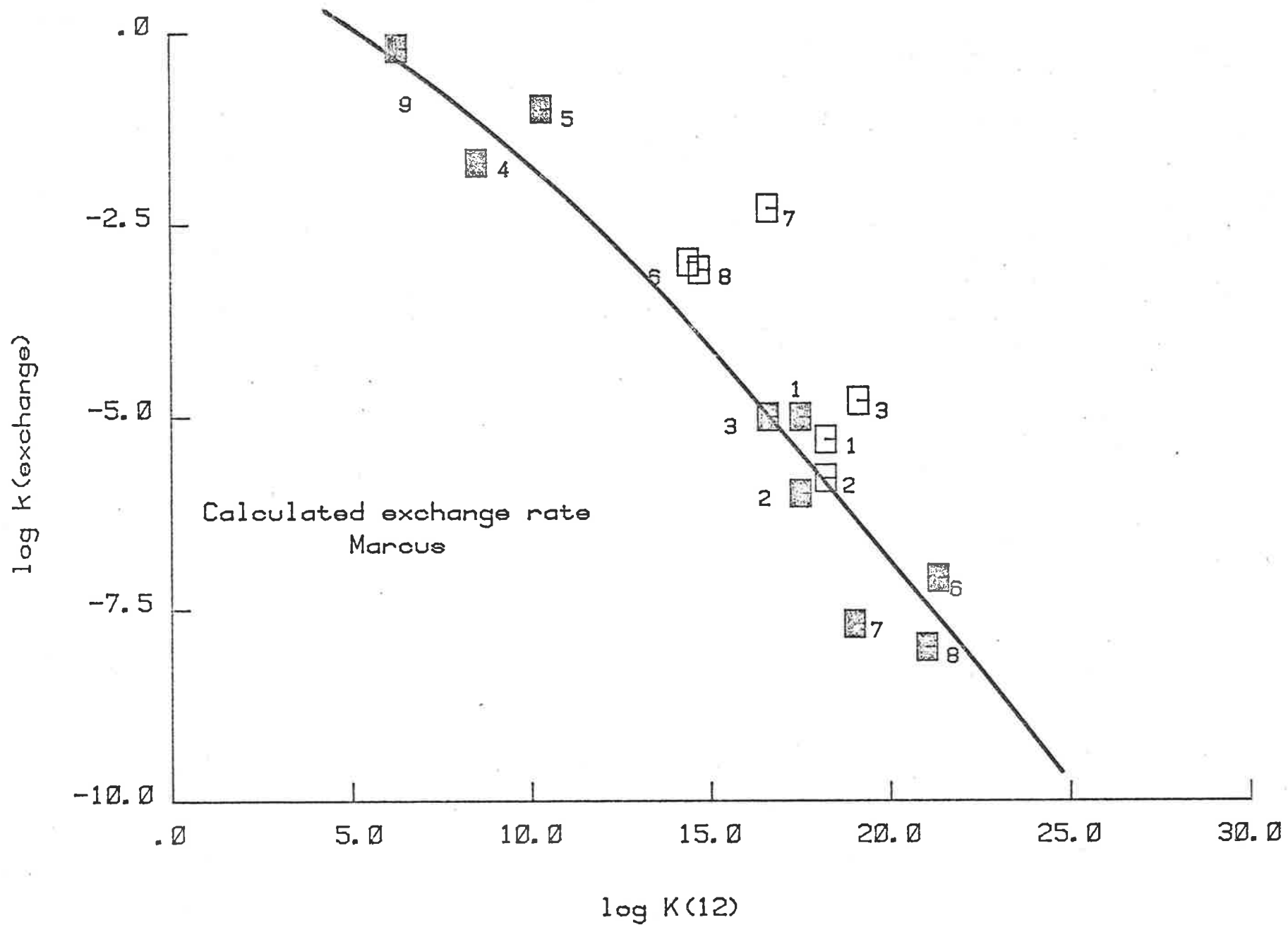
Table (33)

ESTIMATES OF PHOTOCHEMICAL AND THERMAL SELF EXCHANGE RATES FOR COPPER
COMPLEXES - MARCUS THEORY

System	Photochemical		Thermal	
	$\log K_{12}^{\phi}$	$\log k_{ex}^{\phi}$	$\log K_{12}^{th}$	$\log K_{ex}^{th}$
$[\text{Cu}(\text{phen})_2]^{1+,2+}$	17.5	-4.99	18.2	-6.0
$[\text{Cu}(\text{aq})]^{1+,2+}$	17.5	-7.8	18.2	-6.3
$[\text{Cu}(\text{bipy})_2]^{1+,2+}$	16.6	-5.09	19.1	-4.5
$[\text{Cu}(\text{en})_2]^{1+,2+}$	8.5	-1.7	27.2	-13.7
$[\text{Cu}(\text{H}_2\text{EDTA})]^{3-,2-}$	10.3	-1.0	25.4	-10.5
$[\text{Cu}(5\text{-Cl-phen})_2]^{1+,2+}$	21.3	7.1	14.4	-3.0
$[\text{Cu}(\text{Me}_4\text{-phen})_2]^{1+,2+}$	19.0	-7.7	16.6	-2.3
$[\text{Cu}(5\text{-NO}_2\text{-phen})_2]^{1+,2+}$	21.0	-8.0	14.7	-3.1
$[\text{Cu}(\text{diene})]^{1+,2+}$	6.3	-0.15	-	-

Fig. (36) Plots of $\log(k_{\text{exchange}})$ versus $\log K_{12}$ for the copper complexes used as quenchers. The calculated thermal exchange rates ($k_{\text{ex}}^{\text{th}}$) and the photochemical rates (k_{ex}^{ϕ}) are shown as hollow points and full points respectively.

1. $[\text{Cu}(\text{phen})_2]^{1+,2+}$
2. $[\text{Cu}(\text{aq})]^{1+,2+}$
3. $[\text{Cu}(\text{bipy})_2]^{1+,2+}$
4. $[\text{Cu}(\text{en})_2]^{1+,2+}$
5. $[\text{Cu}(\text{H}_2\text{EDTA})]^{2-,3-}$
6. $[\text{Cu}(5\text{-Cl-phen})_2]^{1+,2+}$
7. $[\text{Cu}(\text{Me}_4\text{-phen})_2]^{1+,2+}$
8. $[\text{Cu}(5\text{-NO}_2\text{-phen})_2]^{1+,2+}$
9. $[\text{Cu}(\text{diene})]^{1+,2+}$



in Table (33) to yield values of the Cu(I)-Cu(II) self exchange rates. The values are given in Table (33). If the Marcus relationship accurately described the behaviour of these systems at all ΔG^0 values, then for a given pair of cross-reaction rate constants (excited $*[\text{Ru}(\text{bipy})_3]^{2+}$ electron transfer quenching by Cu(II) and oxidation of Cu(I) by $[\text{Ru}(\text{bipy})_3]^{3+}$) the self exchange rate constants should be the same.

It can be seen that only for the pairs $\text{Cu}_{(\text{aq})}^{2+} - \text{Cu}_{(\text{aq})}^+$, $[\text{Cu}(\text{phen})_2]^{2+} - [\text{Cu}(\text{phen})_2]^{1+}$ and $[\text{Cu}(\text{Me}_4\text{-phen})_2]^{2+} - [\text{Cu}(\text{Me}_4\text{-phen})_2]^{1+}$ is this even approximately true. For these complexes, the ΔG^0 values for the photochemical and thermal reactions are within 15 kJ mol^{-1} . A plot of k_{ex} versus ΔG^0 shows that the calculated self exchange rates have a definite dependence on ΔG^0 , and this dependence is such that the self exchange rate for a given pair of Cu(I)-Cu(II) complexes calculated for a reaction with the more negative ΔG^0 is smaller. This deviation is in the same sense as that observed by Hoselton et al. (1978); the Marcus relationship suggests cross-reaction rates higher than those observed for large, negative ΔG^0 [Fig. (36)].

The Rehm-Weller relationship (eqn. (40)) can also be used to calculate self exchange rates from values of k_{12} and K_{12} . For copper complexes the data are given in Table (34), and shown in the graphical form in Fig. (36). The dependence of the calculated self exchange rates on ΔG^0 is less marked than for the Marcus relationship Fig. (35) but the deviations are in the same sense i.e. for large negative ΔG^0 the calculated cross-reaction rates would be larger than the observed values.

The breakdown of the two theoretical treatments for large reaction free energies [for the data in Tables (33), (34) and (35) ΔG^0 lies between -34 kJ mol^{-1} and -150 kJ mol^{-1}] is expected

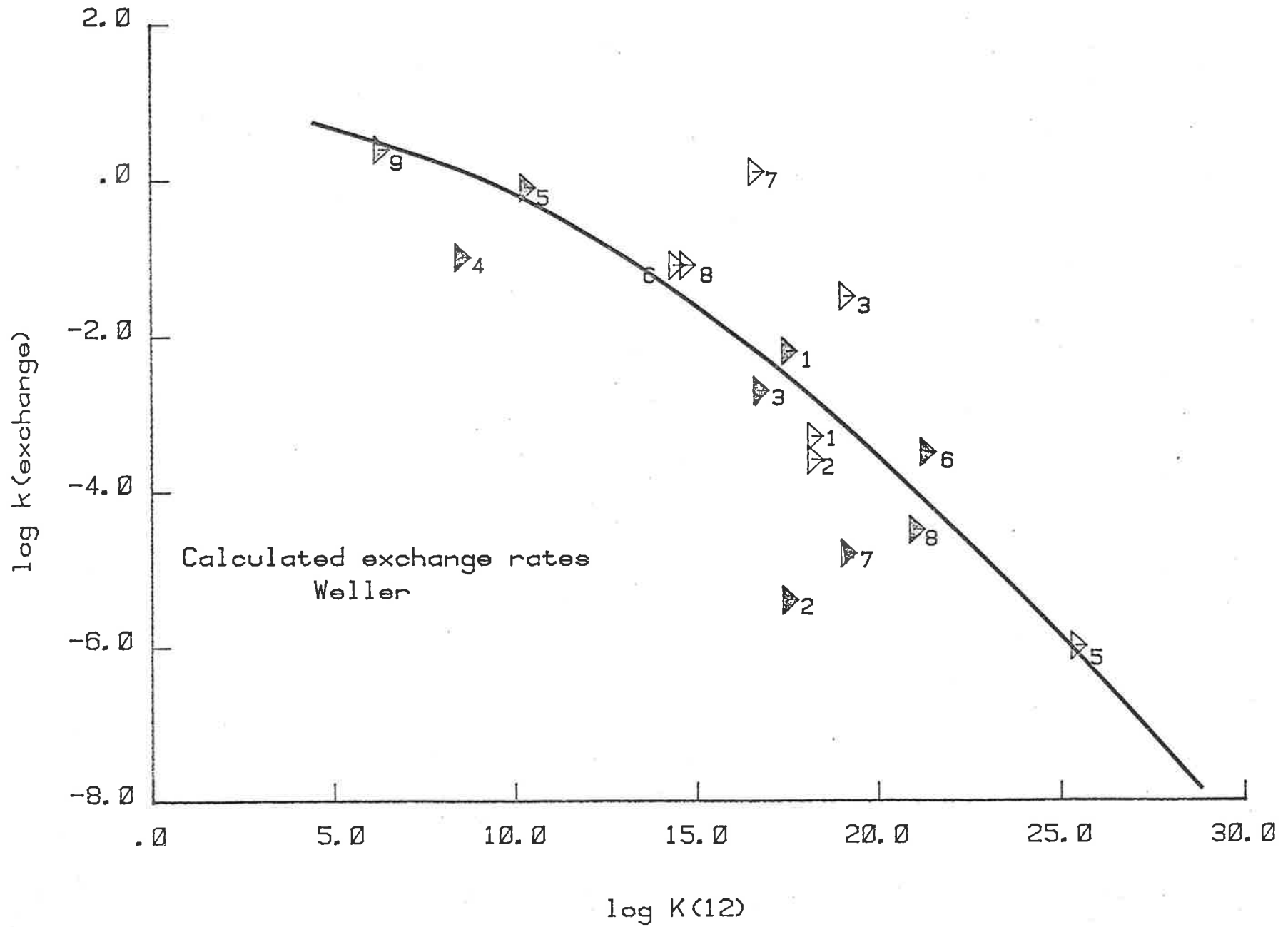
Table (34)

ESTIMATES OF PHOTOCHEMICAL AND THERMAL SELF EXCHANGE RATES FOR COPPER
COMPLEXES - WELLER TREATMENT

System	Photochemical		Thermal	
	$\log K_{12}^{\phi}$	$\log k_{ex}^{\phi}$	$\log K_{12}^{th}$	$\log k_{ex}^{th}$
$[\text{Cu}(\text{phen})_2]^{1+,2+}$	17.50	-2.21	18.20	-3.28
$[\text{Cu}(\text{aq})]^{1+,2+}$	17.53	-5.36	18.2	-3.60
$[\text{Cu}(\text{bipy})_2]^{1+,2+}$	16.66	-2.74	19.11	-1.49
$[\text{Cu}(\text{en})_2]^{1+,2+}$	8.48	-1.0	27.24	-8.73
$[\text{Cu}(\text{H}_2\text{EDTA})]^{3-,2-}$	10.30	+0.06	25.38	-5.95
$[\text{Cu}(5\text{-Cl-phen})_2]^{1+,2+}$	21.32	-3.52	14.38	-1.13
$[\text{Cu}(\text{Me}_4\text{-phen})_2]^{1+,2+}$	19.08	-4.82	16.61	+0.10
$[\text{Cu}(5\text{-NO}_2\text{-phen})_2]^{1+,2+}$	20.96	-4.54	14.73	-1.12
$[\text{Cu}(\text{diene})]^{1+,2+}$	6.26	0.42	-	-

Fig. (35) Plots of $\log(k_{\text{exchange}})$ versus $\log K_{12}$ for the copper complexes used as quenchers. The calculated thermal exchange rates ($k_{\text{ex}}^{\text{th}}$) and the photochemical rates (k_{ex}^{ϕ}) are shown as hollow points and full points respectively.

1. $[\text{Cu}(\text{phen})_2]^{1+,2+}$
2. $[\text{Cu}(\text{aq})]^{1+,2+}$
3. $[\text{Cu}(\text{bipy})_2]^{1+,2+}$
4. $[\text{Cu}(\text{en})_2]^{1+,2+}$
5. $[\text{Cu}(\text{H}_2\text{EDTA})]^{2-,3-}$
6. $[\text{Cu}(5\text{-Cl-phen})_2]^{1+,2+}$
7. $[\text{Cu}(\text{Me}_4\text{-phen})_2]^{1+,2+}$
8. $[\text{Cu}(5\text{-NO}_2\text{-phen})_2]^{1+,2+}$
9. $[\text{Cu}(\text{diene})]^{1+,2+}$



(Hoselton, Sutin, et al., 1977), but the calculated values of the self-exchange rates for such pairs as $\text{Cu}_{(\text{aq})}^{2+} - \text{Cu}_{(\text{aq})}^{+}$, $[\text{Cu}(\text{phen})_2]^{2+} - [\text{Cu}(\text{phen})_2]^{1+}$ and $[\text{Cu}(\text{Me}_4\text{-phen})_2]^{1+}$ are many orders of magnitude below the values estimated for similar complexes by Holwerda et al. (1977) and Augustin and Yandell (1978), and are extremely low. Even the 'accepted' value of the $\text{Cu}_{(\text{aq})}^{2+} - \text{Cu}_{(\text{aq})}^{+}$ exchange rate (ca. $10^{-5} \text{ M}^{-1} \text{ s}^{-1}$) is much lower than values for the aquo-ions of other first row transition metals.

The data are relevant to the discussion of the possible existence of an "inverted Marcus region" for reactions with very negative values of ΔG^0 . The data in Table (33) include reaction pairs for which one member has ΔG^0 in the range $\sim -(65-10) \text{ kJ mol}^{-1}$. Yet all the cross-reaction rates lie between 10^7 and $10^9 \text{ M}^{-1} \text{ s}^{-1}$, values below the diffusion controlled limits for these systems at an ionic strength of 0.1 M. It must be concluded that such an "inverted region" does not exist, and that the Marcus treatment breaks down when the apparent intersection point between the potential energy surfaces describing the reactants and products approach energies equivalent to the lowest vibrational levels of the reactants. Quantum mechanical tunnelling has been suggested as an explanation of similar effects, but current theories are definitely inadequate to describe reactions with very large equilibrium constants. However it would appear that these systems involving Cu(I) and Cu(II) complexes may show markedly great deviations for the Marcus (or Rehm-Weller) relations, and consideration must be given to possible specific effects related to the copper systems. Similarly, the inadequacies of the theories to treat both $[\text{Co}(\text{NH}_3)_6]^{2+} - [\text{Co}(\text{NH}_3)_6]^{3+}$ and $[\text{Co}(\text{sep})]^{3+} - [\text{Co}(\text{sep})]^{2+}$ (sep = sepalchrate) have recently been pointed out by Sargeson

Table (35)
 DATA FOR ΔG_{12}^\ddagger AND ΔG_{12}^0

System	Thermal		Photochemical	
	$\Delta G_{12}^\ddagger / \text{k cal mol}^{-1}$	$\Delta G_{12}^0 / \text{k cal mol}^{-1}$	$\Delta G_{12}^\ddagger / \text{k cal mol}^{-1}$	$\Delta G_{12}^0 / \text{k cal mol}^{-1}$
$[\text{Cu}(\text{phen})_2]^{2+}$	-24.8	5.8	-23.9	5.3
$\text{Cu}^{2+}_{(\text{aq})}$	-24.8	6.0	-23.9	6.9
$[\text{Cu}(\text{bipy})_2]^{2+}$	-26.0	4.8	-22.6	5.8
$[\text{Cu}(\text{H}_2\text{EDTA})]^{2-}$	-37.1	6.6	-11.5	7.2
$[\text{Cu}(5\text{-Cl-phen})_2]^{2+}$	-34.6	5.7	-14.0	6.0
$[\text{Cu}(\text{Me}_4\text{-phen})]^{2+}$	-19.6	5.6	-29.1	5.2
$[\text{Cu}(5\text{-NO}_2\text{-phen})]^{2+}$	-22.7	4.5	-26.0	6.3
$[\text{Cu}(\text{diene})]^{2+}$	-20.1	5.5	-28.6	5.8
	-	-	-8.5	7.4

(1979). The exchange rate for $[\text{Co}(\text{sep})]^{3+} - [\text{Co}(\text{sep})]^{2+}$ was $\sim 10^5$ -fold faster (Creaser et al. 1977) than the parent $[\text{Co}(\text{en})_3]^{3+} - [\text{Co}(\text{en})_3]^{2+}$ ions. The expectation that electron transfer reactions involving Cu(I) and Cu(II) complexes would be slow because of "special" reorganizational barriers associated with the geometrical differences between Cu(I) and Cu(II) species has been referred to on pp. 214, 218. In itself this "special" barrier would be accommodated within the framework of the Marcus theory by very slow self-exchange rates (which reflect the reorganizational barriers) for these systems. However, for systems such as $[\text{Cu}(\text{bipy})_2]^{1+,2+}$, $[\text{Cu}(\text{dmp})_2]^{1+,2+}$ and $[\text{Cu}(\text{NO}_2\text{-phen})_2]^{1+,2+}$ (Augustin & Yandell, 1978) the self-exchange rates are much higher than for comparable Cr(II)-Cr(III) or Co(II)-Co(III) (Sargeson, 1979) systems. The self-exchange rates calculated for the systems in Table (33) are certainly low and may, despite the inadequacies of the Marcus theory, reflect such reorganizational barriers. However the other possibilities exist, especially the validity of the assumption of the "special reorganizational barriers" has never been established and remains untested, and may even lack a sound theoretical basis. That is, there may not be a large energy barrier to the geometry changes in Cu(I) and Cu(II) complexes.

Octahedral Cu(II) complexes are known to exhibit Jahn-Teller distortion. Novack et al. (1971) found that the behaviour of the EPR relaxation of $[\text{Cu}(\text{bipy})_2(\text{H}_2\text{O})_2]^{2+}$, $[\text{Cu}(\text{bipy})(\text{H}_2\text{O})_4]^{2+}$, $[\text{Cu}(\text{bipy})_3]^{2+}$ and $[\text{Cu}(\text{H}_2\text{O})_6]^{2+}$ was anomalous and suggested that in symmetrical coordinated Cu(II) complexes (e.g. $[\text{Cu}(\text{H}_2\text{O})_6]^{2+}$) the rate of intramolecular inversion of the distortion axis was extremely fast (even faster than the rotational tumbling time of the complex) while in assymmetrically coordinated complexes (e.g. $[\text{Cu}(\text{bipy})_2(\text{H}_2\text{O})_2]^{2+}$) intramolecular inversion is slow. Assuming

a random jump of the distortion axis between the three octahedral principal directions, Pouko and Luz (1972) calculated the lifetime of this hopping process to be 16 p sec (25°C) with an activation energy of $\sim 5 \text{ kJ mol}^{-1}$ for aqueous $\text{Cu}(\text{ClO}_4)_2$ solutions. Due to the presence of the fast intramolecular inversion in aqueous and methanolic solutions only weighted averaged parameters over the axial and equatorial ligand molecules could be obtained. The pseudo-first order rate constant for the exchange of solvation shell molecules was estimated to be $7.4 \times 10^7 \text{ s}^{-1}$ having an activation energy of 27.6 kJ mol^{-1} and with the tumbling time of 46 p sec. The rate of exchange of the solvation shell molecules and the molecular tumbling rate for the Cu(II) bis-polypyridine complexes are also expected to be of the same order of magnitude. The rates of substitution and solvent exchange for Cu(II) systems therefore imply small structural barriers to large distortions of the coordination sphere. For Cu(I) complexes, these rates can only be estimated, Cu(I), d^{10} , ion has an ionic radius of 0.96 \AA close to that for Na^+ (0.95 \AA) and the water exchange rate is likely to be comparable (ca. 10^9 s^{-1}) again implying low barrier to coordination sphere distortion.

The rates of quenching (k_q) and thermal back electron transfer (k_{th}) measured in this study and the rates of exchange of the solvation shell molecules are comparable. This rapid intramolecular equilibration of the two extreme geometries, tetrahedral for Cu(I) and octahedral for Cu(II), would lower the structural barriers and facilitate the electron transfers for both the reduction of Cu(II) complexes and their subsequent re-oxidation processes and may be a partial reason for the lack of observation of the 'expected' structural barriers and breakdown

of the application of the Marcus theory to the systems in question.

The dynamic Jahn-Teller effect would also suggest that the self-exchange barrier for Cu(I)-Cu(II) systems might be strongly influenced by the local environment, so that the self-exchange rate would not be a system independent parameter. The influence of the protein structure on the solvent near cytochrome c, for example, may so influence the dynamics of solvent interaction with $\text{Cu}_{(\text{aq})}^+$ and $\text{Cu}_{(\text{aq})}^{2+}$ (and specific interactions with the π -electrons of the heterocyclic rings could have a similar effect on $[\text{Cu}(\text{phen})_2]^{1+}$ and $[\text{Cu}(\text{phen})_2]^{2+}$ complexes) that for these reactions the apparent self-exchange rate differs from that for the same copper complexes in a more "normal" solvent environment. The nature of the factors affecting electron-transfer between Cu(I) and Cu(II) systems is far from being understood, but the present results show that such reactions cannot simply be classed as "slow" on the basis of a hypothetical expectation about the size of reorganisational barriers.

To express concern about the inadequacies of the Marcus theory are the words of my supervisor Dr. G.S. Laurence.

After almost twenty years, the Marcus theory appears to have reached the limits of its usefulness in its current form and needs an improved theoretical treatment.

APPENDIX AFLASH PHOTOLYSIS OF [Co(phen)₃]³⁺ IONA.1 INTRODUCTION

Steady state photolysis of [Co(phen)₃]³⁺ have lead to the suggestion that this complex undergoes photoreduction via the formation of a Co(IV) species which is then transformed to a reactive LMCT excited state which is a precursor to the reduction products (Moggi, Sabbatini & Traverso, 1973). The formation of Co(IV) species is highly unlikely and flash photolysis experiments reinforce this view.

Due to the small quantum yield (4×10^{-3} ; Moggi, Sabbatini & Traverso, 1973) for the photoreduction, the intense $\pi \rightarrow \pi^*$ intraligand absorption in the UV and near UV-region and the very weak absorbances of Co(III) and Co(II) in the visible, the system could not be studied in the same detail as those of the iron(III) complexes.

A.2 EXPERIMENTAL

The preparation, characterization and standardization of the solutions, and the data acquisition and treatment have already been described in Chapter 2. The studies were carried out in aqueous solution at pH = 2, the pH being adjusted with H₂SO₄.

A.3 PRELIMINARY EXPERIMENTS

Preliminary experiments showed that

- (1) No dark reaction could be detected and the room light and the monitoring light had no effect on the flash photolysis runs.
- (2) After flash photolysis, the solution shows a blue shift of 10 nm for the intraligand $\pi-\pi^*$ bands centred at 252 and 287 nm

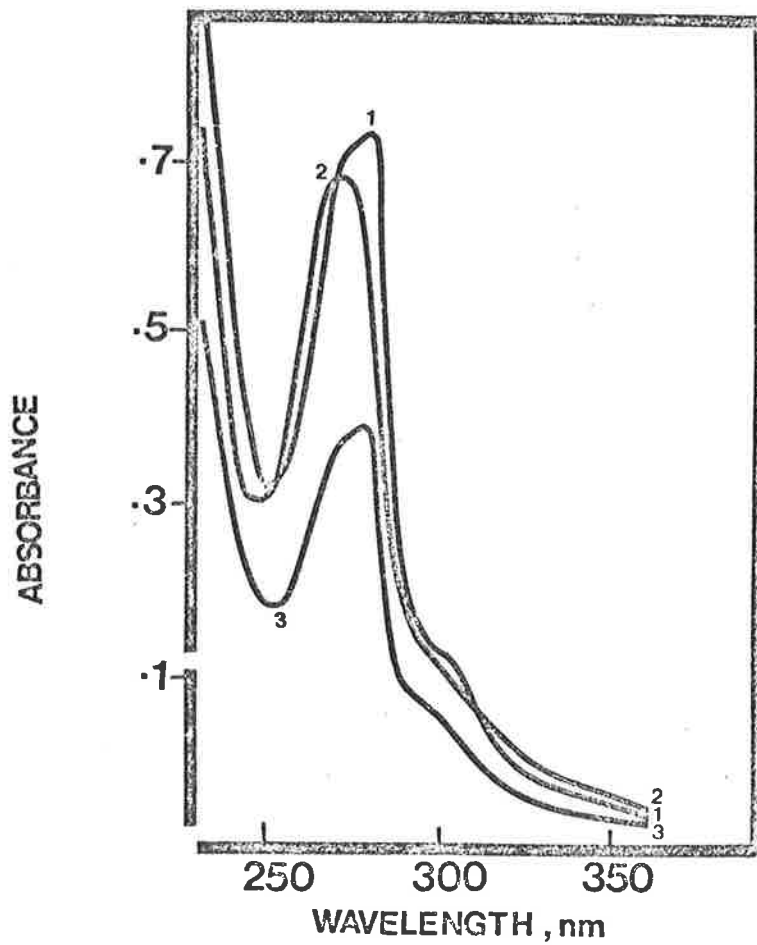


Fig. 37 Absorption Spectra of (1) $[\text{Co}(\text{phen})_3]^{3+}$, (2) Flash Photolysed $[\text{Co}(\text{phen})_3]^{3+}$ and (3) after Shaking the Photolysed Solution with Chloroform.

and of 5 nm for the band at 220 nm [Fig. (37)]. These observations are consistent with the previous findings of Moggi, Sabbatini and Traverso (1973).

- (3) Three isosbestic points at (298 ± 3) nm, (251 ± 3) nm and (307 ± 2) nm were observed between the flash photolysed solution and the Co(III) complex.
- (4) $\text{Co}_{(\text{aq})}^{2+}$ ions were found to be present in the photolysed solution. The production of $\text{Co}_{(\text{aq})}^{2+}$ ions was equivalent to the amount of $[\text{Co}(\text{phen})_3]^{3+}$ destroyed. The detection of the $\text{Co}_{(\text{aq})}^{2+}$ ions was carried out by the thiocyanate method (Vogel, 1961) and the method described by Vydra and Pribil (1960).
- (5) On shaking the photolysed solution with chloroform, the chloroform phase showed the characteristics of the phenanthroline UV-absorption and the aqueous phase showed the spectrum of unreacted $[\text{Co}(\text{phen})_3]^{3+}$. These results are also in agreement with the results of Moggi, Sabbatini & Traverso (1973).
- (6) Purging the solution of O_2 with N_2 had no effect on the amount of $[\text{Co}(\text{phen})_3]^{3+}$ destroyed per flash (4-5%).

A.4 KINETICS OF SECONDARY REACTIONS

The absorbance changes following the flash at 313 nm occurred in three stages: (1) an immediate ($t_{1/2} < 10 \mu\text{sec}$) increase in absorbance (Stage I), (2) decay of the transient absorbance leading to a decrease in absorbance to \sim half of the initial transient absorbance (Stage II) and (3) a slower increase in absorbance. For a $5 \mu\text{M}$ solution in $[\text{Co}(\text{phen})_3]^{3+}$ at $\text{pH} = 2$ the absorbance changes at 313 nm are shown in Fig. (38).

The rate of decrease of the transient absorbance (Stage II) was found to be first order ($k = 22 \pm 1 \text{ s}^{-1}$) and was independent of the concentration of $[\text{Co}(\text{phen})_3]^{3+}$. The rate of increase in

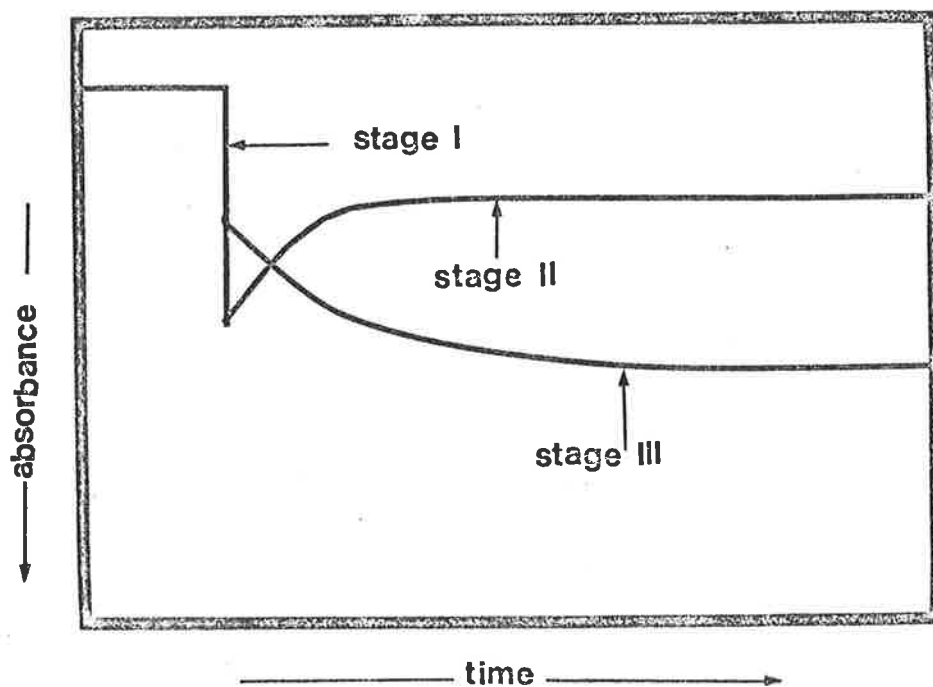
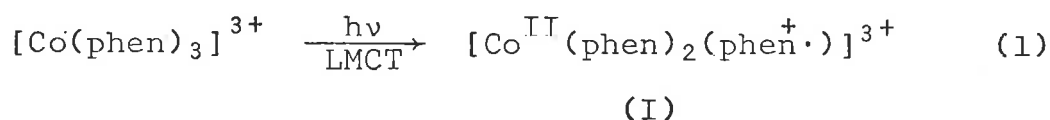


Fig. 38 Three Stages of Reactions in the Flash Photolysis of $[\text{Co}(\text{phen})_3]^{3+}$ Ion

absorbance by the slow process (Stage III) was first order with a half life dependent upon the initial concentration of the complex. The second order rate constant for this process measured from the slope of the straight line plot of the pseudo-first order rate constant versus $[\text{Co}(\text{phen})_3]^{3+}$ concentration (3.0-10.0 μM) was $(5.5 \pm 0.7) \times 10^3 \text{ M}^{-1} \text{ s}^{-1}$. Purging of oxygen from the solution with N_2 or saturating with air had no effect on the changes in absorbance or on the rates of the Stage II and Stage III reactions. All the kinetics were monitored at 313 nm.

A.5 TRANSIENT SPECIES AND PHOTOPRODUCTS

The changes in absorbance are similar to those observed for the other $[\text{M}^{\text{III}}\text{L}_3]^{3+}$ complexes studied [Page (83)]. On the basis of this similarity it is suggested that the initial photochemical reaction is the transfer of an electron from the ligand to the Co(III) centre to produce a Co(II) ligand-radical complex (I): with the Co(II) in the normal high-spin state which it possesses in $[\text{Co}(\text{phen})_3]^{2+}$.

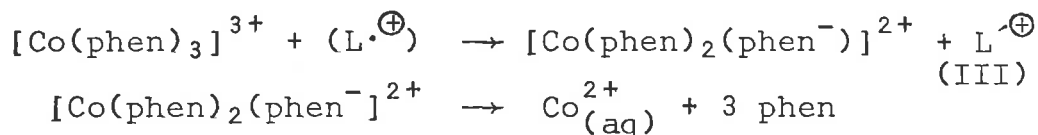


Since the "normal" Co(II) complexes are high-spin and labile, the decrease in transient absorbance (Stage II) may be attributed to the fragmentation of the primary photoproduct (I) to produce weakly absorbing or non-absorbing products.

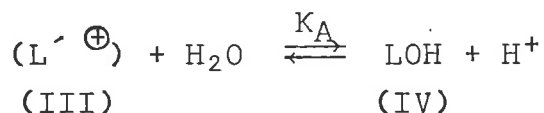


The possible products of reaction (2) are Co(II) and a free ligand radical ($\text{L}^{\cdot\oplus}$). The proposed free ligand-radical ($\text{L}^{\cdot\oplus}$) could not be detected, probably due to high absorption of the Co(III) and Co(II) complexes.

The increase in absorbance (Stage III) is attributed to the reduction of another molecule of $[\text{Co}(\text{phen})_3]^{3+}$ complex by the 'free' ligand radical (II) to



to give $\text{Co}_{(\text{aq})}^{2+}$ and the free phen ligand. The reaction sequence is analogous to that for the iron(III) complexes, modified to allow for the lability of the Co(II) state. The species (III) is a modified ligand, a ligand which has lost two electrons and a proton, and is capable of undergoing acid-base equilibrium with H_2O to give a hydroxy product (IV), in which OH is probably



attached at the 2-(9)-position of the ligand for the reasons already indicated in Chapter (5). Thus the probable products of photolysis of $[\text{Co}(\text{phen})_3]^{3+}$ are $\text{Co}_{(\text{aq})}^{2+}$, free phen and phenOH.

A.6 THERMAL ACID HYDROLYSIS OF M(II) COMPLEXES OF N-HETROCYCLIC LIGANDS

Both $[\text{Co}(\text{phen})_3]^{3+}$ and $[\text{Co}(\text{phen})_3]^{2+}$ are thermodynamically stable and $[\text{Co}(\text{phen})_3]^{2+}$ is relatively inert (Waltz & Pearson, 1969). No studies of the solvolysis of $[\text{Co}(\text{phen})_3]^{3+}$ have appeared as yet but the available data for the rates of the thermal acid hydrolysis of similar Co(II), Fe(II) and Ni(II) complexes should be indicative of the $[\text{Co}(\text{phen})_3]^{2+}$ case. The rates of thermal acid hydrolysis of $[\text{M}(\text{terpy})_2]^{2+}$ (M = Fe(II), Co(II) and Ni(II)) have been estimated by Farina, Hogg and Wilkins (1968).



The hydrolysis is believed to proceed through the rupture of M-N bond which is the rate determining step. The attachment of a proton to the nitrogen atom prevents the rejoining of the severed M-N bond thus facilitating the incorporation of water molecules into the coordination sphere of the metal. The rates of acid catalysed hydrolysis of the relevant M(II) complexes are summarized in Table (36).

Table (36)

RATE CONSTANTS FOR ACID HYDROLYSIS OF M(II) COMPLEXES OF
BIPYRIDINE AND TERPYRIDINE LIGANDS

Reference: Farina, Hogg and Wilkins, 1968

Complex Ion	Temp °C	$\frac{[H^+]}{M}$	Rate Constant s ⁻¹
[Co(terpy) ₂] ²⁺	18.0	0.50	125
[Co(bipy) ₃] ²⁺	18.0	0.50	32
[Co(terpy)] ²⁺	26.0	0.50	0.30
[Ni(bipy) ₃] ²⁺	1.0	1.0	3.8 × 10 ⁻³
[Ni(bipy) ₃] ²⁺	1.0	1.0	5.8 × 10 ⁻³
[Fe(terpy) ₂] ²⁺	35	1.5	3.5 × 10 ⁻³

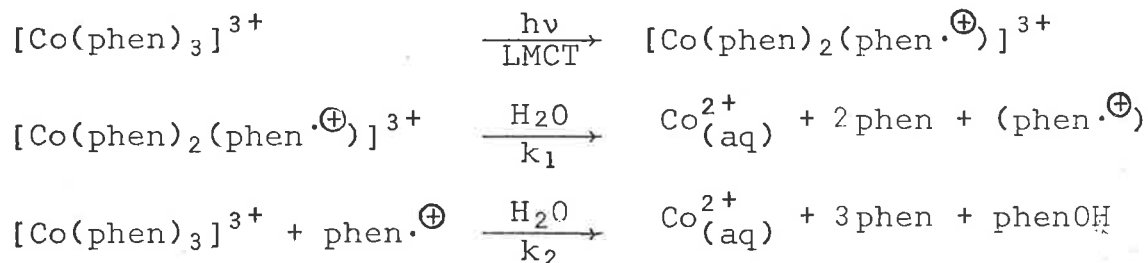
It is obvious that the rate of solvolysis of [Co^{II}(phen)₂(phen·[⊕])]³⁺ would be of the same order of magnitude as for [Co(terpy)₂]²⁺ and [Co(bipy)₃]²⁺. It might be expected the hydrolysis rate for [Co^{II}(phen)₂(phen·[⊕])]³⁺ to be somewhat higher because of the positive charge on one of the rings of the chelating base, which would facilitate the nucleophilic attack by water molecules. The rate of decay of the transient absorbance (Stage II) in the present case (22 ± 1 sec⁻¹) is very close to those

for the Co(II) complexes in Table (36).

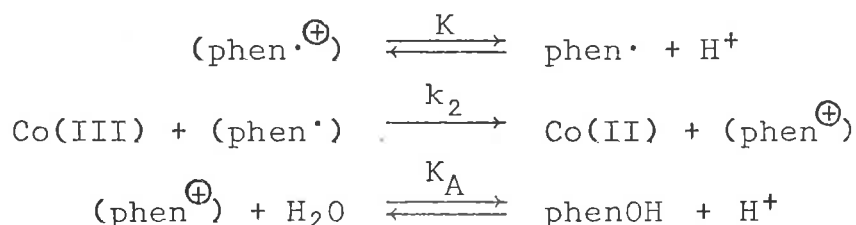
The primary photoproduct (I) cannot be a Co(III) or Co(IV) species as the rates of dissociation of $[\text{Co}^{\text{III}}(\text{phen})_2(\text{OX})]^{2+}$ ($6 \times 10^{-4} \text{ s}^{-1}$; Roy & Benerjea, 1975), $[\text{Co}(\text{phen})_2(\text{mal})]^{1-}$ ($\sim 10^{-4} \text{ s}^{-1}$; Chattopadhyay, Roy & Benerjea, 1978) and $[\text{Co}(\text{phen})_3]^{3+}$ ($3 \times 10^{-4} \text{ s}^{-1}$; Baraona, Rozenblum & Zamudio, 1978) are four orders of magnitude smaller than the rate constant for Stage(II) reaction. The behaviour of the system is so similar (when allowance is made for the lability of the high-spin Co(II) state) to that of Fe(III) and Ru(III) complexes that there is no need to invoke the formation of a Co(IV) species as was suggested by Moggi, Sabbatini and Traverso (1973).

A.7 THE REACTION SCHEME

The reaction scheme



can account for the absorbance changes and the product analysis in the flash photolysis of $[\text{Co}(\text{phen})_3]^{3+}$. It is suggested that the thermal reduction of $[\text{Co}(\text{phen})_3]^{3+}$ by (phen^{\oplus}) radical occurs by a similar outer-sphere mechanism as that for the Fe(III) and Ru(III) complexes [Chapters 4 and 5] and may be represented as



The reaction scheme can explain the stoichiometric equivalent loss of $[\text{Co}(\text{phen})_3]^{3+}$ and the production of $\text{Co}_{(\text{aq})}^{2+}$ similar to that found by Moggi, Sabbatini and Traverso (1973).

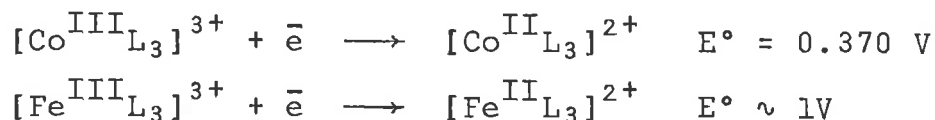
The 'free' (phen^{\oplus}) radical is expected to be more stable than when bound to the metal centre [Chapter 5] due to the increased resonance stabilization of the un-bonded nitrogen atoms. This increased stability of the radical would decrease the rate of thermal reduction of another molecule of the Co(III) complex. The rate of the proposed reduction of $[\text{Co}(\text{phen})_3]^{3+}$ by (phen^{\cdot}) radical (ca. $5 \times 10^3 \text{ M}^{-1} \text{ s}^{-1}$) is three orders of magnitude smaller than that for other $[\text{M}^{\text{III}}\text{L}_3]^{3+}$ complexes (ca. $10^6 \text{ M}^{-1} \text{ s}^{-1}$).

A.8 THE DETAILS OF THE PRIMARY PHOTOCHEMISTRY

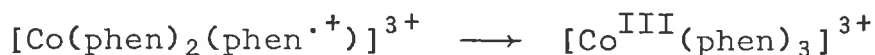
In view of the similarity of the electronic absorption spectra of $[\text{M}^{\text{III}}\text{L}_3]^{3+}$ ($\text{M} = \text{Fe}(\text{III}), \text{Ru}(\text{III})$ complexes in the UV-region), for $[\text{Co}(\text{phen})_3]^{3+}$ the band at 287 nm must essentially correspond to $\pi \rightarrow \pi^*$ (1L) transition having a significant LMCT character (Mayoh & Day, 1978) while the band at ~ 220 nm may be attributed to a LMCT absorption. Because of the similarity of the photochemical behaviour of $[\text{Co}(\text{phen})_3]^{3+}$ to those of other $[\text{M}^{\text{III}}\text{L}_3]^{3+}$ complexes [Chapters 4 & 5] it is concluded that the primary photochemical reaction is the same i.e. the ligand is the electron donor and the photoreduction arises from the internal quenching of the normal free ligand's luminescence by an intramolecular ligand to metal electron transfer [see e.g. Fig. (29)].

The internal luminescence quenching probably can explain the higher photoreduction quantum yield (0.1 ± 0.02) in the sensitization experiments in the presence of free phenanthroline ligand (Moggi, Sabbatini & Traverso, 1973). The quantum yield ca. 10^{-3} for the photoreduction of $[\text{Co}(\text{phen})_3]^{3+}$ is one order

of magnitude smaller than those for the Fe(III) and Ru(III) complexes (ca. 10^{-2}). The difference in the quantum yields may be attributed to the differences in the reduction potentials of the $[M^{III}L_3]^{3+}$ complexes [Table (27)].



The reduction of Fe(III) complex is more spontaneous than that of the Co(III) analogue which would make the thermal back electron transfer (not observed for $[Co(phen)_3]^{3+}$ because of the dissociation of the labile Co(II) species) more efficient. This may



explain the lower quantum yield for the loss of Co(III) complex in the present study.

The photochemical behaviour of $[Co(phen)_3]^{3+}$ is essentially the same as those of its Fe(III) and Ru(III) analogues.

REFERENCES

- Adamczyk, A. and Wilkinson, F. (1972):
J.C.S. Faraday Trans. 2, 68, 2031 (1972).
- Adamson, A.W. (1960a):
J. Inorg. Nucl. Chem., 13, 275 (1960).
- Adamson, A.W. (1960b):
Discuss. Faraday Soc., 29, 163 (1960).
- Adamson, A.W. and Sporer, A.H. (1958):
J. Amer. Chem. Soc., 80, 3865 (1958).
- Al-Shatti, N., Segal, M.G. and Sykes, A.G. (1977):
J. Chem. Soc. Dalton Trans., p.1766 (1977).
- Anbar, M. and Hart, E.J. (1970):
"The Hydrated Electron", Wiley, New York.
- Anbar, M., Munoz, R.A. and Rona, P. (1963):
J. Phys. Chem., 67, 2808 (1963).
- Anderson, C.P., Salmon, D.J., Meyer, T.J. and Young, R.C. (1977):
J. Amer. Chem. Soc., 99, 1980 (1977).
- Arce, J.A., Spodine, E. and Zamudio, W. (1975):
J. Inorg. Nucl. Chem., 37, 1304 (1975).
- Armor, J.N., Furman, R. and Hoffman, M.Z. (1975):
J. Amer. Chem. Soc., 97, 1737 (1975).
- Armor, J.N. and Hoffman, M.Z. (1975):
Inorg. Chem., 14, 444 (1975).
- Asmus, K.D., Moeckel, H. and Henglein, A. (1973):
J. Phys. Chem., 77, 1218 (1973).
- Asmus, K.D., Wigger, A. and Henglein, A. (1966):
Ber. Bunsenges. Phys. Chem., 70, 862 (1966).
- Augustin, M. and Yandell, J. (1978):
J. Chem. Soc. Chem. Commun., p.370 (1978).

- Baker, B.R., Basolo, F. and Neuman, H.M. (1959):
J. Phys. Chem., 63, 371 (1959).
- Baker, B., Ohnavic, M., Sutin, N. (1967):
J. Amer. Chem. Soc., 89, 722 (1967).
- Ballardini, R. et al. (1978):
J. Amer. Chem. Soc., 100, 7219 (1978).
- Balzani, V., Ballardini, R., Sabbatini, N. and Moggi, L. (1968):
Inorg. Chem., 7, 1398 (1968).
- Balzani, V., Bertoluzza, A. and Carassiti, V. (1962):
Bull. Soc. Chim. Belges., 71, 821 (1962).
- Balzani, V., Bolleta, F., Gandolfi, M.T. and Maestri, M. (1979):
Top. Curr. Chem., in press.
- Balzani, V., Bolleta, F. and Moggi, L. (1978):
Spectrosc. Letters, 11, 525 (1978).
- Balzani, V. and Carassiti, V. (1970):
"Photochemistry of Coordination Compounds", Academic Press,
London.
- Balzani, V., Carassiti, V. and Moggi, L. (1964a):
Inorg. Chem., 3, 1252 (1964).
- Balzani, V., Carassiti, V. and Moggi, L. (1964b):
Ann. Chim. Rome, 54, 251 (1964).
- Balzani, V., Laurence, G.S. et al. (1975):
Coord. Chem. Rev., 15, 321 (1975).
- Bandyopadhyay, B.N. and Harriman, A. (1977):
J. Chem. Soc. Faraday Trans. 1, 73, 663 (1977).
- Banfield, T.L. and Hussain, D. (1969):
Trans. Faraday Soc., 63, 1985 (1969).
- Baraona, R., Rozenblum, S. and Zamudio, W. (1978):
J. Inorg. Nucl. Chem., 40, 2043 (1978).

Basolo, F. and Pearson, R.G. (1967):

"Mechanisms of Inorganic Reactions", New York, Wiley.

Baxendale, J.H. (1964):

Radia. Res., Suppl., 4, 139 (1964).

Baxendale, J.H., Barb, W.G., George, P. and Hargrave, K.R. (1955):

Trans. Faraday Soc., 51, 935 (1955).

Baxendale, J.H. and Bridge, N.K. (1955):

J. Phys. Chem., 59, 783 (1955).

Baxendale, J.H. and Fiti, M. (1972):

J. Chem. Soc., Dalton Trans., p.1995 (1972).

Baxendale, J.H. and George, P. (1950):

Trans. Faraday Soc., 46, 55 (1950).

Beilli, E., Gillard, R.D. and Williams, P.A. (1976):

J. Chem. Soc., Dalton Trans., p.1837 (1976).

Bhattacharyya, S.N. and Kundu, K.P. (1973):

Int. J. Radiat. Phys. Chem., 5, 183 (1973).

Billing, D.E. and Hathaway, B.J. (1970):

Coord. Chem., Rev., 5, 143 (1970).

Blau, F. (1898):

Monatsh Chem., 10, 647 (1898).

Bock, C.R., Meyer, T.J. and Whitten, D.G. (1974):

J. Amer. Chem. Soc., 96, 4170 (1974).

Bock, C.R., Meyer, T.J. and Whitten, D.G. (1975):

J. Amer. Chem. Soc., 97, 2909 (1975).

Bolleta, F., Maestri, M. and Moggi, L. (1973):

J. Phys. Chem., 77, 861 (1973).

Brandt, W.W. Mellon, M.G. and Smith, G.F. (1942):

Ind. Eng. Chem., Anal. Ed., 14, 931 (1942).

Brayant, G.M., Fergusson, J.E. and Powell, H.K.J. (1971):

Aust. J. Chem., 24, 257 (1971).

Breck, A.K. and Wan, J.K.S. (1973):

Int. J. Radiat. Phys. Chem., 5, 517 (1973).

Brinen, J.S., Rosebrook, D.D. and Hirt, R.C. (1963):

J. Phys. Chem., 67, 2651 (1963).

Broomhead, J.A., Dwyer, M. and Kane-Maguire, N.A.P. (1968):

Inorg. Chem., 7, 1388 (1968).

Broomhead, J.A. and Grumley, W. (1968a):

J. Chem. Soc. Chem. Commun., p.299 (1968).

Broomhead, J.A. and Grumley, W. (1968b):

J. Chem. Soc. Chem. Commun., p.1211 (1968).

Brown, G.M., Callahan, R.W. and Meyer, T.J. (1975):

Inorg. Chem., 14, 1915 (1975).

Bryant, G.A. and Fergusson, J.E. (1971):

Aust. J. Chem., 24, 275 (1971).

Bunnett, J.F. (1961):

J. Amer. Chem. Soc., 83, 4956 (1961).

Burgess, J. and Prince, R.H. (1966):

J. Chem. Soc. (A), p.6061 (1966).

Burstall, F. and Nyholm, R.S. (1952):

J. Chem. Soc., p.3577 (1952).

Buxton, G.V., Dainton, F.S. and Kalecinski, J. (1969):

Int. J. Radiat. Phys. Chem., 1, 87 (1969).

Campano, D.D. Kantrowitz, E.R., Hoffman, M.Z. and Weinberg, M.S. (1974):

J. Phys. Chem., 78, 686 (1974).

Carassiti, V., Condorelli, G. and Costanzo, L.L. (1964):

Ann. Chim. Rome, 54, 303 (1964).

Carstens, D.W. and Crosby, G.A. (1970):

J. Mol. Spectrosc., 34, 273 (1970).

- Caspari, G., Hughes, R.G., Endicott, J.F. and Hoffman, M.Z. (1970):
J. Amer. Chem. Soc., 92, 6801 (1970).
-
- Chagas, A.P., Tubino, M. and Vichi, E.J.S. (1978):
Inorg. Chim. Acta, 28, L137 (1978).
- Chaisson, D.A. et al. (1972):
J. Amer. Chem. Soc., 94, 6665 (1972).
- Chattopadhyay, B., Roy, J. and Banerjea, D. (1978):
J. Inorg. Nucl. Chem., 40, 2041 (1978).
- Chawla, O.P. and Fessenden, R.W. (1975):
J. Phys. Chem., 79, 2693 (1975).
- Chen, S-N., Cope, V.W. and Hoffman, M.Z. (1973):
J. Phys. Chem., 77, 1111 (1973).
- Chou, M., Creutz, C. and Sutin, N. (1977):
J. Amer. Chem. Soc., 99, 5615.
- Chum, H.L., Koran, D. and Osteryoung, R.A. (1978):
J. Amer. Chem. Soc., 100, 310 (1978).
- Ciampolini, M. and Nardi, N. (1966):
Inorg. Chem., 5, 41 (1966).
- Clark, R.E. and Ford, P.C. (1970):
Inorg. Chem., 9, 227 (1970).
- Cohen, H. and Meyerstein, D. (1971):
J. Amer. Chem. Soc., 93, 4179 (1971).
- Cohen, H. and Meyerstein, D. (1975):
J. Chem. Soc., Dalton Trans., p.2477 (1975).
- Cooper, G.D. and DeGraff, B.A. (1971):
J. Phys. Chem., 75, 2897 (1971).
- Cooper, G.D. and DeGraff, B.A. (1972):
J. Phys. Chem., 76, 2618 (1972).
- Cope, V.W., Chen, S. and Hoffman, M.Z. (1973):
J. Amer. Chem. Soc., 95, 3116 (1973).

Cope, V.W. and Hoffman, M.Z. (1972):

J. Chem. Soc., Chem. Commun., p.227 (1972).

Cordeman, L. et al. (1974):

J. Phys. Chem., 78, 1361 (1974).

Cotton, F.A. and Wilkinson, G. (1972):

"Advanced Inorganic Chemistry", Interscience, London,
3rd ed. (1972).

Creaser, I.I. et al. (1977):

J. Amer. Chem. Soc., 99, 3181 (1977).

Creutz, C. and Sutin, N. (1974):

J. Bio. Chem., 249, 6788 (1974).

Creutz, C. and Sutin, N. (1975):

Proc. Natl. Acad. Sci. U.S.A., 72, 2858 (1975).

Creutz, C. and Sutin, N. (1977):

J. Amer. Chem. Soc., 99, 241 (1977).

Crosby, G.A., Watts, R.J. and Carstens, D.W. (1970):

Science, 170, 1195 (1970).

Crumbliss, A.L. and Gestaut, L.J. (1976):

J. Coord. Chem., 5, 109 (1976).

Curtis, N.F. (1964):

J. Chem. Soc. (A), p.2834 (1964).

David, P.G. (1972):

J. Chem. Soc. Chem. Commun., p.1151 (1972).

David, P.G., Richardson, J.G. and Wehry, E.L. (1971):

Inorg. Nucl. Chem. Letters, 7, 251 (1971).

David, P.G., Richardson, J.G. and Wehry, E.L. (1972):

J. Inorg. Nucl. Chem., 34, 1333 (1972).

David, P.G. and Wehry, E.L. (1973):

Mol. Photochem., 5, 21 (1973).

Davies, G. and Loose, D.J. (1976a):

Inorg. Chem., 15, 694 (1976).

Davies, G., Higgins, R. and Loose, D.J. (1976b):

Inorg. Chem., 15, 700 (1976).

Davies, K.M. and Earley, J.E. (1978):

Inorg. Chem., 17, 3350 (1978).

Davies, R., Green, M. and Sykes, A.G. (1972):

J. Chem. Soc., Dalton Trans., p.1171 (1972).

Day, P. and Sanders, N. (1967):

J. Chem. Soc. (A), p.1530 and 1536 (1967).

DeArmond, K. and Halper, W. (1971):

J. Phys. Chem., 75, 3230 (1971).

DeArmond, M.K. and Hillis, J.E. (1971):

J. Chem. Phys., 54, 2247 (1971).

Demas, N.J. and Adamson, A.W. (1971):

J. Amer. Chem. Soc., 93, 1800 (1971).

Demas, J.N. and Crosby, G.A. (1971):

J. Amer. Chem. Soc., 93, 284 (1971).

Dietrich, M.W. and Wahl, A.C. (1963):

J. Chem. Phys., 38, 1591 (1963).

Dodel, P. and Taube, H. (1965):

Z. Physik. Chem. (Frankfurt), 44, 92 (1965).

Doering, A.G., Porter, G.B. and Karanka, S. (1962):

J. Amer. Chem. Soc., 84, 407 (1962).

Dogliotti, L. and Hayon, E. (1967):

J. Phys. Chem., 71, 3802 (1967).

Durrante, V.A. and Ford, P.C. (1975):

J. Amer. Chem. Soc., 97, 6898 (1975).

Dwyer, F.P. and Davies, N.R. (1954):

Trans. Faraday Soc., 50, 244 (1954).

Dwyer, F.P., Goodwin, H.A. and Gyrafas, E.C. (1963):

Aust. J. Chem., 16, 42 (1963).

Dwyer, F.P. and Gyrafas, E.C. (1952):

J. Amer. Chem. Soc., 74, 4699 (1952).

Elsgernd, H. and Beattie, J.K. (1968):

Inorg. Chem., 7, 2468 (1968).

Endicott, J.F. and Ferrandi, G. (1974):

J. Amer. Chem. Soc., 96, 3681 (1974).

Endicott, J.F., Ferrandi, G.J. and Barber, J.R. (1975):

J. Amer. Chem. Soc. 97, 219 (1975).

Endicott, J.F. and Hoffman, M.Z. (1965):

J. Amer. Chem. Soc., 87, 3348 (1965).

Endicott, J.F. and Hoffman, M.Z. (1965):

J. Amer. Chem. Soc., 87, 3865 (1965).

Endicott, J.F., Hoffman, M.Z. and Beres, L.S. (1970):

J. Phys. Chem., 74, 1021 (1970).

Espenson, J.H. (1967):

J. Amer. Chem. Soc., 89, 1276 (1967).

Falcinella, B., Felgate, P.D. and Laurence, G.S. (1974):

J. Chem. Soc. Dalton Trans., p.1367 (1974).

Farina, R., Hogg, R. and Wilkins, R.G. (1968):

Inorg. Chem., 7, 170 (1968).

Farrington, D.J., Jones, J.G. and Twigg, M.V. (1977):

Inorg. Chim. Acta, 25, L75 (1977).

Favini, G. and Gamba, A. (1966):

Gazz. Chim. Ital., 96, 391 (1966).

Faye, G.H. (1966):

Canad. J. Chem., 44, 2165 (1966).

Fergusson, J.E., Hawkins, C.J., Kane-Maguire, N.A.P. and Lip, H. (1969):

Inorg. Chem., 8, 771 (1969).

Ferrandi, G.J. and Endicott, J.F. (1973):

J. Amer. Chem. Soc., 95, 2371 (1973).

Ferrandi, G.J., Endicott, J.F. and Barber, J.R. (1975):

J. Phys. Chem., 79, 630 (1975).

Fleischauer, P.D. and Adamson, A.W. (eds.), (1975):

"Concepts of Inorganic Photochemistry", Wiley, New York.

Foote, C.S. (1968):

Acc. Chem. Res., 1, 104 (1968).

Ford, P., Rudd, D., Gaunder, R. and Taube, H. (1968):

J. Amer. Chem. Soc., 90, 1187 (1968).

Ford, P.C., Chaisson, D.A. and Stuemer, D.H. (1971):

J. Chem. Soc. Chem. Commun., p.530 (1971).

Ford-Smith, M.H. and Sutin, N. (1961):

J. Amer. Chem. Soc., 83, 1830 (1961).

Fujita, I. and Kobayashi, H. (1972):

Ber. Bunsenges Phys. Chem., 76, 115 (1972).

Furlani, C. (1968):

Coord. Chem. Rev., 3, 141 (1968).

Gafney, H.D. and Adamson, A.W. (1972):

J. Amer. Chem. Soc., 94, 8238 (1972).

Gafney, H.D., Reed, J.L. and Basolo, F. (1973):

J. Amer. Chem. Soc., 95, 7998 (1973).

Geiger, U.P. and Class, E. (1961):

Experientia, 17, 444 (1961).

Ghosh, P., Mukerjee, A.R. and Palit, S.R. (1964):

J. Polym. Sci., Part A, 2, 2817 (1964).

Gijzeman, D.O.L., Kaufman, F. and Porter, G. (1973):

J. Chem. Soc. Faraday Trans. (2), 69, 708 (1973).

Gil, L., Moraga, E. and Bunel, S. (1967):

Mol. Phys., 12, 333 (1967).

Gilkman, T.S. and Podlinyaeva, M.E. (1955):

Ukrain. Khim. Zhur., 21, 211 (1955).

Gillard, R.D. (1975):

Coord. Chem. Rev., 16, 67 (1975).

Gillard, R.D., Hughes, C.T. and Williams, P.A. (1976):

Transition Met. Chem., 1, 51 (1976).

Gillard, R.D., Kane-Maguire, L.A.P. and Williams, P.A. (1977a):

Transition Met. Chem., 2, 12 (1977).

Gillard, R.D., Kane-Maguire, L.A.P. and Williams, P.A. (1977b):

J. Chem. Soc. Chem. Commun., p.1039 (1977).

Gillard, R.D., Kane-Maguire, L.A.P. and Williams, P.A. (1977c):

J. Chem. Soc. Dalton Trans., p.1792 (1977).

Gillard, R.D. and Lyons, J.R. (1973):

J. Chem. Soc. Chem. Commun., p.585 (1973).

Gillard, R.D. and Williams, P.A. (1977):

Transition Met. Chem., 2, 14 (1977).

Gleria, M., Minto, F., Beggiato, G. and Bortolus, P. (1978):

J. Chem. Soc. Chem. Commun., p.285 (1978).

Golinick, G. (1968):

Adv. Photochem., 6, 1 (1968).

Gordon, B.M., Williams, L.L. and Sutin, N. (1961):

J. Amer. Chem. Soc., 83, 2061 (1961).

Gould, E.S. (1959):

"Mechanism and Structure in Organic Chemistry", Holt,
Rinehart and Winston, N.Y.

Gratzel, M., Bansal, K.M. and Henglein, A. (1973):

Ber. Bunsenges Phys. Chem., 77, 11 (1973).

Gratzel, M., Henglein, A., Lilie, J. and Beck, G. (1969):

Ber. Bunsenges Phys. Chem., 73, 646 (1969).

Green, A.A., Edwards, J.O. and Jones, P. (1966):

Inorg. Chem., 5, 1858 (1966).

Grossman, B. and Wilkins, R.G. (1967):

J. Amer. Chem. Soc., 89, 4230 (1967).

Gutierrez, A.R. and Adamson, A.W. (1978):

J. Phys. Chem., 82, 902 (1978).

Hagar, G.D. and Crosby, G.A. (1975):

J. Amer. Chem. Soc., 97, 7031 (1975).

Hagar, G.D., Watts, R.J. and Crosby, G.A. (1975):

J. Amer. Chem. Soc., 97, 7037 (1975).

Haim, A. and Taube, H. (1963):

J. Amer. Chem. Soc., 85, 495 (1963).

Halpern, J. (1961):

Quart. Rev., 15, 217 (1961).

Harriman, A. (1978):

J. Photochem., 8, 205 (1978).

Hayon, E. and McGarvey, J.J. (1967):

J. Phys. Chem., 71, 1472 (1967).

Henning, H., Hempel, K., Ackermann, M. and Thomas, P. (1976):

Z. Anorg. Chem., 422, 65 (1976).

Henning, H., Hempel, K. and Kertscher, P. (1975):

Z. Chem., 15, 491 (1975).

Henning, H., Jurdeczka, K. and Thomas, P. (1976):

Z. Chem., 16, 161 (1976).

Henry, M.S. and Hoffman, M.Z. (1976):

"Sixth IUPAC Symposium on Photochemistry", Abstract No. 43
(1976).

Hipps, K.W. and Crosby, G.A. (1975):

J. Amer. Chem. Soc., 97, 7042 (1975).

- Hoffman, M.Z., Balzani, V. et al. (1975):
J. Amer. Chem. Soc., 97, 728 (1975).
- Hoffman, M.Z. and Kimmel, D.W. (1975):
J. Chem. Soc., Chem. Commun., p.2559 (1975).
- Hoffman, M.Z. and Simic, M. (1970):
J. Amer. Chem. Soc., 91, 533 (1970).
- Hoffman, M.Z. and Simic, M. (1972):
J. Amer. Chem. Soc., 94, 1757 (1972).
- Hoffman, M.Z. and Simic, M. (1973):
J. Chem. Soc. Chem. Commun., p.640 (1973).
- Hoffman, M.Z. and Simic, M. (1973):
Inorg. Chem., 12, 2471 (1973).
- Hoffman, M.Z., Simic, M. and Brezniak, N.V. (1977):
J. Amer. Chem. Soc., 99, 2166 (1977).
- Hoggard, P.E. and Porter, G.B. (1978):
J. Amer. Chem. Soc., 100, 1457 (1978).
- Holwerda, R.A., Wherland, S. and Gray, H.B. (1976):
Ann. Rev. Biophys. Bioengin., 5, 364 (1976).
- Hoselton, M.A. et al. (1978):
J. Amer. Chem. Soc., 100, 2383 (1978).
- Hurst, J.K. (1976):
J. Amer. Chem. Soc., 98, 4001 (1976).
- Ito, H. (1956):
Nippon Kagaku Zasshi, 77, 1399 (1956).
- Jamieson, R.A. and Perone, S.P. (1972):
Anal. Chem., 41, 830 (1972).
- Jamieson, R.A. and Perone, S.P. (1972):
J. Phys. Chem., 76, 830 (1972).
- James, B.R. and Williams, R.J.P. (1961):
J. Chem. Soc., p.2007 (1961).

Jørgensen, K. (1955):

Acta Chemica. Scand., 9, 1362 (1955).

Kane-Maguire, N.A.P., Dunlop, B. and Langford, C.H. (1971):

J. Amer. Chem. Soc., 93, 6923 (1971).

Kane-Maguire, N.A.P. and Langford, C.H. (1971):

J. Chem. Soc. Chem. Commun., p.895 (1971).

Kane-Maguire, N.A.P. and Langford, C.H. (1976):

Inorg. Chem., 15, 464 (1976).

Kantrowitz, E.R., Hoffman, M.Z. and Schilling, K.M. (1972):

J. Phys. Chem., 76, 2493 (1972).

Kearns, D.R. (1971):

Chem. Rev., 71, 395 (1971).

Kelly, T.L. (1971):

Ph.D. Dissertation, Wayne State University, 1971.

Kelly, T.L. and Endicott, J.F. (1972a):

J. Amer. Chem. Soc., 94, 1797 (1972).

Kelly, T.L. and Endicott, J.F. (1972b):

J. Phys. Chem., 76, 1937 (1972).

Kirk, A.D., Hoggard, P.E., Porter, G.B., Rockley, M.G. and Windsor, M.W. (1976):

Chem. Phys. Letters, 37, 199 (1976).

Kirk, A.D., Moss, K.C. and Valentine, J.G. (1971):

Canad. J. Chem., 49, 375 (1971).

Kiss, A. and Császár, J. (1963):

Acta Chim. Acad. Sci. Hung., 38, 405 and 421 (1963).

Kläning, U. and Symons, M.C.R. (1959):

J. Chem. Soc., p.3269 (1959).

Kläning, U. and Symons, M.C.R. (1960):

J. Chem. Soc., p.977 (1960).

Klein, D. and Moeller, C.W. (1965):

Inorg. Chem., 4, 394 (1965).

Knibbe, H., Rehm, D. and Weller, A. (1968):

Ber. Bunsenges Physik. Chem., 72, 257 (1968).

König, E. (1968):

Coord. Chem. Rev., 3, 471 (1968).

Kozlov, Yu.N. and Berdnikov, V.M. (1973):

Russ. J. Phys. Chem., 78, 160 (1973).

Lachish, U., Shafferman, A. and Stein, G. (1976):

J. Chem. Phys., 64, 4205 (1976).

Langford, C.H., Phillips, J., Koningstein, J.A. and Sasseville, R. (1978):

J. Phys. Chem., 82, 622 (1978).

Langford, C.H., Vuik, C.P.J. and Kane-Maguire, N.A.P. (1975a):

Inorg. Nucl. Chem. Letters, 11, 377 (1975).

Langford, C.H., Vuik, C.P.J. and Kane-Maguire, N.A.P. (1975b):

Canad. J. Chem., 53, 3121 (1975).

Larsen, D.W. and Wahl, A.C. (1965):

J. Chem. Phys., 43, 3765 (1965).

Lati, J., Koresch, J. and Meyerstein, D. (1975):

Chem. Phys. Letters, 33, 286 (1975).

Lati, J. and Meyerstein, D. (1975):

Int. Radiat. Phys. Chem., 7, 611 (1975).

Latimer, W. (1952):

"Oxidation Potentials", 2nd ed., Prentice-Hall, Englewood Cliffs, N.J.

Laurence, G.S. and Balzani, V. (1974):

Inorg. Chem., 13, 2976 (1974).

Laurence, G.S. and Thornton, A.T. (1978):

Private Communication.

Laver, J.L. and Smith, P.W. (1970):

Aust. J. Chem., 24, 1807 (1970).

Lee, C.S., Gorton, E.M., Neuman, H.M. and Hunt, Jr., H.R. (1966):

Inorg. Chem., 5, 1397 (1966).

Lilie, J., Beck, G. and Henglein, A. (1971):

Ber. Bunsenges Phys. Chem., 75, 458 (1971).

Lilie, J. and Fessenden, R.W. (1973):

J. Phys. Chem., 77, 674 (1973).

Lincoln, S.F. and Hubbard, C.D. (1974):

J. Chem. Soc. Dalton Trans., p.2513 (1974).

Linschitz, H. and Pekkarinen, L. (1960):

J. Amer. Chem. Soc., 82, 2411 (1960).

Lipeto, M.P. and Endicott, J.F. (1971):

Inorg. Chem., 19, 1420 (1971).

Lucie, J.M., Stranks, D.R. and Burgess, J. (1975):

J. Chem. Soc. Dalton Trans., p.245 (1975).

Lyttle, F.E. and Hercules, D.M. (1966):

J. Amer. Chem. Soc., 88, 4745 (1966).

Lyttle, F.E. and Hercules, D.M. (1969):

J. Amer. Chem. Soc., 91, 253 (1969).

Maestri, M. et al. (1973):

J. Amer. Chem. Soc., 95, 7864 (1973).

Maestri, M., Bolleta, F., Manfrin, F., Moggi, L. and Balzani, V.
(1976):

"Sixth IUPAC Symposium on Photochemistry", Abstract No. 65
(1976).

Maki, N. (1969):

Bull. Chem. Soc. Japan, 42, 2275 (1969).

Malik, G.M. and Laurence, G.S. (1978):

Inorg. Chimica Acta, 28, L149-151 (1978).

- Malin, J.M. and Swinehart, J.H. (1968):
Inorg. Chem., 7, 250 (1968).
- Malone, S.D. and Endicott, J.F. (1972):
J. Phys. Chem., 76, 2223 (1972).
- Marcus, R.A. (1956):
J. Chem. Phys., 24, 966 (1956).
- Marcus, R.A. (1959):
Can. J. Chem., 37, 155 (1959).
- Marcus, R.A. (1960):
Discuss. Faraday Soc., 29, 21 (1960).
- Marcus, R.A. (1963):
J. Phys. Chem., 67, 853 (1963).
- Marcus, R.A. (1964):
Ann. Rev. Phys. Chem., 15, 155 (1964).
- Marcus, R.A. (1968):
J. Phys. Chem., 72, 891 (1968).
- Marcus, R.A. and Sutin, N. (1975):
Inorg. Chem., 14, 213 (1975).
- Martin, B., McWhinnie, W.R. and Waind, G.M. (1961):
J. Inorg. and Nucl. Chem., 28, 2937 (1961).
- Mason, S.F. and Norman, B.J. (1969):
J. Chem. Soc. (A), p.1428 (1969).
- Matheson, M.S. and Dorfman, L.M. (1969):
"Pulse Radiolysis", M.I.T. Press, Cambridge, Mass.
- Matheson, M.S., Mulac, W.A. and Rabani, J. (1963):
J. Phys. Chem., 67, 2613 (1963).
- Matheson, R.A. (1967):
J. Phys. Chem., 71, 1302 (1967).
- Matsura, N. et al. (1967):
Bull. Chem. Soc. Japan, 40, 2024 (1967).

Mayoh, B. and Day, P. (1978):

Theoret. Chim. Acta (Berl.), 49, 259 (1978).

McArdle, J.V. et al. (1977):

J. Amer. Chem. Soc., 99, 2483 (1977).

McConnell, H.M. and Weaver, H.E. (1956):

J. Chem. Phys., 25, 307 (1956).

McMillin, D.R., Brucker, M.T. and Ahn, B.T. (1977):

Inorg. Chem., 16, 943 (1977).

Meyer, T.J. (1978):

Account Chem. Res., 11, 94 (1978).

Meyer, T.J. and Taube, H. (1968):

Inorg. Chem., 7, 2369 (1968).

Meyerstein, D. (1971a):

Inorg. Chem., 10, 638 (1971).

Meyerstein, D. (1971b):

Inorg. Chem., 10, 2244 (1971).

Meyerstein, D. (1978):

Acc. Chem. Res., 11, 43 (1978).

Miesel, D., Levanon, H. and Czapski, G. (1974):

J. Phys. Chem., 78, 779 (1974).

Moggi, L., Sabbatini, N. and Traverso, O. (1973):

Mol. Photochem., 5, 11 (1973).

Moggi, L., Varani, G., Sabbatini, N. and Balzani, V. (1971):

Mol. Photochem., 3, 141 (1971).

Montasti, E., Pelizzetti, E., Baiocchi, C. (1977):

J. Chem. Soc. Dalton Trans., p.132 (1977).

Muir, M.M. and Huang, W.L. (1973a):

Inorg. Chem., 12, 1831 (1973).

Muir, M.M. and Huang, W.L. (1973b):

Inorg. Chem., 12, 1930 (1973).

- Natarajan, P. and Endicott, J.F. (1972):
J. Amer. Chem. Soc., 94, 5909 (1972).
- Natarajan, P. and Endicott, J.F. (1973a):
J. Amer. Chem. Soc., 95, 2470 (1973).
- Natarajan, P. and Endicott, J.F. (1973b):
J. Phys. Chem., 77, 1823 (1973).
- Natarajan, P. and Endicott, J.F. (1973c):
J. Phys. Chem., 77, 2049 (1973).
- Navon, G. and Sutin, N. (1974):
Inorg. Chem., 13, 2159 (1974).
- Neta, P. and Dorfman, L.M. (1968):
Adv. Chem. Ser., No. 81, 222 (1968).
- Neta, P., Madhavan, V., Zemel, H. and Fessenden, R.W. (1977):
J. Amer. Chem. Soc., 99, 163 (1977).
- Newton, T.W. and Baker, F.B. (1964):
Inorg. Chem., 3, 569 (1964).
- Noack, M. et al. (1971):
J. Phys. Chem., 54, 1342 (1971).
- Nord, G., Pederson, B. and Fraver, O. (1978):
Inorg. Chem., 17, 2233 (1978).
- Nord, G. and Wernberg, O. (1972):
J. Chem. Soc. Dalton Trans., p.866 (1972).
- Nord, G. and Wernberg, O. (1975):
J. Chem. Soc. Dalton Trans., p.845 (1975).
- Nord, K. (1976):
Inorg. Chem., 15, 1921 (1976).
- Norton, Jr., K. and Hurst, J.K. (1978):
J. Amer. Chem. Soc., 100, 7237 (1978).
- Ohno, T. and Kato, S. (1969):
Bull. Chem. Soc. Japan, 42, 3385 (1969).

O'Neill, P., Schulte-Frohlinde, D. (1977):

J. Phys. Chem., 81, 26 (1977).

Orgel, L.E. (1961):

J. Chem. Soc., p.3683 (1961).

Pagsberg, P. and Floryan, E.S. (1976):

Int. J. Radiat. Phys. Chem., 8, 425 (1976).

Palit, S.R. and Murkejee, A.R. (1962):

J. Poly. Sci., 58, 1243 (1962).

Palmer, J.M., Papaconstantinou, E. and Endicott, J.F. (1969):

Inorg. Chem., 7, 1516 (1969).

Palmer, J.M. et al. (1969):

Inorg. Chem., 8, 1516 (1969).

Palmer, R.A. and Piper, T.S. (1966):

Inorg. Chem., 5, 864 (1966).

Parker, C.A. and Hatchard, C.J. (1959):

J. Phys. Chem., 63, 22 (1959).

Parker, O.J. and Espenson, J.H. (1969a):

J. Amer. Chem. Soc., 91, 1313 (1969).

Parker, O.J. and Espenson, J.H. (1969b):

Inorg. Chem., 8, 1523 (1969).

Paszyc, S. and Norrish, R.G.W. (1963):

Rocz. Chem., 37, 1305 (1963).

Patterson, J.I.H. and Perone, S.P. (1972):

Anal. Chem., 44, 1978 (1972).

Patterson, J.I.H. and Perone, S.P. (1973):

J. Phys. Chem., 77, 2437 (1973).

Pecht, I. and Anbar, M. (1969):

J. Chem. Soc. (A), p.1902 (1969).

Perkampus et al. (1968):

Z. Naturforsch. A, 23, 840 (1968).

Penkelt, S.A. and Adamson, A.W. (1965):

J. Amer. Chem. Soc., 87, 2514 (1965).

Pfeiffer, P., Welderman, Br. (1950):

Zeitch. Anorg. Chemie., Baud 261, p.203 (1950).

Pfeil, A. (1971):

J. Amer. Chem. Soc., 93, 5395 (1971).

Pflaum, R.T. and Brandt, W.W. (1955a).

J. Amer. Chem. Soc., 76, 6215 (1955).

Pflaum, R.T. and Brandt, W.W. (1955b):

J. Amer. Chem. Soc., 77, 2019 (1955).

Pouko, N. and Luz, L. (1972):

J. Chem. Phys., 57, 3311 (1972).

Price, H.J. and Taube, H. (1968):

Inorg. Chem., 7, 1 (1968).

Rabani, J., Klug-Roth, D. and Lilie, J. (1973):

J. Phys. Chem., 77, 1169 (1973).

Rabani, J., Stein, G. (1962):

Trans. Faraday Soc., 58, 2150 (1962).

Rabold, G.P. and Piette, L.H. (1968):

Spectrosc. Letters, 1, 225 (1968).

Reed, J.L., Gafney, H.D. and Basolo, F. (1974):

J. Amer. Chem. Soc., 96, 1363 (1974).

Reed, J.L., Wang, F. and Basolo, F. (1972):

J. Amer. Chem. Soc., 94, 7173 (1972).

Rehm, D. and Weller, A. (1969):

Ber. Bunsenges Phys. Chem., 73, 834 (1969).

Rehm, D. and Weller, A. (1970):

Isr. J. Chem., 8, 259 (1970).

Reynold, W.L. and Lumry, R.W. (1966):

"Mechanisms of Electron Transfer", New York, The Ronald Press.

- Richards, A.F., Ridd, J.H. and Tobe, M.L. (1963):
Chem. Ind. (London), p.1726 (1963).
- Roche, T.S. and Endicott, J.F. (1972):
J. Amer. Chem. Soc., 94, 8622 (1972).
- Roche, T.S. and Endicott, J.F. (1974):
Inorg. Chem., 13, 1575 (1974).
- Rowan, N.S., Hoffman, M.Z. and Milburn, M. (1974):
J. Amer. Chem. Soc., 96, 6060 (1974).
- Roy, J. and Banerjea, D. (1975):
J. Inorg. Nucl. Chem., 38, 1313 (1975).
- Ruff, I. and Zimonyi, M. (1973):
Electrochim. Acta, 18, 515 (1973).
- Sadisvian, N. and Endicott, J.F. (1966):
J. Amer. Chem. Soc., 88, 5468 (1966).
- Saji, T. and Aoyagui, S. (1975):
J. Electroanal. Chem. Interfacial Electrochem., 58, 401 (1975).
- Samotus, A. (1973a):
Advan. Mol. Rel. Processes, 5, 121 (1973).
- Samotus, A. (1973b):
Rocz. Chem., 17, 265 (1973).
- Sargeson, A.M. (1979):
Chem. Britain, 15, 23 (1979).
- Scandola, F., Bartocci, C. and Scandola, M.A. (1973):
J. Amer. Chem. Soc., 95, 7898 (1973).
- Scandola, F., Bartocci, C. and Scandola, M.A. (1974):
J. Phys. Chem., 78, 572 (1968).
- Scheerer, R. and Grätzel, M. (1977):
J. Amer. Chem. Soc., 99, 865 (1977).
- Schilt, A.A. and Smith, G.F. (1956):
J. Phys. Chem., 60, 1516 (1956).

Schulman, S.G., Tidwell, P.T., Cetorelli, J.J. and Winefordner, J.D. (1971):

J. Amer. Chem. Soc., 93, 3179 (1971).

Schunn, R.A. (1966):

Quart. Rev., 20, 245 (1966).

Sekested, K., Holeman, J. and Hart, E.J. (1977):

J. Phys. Chem., 81, 1363 (1977).

Shagisultanova, G.A. et al. (1973):

Zhur. Fiz. Khim., 46, 2407 (1972).

Shakhashiri, B.Z. and Gordon, G. (1968):

Inorg. Chem., 11, 2454 (1968).

Shakhashiri, B.Z. and Gordon, G. (1969):

J. Amer. Chem. Soc., 91, 1103 (1969).

Sharma, V.S. and Schubert, J. (1971):

Inorg. Chem., 10, 251 (1971).

Shaw, K. and Espenson, J.H. (1968):

Inorg. Chem., 7, 1619 (1968).

Sidgwick, N.V. (1959):

"The Elements and Their Compounds", Vol. 1, Oxford University Press, Oxford.

Siiman, O., Young, M. and Carey, P.R. (1976):

J. Amer. Chem. Soc., 98, 744 (1976).

Simic, M. and Hoffman, M.Z. (1972):

Proc. 14th Internat. Conf. Coord. Chem., Toronto, p.501.

Smith, G.F. and Banick, W.M. (1959):

Talanta, 2, 348 (1959).

Smith, G.F. and Richter, F.P. (1944):

Ind. Eng. Chem., Anal. Ed., 16, 580 (1944).

Solenberger, J.C. (1969):

Ph.D. Thesis, Washington University, St. Louis, Ma. (1969).

- Sone, K., Krumholtz, P. and Stammreich, H.J. (1955);
J. Amer. Chem. Soc., 77, 777 (1955).
- Stalnaker, N.D., Solenberger, J.C. and Wahl, A.C. (1977):
J. Phys. Chem., 81, 601 (1977).
- Steel, C. and Linschitz, H. (1962):
J. Phys. Chem., 66, 2577 (1962).
- Stranks, D.R. (1960):
Discuss. Faraday Soc., 29, 116 (1960).
- Street, A.J., Goodall, D.M. and Greenhow, R.C. (1978):
Chem. Phys. Letters, 56, 326 (1978).
- Sundarajan, S. and Wehry, E.L. (1972a):
J. Phys. Chem., 76, 1528 (1972).
- Sundarajan, S. and Wehry, E.L. (1972b):
J. Chem. Soc. Chem. Commun., p.1135 (1972).
- Sundarajan, S. and Wehry, E.L. (1972c):
J. Inorg. Nucl. Chem., 34, 3699 (1972).
- Sutin, N. (1968):
Accounts Chem. Res., 1, 225 (1968).
- Sutin, N. and Gordon, B.M. (1961):
J. Amer. Chem. Soc., 83, 70 (1961).
- Taube, H. (1959):
Adv. Inorg. Chem. Radiochem., 1, 1 (1959).
- Taube, H. and Gould, E.S. (1969):
Accounts Chem. Res., 2, 231 (1969).
- Thomas, J.K. (1965):
Trans. Faraday Soc., 61, 702 (1965).
- Thornton, A.T. and Laurence, G.S. (1973); (1974).
J. Chem. Soc., Dalton Trans., p.1632 (1973), p.142 (1974).
- Thornton, A.T. and Laurence, G.S. (1978a):
Abstracts of the 9th AINSE Conf., Lucas Heights, Australia,
p.25 (1978).

Thornton, A.T. and Laurence, G.S. (1978b):

Int. J. Radiat. Phys. Chem., 11, 311 (1978).

Tokel-Takvoryan, N.E., Hemingway, R.E. and Bard, A.J. (1973):

J. Amer. Chem. Soc., 95, 6582 (1973).

T.Ng, F.T., Henry, P.M. (1976):

J. Amer. Chem. Soc., 98, 3606 (1976).

Treitel, I.M., Flood, M.T., Marsh, R.E. and Gray, H.B. (1969):

J. Amer. Chem. Soc., 91, 6512 (1969).

Valee, B.L. and Williams, R.J. (1968):

J. Biochem., 59, 498 (1968).

Vaudo, A.F., Kantrowitz, E.R. and Hoffman, M.Z. (1971):

J. Amer. Chem. Soc., 93, 6698 (1971).

Vaudo, A.F., Kantrowitz, E.R., Hoffman, M.Z., Papaconstantinou, E. and Endicott, J.F. (1972):

J. Amer. Chem. Soc., 94, 6655 (1972).

Vogel, A.I. (1961):

"Quantitative Inorganic Analysis", Longmans, London, 3rd ed.

Vogelman, E. et al. (1975):

Z. Phys. Chem., Neue Folge, 101, 321 (1975).

Vogler, A. and Adamson, A.W. (1968):

J. Amer. Chem. Soc., 90, 5943 (1968).

Voorst, J.D.W. and Hammerick, P. (1966):

J. Chem. Phys., 45, 3914 (1966).

Vydra, F. and Pribil, R. (1960):

Talanta, 5, 44 (1960).

Wagestian, H.F. and Hamond, G.S. (1971):

Theor. Chim. Acta, 20, 186 (1971).

Waltz, W.L. and Adamson, A.W. (1969):

J. Phys. Chem., 73, 4250 (1969).

- Waltz, W.L. and Pearson, R.G. (1969):
J. Phys. Chem., 73, 1941 (1969).
-
- Watts, R.J. and Crosby, G.A. (1972):
J. Amer. Chem. Soc., 94, 2606 (1972).
- Watts, R.J., Harrington, J.S. and Van Houten, J. (1977):
J. Amer. Chem. Soc., 99, 2179 (1977).
- Wehry, E.L. (1967):
Quart. Rev. (London), 28, 51 (1967).
- Wehry, E.L. and Ward, R.A. (1971):
Inorg. Chem., 10, 2660 (1971).
- Weller, A. (1967):
Nobel Symposium, 5, 413 (1967).
- Wells, A.F. (1962):
"Structural Inorganic Chemistry", University Press, Oxford,
3rd ed.
- Wells, W.L. and Endicott, J.F. (1971):
J. Phys. Chem., 75, 3075 (1971).
- Whitburn, K.D. (1976):
Ph.D. Thesis, The University of Adelaide, South Australia.
- Wilkins, R.G. and Yelin, R.E. (1968):
Inorg. Chem., 7, 2667 (1968).
- Wilson, R.I. et al. (1971):
Int. J. Radiat. Phys. Chem., 3, 311 (1971).
- Woodruff, W.H. and Margerum, D.W. (1973):
Inorg. Chem., 12, 962 (1973).
- Wright, R.C. and Laurence, G.S. (1972):
J. Chem. Soc. Chem. Commun., p.132 (1972).
- Yandell, J.K., Fay, D.P. and Sutin, N. (1973):
J. Amer. Chem. Soc., 95, 1131 (1973).

Yoneda, G.S., Blackmer, G.L. and Holwerda, R.A. (1977):

Inorg. Chem., 16, 3376 (1977).

Young, R.C., Keene, F.R. and Meyer, T.J. (1977):

J. Amer. Chem. Soc., 99, 2468 (1977).

Young, R.C., Nagle, J.K., Meyer, T.J. and Whitten, D.G. (1978):

J. Amer. Chem. Soc., 100, 4773 (1978).

Zarnegar, P.P., Bock, C.R. and Whitten, D.G. (1973):

J. Amer. Chem. Soc., 95, 4367 (1973).

Zemel, H. and Fessenden, R.W. (1975):

J. Phys. Chem., 79, 2773 (1975).

Zuberbühler, A. (1967):

Helv. Chim. Acta, 50, 466 (1967).

Zuberbühler, A. (1969):

Chimia, 23, 416 (1969).

Zuberbühler, A. (1970):

Helv. Chim. Acta, 53, 669 (1970).

Zwickel, A.M. and Taube, H. (1960):

Discuss. Faraday Soc., 29, 42 (1960).

Zwickel, A.M. and Taube, H. (1961):

J. Amer. Chem. Soc., 83, 793 (1961).

ADDENDUM

Page	line	now reads	should be
(v)	23	$[\text{Fe}(\text{phen})_3]^{3+}$	$[\text{Fe}(\text{Me}_4\text{-phen})_3]^{3+}$
28	5	Norvisch	Norrish
28	6	DeGraffe	DeGraff
60	4	Fig. ().	Fig. (8).
95	3	$[\text{Fe}(\text{phen})_3]^{3+}$	$[\text{Fe}(\text{Me}_4\text{-phen})_3]^{3+}$
169	12	ddition	addition
181	9	rules	ruled
266	1	Ferrandi	Ferraudi
266	3	Ferrandi	Ferraudi